UNIVERSITAT POLITÈCNICA DE VALÈNCIA

ESCOLA TÈCNICA SUPERIOR D'ENGINYERIA DEL DISSENY

Hybrid inorganic-organic materials for the optical recognition of neutral and anionic species.

PhD. THESIS

Submitted by

Maria Comes Navarro

PhD. Supervisor:

Dr. Ramón Martínez Máñez
Dr. Luis A. Villaescusa Alonso

València 2015

Escuela Técnica Superior de Ingeniería del Diseño

Instituto Interuniversitario de Reconocimiento Molecular y Desarrollo Tecnológico

RAMÓN MARTÍNEZ MÁÑEZ, PhD in Chemistry and Professor at the Universitat Politècnica de València, and LUIS ÁNGEL VILLAESCUSA ALONSO PhD in Chemistry and Lecturer at the Universitat Politècnica de València,

CERTIFY:

That the work *"Hybrid inorganic-organic materials for the optical recognition of neutral and anionic species"* has been developed by Maria Comes Navarro under their supervision in the Centro de Reconocimiento Molecular y Desarrollo Tecnológico de la *Universitat Politècnica de València*, as a thesis Project in order to obtain the degree of PhD in Chemistry at the *Universitat Politècnica de València.*

December 16th, 2015.

Dr. Ramón Martínez Máñez

Dr. Luis Ángel Villaescusa Alonso

"La verdadera ciencia enseña, sobre todo, a dudar y a ser ignorante"

Ernest Rutherford

"*... dove la natura finisce di produrre le sue spezie, l'uomo quivi cominicia con le cose naturali, con l'aiutorio di essa natura, a creare infinite spezie...*"

(...donde la naturaleza termina de producir sus propias especies, el hombre comienza, utilizando cosas naturales y con la ayuda de esta naturaleza, a crear una infinidad de especies...).

Leonardo da Vinci

Als meus pares i al meu germà,
a Vicent, Laia i Maria.

Agraïments.

Agradecimientos. Acknowledgements.

Quisiera aprovechar las primeras líneas de mi trabajo de tesis para expresar públicamente mi agradecimiento a las numerosas personas que, de una forma u otra, han tenido que ver con el mismo. Ciertamente, son muchas más de las que voy a nombrar, pero éstas sin duda son las que destacadamente tienen mi reconocimiento.

En primer lugar, a mis directores de tesis. Dr. Ramón Martínez Máñez, que desde el momento en que me ofreció la oportunidad de formar parte de su grupo, siempre he recibido de él palabras de ánimo y apoyo a este trabajo de investigación. Y asimismo, al Dr. Luis A. Villaescusa, por contagiarme su pasión por la síntesis de nuevos materiales, además de su inestimable ayuda en todo el trabajo de laboratorio y de redacción, para poder presentar finalmente esta tesis.

A los profesores del grupo de investigación, Loles y Juan, por el tiempo y las atenciones que me han dedicado. A Félix, por su incondicional ayuda. A mis compañeros del laboratorio 2.6, Ana Belén, Mª Jesús, Carmen, Elena, Hanoi, Rosa, Ana y Bea. En todos ellos he encontrado no sólo el apoyo investigador, sino también incluso una estrecha amistad.

No quiero olvidarme tampoco de la gente del Departamento de Química, profesores, compañeros de otros laboratorios, personal de administración y técnicos de laboratorio, porque han sido muy amables en todo momento, facilitándome cuanto he necesitado.

Quiero agradecer también a mis compañeros del ICMUV, por el tiempo que trabajé con ellos previos a mi beca en la UPV. Parte de la caracterización de los sólidos de este trabajo se debe a su colaboración. Especial mención a Vicent Primo, gran compañero y buen amigo.

Acknowledgements

I would like to thank Gerhard Mohr for giving me the opportunity to work and learn in his laboratory in Jena (Germany) and to all the people who made my stay pleasant and easy, especially to Anja.

De caràcter diferent és el recolzament que he rebut dels meus companys i companyes d'Eivissa, Anna, Xus, Maria Jose, Esther, Ricard, Joan, Cati… als que també vull agrair les seves paraules d'ànim, que han sigut de gran ajuda en aquesta darrera etapa de redacció.

Agrair especialment el suport que he rebut de la meva familia. Ells ben saben el que ha costat aquesta tesi. A Vicent, pel seu recolzament incondicional. Gràcies, moltes gràcies per tot. De les meves filles, Laia i Maria, només desitge que un dia comprenguen per què els vaig privar de tantes hores de gaudir juntes.

Resum

La tesis doctoral que es presenta sota el títol "***Hybrid inorganic-organic materials for the optical recognition of neutral and anionic species***" ha tingut com objectiu principal la síntesi i caracterització de materials híbrids orgànic-inorgànics basats en la combinació dels principis de la Química Supramolecular i la Ciència dels Materials.

Estudis recents corroboren que la cooperació entre aquestes dues àrees de la Química permet simular el que ja fa milions d'anys realitzen de forma natural els organismes vius. A nivell cel·lular, moltes de les funcions vitals estan relacionades amb l'habilitat d'un receptor concret per a reconèixer una espècie determinada, donant una resposta específica. Però el que és més interessant, és que als organismes vius, la majoria d'aquests sistemes no existeixen en forma de molècules dissoltes, sinó que estan units amb major o menor flexibilitat a un esquelet bio(in)orgànic.

Quan imitem aquests sistemes tenint en compte la química supramolecular i analítica, ens trobem que necessitem d'una molècula indicadora que sigui capaç d'unir-se a l'espècie que volem detectar i que alhora, aquesta unió produeixi un canvi en les propietats fisico-químiques de l'entitat per produir una senyal. Però a més, si aprofitem el fet que els materials silícics nanoestructurats presenten una alta estabilitat física i química i que proporcionen cavitats on es pot allotjar el sistema sensor, tenim la combinació híbrida orgànica-inorgànica sintètica semblant a la natural.

Per tal de desenvolupar aquesta idea, hem utilitzat sistemes sensors ampliament estudiats en procediments de reconeixement molecular en

dissolució aquosa i els hem aplicat als materials híbrids orgànic-inorgànics. Així el present treball de Tesis s'ha estructurat en dues parts: per una banda, la síntesis i caracterització de materials sòlids inorgànics porosos funcionalitzats per l'estudi i detecció d'amines utilitzant el procediment de "dosímetre químic", i per altra banda, s'ha realitzat la síntesis i caracterització de sòlids inorgànics porosos funcionalitzats per a l'estudi i detecció d'espècies aniòniques mitjançant el procediment d' "assajos per desplaçament".

Resumen

La tesis doctoral que se presenta bajo el título "*Hybrid inorganic-organic materials for the optical recognition of neutral and anionic species*" ha tenido como objetivo principal la síntesis y caracterización de materiales híbridos orgánico-inorgànicos basados en la combinación de los principios de la Química Supramolecular y la Ciencia de los Materiales.

Recientes estudios corroboran que la cooperación entre estas dos áreas de la Química permite simular lo que ya hace millones de años realizan de forma natural los organismos vivos. A nivel celular, muchas de las funciones vitales están relacionadas con la habilidad de un receptor concreto para reconocer una determinada especie, dando una respuesta específica. Pero lo que resulta más interesante, es que en los organismos vivos, la mayoría de estos sistemas no existen en forma de moléculas disueltas, sino que están unidos con mayor o menor flexibilidad a un esqueleto bio(in)orgánico.

Cuando imitamos estos sistemas teniendo en cuenta la química supramolecular y analítica, nos encontramos que necesitamos de una molécula indicadora que sea capaz de unirse a la especie que queremos detectar y que a su vez, esta unión produzca un cambio en las propiedades físico-químicas de la entidad para producir una señal. Pero además, si aprovechamos el hecho de que los materiales silíceos nanoestructurados presentan una alta estabilidad física y química y que proporcionan cavidades donde alojar al sistema sensor, tenemos la combinación híbrida orgánico-inorgánico sintética similar a la natural.

Con el objetivo de desarrollar esta idea, hemos utilizado sistemas sensores ampliamente estudiados en procedimientos de reconocimiento

molecular en disolución acuosa y los hemos aplicado a los materiales híbridos orgánico-inorgànicos. De esta manera, el trabajo de tesis se ha estructurado en dos partes: por un lado, la síntesis y caracterización de materiales sólidos inorgánicos porosos funcionalizados para el estudio y detección de aminas utilizando el procedimiento de "dosímetro químico", y por otro lado, se ha llevado a cabo la síntesis y caracterización de sólidos inorgánicos porosos funcionalizados para el estudio y detección de especies aniónicas mediante el procedimiento de "ensayos por desplazamiento".

Abstract

The doctoral thesis presented under the title "*Hybrid inorganic-organic materials for the optical recognition of neutral and anionic species*" has had as its main objective the synthesis and characterization of organic-inorganic hybrid materials based on the combination of the principles of Supramolecular Chemistry and Materials Science.

Recent studies confirm that cooperation between these two areas of Chemistry allow the simulation of what natural living beings have been doing for millions of years in a natural way. At cellular level, many vital functions are related to the ability of a particular receptor to recognize a particular species, giving a specific answer. But what is more interesting is that in living organisms, most of these systems do not exist as dissolved molecules, but are bounded to a (bio)organic skeleton with more or less flexibility.

When we imitated these systems bearing in mind the supramolecular and analytical chemistry, we find that we need a sensory molecule able to join with the specie that we want to detect and at the same time, this union must produce a change in its physico-chemical properties giving as a result a signal. But moreover, if we take advantatge of the fact that siliceous nanostructured materials present a high physical and chemical stability and that they have cavities where the sensor system can be incorporated into, we have the synthetic hybrid organic-inorganic combination similar to the natural one.

In order to develop this idea, we have used sensor systems widely studied in molecular recognition processes in aqueous media and we have applied them to the inorganic-organic hydrid materials. Therefore,

Abstract

the present work thesis has been structured in two parts: on the one hand, the synthesis and characterization of the functionalized inorganic porous solid materials by the study and detection of amines using the "chemodosimeter" approach. On the other hand, we have made the synthesis and characterization of the organic functionalized inorganic porous solid materials for the study and detection of anionic species through the displacement assays approach.

Results of this thesis and other contributions have resulted in the following scientific publications:

1. Maria Comes, M.Dolores Marcos, Ramón Martínez-Máñez, Félix Sancenón, Juan Soto, Luis A. Villaescusa, Pedro Amorós and Daniel Beltrán. **Chromogenic discrimination of primary aliphatic amines in water with functionalized mesoporous silica**. *Advanced Materials*, **2004**, 16, 1783-1786.

2. Maria Comes, Luis A. Villaescusa, María Dolores Marcos, Ramón Martínez-Máñez, Félix Sancenón, and Juan Soto. **N-Methyl,N-(propyl-3-trimethoxysilyl)Aniline, an Intermediate for Anchoring Dyes on Siliceous Supports.** *Synthetic Communications,* **2005**, 35, 1511-1516.

3. Sara Basurto, Tomás Torroba, Maria Comes, Ramón Martínez-Máñez, Félix Sancenón, Luis Villaescusa, and Pedro Amorós. **New Chromogenic Probes into Nanoscopic Pockets in Enhanced Sensing Protocols for Amines in Aqueous Environments**. *Organic Letters*, **2005**, 7, 24, 5469-5472.

4. Maria Comes, Gertrudis Rodríguez-López, M. Dolores Marcos, Ramón Martínez-Máñez, Félix Sancenón, Juan Soto, Luis A. Villaescusa, Pedro Amorós, and Daniel Beltrán. **Host Solids Containing Nanoscale Anion-Binding Pockets and Their Use in Selective Sensing Displacement Assays**. *Angewandte Chemie International Edition*, **2005**, 44, 2918-2922.

5. Beatriz García-Acosta, Maria Comes, Julia L. Bricks, Margarita A. Kudinova, Vladimir V. Kurdyukov, Alexei I. Tolmachev, Ana B. Descalzo, M. Dolores Marcos, Ramón Martínez-Máñez, Ana Moreno, Félix Sancenón, Juan Soto, Luis A. Villaescusa, Knut

Rurack, Jose M. Barat, Isabel Escriched and Pedro Amorós. **Sensory hybrid host materials for the selective chromo-fluorogenic detection of biogenic amines.** *Chemical Communications,* **2006**, 2239-2241.

6. Maria Comes, M. Dolores Marcos, Ramón Martínez-Máñez, M. Carmen Millán, Jose Vicente Ros-Lis, Félix Sancenón, Juan Soto, and Luis A. Villaescusa. **Anchoring Dyes into Multidimensional Large-Pore Zeolites: A Prospective Use as Chromogenic Sensing Materials.** *Chemistry. A European Journal,* **2006**, 12, 2162-2170.

7. Lenin Huerta, Jamal El Haskouri, David Vie, Maria Comes, Julio Latorre, Carmen Guillem, M. Dolores Marcos, Ramón Martínez-Máñez, Aurelio Beltrán, Daniel Beltrán, and Pedro Amorós. Nanosized **Mesoporous Silica Coatings on Ceramic Foams: New Hierarchical Rigid Monoliths.** *Chemistry of Materials*, **2007**, 19, 1082-1088.

8. José V. Ros-Lis, Rosa Casasús, Maria Comes, Carmen Coll, M. Dolores Marcos, Ramón Martínez-Máñez, Félix Sancenón, Juan Soto, Pedro Amorós, Jamal El Haskouri, Nuria Garró, and Knut Rurack. **A Mesoporous 3D Hybrid Material with Dual Functionality for Hg^{2+} Detection and Adsorption**. *Chemistry. A European Journal*. **2008**, 14, 8267-8278.

9. Maria Comes, María D. Marcos, Ramón Martínez-Máñez, Félix Sancenón, Juan Soto, Luis A. Villaescusa and Pedro Amorós. **Hybrid Materials with nanoscopic anion-binding pockets for the colorimetric sensing of phosphate in water using displacement assays**. *Chemical Communications*, **2008**, 3639-3641.

10. Maria Comes, M. Dolores Marcos, Ramón Martínez-Máñez, Félix Sancenón, Luís A. Villaescusa, Anja Graefe and Gerhard J. Mohr. **Hybrid functionalised mesoporous silica-polymer composites for enhanced analyte monitoring using optical sensors.** *Journal of Materials Chemistry,* **2008**, 18, 5815-5823.

11. Maria Comes, Elena Aznar, María Moragues, M. Dolores Marcos, Ramón Martínez-Máñez, Félix Sancenón, Juan Soto, Luis A. Villaescusa, Luis Gil, and Pedro Amorós. **Mesoporous Hybrid Materials Containing Nanoscopic "Binding Pockets" for Colorimetric Anion Signaling in Water by using Displacement Assays.** *Chemistry. A European Journal,* **2009**, 15, 9024-9033.

Content

CHAPTER 5. BIOMIMETIC "BINDING POCKETS" IN HYBRID ORGANIC-INORGANIC MATERIALS FOR DISPLACEMENT ASSAYS.

General objectives

The combination of the properties of organic and inorganic building blocks within a single material is particularly because of the possibility to combine the enormous functional variation of organic chemistry with the advantages of a thermally stable and robust inorganic substrate.

In this context, this thesis aims to develop organic-inorganic hybrid supports and explore their application in the field of the recognition and signaling of chemical species.

The general objectives of this project are,

- To prepare new hybrid organic-inorganic siliceous materials with different functionalizations to improve the selectivity and sensitivity of sensory system, to characterize their structure and study their properties.
- To test these materials in recognition and signaling protocols in the detection of chemical species.

Outline of this thesis

The present work thesis has been structured in different chapters:

- In the first chapter, there is an introduction about supramolecular chemistry applied to molecular recognition processes and some new concepts related to the preparation of novel "hetero-supramolecular" hybrid organic-inorganic materials for signaling applications.

- The second chapter describes the working plan designed for this thesis work.

- Third chapter includes in detail the different characterization techniques used for the exhaustive study of the novel hybrid materials synthesized in the present work.

- Chapter 4 and 5 contain works developed in this thesis that were gathered together taking into account the used sensing protocol. Chapter 4 includes four publications based on hybrid materials that used the chemodosimeter approach, whereas Chapter 5 includes two publications which take advantage of displacement assays.

- Chapter 6 includes general conclusions and some comments about future perspectives in this field.

Abbreviations

ADP	Adenosine Diphosphate
**BEA*	Zeolite Beta
AMS	anionic mesoporous surfactant
ATP	Adenosine Triphosphate
Azo	Azo pyridin derivative
BET	Brunauer, Emmett and Teller Model
BJH	Barret, Joyner and Halenda Model
CTAB	Hexadecyltrimethylammonium Bromide
DMF	dimethylformamide
DMSO	dimethylsulphoxide
DSC	differential scaning calorimetry
EA	elemental analysis
FAU	Faujasite
GMP	Guanosine monophosphate
HMDS	hexamethyldisilazane
HT	Hydrothermal treatment
IR	Infra Red
IZA	International Zeolite Association
LC	liquid crystal
LCT	liquid crystal templating
MCM	Mobile Crystalline Material
MeCN	acetonitrile
MFI	ZSM-5, Zeolite Socony Mobil-five
MHA	16-mercaptohexadecanoic acid
MPTMSA	N-methyl-N-propyl-3-(trimethoxisilyl)aniline
MS	Mass spectrometry
MSN	Mesoporous Silica Nanoparticles
NMR	Nuclear Magnetic Resonance
OFMS	Organic functionalised molecular sieves
OSDA	Organic structure-directing agent
PMOs	Periodic Mesoporous Organosilicas
pXRD	powder X-ray diffraction

$Ru(bipy)_3^{2+}$	Tris(2,2'bipyridyl)Ruthenium(II)
SAMs	self-assembled monolayer surfaces
SBA	Santa Barbara Amorphous Material
SDAs	structure directing agents
SEM	Scanning Electron Microscopy
SLC	silicatropic liquid crystal
SMPS	Silica Mesoporous supports
STEM	Scanning transmission electron microscopy
STEM-EDX	Scanning transmission electron microscopy-
TEA	tetraethylammonium
TEA+	tetraethylammonium cation
TEAH3	Triethanolamine
TEM	Transmission Electron Microscopy
TEOS	Tetraethylorthosilica
TFA	4-trifluorocetylazobenzene
TFAA	trifluoroacetylaniline
TGA	Termogravimetric Analysis
TMOS	tetramethylorthosilica
TPA+	tetrapropylammonium cation
UVM-7	Universidad Valencia Material
UV-vis	Ultraviolet-visible
VOC	volatile organic compounds
XRD	X-ray diffraction

Chapter 1

Introduction

1.1. Supramolecular chemistry.

Supramolecular Chemistry was defined by Jean-Marie Lehn[1] as the "chemistry of molecular assemblies and of the intermolecular bond". In other words, this may be expressed as "chemistry beyond the molecule"[2] and refers the area of the chemistry focused on the chemical systems made up by a discrete number of assembled molecular subunits or components. Other definitions of supramolecular chemistry are "the

[1] Lehn was awarded by the 1987 Nobel Prize for Chemistry shared with Donald J. Cram and Charles J. Pedersen in recognition of their work in this area.

[2] J.-M. Lehn, *Supramolecular Chemistry. Concepts and Perspectives*. VCH, **1995.**

chemistry of the non-covalent bond" and "non-molecular chemistry". While traditional chemistry centers its study on the covalent bond, supramolecular chemistry includes also the weaker and reversible noncovalent interactions between molecules (hydrogen bonding, metal coordination, hydrophobic forces, van der Waals forces, π-π interactions, halogen bonding and electrostatic and/or electromagnetic effects)

Originally supramolecular chemistry was defined in terms of the non-covalent interaction between a "host" and a "guest" molecule, as shown in Figure 1.1. which illustrates the relationship between molecular and supramolecular chemistry. In addition to the difference in the type of bonds used, supramolecular species are thermodynamically less stable, kinetically more labile, and dynamically more flexible than molecules.

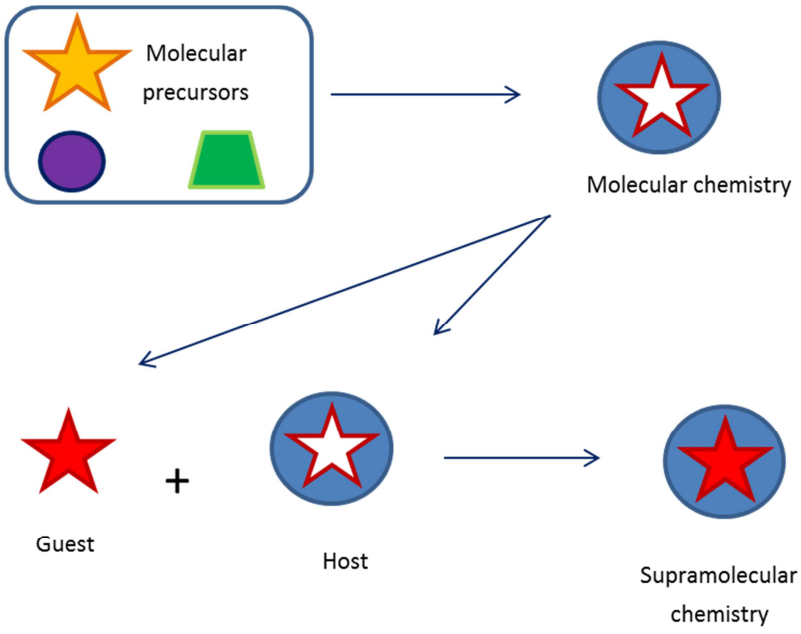

Figure 1.1. Comparision between the scope of molecular and supramolecular chemistry.

In the context of the Supramolecular chemistry, we generally consider a molecule (a "host") binding another molecule (a "guest") to produce a "host-guest" complex or supermolecule. Commonly the host is a large molecule or aggregate such as an enzyme or synthetic cyclic compound possessing a sizeable, central hole or cavity. The guest may be a monoatomic cation, a simple inorganic anion, an ion pair or a more sophisticated molecule such a hormone, pheromone or neurotransmitter. More formally, the host is defined as the molecular entity possessing *convergent* binding sites and the guest possesses *divergent* binding sites. In turn a binding site is defined as a region of the host or guest capable of taking part in a non-covalent interaction. The host-guest relationship has been defined by Donald Cramm (another Supramolecular Chemistry Nobel Laureate)[3] as *"…a host-guest relationship involves a complementary stereoelectronic arrangement of binding sites in host and guest…"*

In these host-guest interactions, there is an equilibrium between the unbound state, in which host and guest are separate from each other, and the bound state, in which there is a structurally defined host-guest complex. In order to rationally and confidently design synthetic systems that perform specific functions and tasks, it is very important to understand this thermodynamics of binding between host and guest.

$$H + G \rightleftarrows HG \qquad K_{eq}$$

H: "host", G: "guest", HG: "host-guest complex"

[3] Cram, D. J., Preorganisation –from solvents to spherands. *Angew. Chem., Int. Ed. Engl*. **1986**, 25, 1039-1134.

At this point, it is important to note, that the strength of the binding between a host and a guest is controlled by the intermolecular forces that both components could stablish. For improving the specificity, the degree of complexity should be higher to create an adequate host to accomplish the task. Precisely, this is the primary aim within supramolecular chemistry, the design and construction of supramolecular species from component units with specific properties which may be tailored to perform new functions depending on the desired application.

The effects resulting from molecular recognition are wide ranging. The physical characteristics of the supermolecule (formed upon host-guest interaction) can differ radically from that of either the substrate or receptor alone, with corresponding effects on reactivity, optical behavior, charge distribution, etc. "Information" in a supermolecule may be stored in multiple forms: in the architecture of the receptor, in its binding sites, and in the ligand layer surrounding the bound receptor. Depending on the characteristics of the supermolecule formed, this information may be observed directly (as in the case of fluorescence or a chemical reaction occurring) or may contribute to such secondary effects as reactivity, kinetic effects and so on.

1.2. Molecular recognition processes for sensing applications.

1.2.1. From receptors to molecular sensors.

Over the last years, have been noticed an important increment in the design of molecular receptors for their application in different areas of molecular recognition. One of them is that related with sensing. In order to achieve the detection of a selected guest, the receptor (or host) must

be functionalized with a reporter molecule. The underlying idea is that coordination of the guest with the receptor could change the physical or chemical properties of the reporter that could be detectable (signaling process). These supramolecular entities formed by receptors and reporters are called molecular sensors or chemosensors.

The concept of "signaling" refers to the transduction of a recognition event through changes of a certain physical property such as a shift or intensity change in colour, fluorescence, or a redox wave. Particularly, colour changes as signaling events have been widely used because it requires the use of inexpensive equipment or no equipment at all as colour changes can be detected by the naked eye.

A general approach for the development of chemical sensors is the coupling of, at least two units, each one displaying a precise function:

- The binding site, where resides the function of coordination to a certain molecule,
- And the signaling subunit, which translates the microscopic interaction between the binding site and the guest molecule into a measurable macroscopic signal (forexample colour or emission changes).

Many chemosensors displays change in either colour[4,5] or fluorescence[6] in the presence of a certain guest although change in electrochemical properties such as the oxidation potencial of redox active groups have

[4] Löhr, H.-G.; vögtle, F*. Acc. Chem. Res*. **1985**, 18,65

[5] Takagi, M; Ueno, K. *Top. Curr. Chem*. **1984**, 121, 39.

[6] Czarnik, A. W. *Acc. Chem. Res*. **1994**, 27, 302.

also been widely used.[7,8] In this sensing process, information at the molecular level, such as the presence or not of a certain guest in solution, is amplified to a macroscopic level; hence, sensing might open the door to the determination (qualitative or quantitative) of certain guests.

The development of molecular chemosensors has been especially important in the case of cation recognition process, mainly for alkaline and alkaline earth metal, using crown ethers as molecular receptors.[9] Anion recognition is also an important area of increasing research in supramolecular chemistry originated from the fundamental role that anions play in nature: biologically, chemically, biomedically and environmentally.[10] The development of abiotic receptors for anionic species has been extensively explored during the last 20 years, and several host molecules have been designed, synthesized and anion recognition studies investigated over the years. These include protonated polyamines, quaternary ammonium derived receptors, Lewis acidic centers, etc.[11]

---

[7] Beer, P. D. Chem. Commun. **1996**, 689.

[8] Beer, P. D. *Coord. Chem. Rev*. **2000**, 205, 131.

[9] (a) Valeur, B.; Leray, I. *Coord. Chem. Rev.* **2000**, 205, 3; (b) de Silva, P.; Gunaratne, H. Q. N.; Gunnlaugsson, T.; Huxley, A. J. M.; McCoy, C. P.; Rademacher, J. T.; Rice, T. E. *Chem. Rev.* **1997**, 97, 1515; (c) Yin, J.; Hu, Y.; Yoon, J. *Chem. Soc. Rev.* **2015**, 44, 4619; (d) Yeung, M. C.; Yam, V. W. *Chem. Soc. Rev.* **2015**, 44, 4192.

[10] Beer, P. D.; Gale, P. A. *Angew. Chem. Int. Ed.* **2001**, 40, 486.

[11] (a) Martínez-Máñez, R.; Sanceón, F. *Chem. Rev.* **2003**, 103, 4419; (b) Santos-Figueroa, L. E.; Moragues, M. E.; Climent, E.; Agostini, A.; Martínez-Máñez, R.; Sancenón, F. *Chem. Soc. Rev.* **2013**, 42, 3489; (c) Gale, P. A.; Caltagirone, C. *Chem. Soc. Rev.* **2015**, 44, 4212.

Three main approaches have been used for the development of optical chemosensors, namely (i) binding site-signaling subunit, (ii) displacement and (iii) chemodosimeter. The main differences in the three approaches are related with the spatial disposition of the binding sites and signaling subunits. Binding sites and signaling units can be covalently linked (binding site-signaling subunit approach) or not (displacement approach). In both approaches the guest coordination and the change in color or fluorescence are in principle reversible. In addition to these approaches, analyte detection by fluorescence or color changes can also be observed using irreversible reactions. In this case, the term chemosensor should not strictly be applied and it should be used terms such as reagents, reactants, or chemodosimeters.

1.2.2. Optical molecular sensors.

1.2.2.1. Binding site-signaling subunit approach.

The vast majority of chemosensors were constructed using this paradigm in which the binding site and the signaling subunit are linked through the formation of covalent bonds (see Figure 1.2).[12]

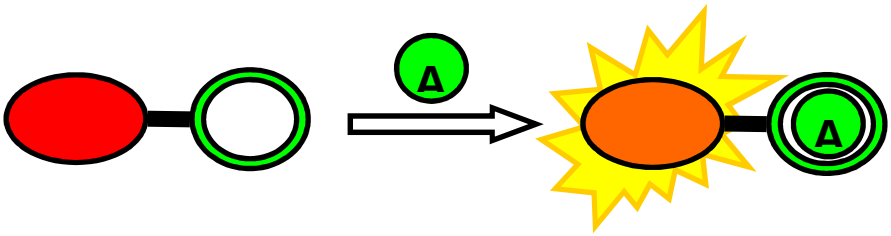

Figure 1.2. Anion chemosensor based on the binding site-signaling subunit approach.

[12] Bissell, R. A.; de Silva, P; Gunaratne, H.Q. N.; Lynch, P. L. M.; Maguire, G. E. M.; Sandanayake, K. R. A. S. *Chem. Soc. Rev*. **1992**, 187.

As can be seen in Figure 1.2., the coordination site binds an anion in such a way that the properties of the signaling subunit are changed giving rise to variations either in the color (chromogenic chemosensor) or in its fluorescence behavior (fluorogenic chemosensor). The chemosensors prepared using this approach requires a significant synthetic effort because the binding site and the signaling subunit must be linked in such a way that the properties of the latter changes upon coordination of the guest with the former. Besides, one important drawback of the chemodosimeters constructed under this paradigm is the fact that many of them only work in organic solvents or in water-organic solvent mixtures. In spite of these facts, this approach has been the most commonly used for the designd of chemosensors.

1.2.2.2. Displacement approach.

In the case of displacement approach, the binding site and the signaling subunit are not covalently attached but form a coordination complex (molecular ensemble). Then when a target molecule interacts with the binding site induced a displacement reaction. The binding site coordinates the target molecule whereas the signaling subunit is displaced to the solution retrieving its non-coordinated spectroscopic behavior (as is schematized in Figure 1.3).[13]

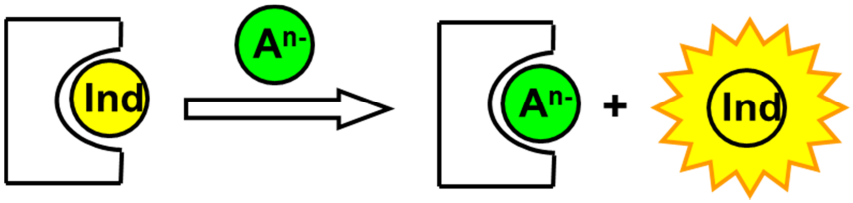

Figure 1.3. Anion chemosensors based on the displacement approach.

[13] Wiskur, S. L.; Aït-Haddou, H.; Lavigne, J.J.; Anslyn, E. V. *Acc. Chem. Res.* **2001**, 34, 963.

If the spectroscopic characteristics of the signaling subunit in the molecular ensemble are different to those in its no-coordinated state, then the displacement process is coupled to a signaling event. As it can be inferred, the stability constant for the formation of the complex between the binding site and the signaling subunit has to be lower than that between the binding site and the target molecule. Additionally, selectivity can be achieved by choosing an indicator-binding site coupled with a formation stability constant larger than that between the signaling unit and the potentially interfering species.

This approach has some advantages over the binding site-signaling subunit, as for instance, the noncovalent anchoring binding sites and indicator groups allows a large number of combinations to be tested with minimum effort in order to obtain tuned sensing systems. Also, the sensing ensembles used usually worked in water opening the possibility of application in real detection protocols.

1.2.2.3. Chemodosimeter approach.

This approach involves the use of specific chemical reactions (usually irreversible) induced by the presence of target molecules that are coupled to a color or emission variation.[14] If the chemical reaction is irreversible, the use of the term chemosensor can not strictly be used and we will refer to these systems as chemodosimeters or chemoreactants. Figure 1.4. shows schematically two examples, one in

[14] (a) Chae, M. –Y; Czarnik, A. W. *J. Am. Chem. Soc*. **1992**, 114, 9704; (b) Dujols, V.; Ford, F.; Czarnik, A. W. *J. Am. Chem. Soc., Perkin Trans. 1* **2000**, 3155; (c) Yang, Y.; Zhao, Q.; Feng, W.; Li, F. *Chem. Rev.* **2013**, 113, 192; (d) Chen, X.; Zhou, Y.; Peng, X.; Yoon, J. *Chem. Soc. Rev.* **2010**, 39, 2120.

which the molecule reacts with the chemodosimeter remaining covalently bonded to the product and the other in which the molecule catalyzes a chemical reaction. In those examples, as the final compounds are chemically different to the original one, the spectroscopic characteristics should change, allowing detection of the molecule guest.

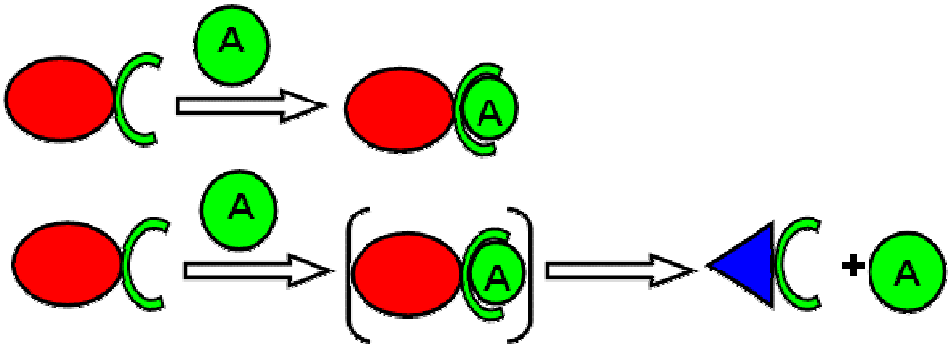

Figure 1.4. Chemodosimeters or chemoreactands. In the first sequence, the analyte reacts with the chemodosimeter and remains covalently attached, and in the second sequence, the analyte catalyzes a chemical reaction.

The underlying idea of these irreversible systems is to take advantage of the selective reactivity that certain molecules may display. Hence, the use of molecule-induced reactions has advantages as the high selectivity usually reached and also an accumulative effect that is related with the molecule concentration.

1.3. Hybrid materials for molecular recognition process.

As stated above chemosensors usually have several limitations when applied to real recognition protocols:

- Sometimes requires extensive and time-consuming synthetic efforts to finally obtain somewhat complex receptors for

improving the selectivity and discrimination of similar target molecules.

- In the case of the displacement approach, one restriction is that the spectroscopic characteristics of the indicator in the molecular ensemble must be different to those in its non-coordinated form.
- Targeting small organic molecules for which no artificial recognition motif is easily available is also a serious drawback.

In an attempt to overcome these above cited limitations, new concepts related to the preparation of novel "hetero-supramolecular" hybrid organic-inorganic materials for signaling applications have been studied recently.[15] As we will see below, these hybrid ensembles usually take advantage of the merging of inorganic materials with classical supramolecular principles, often resulting in an improved selectivity and sensitivity compared with the free, molecular hosts. By using this simple concept many hybrid materials for the recognition of anions,[16] cations[17]

[15] (a) Descalzo, A. B.; Martínez-Máñez, R.; Sancenón, F.; Hoffmann, K.; Rurack, K. *Angew. Chem. Int. Ed.* **2006**, 45, 5924; (b) Martínez.Máñez, R.; Sancenón, F.; Hecht, M.; Biyical, M.; Rurack, K. *Anal. Bioanal. Chem.* **2011**, 399, 55; (c) Biyical, M.; Hecht, M.; Martínez-Máñez, R.; Rurack, K, Sancenón, F. *Supramol. Chem.* **2012**, 3669.

[16] Descalzo, A. B.; Jiménez, D.; Marcos, M. D.; Martínez-Máñez, R.; Soto, J.; El Haskouri, J.; Guillem, C.; Beltrán, D.; Amorós, P.; Borrachero, M. V. *Adv. Mater.* **2002**, 14, 966; (b) Beer, P. D.; Cormode, D. P.; Davis, J. J. *Chem. Commun.* **2004**, 414.

[17] (a) El-Safty, S. A.; Prabhakaran, D.; Ismail, A. A.; Matsunaga, H.; Mizukami, F. *Chem.* Mater. **2008**, 20, 2644; (b) El-Safty, S. A.; Prabhakaran, D.; Yoshimichi, Y.; Mizukami, F. *Adv. Funct. Mater.* **2009**, 18, 1739; (c) El-Safty, S. A.; Ismail, A. A.; Matsunaga, H.; Nanjo, H.; Mizukami, F. *J. Phys. Chem. C* **2008**, 112, 4825.

or neutral species[18] has been described recently. Besides, this approach allows the creation of hybrid sensing ensembles to target analytes for whose selectivity is difficult to achieve by conventional methods.

Several factors should be taken into account in order to prepare hybrid organic-inorganic sensory materials:

1. Preorganization is one of the key concepts in supramolecular chemistry, and thus, in molecular recognitions processes. It determines the tendency of a host molecule and its coordination sites to assume a conformation that is ideally suited to bind a guest molecule, leading a complex with increased stability. Increased preorganization can also be achieved by immobilizing (simple) ligands on solid supports such as porous nanoparticles, whether bulk or mesoporous, or other nanostructured solids.

   In some specific cases, for instance the ones observed for spherical of both gold and silica nanoparticles, recognition characteristics are improved due to the reduction of conformational flexibility of the hosts on solid supports, behavior termed as *the surface chelate effect*. This thermodynamic effect of the enhancement of classical recognition features is basically due to entropic factors related with the pre-organization of the coordination sites on the surface that reduce the conformational flexibility of the receptors and increase their effective concentration at the surface. This results in a remarkable improvement of the recognition characteristics. From a molecular viewpoint, surface functionalization creates a multidentate

[18] (a) Boal, A. K.; Rotello, V. M. *J. Am. Chem. Soc.* **2000**, 122, 734; (b) Boal, A. K.; Rotello, V. M. *J. Am. Chem. Soc.* **1999**, 121, 4914.

coordination environment that displays a statistical advantage in relation to coordination when compared to the molecular receptor.

A pioneering study introducing the principle of enhanced recognition through pre-organization of a self-assembled monolayer of thiol-functionalized ligands on gold nanoparticles was reported by Major and Zhu, who investigated the formation of Cu^{2+} complexes with SAMs of 16-mercaptohexadecanoic acid (MHA) on gold surfaces in relation to using molecular mono- and bidentate carboxylates.[19] The authors found that the formation constant for the Cu^{2+} complex with the pre-arranged MHA was 119 times greater than with succinic acid, and 213 times greater than with glutaric acid in aqueous solutions. Since bidentate ligands generally form more stable complexes than monodentate ligands, the authors proposed that the monodentate MHAs are pre-organized on the "flat" gold surface and act as a multidentate coordinating layer, able to form a more stable Cu^{2+} complex than bidentate carboxylates (see Figure 1.5).

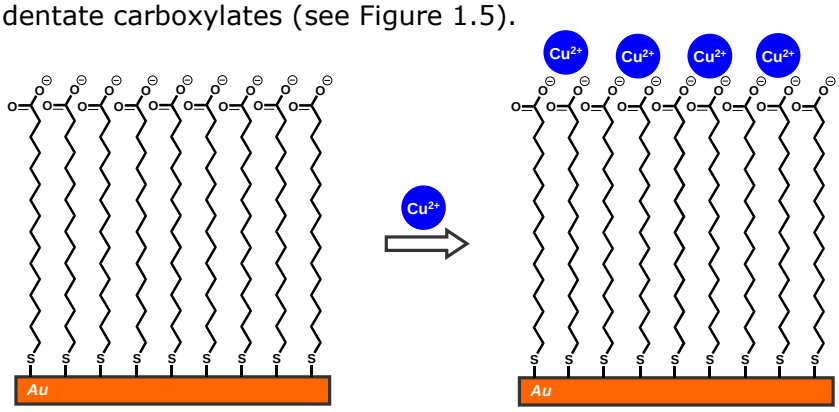

Figure 1.5. Schematic illustration of the surface chelate effect. Adapted from *Angew. Chem. Int. Ed*. **2006**, 45, 5924-5948.

[19] Major, R. C.; Zhu, X. –Y. J. Am. Chem. Soc. 2003, 125, 8454.

Something similar has been reported for coordinating dendrimers that show a "positive dendritic effect," which is related to the capability of dendrimers to achieve a better recognition as the generation of the dendrimer increases.[20] The ability to show enhanced coordination is at the heart of the basic concept of supramolecular chemical amplification; the step from the molecule itself to the hetero-supramolecular ensemble thus results in new properties, which are not simply an extrapolation of the solution conduct to the surface, but to its own unique features.

2. However, the simple enhancement of the coordination, which is driven by the "surface chelate effect," is not sufficient for the development of sensing protocols, and the recognition process must be coupled with a signaling event. In order to translate this approach into a more modular or even combinatorial system design, several researchers began to anchor binding sites and signaling units independently in close proximity to the surface, hoping for additional cooperative effects. If the distance between a receptor site and its next-neighbour fluorophores is close enough, long-range processes such as electron or energy transfer should still be operative and all signaling units within the active interaction distance might funnel their energy to the bound receptor. This approach also permits to adjust the ratio of grafted ligand to grafted fluorophore in a straightforward manner if for instance different concentration ranges have to be assessed in different analytical applications. In addition to modularity, such an approach would also overcome synthetic problems connected

[20] D. Astruc, M.-C. Daniel, J. Ruiz*, Chem. Commun.,* **2004***,* 2637–2649.

to the conventional preparation of complex receptors. Among the first to establish this strategy were Tecilla and Tonellato.[21] They developed a fluorescent sensor for Cu^{2+} using silica nanoparticles functionalized with both ligands for the selective coordination of Cu^{2+} and fluorescent dyes which can be quenched in the presence of the paramagnetic guest. This comparatively simple system indeed allowed the detection of Cu^{2+} concentrations down to the nanomolar level in DMSO-water solutions. The authors demonstrated that coordination of a single metal ion led to the quenching of up to 10 fluorescent groups, i.e., to amplified signaling (Figure 1.6).

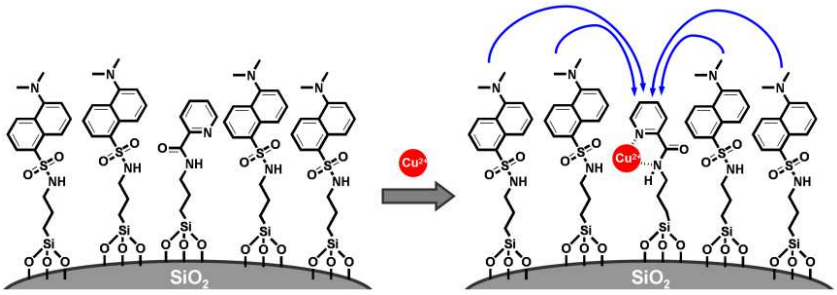

Figure 1.6. Cu^{2+}-amplified quenching of dansylated silica nanoparticles. Adapted from *Angew. Chem. Int. Ed.* **2006**, 45, 5924-5948.

3. Finally, polarity and size are two essential parameters in supramolecular chemistry for host-guest interactions as well. The combination of inorganic nanostructured or porous supports with organic functions is especially suitable for such purposes, because the former determining size control and the latter governing polarity features.

[21] (a) Rampazzo, E.; Brasola, E.; Marcuz, S.; Mancin, F.; Tecilla, P.; Tonellato, U. *J. Mater. Chem.* **2005**, 15, 2687; (b) Brasola, E.; Mancin, F.; Rampazzo, E.; Tecilla, P.; Tonellato, U. *Chem. Commun.* **2003**, 3026.

1.4. Hybrid organic-inorganic porous materials.

The term "hybrid" is used in the specific case of the hybrid organic-inorganic porous siliceous materials to mean those hybrid materials that are constituted by organic components or networks intimately mixed at the molecular level with a porous siliceous skeleton.

Depending on the interactions between the organic and the inorganic part, hybrid silica materials can be divided into two families[22]:

a) materials, in which either the organics are entrapped (or embedded) in the inorganic matrix without any interaction or the organic and inorganic components are linked together through non-covalent weak bonds such as van der Waals, hydrogen bond, hydrophobic or ionic interactions.

These hybrid materials can be synthesized by (i) adsorption of the organic species into the pores of the support or (ii) construction of the organic molecules piece by piece within the confines of cavities of the support (the "ship-in-bottle" technique) as is represented in the figure 1.7.

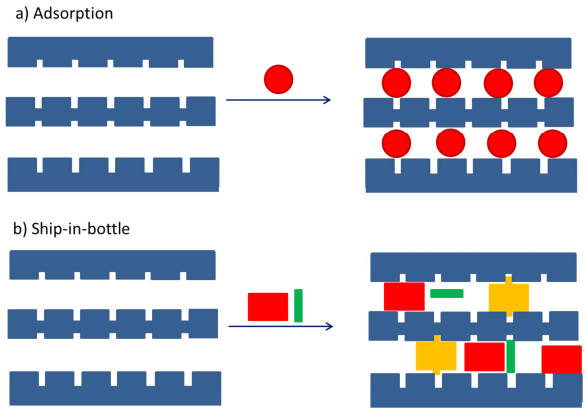

Figure 1.7. Organic functionalization of the inorganic matrix by a) adsorption and b) ship-in-bottle technique.

[22] Sanchez, C; Ribot, F. *New J. Chem.*, **1994**, 18, 1007.

Following the strength of these interactions, the two phases of these materials can be separated by classical techniques such as extraction of the organics with an organic solvent.

b) materials, in which the organic and inorganic components are linked together through strong covalent or iono-covalent chemical bonds (Figure 1.8.) As a result, they form a unique continuous phase whose components can not be separated by analytical methods.

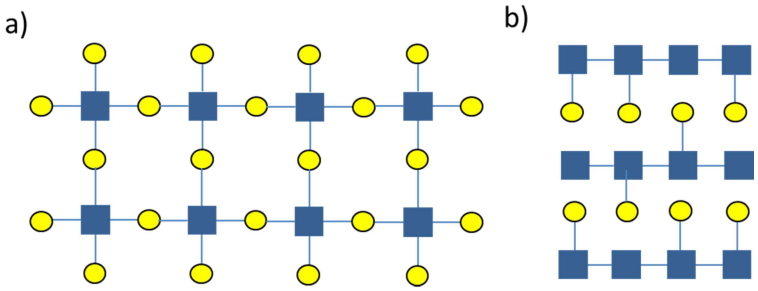

Figure 1.8. Organic functionalization of the inorganic matrix by covalent bond, a) as a part of the inorganic matrix or b) organic modification of the pore structure or surface. The squares and the circles denote the inorganic and organic components respectively.

If the hybrid organic-inorganic porous materials are used in supramolecular applications, the **organic moiety** should provide useful molecular receptor groups to the hybrid material capable to carry out the molecular recognition process and the **inorganic structure** must be selected according to the properties that we would like to ensure (porous-size, channels, cages, more/less hydrophobicity, etc.) in the final hybrid organic-inorganic material.

Siliceous-porous matrices present some advantatges, as is the varied distribution of sizes, shapes and volumes of the void spaces that directly relates to their ability to act as an active part in the supramolecular recognition process. In addition, its stability over a fairly wide range of pH (excluding alkaline), relative inertness in many environments, and transparency in the UV-visible spectrum are also some important characteristics.

Obviously, the versatilitiy in choosing the organic moiety and the fine tune of the inorganic structure allows one to control the properites of the materials and to optimize them for a specific guest recognition process.

1.4.1. Porous materials.

The development of porous materials with large specific surface areas have been since decades a field of extensive research, particularly with regard to potential applications in areas such as adsorption, chromatography, catalysis, drug delivery and sensor technology.

According to the international Union of Pure and Applied Chemistry (IUPAC), pore sizes are classified into three main categories, namely micropores, mesopores and macropores characterized by pore sizes less than 2 nm, between 2 and 50 nm, and larger than 50 nm respectively.[23]

In figure 1.9. the pore diameter of three representative classes of silica materials with micro-, meso- and macropores are despicted.

[23] a) G. Zhao, *J. Mater. Chem.*, **2006**, 623. b) D. Schaefer, *MRS Bulletin*, **1994**, *14*, 6.

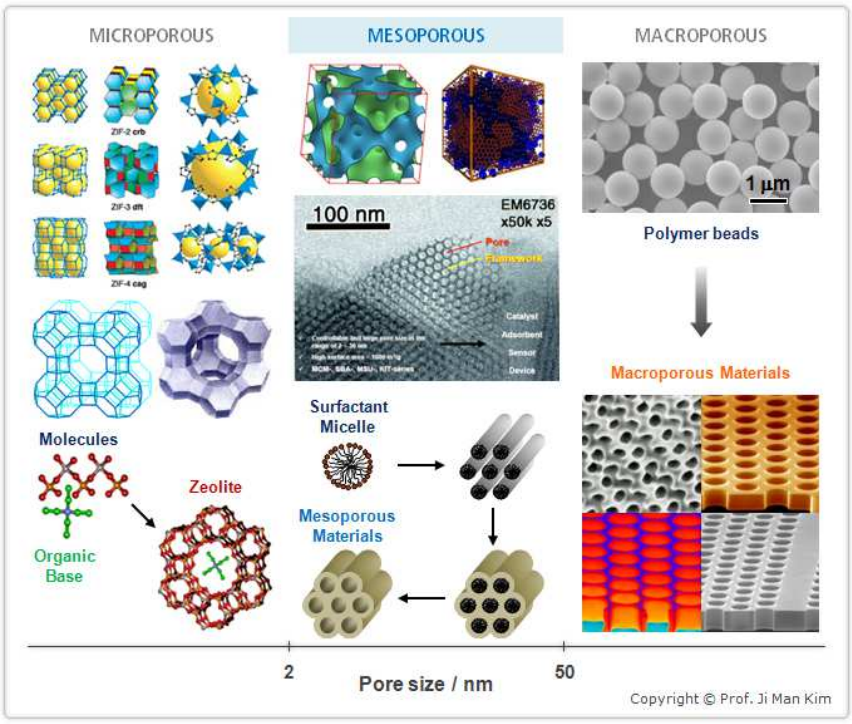

Figure 1.9. Classification of the porous materials by their pore size. (International Union of Pure and Applied Chemistry) Reference: *Pure and Applied Chemistry*, 1994, **66**, 1739-1758. Copyright © Prof. Ji Man Kim.

1.4.1.1. Synthesis of mesoporous materials.

Mesoporous materials are characterized by very large specific surface areas, ordered pore systems and well-defined pore radius distributions, and exceed zeolite molecular sieves (within the range 2-10 nm). An upsurge in the use of mesoporous materials for applications in areas such as adsorption, chromatography, catalysis, etc. began in 1992 with the development by the Mobil Oil Company of the class of periodic

mesoporous silicas known as the M41S phase[24,25,26,27]. The most well-known representatives of this class include the silica solids MCM-41 (with a hexagonal arrangement of the mesopores), MCM-48 (with a cubic arrangement of the mesopores) and MCM-50 (with a laminar structure). See figure 1.10.

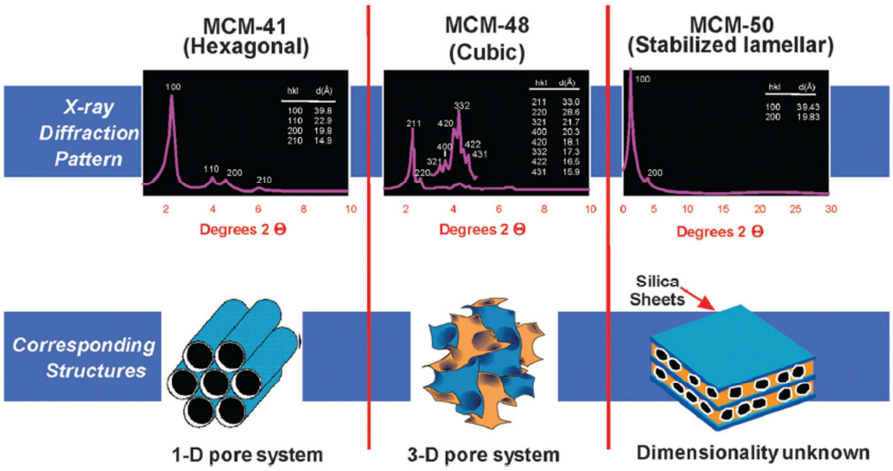

Figure 1.10. Scheme of the M41S family of mesoporous molecular sieves, including MCM-41, MCM-48 and MCM-50. *(Reprinted with permission from C. T. Kresge and W. J. Roth, Chem. Soc. Rev., 2013, 42, 3663. Copyright © 2013 The Royal Society of Chemistry).*

---

[24] C. T. Kresge, M. E. Leonowicz, W. J. Roth, J. C. Vartuli and J. S. Beck, *Nature*, **1992**, *359*, 710.

[25] C. T. Kresge, M. E. Leonowicz, W. J. Roth and J. C. Vartuli, Synthetic Mesoporous Crystalline Material, US Patent 5,098,684, March 24, **1992.**

[26] C. T. Kresge, M. E. Leonowicz, W. J. Roth and J. C. Vartuli, Synthetic Porous Crystalline Material, Its Synthesis, US Patent 5,102,643, April 7, **1992.**

[27] J. S. Beck, J. C. Vartuli, W. J. Roth, M. E. Leonowicz, K. D. Schmidt, C. T. W. Chu, D. H. Olson, E. W. Sheppard, S. B. McCullen, J. B. Higgins and J. L. Schlenker, *J. Am. Chem. Soc.*, **1992**, *114*, 10834.

Ordered mesoporous materials, based on MCM-41 (Mobile Crystalline Material), are silicates with remarkable features such as pores with well-defined sizes and uniform shapes that are ordered to yield arrays of non-intersecting channels in a hexagonal arrangement. The walls of the channels are amorphous SiO_2 and the porosity can be as high as 80% of their total volume[28].

The use of alkoxysilanes as inorganic precursor (normally tetraethyl- (TEOS) or tetramethylorthosilica (TMOS))[29] (i) provides monomeric Si species in a uniform distribution from the start of the sol-gel process and (ii) makes room-temperature processing possible, enabling the addition of organic moieties if we would like to prepare a hybrid material. The kinetics are influenced by various factors, like (i) the activities of H^+or OH^- in acidic or basic solutions, (ii) the type of organic solvent, (iii) the H_2O/TEOS ratio, or (iv) the nature of the alkoxy group in the precursor.

Polymerization of silica precursors occurs via hydrolysis and condensation reactions; the hydrolysis reaction replaces the alkoxide groups (OR) with hydroxyl groups (OH) to produce silanol groups (≡Si-OH) and subsequent condensation reactions involving the silanol groups lead to siloxane bonds (≡Si-O-Si≡). The detailed reaction mechanisms under a) acidic conditions and b) basic conditions are represented in the follow figure 1.11:

[28] Monnier, A.; Schüth, F.; Huo, Q.; Kumar, D.; Margolese, D.; Maxwell, R.S.; Stucky, G.D.; Krishnamurty, M.; Petroff, P.; Firoouzi, A.; Janicke, M.; Chmelka, B.F. *Science ,* **1993**, *261*, 1299–1303.

[29] G. S. Attard, J. C. Glyde, C. G. Göltner, *Nature* **1995**, 378, 366-368.

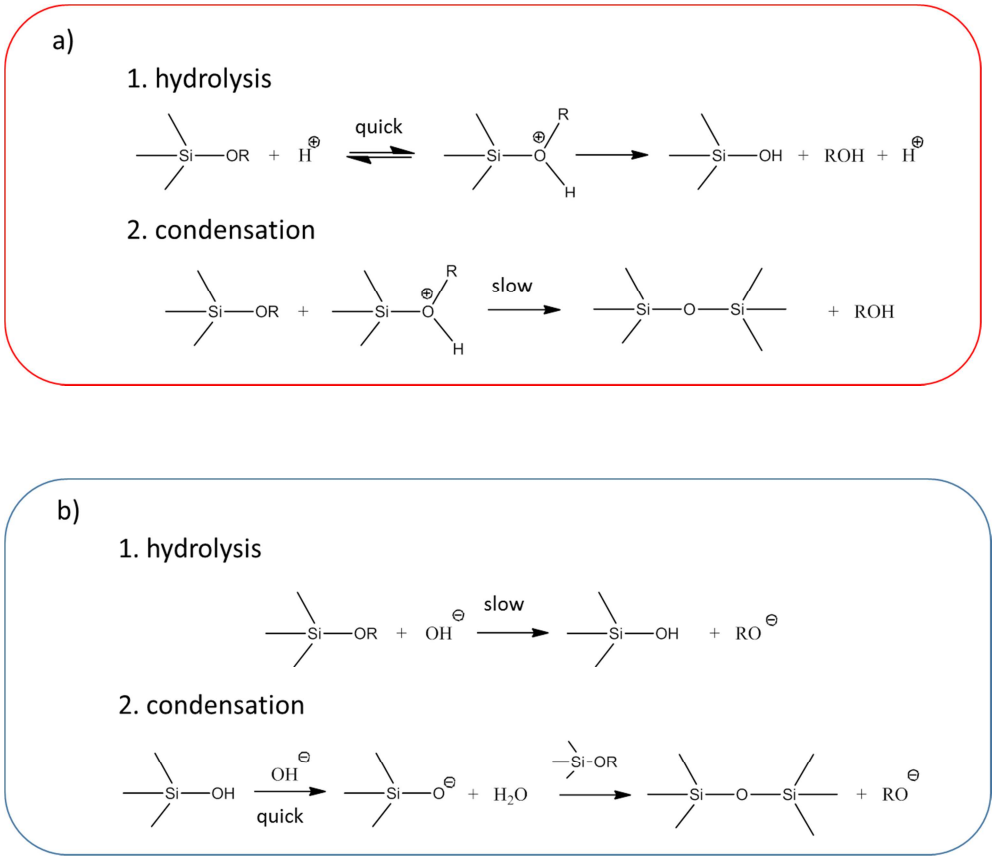

Figure 1.11. Hydrolysis and condensation reactions under a) acid conditions and b) basic conditions.

The ratio of the rate constants of hydrolysis and condensation determines the size and nature of the polycondensate structures in the sol, e.g., the length of linear chains, the degree of branching, or the density. Consequently, the physical properties of the gels depend on these polycondensate structures and their degree of crosslinking.[30]

[30] U. Schubert y N. Hüsing, *Synthesis of inorganic materials*; Wiley-VCH, **2005.**

In the preparation of the mesoporous structures, it is used as a template a surfactant molecule (specie with at least two parts: a hydrophilic (head group) and hydrophobic (tail)), also called structural director agents, SDA. Surfactants have two fundamental characteristics, a) the tendency to accumulate at an interface (e.g. water-air) and b) their tendency to form aggregates in a solution called micelles. The formation of micelles reduces the free energy of the system since the monomers absorb at the interface by rearranging hydrophobic groups in contact with the water. The formation of micelles depends on the concentration of the surfactant in the solution, and the limit at which the micelles start to form is called the critical micellar concentration (CMC). Surfactants in a lyotropic system can form different liquid crystal (LC) phases including isotropic micellar, micellar cubic, hexagonal columnar, bicontinuous cubic, lamellar, and reversed micelle phases depending on the concentration and temperature of the system.

Another fundamental condition for this method is that an attractive interaction between the template and the silica precursor is produced to ensure the inclusion of the structure director without phase separation taking place. Depending of the polarity of the head group, surfactants are classified as anionic, cationic, non-ionic (neutral) and zwitterionic. The diferent interactions that can take place between the inorganic components and the head groups of the surfactants according to the suggestion of Huo et al. are:[31]

[31] Q. Huo, D. I. Margolese, U. Ciesla, P. Feng, T.E. Gier, P. Sieger, R. Leon, P. M. Petroff, F. Schüth, G. D. Stucky, *Nature* **1994**, 368, 317-321; Q. Huo, D. I. Margolese, U. Ciesla, D. G. Demuth, P. Feng, T.E. Gier, P. Sieger, A. Firouzi, B. F. Chmelka, F. Schüth, G. D. Stucky, *Chem. Mater*. **1994,** 6, 1176-1191.

a) If the reactions take place under basic conditions (where the silica species are present as anions) and cationic quaternary ammonium surfactants are used as the SDA, the synthetic pathway is termed S^+I^- (S for designed surfactant species and I for designed inorganic species) as is schematized in a) in the Figure 1.12.

b) If the reactions take place under acidic conditions, whereby the silica species are positively charged, the interaction with the cationic surfactant and the silica species needs a mediator ion X^- (usually a halide) as is schematized in b) in the Figure 1.12. This pathway is designed as $S^+X^-I^+$. See b)

c) If a negatively charged surfactants are used as the SDA, it is possible to work in basic media, whereby again a mediator ion M^+ must be added to ensure interaction between the equally negatively charged silica species. The synthetic pathway is designed as $S^-M^+I^-$, as is shown in the Figure 1.12 c).

d) In the case of the acidic media, the mediator ion is not required. This pathway is designed as S^-I^+ and is schematized in the section d) of the Figure 1.12.

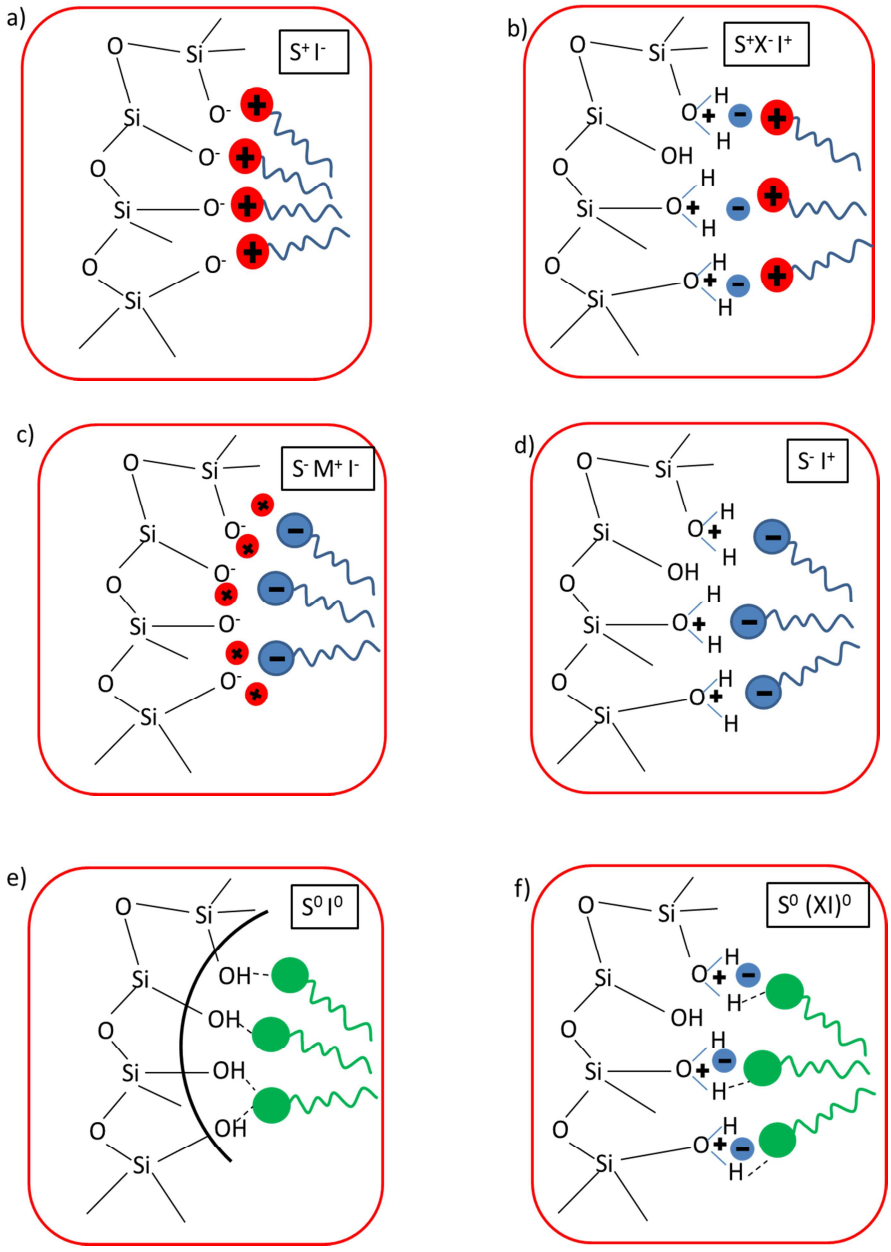

Figure 1.12. Interactions between the inorganic species and the head group of the surfactant with the consideration of the possible synthetic pathway in acidic and basic media.

Moreover, is still possible use a non-ionic structure director, whereby uncharged silica species (S^0I^0) or ion pairs ($S^0(XI)^0$) can be present. The attractive interactions are mediated through hydrogen bonds. See Figure 1.12 e) and f).

A large number of studies have been carried out to investigate the mechanism of formation of surfactant-templated mesoporous materials. Firstly, scientists in Mobil Corporation proposed two models, namely[32]: (a) the liquid crystal templating (LCT) mechanism and (b) the co-operative mechanism (see Figure 1.13)

In the LCT model, surfactants initially form pre-defined lyotropic liquid crystalline phases followed by the migration and polymerization of the inorganic silicate species. In the co-operative mechanism, surfactants and silicate species co-assemble to form an organic-inorganic mesostructure. The LCT mechanism is limited by the surfactant concentration, as is the case of the mesoporous materials, which should be formed only above the critical micellar concentration (CMC) of the particular surfactant. Davis et al[33] proposed a new mechanism where the formation of an ordered liquid crystal phase is not a prerequisite for the formation of an ordered mesostructured and different structures can be accessible by various synthesis precursors and conditions, even when the surfactant concentration is below its corresponding critical micellar concentration, CMC.

---

[32] J. S. Beck, J. C. Vartuli, W. J. Roth, M. E. Leonowicz, C. T. Kresge, K. D. Schmitt, C. T. W. Chu, D. H. Olson, E. W. Sheppard, S. B. McCullen, J. B. Higgins and J. L. Schlenker, *J. Am. Chem. Soc.*, **1992**, 114, 10834.

[33] C.-Y. Chen, S. L. Burkett, H.-X. Li and M. E. Davis, *Microporous Mater.*, **1993**, 2, 27-34

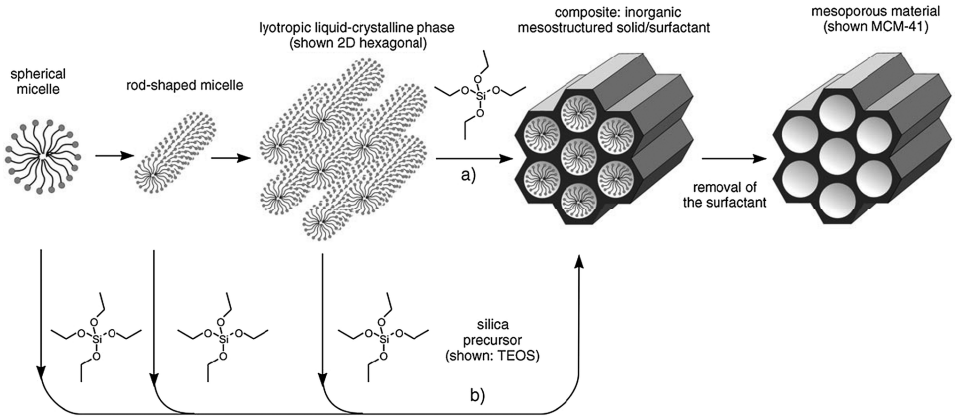

Figure 1.13. Formation of mesoporous materials by structure-directing agents: a) liquid-crystal templating mechanism, b) co-operative mechanism.

Davis et al[33] suggested that randomly ordered rod-like organic micelles interact with silicate species to yield two or three monolayers of silica encapsulated aroung the external surfaces of the micelles. Subsequent polymerization of silicates leads to a hexagonal structure analogous to MCM-41. The co-operative mechanism was further developed by Stucky *et al*, who proposed a silicatropic liquid crystal (SLC) mechanism.[34] The SLC mechanism was explained on the basis of (1) ion-exchange between surfactant halide counterions and silicate anions, (2) a true cooperative self-assembly of the silicates and surfactants leading to a liquid-crystal-like mesophase, followed by (3) condensation of the silicate species giving the desired mesoporous structure. In the co-

[34] A. Firouzi, D. Kumar, L. M. Bull, T. Besier, P. Sieger, Q. Huo, S. A. Walker, J. A. Zasadzinski, C. Glinka, J. Nicol, D. Margolese, G. D. Stucky and B. F. Chmelka, *Science*, **1995**, 267, 1138-1143.

operative templating mechanism,[35,36,37] the degree of ionization of the silicate species and its hydrolysis and condensation rates influence the ordering of the surfactant micelles in the solution, directing them towards the desired liquid crystal phase. The key aspect is the interaction between silicate species and surfactants; charge matching is an important parameter for achieving the desired of mesostructured.

The formation of the pore structures depends on the synthesis conditions such as temperature, reaction time, pH, solvents, silica/surfactant ratio, hydrothermal treatment (HT) and drying/calcination routes.[38,39,40,41] Synthesis pH and hydrothermal treatment are the common parameters that induce phase transformation, and the maintenance of structures with high porosity requires careful removal of solvents to avoid pore collapse via the high surface tensions in the capillaries.

---

[35] A. Firouzi, D. Kumar, L. M. Bull, T. Besier, P. Sieger, Q. Huo, S. A. Walker, J. A. Zasadzinski, C. Glinka, J. Nicol, D. Margolese, G. D. Stucky and B. F. Chmelka, *Science*, **1995**, 267, 1138-114.

[36] Q. S. Huo, D. I. Margolese, U. Ciesla, D. G. Demuth, P. Y. Feng, T. E. Gier, P. Sieger, A. Firouzi, B. F. Chmelka, F. Schuth and G. D. Stucky, *Chem. Mater.*, **1994**, 6, 1176-1191.

[37] Q. S. Huo, D. I. Margolese, U. Ciesla, P. Y. Feng, T. E. Gier, P. Sieger, R.Leon, P. M. Petroff, F. Schuth and G. D. Stucky, *Nature*, **1994**, 368, 317-321.

[38] A. F. Gross, V. H. Le, B. L. Kirsch, A. E. Riley and S. H. Tolbert, *Chem. Mater.*, **2001**, 13, 3571-3579.

[39] A. F. Gross, S. Yang, A. Navrotsky and S. H. Tolbert, *J. Phys. Chem. B*, **2003**, 107, 2709-2718.

[40] S. H. Tolbert, C. C. Landry, G. D. Stucky, B. F. Chmelka, P. Norby, J. C. Hanson and A. Monnier, *Chem. Mater.*, **2001**, 13, 2247-2256.

[41] M. T. Anderson, J. E. Martin, J. G. Odinek and P. P. Newcomer, *Chem. Mater.*, **1998**, 10, 311-321.

Ordered mesoporous structures can be classified according to their structural dimensions and pore geometry:

- Structures (2D- or 3D-) with cylindrical pores such as MCM-48, AMS-6, FDU-5, AMS-10, MCM-41 and SBA-15 that possess uniform diameters. (Figure 1.14 (a), (b))
- Structures (3D-) with interconnected cage type pores such as FDU-1, FDU-12, SBA-16, SBA-1, SBA-6, SBA-2, SBA-12 and AMS-8 consist of spherical or ellipsoidal cages that are 3D connected by smaller cage-connecting pores called windows. These mesocaged materials possess features of both the microporous domain in the form of narrow windows and mesoporous voids in the form of cages. ((Figure 1.14 (d), (e))

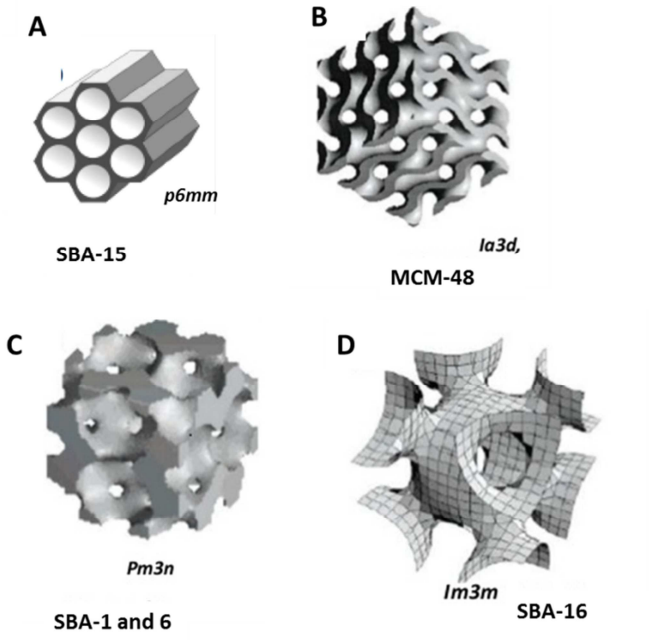

Figure 1.14. Some representative porous geometries of mesoporous structures, a) 2D hexagonal, b) bicontinous cubic, c) cage type *Pm3n* and d) cage type *Im3m*.

In the current work, we have employed mesoporous MCM41-type material UVM-7[42], which consists of small (12-17 nm), soldered, mesoporous particles that generate a bimodal pore system of 3.0-3.2 nm surfactant mesoporous and 20-70 nm textural pores. This bimodal pore system can offer different advantages:

- The textural porosity facilitates the movement of the active species through the solid.
- Presents a very large specific surface area of over 1100 m^2/g.
- And its synthetic conditions permit the inclusion of an organic precursor in the synthesis gel.

1.4.1.2. Synthesis of microporous crystalline materials

Zeolites are members of a large family of crystalline aluminosilicates containing pores and cavities of molecular dimensions (2-12 Å). The term zeolite comes from the Greek words for boil and stone. Many of them occur as natural minerals, and 229 framework type codes have been assigned to date[43] (176 of these appear in the 6th edition of the *Atlas of Zeolite Framework Types* and 53 additional codes have since been approved). It is the synthetic varieties which are among the most widely used sorbents, catalysts and ion-exchange materials in the world.

Strictly defined, zeolites are aluminosilicates with tetrahedrally-connected framework structures based on corner-sharing aluminate (AlO_4) and silicate (SiO_4) tetrahedral. Conceptually, they may be considered as pure silica frameworks with Si substituted by Al. This

[42] J. El Haskouri, D. Ortiz de Zárate, C. Guillem, J. Latorre, M. Caldés, A. Beltrán, D. Beltrán, A. B. Descalzo, G. Rodríguez-López, R. Martínez-Máñez, M. D. Marcos, and P. Amorós, *Chem. Commun*. **2002**, 4, 330.

[43] http://www.iza-structure.org/

$Al^{3+} \Leftrightarrow Si^{4+}$ substitution gives an overall negative charge to the framework. This is balanced by the presence of extra-framework charge-balancing cations located within the pore space, coordinated to framework O atoms, which is also able to take in neutral atoms and molecules small enough to enter via the pore windows.

A simplified empirical formula for an aluminosilicate zeolite is

$$M^{n+}_{x/n} Al_x Si_{1-x} O_2 \cdot_y X$$

where x can vary from 0-0.5 and M^{n+} represents inorganic or organic cations. In the as-prepared zeolites they are typically alkali or alkali earth metal cations or alkylammonium cations, but after post-synthetic modifications they can be ion exchanged to almost any inorganic cation or replaced by protons. X represents neutral guest molecules or included species.[44]

Zeolite structures are also commonly described in terms of the size (i), geometry (ii) and connectivity of the pore space (iii) defined by their frameworks.

- The size of the channels or pore openings (windows) that control molecular access into the pores is given in terms of the limiting ring size. Zeolites with channels or windows described by planar eight-membered rings of siliceous atoms (or oxygen atoms) 8MRs have pore sizes around 4Å and are known as "small pore", those with planar 10MR window or channels as "medium pore" (5.5 Å) and those with 12 MR window or channels as large pore (7.5 Å). In addition, zeolites with 7MR, 9MR and 11 MR openings

[44] Breck, D. W. *Zeolite Molecular Sieves*; Wiley: New York, 1974; Barrer, R. M. *Hydrothermal Chemistry of Zeolites*; Academic Press: London, 1982; Szostak, R. *Molecular sieves- Principles of Synthesis and Identification*, 1st ed.; Van Nostrand Reinhold: New York, 1989; 2nd ed.; Blackie: London, 1998.

are known. Some structures contain openings limited by 14 MRs or even 20 MRs (referred to as extralarge pore solids).

- The pores space geometry may be described in terms of channels, which may be uniform or non-uniform in cross section and may intersect with other channels or for other structures in terms of cages, linked via windows.
- Finally, the connectivity of pore space can be one dimensional, 1D, (unconnected channels), 2D (where any point in a plane in the pore system can be accessed from any other point in that plane) or 3D, where any part of the pore space is accessible from any other point within the crystal.[45]

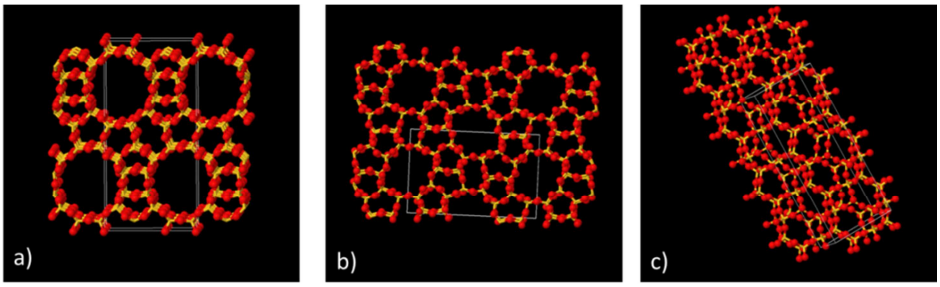

Figure 1.15. Some representations of the frameworks type a) BEA*, b) MFI and c) FRA. Siliceous and oxygen atoms are represented by yellow sticks and red balls. *3D Drawings obtained by the Java Applet Jmol from the Database of Zeolite Structures official website.*

The synthesis of zeolites is carried out under hydrothermal conditions. Commonly, an aluminate solution and a silicate solution are mixed together in an alkaline medium to form a milky gel or in some instances, clear solutions. Various cations or anions can be added to the synthesis mixture. Synthesis proceeds at elevated temperatures (60-200 ºC) where crystals form through a nucleation step. Before the 1960s,

[45] M. E. Davis, *Nature*, **2002**, *147*, 813-821.

zeolites were synthesized using only inorganic reagents. In general, the products obtained had a low Si/Al ratio framework (Si/Al <10) and hydrophilic properties (due to the anionic Al sites which are charge compensationed with cations such as Na^+ or K^+). In the 1960s, however, a new synthesis method using organic compounds, particularly quaternary ammonium salts, was established. These organic compounds, most frequently organic cations, are now being generally referred to as Organic Structure Directing Agents (OSDAs), Structure Directing Agents (SDAs) or templates, allowed the synthesis of new zeolites structures formed around them via hydrophobic interactions. The role of organic cations can go from pore filling to a true templating effect dominated by a geometric specificity.[46] Most frequently, they seem to display some kind of specificity by which, in the appropriate range of synthetic conditions, they are able to direct the crystallization to a particular zeolite structure. A strong interaction between organic molecules and inorganic species may cause the self-assembly of molecular sieve precursors. However, it has also been shown that several other factors, in addition to the presence of OSDA, play a role in determining the phase selectivity of a zeolite crystallization, as for instance, the nature and concentration of heteroatoms, the nature of source of inorganic components or the concentration of the synthesis mixture.

Classic synthesis of zeolites are carried out in alkaline conditions, since hydroxide anions are used as a mineralizer. It helps solubilize and mobilise silica and alumina affording a high supersaturation and catalyzing the breaking and formation of Si-O-T bridges, thus allowing the reorganization of amorphous gels and other solids to produce zeolites. However, by the end of the 1970s, Flanigen and Patton

[46] M. E. Davis, R.F. Lobo, *Chem Mater.*, **1992**, 4, 756.

substituted hydroxide by fluoride to produce an all-silica version of zeolite ZSM-5.[47] The synthesis made use of the classical organic structure-directing agent (OSDA) for MFI zeolites, TPA^+ (tretrapropylammonium cation), which they also used successfully to produce the same pure-silica zeolite by the hydroxide route at high pH. In the fluoride route, the synthesis proceeded at much lower alkalinities than traditional zeolite synthesis, leaving a pH close to neutral. Calcination of the as-made material (containing TPA^+ and F^-) allowed to obtain a new microporous crystalline polymorph of silica, highly hydrophobic and devoid of any ion-exchange properties.

From that time, the synthesis of zeolites by the so-called "fluoride route" has been extensively developed and has allowed not only the discovery of new framework zeolite types, but also a dramatic change in some of the most characteristic properties of the obtained zeolites.

The chemistry of the fluoride route to zeolites, particularly pure-silica zeolites, is indeed interesting for several reasons. First, in addition to allow the crystallization at pH close to neutral, fluoride ends up occluded into the zeolite, affording charge-balance of the generally cationic OSDA. A second interesting aspect of the fluoride route is that the obtained zeolite is devoid of connectivity defects in its network of siloxane bridges (silica zeolites synthesized at high pH present a large concentration of defects forming nests of Si-OH groups hydrogen bonded to SiO^-). And finally, another interesting feature of the fluoride route is that it may be argued that the fluoride anion displays significant structure-directing effects. Supporting this, there are several new zeolite structures that, so

[47] E.M. Flanigen and R. L.Patton, *U.S. Patent* 4,073,865, **1978**

far, cannot be made in the absence of fluoride, at least as pure-silica materials.[48]

The Zeolites materials synthesized in this thesis work have been crystallized under hydrothermal conditions using tetraethylammonium hydroxide as SDA and fluoride anions as mineralizers. The high silica zeolite obtained in these synthetic conditions has been the Zeolite Beta which presents some advantages for designing the hybrid organic-inorganic material for sensing applications due to different reasons:

1. Zeolite beta contains a 3D system of large pores circumscribed by rings of 12 tethrahedra (12MR), providing ideal space for the incorporation, stabilization and organization of organic species. Moreover, its 3D porous structure makes more difficult its pore blockage.

   The complex structure of zeolite beta has been described as a disordered intergrowth of two mostly polymorphs (called A and B), both circumscribed by rings of 12 tethrahedra (12MR) as is shown in figure 1.16. (Table 1.1. shows the structural properties of the polymorphs A and B of the beta zeolite).

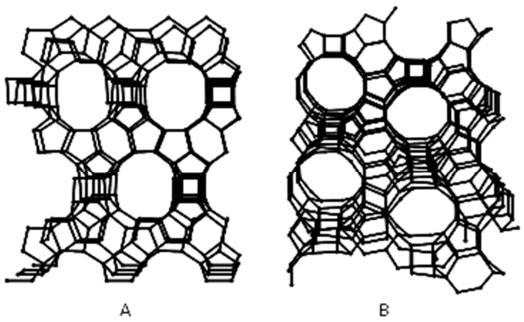

Figure 1.16. Two of the main polymorphs of zeolite Beta. *Polymorph A* (along [100]) and *Polymorph B* (along [110]).

[48] Porous materials. M. A. Camblor, S. B. Hong. Wiley, **2011**, 264-323.

Structure	*Spacial group*	*Crystalline System*	*a (Å)*	*b (Å)*
Pol A	$P4_122$ or P_4322	Tetragonal	12.66	12.66
Pol B	C2/c	Monoclinic (β = 114.8)	17.90	17.92

Table 1.1. Structural properties of the Polymorphs A and B of the beta zeolite.

2. Zeolite beta can be synthetised using about 25 different SDA when fluoride route is employed[49]. It suggests that variations in the composition of the synthesis mixture, as the incorporation of organosilanes, still can make it possible the crystallization of zeolite Beta. Tetraethylammonium (TEA) is one of these SDA whose size is small enough compared with the pore opening of the zeolite Beta structure to be removed by solvent extraction. Table 1.2. shows the experimental values of zeolite beta in pure silica composition.

	Pore diameter (Å)(1)	*Vμp (cm^3/g)(3)*	*S_{BET} (m^2/g)*
Zeolite Beta	5.6 and 6.8	0.19	~ 450

Table 1.2.Experimental values of high pure silica Zeolite Beta.

3. Pure-silica zeolite beta can be prepared in fluoride media which allows working at near to neutral pH, increasing the stability of

[49] M. A. Camblor, P. A. Barret, M-J. Díaz-Cabañas, L. A. Villaescusa, M. Puche, T. Boix, E. Pérez, H. Koller. *Microporous and Mesoporous Materials*, 48, **2001**, 11-22.

the organic species in the strong synthesis media (about weeks at temperatures of 150-175 ºC).

4. On the other hand, as has been previously described by Davis *et al.*,[50] zeolite extraction is fully achieved when using pure silica framework composition in comparison to aluminosilicate counterpart, whose interaction via charge-balancing ionic interactions with the SDA and the silicate framework is stronger.

1.4.2. Covalent functionalization of microporous and mesoporous materials.

One important way of modifying the physical and chemical properties of porous silicates has been the incorporation of a functional organic component. As it has been described previously, organic functionalization in porous materials can be carry out (i) without any interaction with the organic and the inorganic components or linked together through non-covalent weak bonds or (ii) through strong covalent chemical bonds with the organic and inorganic components.

Some parameters should be controlled when we design the synthesis of a hybrid organic-inorganic material:

- The control over the amount of organic-groups incorporated in the structure of the porous material.
- The distribution of the organic molecules in the porous matrix (inside or outside the channels or porous of the silica material) and their uniform coverage.
- And the stability of the organic functionalization.

[50] C. W. Jones, K. Tsuji, T. Takewaki, L. W. Beck, M. E. Davis, Micro. and Meso. Mater., 48, **2001**, 57-64.

The organic functionalization by covalent bonding of the inorganic matrix avoids some of the considerations explained above and prevents leaching and/or aggregation.

Most of the reported examples when the organic moiety is bonded covalently, involve the use of MCM-41 (2D hexagonal, prepared under basic conditions using cationic surfactants)[51], MCM-48 (cubic, basic conditions, cationic surfactants), FSM-16 (2D hexagonal, derived from the layered polysilicate kanemite)[52], HMS (acidic conditions with neutral amine templates)[53], SBA-1 (cubic, acidic conditions, cationic surfactants)[54], SBA-3 (2D hexagonal, acidic conditions, cationic surfactants), SBA-15 (2D hexagonal, acidic conditions, prepared with block-copolymer templates)[55] or silica nanotube matrices in which certain selective probe molecules are covalently anchored to the pore walls. These materials have a suitable ability to interact with atoms, ions and molecules on their external and internal surface when are

[51] J. S. Beck, J. C. Vartuli, W. J. Roth, M. E. Leonowicz, C. T. Kresge, K. D. Schmitt, C. T.-W. Chu, D. H. Olson, E. W. Sheppard, S. B. McCullen, J. B. Higgins, J. L. Schlenker, *J. Am. Chem. Soc.* **1992**, 114, 10 834.

[52] S. Inagaki, Y. Fukushima, K. Kuroda, *J. Chem. Soc., Chem. Commun*. **1993**, 680.

[53] P. T. Tanev, T. J. Pinnavaia, *Science* **1995**, 267, 865.

[54] Q. Huo, D. I. Margolese, U. Ciesla, D. G. Demuth, P. Feng, T. E. Gier, P. Sieger, A. Firouzi, B. F. Chmelka, F. Schüth, G. D. Stucky, *Chem. Mater*. **1994**, 6, 1176; Q. Huo, D. I. Margolese, U. Ciesla, P. Feng, T. E. Gier, P. Sieger, R. Leon, P. M. Petroff, F. Schüth, G. D. Stucky, *Nature* **1994**, 368, 317.

[55] D. Zhao, J. Feng, Q. Huo, N. Melosh, G. H. Fredrickson, B. F. Chmelka, G. D. Stucky, *Science* **1998**, 279, 548; D. Zhao, Q. Huo, J. Feng, B. F. Chmelka, G. D. Stucky, *J. Am. Chem. Soc*. **1998**, 120, 6024.

adequately functionalized. In contrast, there has been little success in the functionalization of microporous materials with organosilanes.[56]

Strategies for preparation of organic-inorganic nanostructured materials are diverses and depend on the way of the organic functionalization selected will permit precise control over the surface properties and pore sizes of the mesoporous sieves[57]. Organosilanes of the type $(R'O)_3SiR$, where **R** is the organic residue, are the reagents of choice for stable and reliable functionalization of most of the inorganic supports.

In the next section, it will be described the main three pathways available for the synthesis of porous hybrid materials based on organosilica units covalently bonded: 1) the subsequent modification of the pore surface of an inorganic silica material (the so called grafting), 2) the simultaneous condensation of corresponding silica and organosilica precursors (co-condensation), and 3) the incorporation of organic group as bridging components directly and specifically into the pore walls by the use of bisilylated single-source organosilica precursors (periodic porous organosilicas), as is schematized in the figure 1.17.

[56] K. Tsuji, C. W. Jones, M. E. Davis, *Microp. and Mesop. Mater*. 29, **1999**, 339-349.

[57] D. Brühwiler, G. Calzaferri, *Microp. and Mesop. Mater*, 72, **2004**, 1-23.

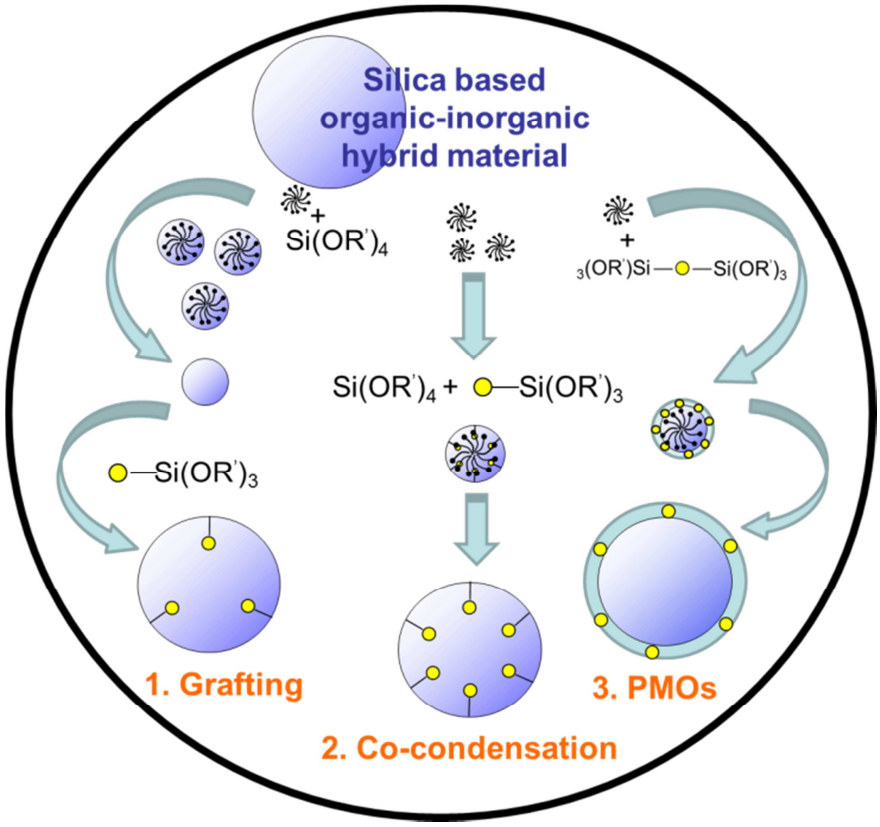

Figure 1.17. Organic functionalization methods for porous materials by covalent bond. Adapted from *Angew. Chem. Int. Ed*. **2006**, 45, 3216-3251.

1.4.2.1. Organic functionalization of the inorganic matrix by the Grafting methods.

Grafting refers to post-synthesis modification of a pre-synthesized porous support by attachment of functional molecules to the surface of the inorganic matrix, usually after surfactant removal. Porous silicates materials possess surface silanol (Si-OH) groups that can be present in high concentration and act as convenient anchoring points for organic functionalization.

Surface modification with organic groups is most commonly carried out by silylation, although modification of silanol groups is also possible by esterification (with ethanol for example), which occurs on free (≡Si-OH) and germinal silanol (=Si(OH)$_2$) groups, as is schematized in figure 1.18. For this reason, is important to maintain a large number of surface silanol groups after removal of the surfactant (carried out by calcination or by appropriate solvent-extraction methods).

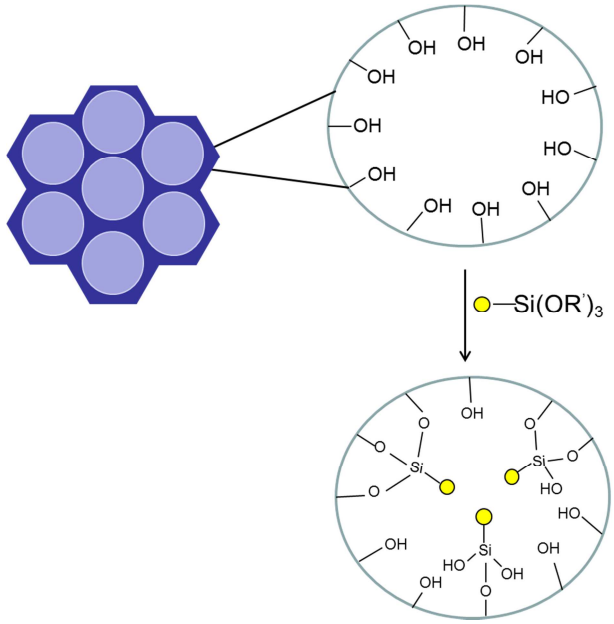

Figure 1. 18. Scheme for the functionalization of porous silicates by grafting.

If the surfactant is removed by calcination, this process promotes condensation of unreacted silanol groups, and many surface groups are lost at typical calcination temperatures; in this case, the surface can be rehydrated by boiling calcined mesoporous silicate in water and

removing excess water by azeotropic distillation with toluene or benzene.[58]

In the case that the surfactant is removed by extraction with acid/alcohol mixtures, it minimizes loss of surface silanols, although post-extraction thermal treatments can increase the surface reactivity for silylation and strengthen the walls through additional condensation.[59]

Moreover, the grafting process can be carried out with *passive* surface groups (groups that exhibit low reactivity such as alkyl groups or phenyl groups) or with *reactive surface groups* (silane-coupling agents such as olefins, nitriles, alkylthiols, alkyl amines, alkyl halides, epoxides and some other surface groups that are reactive and permetted further functionalizations).[60]

- The functionalization by the grafting procedure *with passive surface groups* can be used to tailor the accessible pore sizes of porous solids, increase the surface hydrophobicity, passivate silanol groups and thereby protect the framework towards hydrolysis. The pore diameters could be progressively decreased using longer alkyl chain lengths of chloroalkyldimethylsilanes for instance and the size of the silylating groups affected the degree of silylation and the concurrent surface hydroxyl consumption

[58] J. Liu, X. Feng, G. E. Fryxell, L.-Q. Wang, A. Y. Kim, M. Gong, *Adv. Mater*. **1998**, 10, 161; X. Feng, G. E. Fryxell, L.-Q. Wang, A. Y. Kim, J. Liu, K. M. Kemner, *Science* **1997**, 276, 923.

[59] X. S. Zhao, G. Q. Lu, *J. Phys*. Chem. B **1998**, 102, 1556.

[60] A. Stein, B. J. Melde, R. C. Schroden, *Adv. Mater*. **2000**,12, 1403-1419

(best surface coverage was obtained with the sterically less demanding silyl groups).[61]

- In the case of the organic functionalization *with reactive surface groups*, the grafting procedure allows functionalizing the external surface of the inorganic porous material with an active group which is a precursor of any other functional group. The reactive groups on the external surface are more accessible in the subsequent reactions.[62]

Multiple grafting has also been demonstrated. For instance, if uncovered areas remain after silylation (leaving hydrophilic sites) they can be passivated by trimethylsilylation which changes the hydrophobicity of the surface and thereby controls adsorption of polar/non-polar molecules. These multiple functionalizations have been achieved and well-controlled by two different methods as is schematized in figure 1.19.:

- The first approach assume that silanol groups on the external surface in calcined MCM-41 sample are kinetically more accessible for functionalization and the second functionalization is almost entirely on the internal surface of MCM-41, as is described by Sherphard et al.[63]

- The alternative approach for selective functionalization of external and internal MCM-41 surfaces was described by Juan

[61] T. Kimura, S. Saeki, Y. Sugahara, K. Kuroda, *Langmuir*, **1999**, 15, 2794.

[62] J. H. Clark, D. J. Macquarrie, *Chem. Commun*. **1998**, 853.

[63] D. S. Shephard, W. Zhou, T. Maschmeyer, J. M. Matters, C. L. Roper, S. Parsons, B. F. G. Johnson, M. J. Duer, *Angew. Chem. Int. Ed*. **1998**, 37,2719.

and Ruiz-Hitzky.[64] In this case, the first (external) grafting step is carried out with the as-synthesized mesoporous sieve whose pores are still filled with the surfactant template. Then the template is extracted and the internal pore surfaces are functionalized with a second organosilane group.

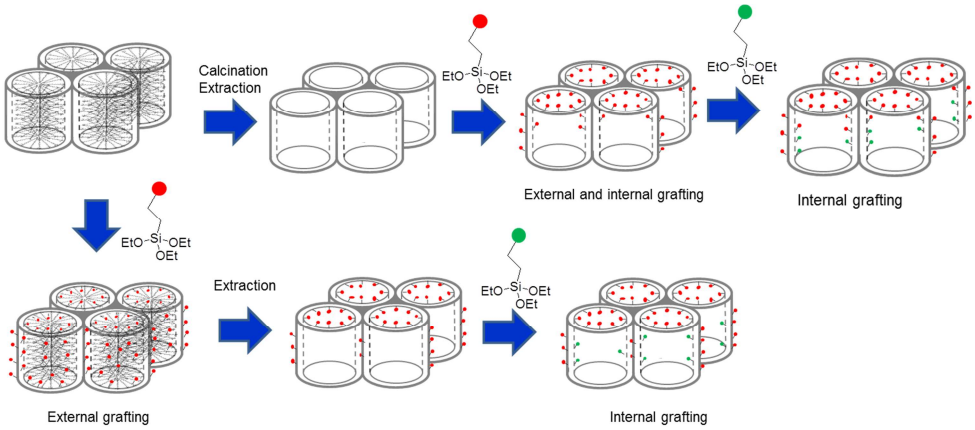

Figure 1.19. Methods of selective grafting on external and internal surfaces of mesoporous silicates.

In the particular case of the microporous materials, it should be taken into account that functionalization by grafting occurs exclusively on the external surface because the microporous sizes restrict the acces to the internal microporous surface for most organosilane reactants (these silanes are usually too big to penetrate into the zeolites pores).

1.4.2.2. Organic functionalization of the inorganic matrix by co-condensation methods.

Co-condensation of a tetraalkosysilane ($(RO)_4Si$) and one or more organoalkoxysilanes ($(R'O)_3SiR$) with Si-C bonds is an alternative

[64] F. de Juan, E. Ruix-Hitzky, *Adv. Mater.* **2000**, 12, 430.

method of producing inorganic-organic hybrid materials by sol-gel chemistry. These co-condensation reactions are carried out in the presence of a structure directing agent (SDA) leading to materials with organic residues anchored covalently to the pore walls (see Figure 1.20.)

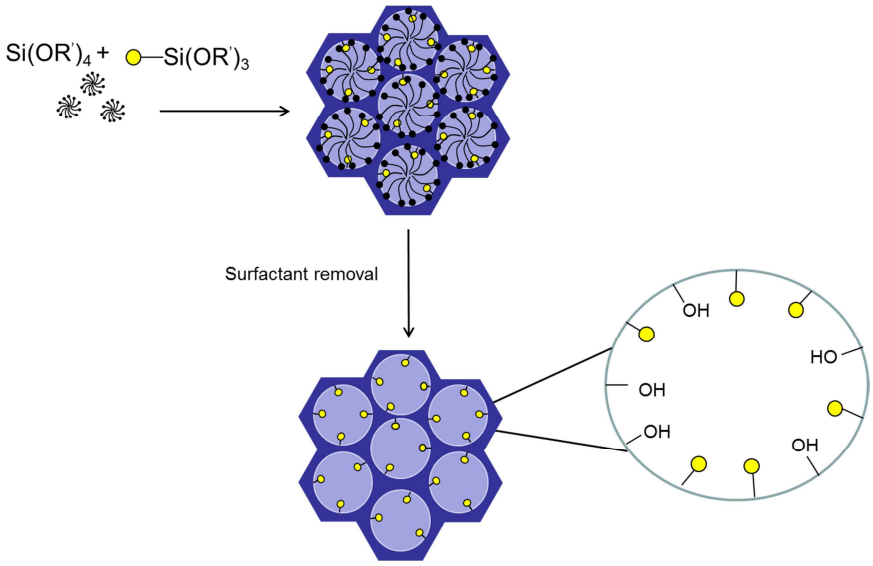

Figure 1.20. Synthesis of hybrid mesoporous silicates by co-condensation.

The co-condensation procedure allows the incorporation of a relatively large amount of functional groups, which generally falls between 2 and 4 meq/g, in the most favourable cases.[65] Due to the synthesis process, the organic groups **R** are bonded to silicon atoms most of them located into the pores and the organic units are generally more homogeneously distributed than in materials synthesized with the grafting process.

However, there are some disadvantages that should be taken into account when this method is used:

[65] A. Stein, B. J. Melde y R. C. Schroden, *Adv. Mater.*, 12, **2000**, 1403-1419

- The degree of mesoscopic order of the products decreases when the trialkoxyorganosilane concentration is increased in the reaction mixture. For microporous materials, co-condensation methods tend to interfere with crystallization.
- As a consequence of the increase of the homocondensation reactions between silane groups, the ratio of terminal organic groups that are incorporated into the pore-wall network is, generally, lower than would correspond to the starting concentration in the reaction mixture.
- The incorporation of the organic groups can lead to a reduction in the pore diameter, pore volume, and specific surface areas.
- And finally, only the extraction method is available to carry out the removal of the surfactant, avoiding the calcination that would destroy the structure of the material due to the presence of organic groups in the skeleton.

However, the co-condensation reactions can be carried out under a wide range of reaction conditions (cationic, neutral or anionic surfactant under basic, neutral or acidic reaction conditions) and depending on this synthesis conditions, the limit and the ordering of the organoalkoxysilane incorporation into the hybrid mesostructured materials can be very different. [66,67,68,69] Moreover, solvent extraction provides straight away the organic functionalized porous material.

On the other hand, some disadvantages can arise if a relative large extension of functionalisation is required, since they have been found

[66] S. L. Burkett, S. D. Sims, S. Mann, *Chem. Commun*. **1996**, 1367.

[67] D. J. Macquarrie, *Chem. Commun*. **1996**, 1961.

[68] Q. Huo, D. I. Margolese, G. D. Stucky, *Chem. Mater*. **1996**, 8, 1147.

[69] M. H. Lim, C. F. Blanford, A. Stein, *J. Am. Chem. Soc*. **1997**, 119, 4090

buried in the silica wall, decreasing the degree of mesoscopic order of the solid. For microporous materials, co-condensation methods tend to interfere with the crystallization of the target phase.

In 2003, Che *et al.*[70] developed a method to prepare highly functionalised materials named AMS (Anionic Mesoporous Surfactant). The method makes use of anionic surfactants and of the so-called co-structure-directing agent. Thus, the interaction between the inorganic wall and the surfactant is achieved through this co-structuring agent, which, in the case of anionic surfactants, can be organoalkoxysilanes derivatives capable to bear a positive charge (see Figure 1.21)

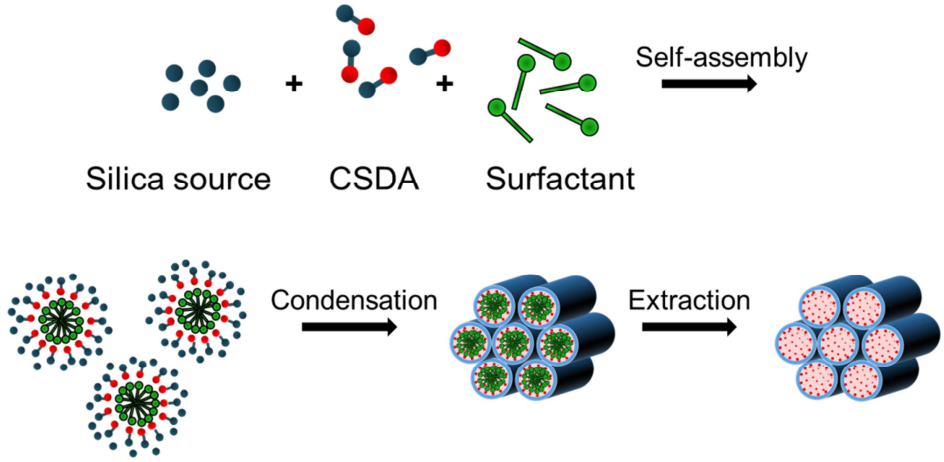

Figure 1.21. Scheme of the interactions between CSDA and headgroup of surfactant in the co-structure-directing synthesis of mesoporous silicas. The interactions can be electrostatic, covalent, hydrogen bonding and π-π interaction, etc., which gives rise to mesoporous silicas with regularly arranged functional groups following the arrangement of headgroups of surfactant.

[70] S. Che, A. E. Garcia-Bennett, T. Yokoi, K. Sakamoto, H. Kunieda, O. Terasaki and T. Tatsumi, *Nature Materials*, **2003**, 2, 801.

The method is highly versatile, since there are plenty of factors that can be used to prepare the phase with the desired properties, SDA, CSDA as well as the synthesis conditions (composition, temperature, pH, time, source of silica, solvent, etc).

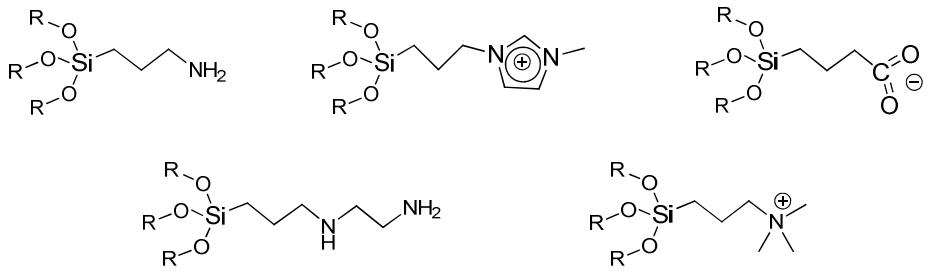

Figure 1.22. Some of the co-structure agent for the meso-organization of the hybrid silica porous materials.

This approach has provided a large amount of different materials with a variety of empty space distribution (cages, straight channels, bicontinuos, etc) specific areas (up to around 1000 m^2/g) and dimensions of pores (ranging from 2 to 7 nm) and pore volume (up to 0.7 cm^3/g)[71,72,73,74]. The extraction of the porogen "guarantees" the presence of functional groups on the inner surface, with values of about 1 organic group per 20 $Å^2$.

[71] R. Atluri, N. Hedin and A.E. Garcia-Bennett. *J. Am. Chem. Soc,* **2009**, 131, 3189.

[72] A. E. Garcia-Bennett , O. Terasaki , S. Che and T. Tatsumi , *Chem. Mater.* **2004** , *16* , 813.

[73] A. E. Garcia-Bennett , N. Kupferschmidt , Y. Sakamoto , S. Che and O. Terasaki , *Angew. Chem. Int. Ed.* **2005** , *44* , 5317 .

[74] C. Gao , Y. Sakamoto , K. Sakamoto , O. Terasaki and S. Che , *Angew. Chem. Int. Ed.* **2006** , *45* , 4295 .

Mesophase	Mesostructure	*Adsorption properties*		
		Surface Area (m^2/g)	Pore volume (cm^3/g)	Pore diameter (Å)
AMS-1	3D-hexagonal	501	0.32	23
AMS-2	3D-cubic Modulated	963	0.70	28
AMS-3	2D-hexagonal *p6mm*	387	0.51	62
AMS-4	3D-cubic and hexagonal	760	0.79	40
AMS-5	Lamellar	-	-	-
AMS-6	Bicontinuous 3d-cubic *Ia-3d*	667	0.65	32
AMS-7	3d-disordered	301	0.33	23
AMS-8	3d-cubic *Fd-3m*	271	0.22	23
AMS-9	Tetragonal $P4_2/mnm$	872	0.60	38
AMS-10	Bicontinuous cubic Pn-3m	493	0.65	47

Table 1.3. Structural data derivates from XRD and N_2 isotherms obtained for the *AMS-n* materials. [75]

This strategy has been extended to the preparation of mesoporous materials using non surfactant porogen agents, for example folic acid[76]. or guanosine monophosphate.[77]

[75] C. Gao and S. Che. *Adv. Funct. Mater*. **2010**, 20, 2750–2768.

[76] R. Atluri, N. Hedin and A.E. Garcia-Bennett. *J. Am. Chem. Soc,* **2009,** 131, 3189.

[77] C. J. Bueno-Alejo, L. A. Villaescusa, and A. E. Garcia-Bennett. *Angew. Chem. Int. Ed*. **2014**, 53, 12106 –12110.

Folic acid self assembles in columnar hexagonal liquid crystalline phases where the columns consist of stacked arrays of pterine tetramers held together by Hoogsteen type hydrogen bonds and π-π stacking interactions. It leaves carboxylate groups pointing to the external surface of the supramolecular columns which interacts to the silica through the co-structuring directing agent, which in that case was (3-Aminopropyl)triethoxysilane (APES) to form the hybrid mesoestructure (figure 1.23). If the design of the material is focused on the porogen, it is possible to encapsulate it for its subsequent delivery. In this case, the material is a delivery vehicle for the release of folic acid.[78]

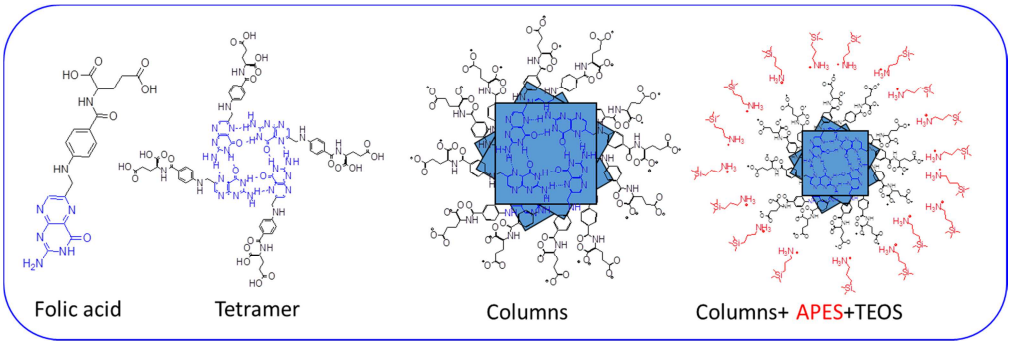

Figure 1.23. Scheme of the self-assembling of folic acid and the synthetic strategy for the preparation of NFM-1.

Similar to the grafting procedure, incorporation of two or more functional groups in a one-pot synthesis is also possible, although the location of functional groups is not as controlled as that produced by the grafting processes described earlier; the functional groups are randomly distributed in the product.[79]

[78] R. Atluri, N. Hedin, A. E. Garcia-Bennett, *J. Am. Chem. Soc*. **2009**, 131, 3189.

[79] S. R. Hall, C. E. Fowler, B. Lebeau, S. Mann*, Chem. Commun*. **1999**, 201.

1.4.2.3. Periodic mesoporous organosilicas.

An alternative method to synthesized organically functionalized mesoporous silica materials is the hydrolysis and co-condensation reactions of bridged organosilica precursors of the type $(R'O)_3$-R-$Si(OR')_3$.[80] In contrast to the organically functionalized silica phases, which are obtained by postsynthetic or direct synthesis, the organic units in this case are incorporated in the three-dimensional network structure of the silica matrix through two covalent bonds and thus distributed totally homogeneously in the pore walls. (see Figure 1.24)

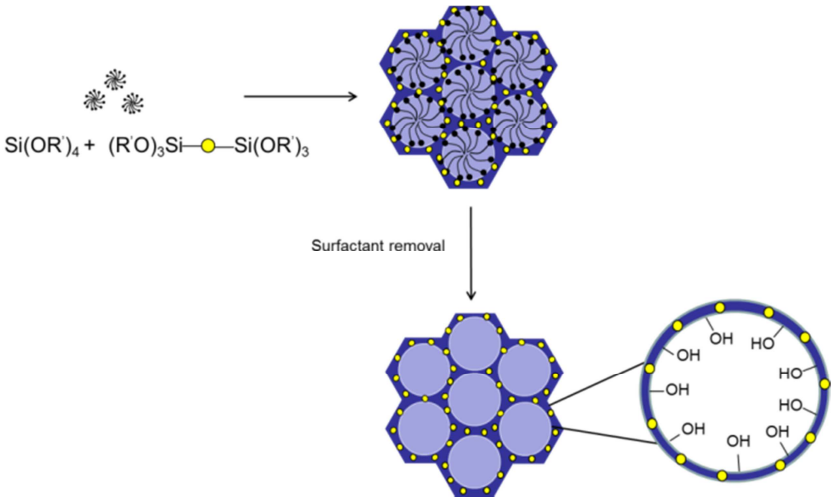

Figure 1.24. General synthetic pathway to PMOs that are constructed from bissilylated organic bridging units.

These organic units are incorporated into the synthesis gel, and even without surfactant templating, these materials can be obtained as porous aero- and xerogels with high surface area and high thermal

[80] D. A. Loy, K. J. Shea, *Chem. Rev.* **1995**, 95, 1431 – 1442; K. J. Shea, D. A. Loy, *Chem. Mater*. **2001**, 13, 3306 – 3319.

stability but generally exhibiting completely disordered porous systems with a relatively wide distribution of the pore radii. If surfactants are added to these types of synthesis, the uniformity of channels can be improved and periodically organized pore system is obtained. These materials are designed as a *periodic mesoporous organosilicas (PMOs)*.

The inclusion into the walls of the organic moiety by this method permits stoichiometric incorporation of organic groups in the silicate networks, resulting in higher loadings of organic functional groups than by grafting methods or by direct synthesis of mesoporous silicates with organic groups.

1.5. Applications of organic-inorganic siliceous hybrid materials for sensing.

Having as a reference the living nature and borrowing concepts and strategies from its, have been developed hybrid systems that mimic biological functions, as for instance, discriminating between closely related species and recognize target analytes through chromo-fluorogenic responses. This principle of operation has been mainly presented in biomimetic hybrid systems that are based on pre-organized nanoscopic siliceous porous solids.

The convergence of the properties of organic and inorganic building blocks in the same material is particularly interesting due to the possibility to combine the enormous functional variation of organic chemistry with the advantages of a thermally stable and rigid inorganic structure. This symbiosis can lead to materials whose properties are very different from those of their individual ones.

Particularly, in hybrid organic-inorganic materials for sensing applications, the porous structure enables the access of analyte molecules to the indicator dye centers, which could be adsorbed[81], occluded[82] or anchored in the pores of the mineral host, as has been described before. Furthermore, the advantages of an inorganic matrix for anchoring covalently functional chromophores are attributed to the more rigid environment as well as much higher migration stability, strongly increased photostability and low absorption and emission in the visible spectrum.

1.5.1. Binding pockets

The first reported example that used the concept of binding pockets made use of mesoporous silica supports in whose surface had been anchored suitable binding sites creating sensory materials with nanometer-sized that show enhanced recognition features. The basic strategy needs to use a 3D porous solid support which is functionalized with a large number of recognition centers on its surface area. In a second step, another molecular entity is grafted onto the walls of the material to fine-tune the polarity around the recognition centers.

As will be described, these systems show advanced features because, in addition to simple recognition at the binding site, there is an additional supramolecular control that is governed by the size and polarity of the nanoscopic pore and a hydrophilic/lipophilic partitioning or extraction. This approach usually results in a remarkably enhanced response and

[81] G. Calzaferri, S. Huber, H. Maas, C. Minkowski. *Angew. Chem. Int. Ed.* **2003**, 42, 3732-3758.

[82] G. Schulz-Ekloff, D. Wöhrle, B. van Duffel, R.A. Schoonheydt, *Microporous and Mesoporous Materials*, **2002**, 51, 91-138.

selectivity with respect to analogous molecular probes. In terms of bio-inspired concepts, these systems try to mimic the principle of operation of enzymes, which succeed in processing target substrates by extracting them into specific bonding pockets. These concepts are embedded in a wider concept of biomimetic chemistry as a part of the science that tries to imitate nature's methods, mechanisms and processes.[83,84,85]

The basic principle of operation is sketched in the example shown in Figure 1.25, which was designed to selectively sense linear long-chain carboxylates. The hybrid system consisted of a mesoporous MCM-41-type material that was functionalized in two steps. First, a urea-phenoxazinone derivative is anchored onto the surface of the mesoporous solid of the MCM-41-type. Therefore, the anchoring of the sensor molecule at low concentrations results in a functionalized material that contains the signaling receptor almost exclusively within the pores. The urea-phenoxazinone derivative is the signaling-recognition unit as it is able to act at the same time as an anion receptor through hydrogen bonding between the carboxylate groups of the target guest and the urea group, and the signaling reporter through a modulation of the electron distribution in the phenoxazine group upon carboxylate–urea coordination, which results in changes in absorption and fluorescence. In a second step, the inner surface of the mesoporous support was further functionalized with trimethylsilane with the aim of transforming the hydrophilic inner walls of the silica skeleton into hydrophobic pockets by transformation of -OH groups to $-Si(Me)_3$

[83] O. H. Schmitt*,* Proc. 3rd Intl. Biophysics Congress (Boston, MA, 29 Aug. to 3 Sept. 1969) p 297.

[84] Y. Bar-Cohen*, Bioinsp. Biomim.,* **2006***, 1,* **P1–P12***.*

[85] J. F. V. Vincent, O. A. Bogatyreva, N. R. Bogatyrev, A. Bowyer, A.-K. Pahl, *J. R. Soc. Interface*, **2006**, *3*, 471.

moieties[86]. This solid displays a remarkable response to long-chain carboxylates in water thereby exhibiting a bathochromic shift of the absorption band and an enhancement of the fluorescence emission. The authors demonstrated that short-chain carboxylates, inorganic cations, anions and biological species such as triglycerides, cholesterol, bile acids or organic phosphates gave no remarkable response; i.e. the solid is highly selective. The performance of the hydrophobic hybrid solid suggests that, after extraction of the long-chain carboxylates into the pores, the water content in the hydrophobic layer at the inner wall is presumably reduced so that hydrogen bonding between carboxylate and urea can occur. The integration of functionality and signaling is clearly shown if one takes into account that neither the urea-phenoxazinone probe molecule nor the hybrid material that is solely functionalized with the urea-phenoxazinone probe (but not being hydrophobized) are able to sense the target analytes in water. In biomimetic terms, selective signaling is achieved here in a similar way as many proteins; i.e., the substrate is extracted into a hydrophobic pocket where the active site–substrate complex is shielded from competitive water molecules.

[86] A. B. Descalzo, K. Rurack, H. Weisshoff, R. Martínez-Máñez, M. D. Marcos, P. Amorós, K. Hoffmann, J. Soto, *J. Am. Chem. Soc.*, **2005**, *127*, 184–200.

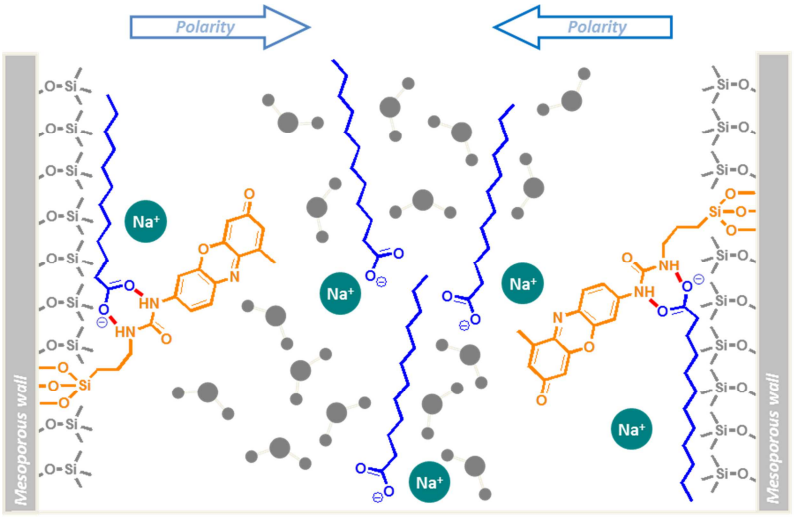

Figure 1.25. Schematic model of a biomimetic material for the sensing of long-chain carboxylates. Adapted from *Supramolecular Chemistry: From Molecules to Nanomaterials* © 2012 John Wiley & Sons.

Lin's group reported two other examples of functional discrimination by size and polarity for enhanced signaling. For example, a mesoporous material was first functionalized with *o*-phthalic hemithioacetal moieties that are able to react with amines to produce a highly fluorescent isoindole chromophore. The solid was then hydrophobized with different groups such as propyl, phenyl and pentafluorophenyl[87]. Interestingly, some of these solids displayed a remarkably selective and differentiable response to dopamine *versus* the less lipophilic glucosamine. The authors also demonstrated that this selectivity was not observed when using amorphous silica functionalized with the same organic groups, thereby stressing the importance of the 3D mesoporous structure. In a further interesting study, the authors coated mesoporous materials with

[87] V. S.-Y. Lin, C.-Y. Lai, J. Huang, S.-A Song, S. Xu, *J. Am. Chem. Soc.*, **2001**, *123*, 11510.

poly(lactic acid)[88]. This coating acts as a "molecular gate keeper" that is able to regulate the penetration of certain amines into the nanoscopic pores using coulombic forces. A large difference in the diffusion rates into the pores and, therefore, a selective signaling of the neurotransmitter dopamine in relation to tyrosine and glutamic acid was observed. The discrimination relies on the ratio between the charges at neutral pH of the gate keeper (negatively charged) and the charge of the guests; i.e., whereas dopamine is positively charged, tyrosine and glutamic acid are negatively charged. Thus, the latter are repelled by the negatively charged poly(lactic acid) coating (Figure 1.26).

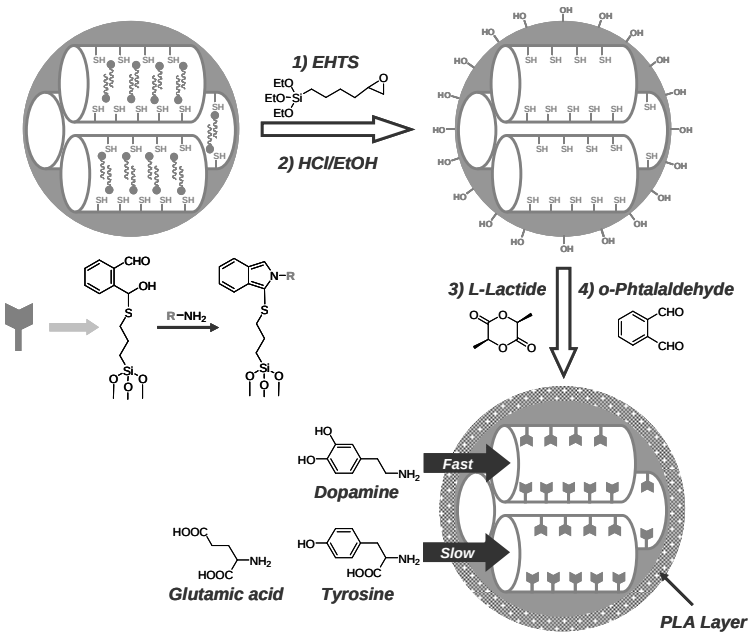

Figure 1.26. Schematic representation of the synthesis of PLA-coated a fluorescent sensor material for detection of amine-containing neurotransmitters (dopamine, glutamic acid and tyrosine). Adapted from *J. Mater. Chem.*,**2011**, 21, 12588-12604.

[88] D. R. Radu, C.-Y. Lai, J. W. Wiench, M. Pruski, V. S.-Y. Lin, *J. Am. Chem. Soc.,* **2004**, *126*, 1640.

These examples demonstrate that selective molecular recognition can be achieved by integrating functionality related with polarity and size discrimination with a signaling event. In fact, within a biomimetic perspective, the confinement of signaling groups into the modified solid structure leads to additional recognition advantages that take profit of both (i) the extraction of the guest from water that is limited by polarity and size and (ii) the selective reactivity of the binding site with the guest. These recognition benefits are especially obvious when one compares the response of the "binding pockets" with the analogous molecular probes with other non-porous supports.

Discrimination by polarity has also been used for the design of robust sensors for vapor detection. For instance, a mesoporous silica material containing a covalently anchored phenoxazinone probe has been used as an optical sensory hybrid for the detection of volatile organic compounds (VOC). The indication mechanism relies on the property of certain phenoxazinone derivatives to behave as fluorescent solvatochromic dyes[89]. As in the above cases, the mesoporous material was first functionalized with the dye and then re-functionalized with hexamethyldisilazane, which results in a fine control of the inner surface polarity and yields a rather hydrophobic hybrid sensory material. This derivative shows enhanced performance as optical sensor for VOCs when compared with the analogous non-hydrophobized material. For instance, the former allows the indication of VOCs over a larger polarity range; and, the color and fluorescence changes distinctly exceeding those of the latter, hydrophilic material. Additionally, the hydrophobic material shows a faster response, better reversibility and displays

[89] A. B. Descalzo, M. D. Marcos, C. Monte, R. Martínez-Máñez, K. Rurack, *J. Mat. Chem.*, **2007**, *17*, 4716.

minimal interference from environmental humidity. Moreover, when compared with other inorganic hosts for VOCs detection such as zeolites[90], the mesoporous hybrid has the advantage of larger pore diameters, which enable faster diffusion rates and better surface tailoring. This hybrid approach may also show advantages compared to sensory polymers because of the facile covalent functionalization of inorganic supports, the highly ordered 3D structure and the avoidance of swelling problems[91,92].

By analogy to the aforementioned, porphyrin-doped mesoporous silica films have been used for the detection of TNT vapours by quenching of the porphyrin emission[93]. The authors demonstrated that the use of mesoporous phases shows distinct advantages in terms of response when compared with functionalized amorphous silica.

1.5.2. Molecular gates.

A gate-like ensemble here refers to a mesoporous 3D skeleton that is functionalized with molecules that can be switched (by different means) to control either the release of a confined guests from the porous host or the entrance (or access) of molecular species to certain sites or into the pores. The triggers used for switching the state of the gate can be of chemical (e.g., ionic species) or physical nature (e.g., light). Most of these gate-like systems have been developed as scaffoldings for cargo delivery. However, applications in delivery are only one side of the

[90] J. L. Meinershagen, T. J. Bein, *J. Am. Chem. Soc.*, **1999**, *121*, 448.

[91] T. A. Dickinson, J. White, J. S. Kauer, D. R. Walt, *Nature*, **1996**, *382*, 697.

[92] T. A. Dickinson, K. L. Michael, J. S. Kauer, D. R. Walt, *Anal. Chem.*, **1999**, *71*, 2192.

[93] S. Tao, G. Li, *Colloid Polym. Sci.*, **2007**, *285*, 721.

medal. Recent works have demonstrated that nanoscopic gate-like scaffoldings can also be successfully employed in sensing protocols.

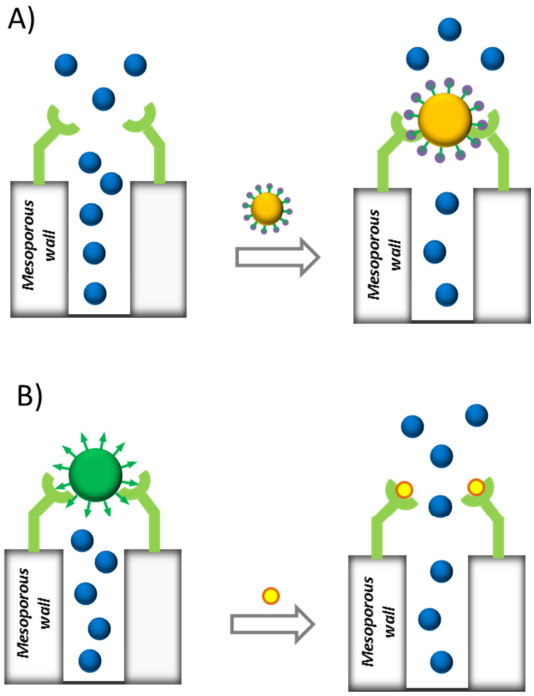

Figure 1.27. Scheme of the recognition paradigm using nanoscopic gate-like scaffoldings: (A) inhibition of dye release due to analyte coordination with grafted binding sites; (B) uncapping of the pores by an analyte-induced displacement reaction. Adapted from *Supramolecular Chemistry: From Molecules to Nanomaterials* © 2012 John Wiley & Sons.

When using gated concepts for sensing, two possible situations are envisioned (see Figure 1.27). In one, pores are open and the reporter is delivered to the solution, whereas in the presence of a given analyte, this molecule can bind to receptors on the external surface of the silica mesoporous supports closing the gate. As capping of the mesoporous support is selectively achieved in the presence of a target analyte, the design of a probe can be envisioned. In the second approach, the

starting material is capped and the presence of a target guest induces pore opening and dye delivery due to competitive binding. Of both these approaches, the second is perhaps the most interesting because it is able to show a signal when the reporter is released (i.e. off-on behavior), which is generally easier to measure than dye delivery inhibition (i.e. on-off behavior).

- *On-off behavior*

A first proof-of-concept was reported for an MCM-41 mesoporous support containing $[Ru(bpy)_3]^{2+}$ dye in the inner pores and functionalized on the external surface with 3-[2-(2-aminoethylamino)ethylamino]propyl trimethoxysilane acting as a gate. At a neutral pH, in which the experiments were carried out, the gate was open and delivery of the ruthenium complex was detected chromo-fluorogenically. Among several anions tested, ATP and ADP were selectively able to close the gate whereas other anions such as Cl^-, SO_4^{2-} or GMP were too small or formed too weak complexes with the functionalized surface to effectively close the pore openings and stop leaching of the $[Ru(bpy)_3]^{2+}$ indicator (Figure 1.28).[94]

[94] R. Casasús, E. Aznar, M. D. Marcos, R. Martínez-Máñez, F. Sancenón, J Soto, and P. Amorós, *Angew. Chem. Int. Ed.*, **2006**, 45, 6661–6664.

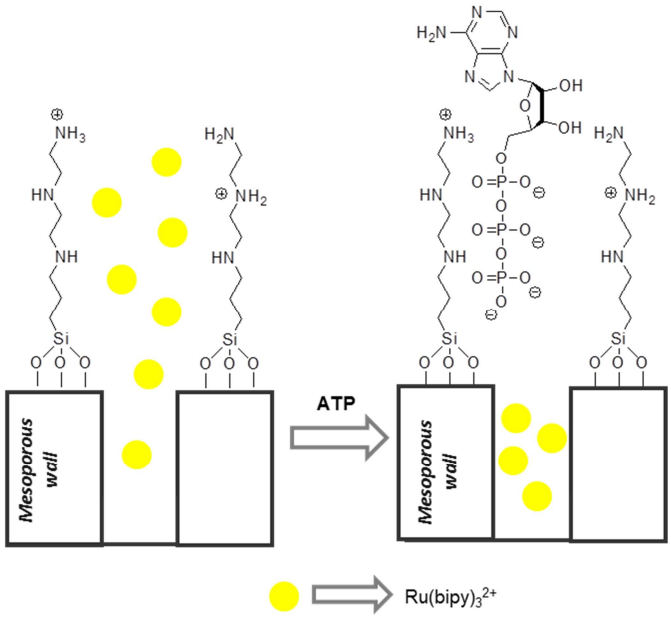

Figure 1.28. ATP signaling protocol via inhibition of dye delivery using nanoscopic gate-like scaffoldings. Adapted from *Angew. Chem. Int. Ed.*, **2006**, 45, 6661–6664.

In a complementary study, the same authors studied the behavior of a similar amine-functionalized material obtained by anchoring suitable polyamines onto the pore outlets of the mesoporous materials loaded with $Ru(bipy)_3^{2+}$.[95] A pH-driven open/close mechanism was observed that emerged from a hydrogen-bonding interaction between amines at a neutral pH (open gate) and Coulombic repulsions at an acidic pH between closely located polyammoniums at pore openings (closed gate). In addition to the pH-driven protocol, the opening/closing of the gate-like ensemble could also be modulated by an anion-controlled mechanism. Choice of a certain anionic guest resulted in a different gate-like ensemble behavior, which ranged from basically no action (chloride) to

[95] R. Casasús, E. Climent, M. D. Marcos, R. Martínez-Máñez, F. Sancenón, J. Soto, P. Amorós, J. Cano, E. Ruiz, *J. Am. Chem. Soc.*, **2008**, *130*,1903-1917.

complete (ATP) or partial pore blockage, depending on pH (sulfate and phosphate). The authors explained the remarkable anion-controllable response of the gate-like ensemble in terms of anion complex formation with tethered polyamines.

Based in this same open-closed mechanism, C. Coll and coworkers, developed a new chromo-fluorogenic sensing system capable of detecting long-chain carboxylates by the use of mesoporous silica nanoparticles loaded with $[Ru(bipy)_3]^{2+}$ and functionalized on the external surface with imidazolium binding sites.[96] It was found that short carboxylates, such as acetate, butanoate, hexanoate and octanoate, were unable to induce pore blockage, whereas presence of larger carboxylates, such as decanoate and dodecanoate inhibited dye release, most likely due to the electrostatic interaction of these carboxylates with the imidazolium binding sites on the surface and the formation of a dense hydrophobic monolayer around pore outlets (see Figure 1.29). In particular, dodecanoate completely inhibited dye delivery at the millimolar level. In a similar study, the same authors[97] developed another sensing system, also for the optical detection of long-chain carboxylates, based on the use of silica mesoporous solids loaded with $[Ru(bipy)_3]^{2+}$ and functionalizated on the external surface with thiourea or urea binding sites. In general, a similar result to that found for their previous solid functionalized with imidazolium was observed.

[96] C. Coll, R. Casasús, E. Aznar, M. D. Marcos, R. Martínez-Máñez, F. Sancenón, J. Soto, P. Amorós, *Chem. Commun.* **2007**, 1957-1959.

[97] C. Coll, E. Aznar, R. Martínez-Máñez, M. D. Marcos, F. Sancenón, J. Soto, P. Amorós, J. Cano, E. Ruiz, *Chem. Eur. J.* **2010**, 16, 10048-10061.

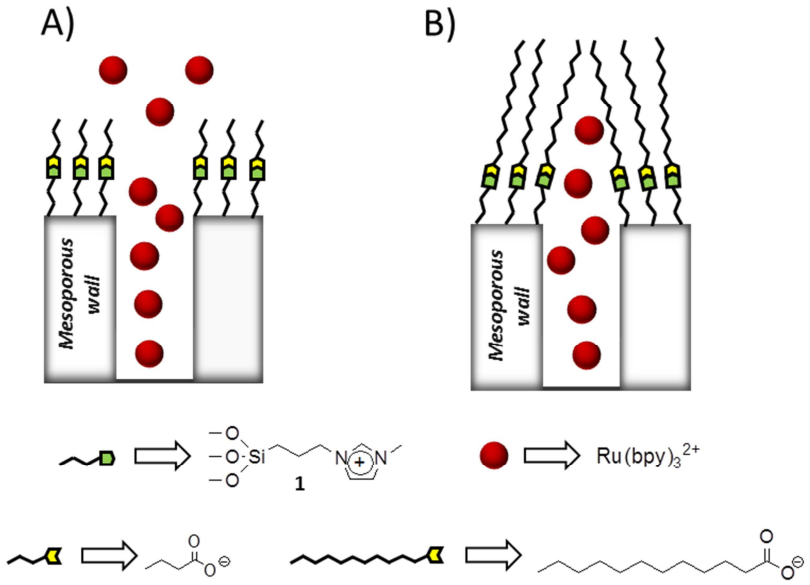

Figure 1.29. Micrometric silica mesoporous supports functionalized with imidazolium binding sites for the detection of long-chain carboxylates. Adapted from *Chem. Commun*. **2007**, 1957–1959.

- ***Off-on behaviour***

The first example reported where the off-on approach had been used for sensing, was developed by E. Climent and coworkers.[98] Gated silica mesoporous materials were used in this case for sensing of cation CH_3Hg^+. The gated material consisted of a mesoporous support loaded with dye safranin O and capped with 2,4-bis-(4-dialkylaminophenyl)-3-hydroxy-4-alkylsulfanylcyclobut-2-one groups (APC). APC moieties were readily formed by the reaction of a squaraine dye and thiol units, which were previously anchored to the external surface of the mesoporous support. When CH_3Hg^+ was added to the acetonitrile:toluene 4:1 v/v suspension of the APC-capped

[98] E. Climent, M. D. Marcos, R. Martinez-Máñez, F. Sancenón, J. Soto, K. Rurack, P. Amorós, *Angew. Chem. Int. Ed.*, **2009**, *48*, 8519-8522.

support safranin O release was observed. This uncapping process derived from the reaction of methylmercury with the thiol group on APC moieties, which resulted in the coordination of the cation to thiols and in both, the release of the bulky squaraine chromophore and the delivery of the entrapped safranin O reporter (see Figure 1.30).

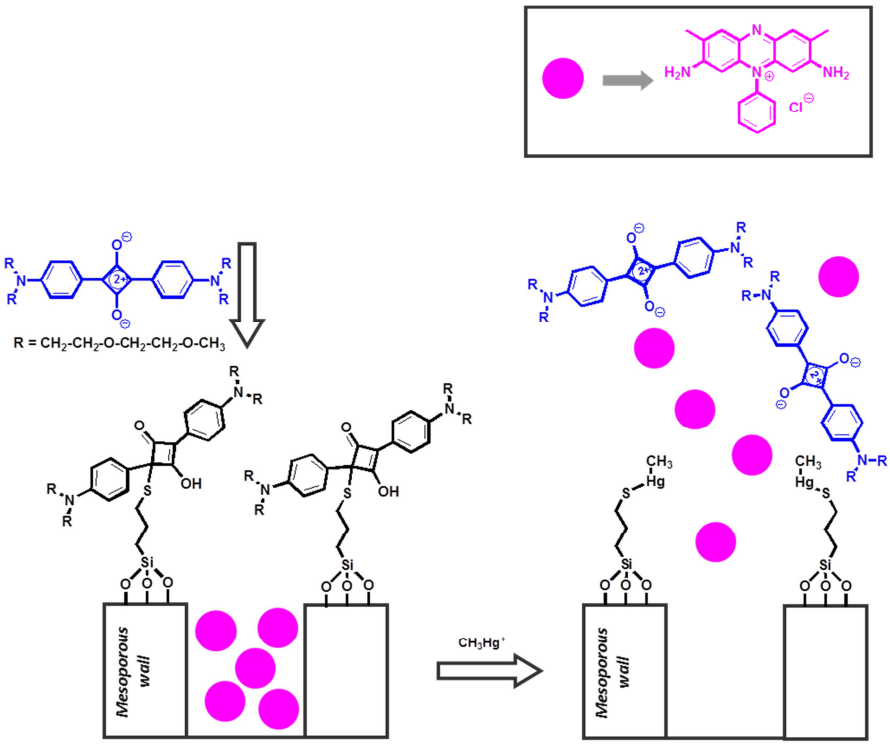

Figure 1.30. Micrometric silica mesoporous support loaded with safranine and capped with APC groups for the detection of methylmercury. Adapted from *J. Mater. Chem.*, **2011**, 21, 12588-12604.

The chromogenic indication reaction allowed the detection of CH_3Hg^+ down to 0.5 ppm, whereas the use of standard fluorometric methods reduced the LOD to below 2 ppb. Experiments were done in acetonitrile:toluene 4:1 v/v mixtures to achieve discrimination from

Hg^{2+} given its low solubility in this medium. This procedure was successfully tested to optically determine methylmercury in fish samples by a simple extraction procedure with toluene and CH_3Hg^+ detection with the APC-capped solid. These real fish samples were also spiked with cations Na^+, K^+, Ca^{2+}, Mg^{2+}, Cu^{2+}, Ni^{2+}, Zn^{2+}, Ag^+, Pd^{2+}, Cd^{2+}, Au^{3+} and Tl^+ and various organic species, e.g. sodium lauryl sulfate, cysteine, histamine, ethanol, heptylamine, hexanethiol. However, none of these species affected the response of the capped material to CH_3Hg^+.

Those new sensing systems based in the molecular gated nanoscopic hybrid materials conceptually differs from classic supramolecular "binding site-signaling subunit" systems because the new protocol disconnects the recognition step from the signaling event, but offers several advantages:

- Signaling event is independent of the host-guest interaction.
- Due to the possible use of different 3D supports, a large range of gate-like systems and a number of reporters which display chromogenic, fluorogenic or electrochemical responses, a variety of novel signaling systems based on gate-like scaffoldings can be designed with minimum effort.

1.6. Conclusions

In this chapter, some relevant supramolecular concepts related to the field of hybrid organic-inorganic materials have been reviewed and an account of representative examples published in this area applied to signaling applications has been given. Sensing concepts arising from the combination of supramolecular functions of suitable molecules and pre-

organized nanoscopic inorganic supports, often covalently linked, have been introduced and discussed.

Chapter 2

Work plan

The work of this thesis has been divided into several tasks:

Task 1: Synthesis and characterization of hybrid organic-inorganic materials for chemosensor protocols.

This first task has been organized in the following items:

1.1. The optimization of the synthesis of a trialkoxysiliyl derivative as an organic precursor for yielding dyes anchored to siliceous surfaces. Concretely, we have been working on the development of new dyes for sensing applications that are obtained from electrophilic aromatic substitution of N,N'-substituted anilines.

1.2. The organic functionalization with a pendant aniline subunit of the mesoporous MCM-41 type material UVM-7 by co-condensation

in order to have a precursor of different dyes within the mesoporous structure, the control of the amount of aniline incorporated into the siliceous matrix and the characterization of the final hybrid solid.

1.3. To study the different post-functionalizations with hydrophobic groups in order to tune the polarity of the surface and to compare the different properties of these hybrid materials.

1.4. The organic functionalization with a pendant aniline subunit of a microporous material (pure silica zeolite beta) in order to have a precursor of different dyes in a microporous structure, to control the aniline content and to characterize the structure of the final hybrid material.

1.5. To test the use of these hybrid materials as chemosensors.

Task 2: Synthesis and characterization of hybrid organic-inorganic materials for chromogenic displacement assays.

This second task has been organized according to these different items:

2.1. Organic functionalization of the mesoporous MCM-41 type material UVM-7 with different anion-binding sites and structural characterization of the hybrid solids.

2.2. To load the different hybrid materials with a property dye.

2.3. To test these hybrid organic-inorganic materials for their use as anion sensing by displacement protocols.

Chapter 3

Techniques of characterization

As it has been described, the properties of the organic functionalized materials obtained depend on the method of the incorporation of the organic moiety and the type of organic group used. Physical parameters as surface area, porosity and morphology are significantly affected by some of these parameters. Chemicals analysis provides information about the amount of organic species anchored in the material. A brief summary of the different material characterization methods is presented in this chapter.

3.1. Thermogravimetric Analysis

Thermogravimetric analysis (TGA) is a widely used analytical method for determining changes in the mass of a material as a function of temperature. It provides an idea of thermal stability of a given material,

including structural decomposition, oxidation, corrosion, moisture adsorption/desorption. In hybrid organic-inorganic materials it is used to determine the loading of organic components.

The record is the *thermogravimetric* or *TG curve*, where the mass is plotted on the ordinate decreasing downwards and temperature (T) or time (t) on the abscissa increasing from left to right (Figure 3.1.)

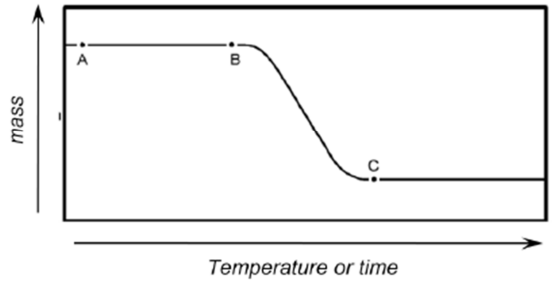

Figure 3.1. Thermogravimetric curve.

In the TG curve of hybrid materials the first weight loss corresponds to the thermodesorption of physically adsorbed water or solvent molecules from the silica surface and it can be observed in the region A-B with a slightly negative slope (temperatures in the range of 20-200 ºC). The second region between 400 and 600 ºC can be attributed to the thermal decomposition of the chemically bonded organic groups. At temperatures exceeding 700 ºC (region after point C) the organic component of hybrid materials is destroyed completely and thus, from the residual mass the inorganic content of the hybrid material can be determined.

Simultaneous TGA-DSC (Differential Scanning Calorimetry) measures both heat flow and weight changes in a material as a function of temperature or time in a controlled atmosphere. The simultaneous

measurement of these properties simplifies the interpretation of the results as complementary information is obtained (for instance, if certain events are endothermic or exothermic)

The Thermo-gravimetric analyses for this thesis work were carried out on a TGA/SDTA 851e Mettler Toledo balance, using an air standardized atmosphere (80 mL/min) with a heating program consisting in a first heating ramp of 10 °C per minute from 393 K to 1273 K, and then a plate at 1273 during 30 minutes.

3.2. Elemental Analysis.

The composition of hybrid materials is determined by elemental analysis. The carbon, hydrogen, nitrogen, sulphur, chlorine, bromine or iodine coming from the organic fragment can be analysed by combustion. The amount of other elements such as silicon can be determined for comparing the TGA results with the EA ones.

The theoretical and experimental contents can considerably differ and, generally, less organic functionality than expected is loaded in the hybrid material. Discrepancy between the two values also comes from traces of surfactant or high-boiling point solvent remaining in the material after the processing.

3.3. Infrared spectroscopy

Infrared spectroscopy (IR) allows the qualitative identification of functional groups present in the material which have representative signals. The use of this technique is limited to hybrid materials with low organic fragment dilution in the inorganic framework. When the ratio

tetraalkoxysilane/organosilane is higher than 10, the IR spectrum shows mainly bands corresponding to Si-O-Si vibrations (around 1100 cm^{-1}), surface adsorbed water and silanol species (3500-3200 cm^{-1}).

With the hybrid materials, the infrared spectra show an intensity decrease of the silanols band at 1080 cm^{-1} due to the organic functionalization and appear new bands related to this functionalization, as for instance, bands at 2940 cm^{-1} due to the stretching C-H vibrations (related to the functionalization with CH_3 groups) or a band assignable to the NH-δ vibration at 1670 and 1600 cm^{-1} (related with the functionalization with NH_2 groups).

In this thesis work, IR spectra have been recorded on a Jasco FT/IR-460 Plus between 400 and 4000 cm^{-1} diluting the solids in KBr pellets.

3.4. Surface area analysis

Gas adsorption-desorption measurements are used for determining the surface area, the average pore size and pore volume distributions of a variety of different solid materials.

N_2-sorption analyses are performed at 77 K from thoroughly degassed samples. The adsorption isotherm is built by adding controlled doses of nitrogen gas on the cold sample, and monitoring the corresponding relative pressure in the surrounding environment (P/P_0). When P/P_0 reaches 1, spontaneous liquefaction of N_2 occurs. Under these conditions consecutive molecular layers of nitrogen can be adsorbed on the solid surface.

The graphic representing the relationship, at constant temperature, between the amount adsorbed and the equilibrium pressure of the gas is known as the *adsorption-desorption isotherm.* In some cases, a hysteresis loop is observed when adsorption and desorption curves do not match. In 1940 S. Brunauer, L. S. Deming, W. E. Deming and E. Teller classified isotherms in five different types. Later on, in 1985 the *International Union of Pure and Applied Chemistry* (IUPAC) expanded this classification to six types (Figure 3.2.)

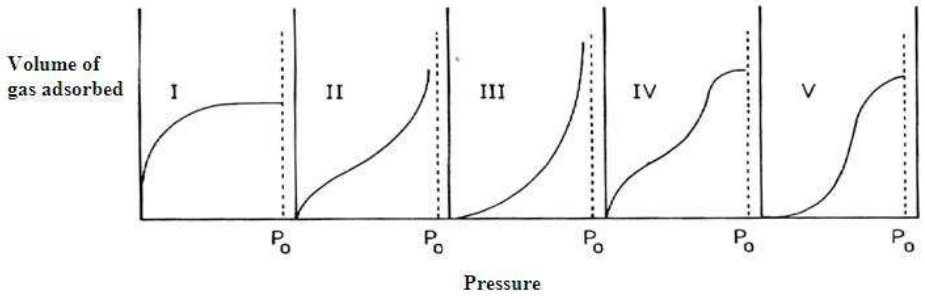

Figure 3.2. The five types of adsorption isotherms in the Brunauer classification.

Types I and IV are of special interest. The type I isotherm is typical of microporous zeolites. The steep initial slope corresponds to the monolayer adsorption within the porous lattice: primary micropore filling. Mesoporous solids, on the other hand, follow a Type IV isotherm. They have a characteristic hysteresis loop, which is associated with capillary condensation taking place in mesopores, and the limiting uptake over a range of high relative pressure. Such hysteresis loops may exhibit a variety of shapes classified by IUPAC in four types (H1, H2, H3 and H4), being the most frequent the types H1 and H2. Although the effect of various factors on adsorption hysteresis is not fully understood, the shapes of hysteresis loops have often been identified with specific pore structures, as for instance, mesostructured materials

like SBA-15, MCM-41 or MCM-48 exhibit Type H1 of hysteresis and Type H2 of hysteresis is representative for materials with higher disorder.

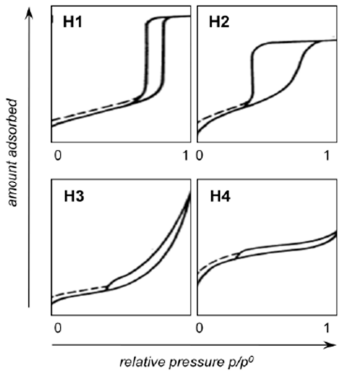

Figure 3.3. Types of hysteresis loops according to the IUPAC classification.

In summarize, the curve shape gives information about the pore size (P/P_0 from the hysteresis point), about the pore volume (the area limited by adsorption and desorption curves) and about the diameter distribution (related with the slope of the hysteresis).

The most common method of obtaining data on the specific surface area of samples from adsorption data is the use of the Brunauer-Emmett-Teller (BET) equation (equation 1). This equation describes multilayer physical adsorption, extending the theory of gases form the Langmuir equation for the adsorption of a monolayer of gas on a surface. The BET equation assumes that a monolayer of gas adsorbed will possess a fixed heat of adsorption (H_1), subsequent layers having heats of adsorption equal to the latent heat of evaporation (H_L).

$$\frac{P}{V(Po-P)} = \frac{1}{Vmc} + \frac{c-1}{Vmc}\left(\frac{P}{Po}\right) \quad \text{(eq .1)}$$

V is the volume of gas adsorbed at a particular gas pressure *P*. P_o is the satured vapour pressure of the gas adsorbed, V_m the monolayer volume and *c* is the monolayer constant (equation 2), where *R* is the gas constant and *T* the temperature in Kelvin.

$$c = \exp\left(\frac{H1-HL}{RT}\right) \qquad \text{(eq.2)}$$

The slope and intercepts of the BET plot ($P/V(P_0-P)$ *vs* P/P_0) allows the elucidation of V_m and *c* (equation 3).

$$Vm = \frac{1}{slope + intercept}$$

$$c = \frac{slope}{intercept} + 1 \qquad \text{(eq.3)}$$

V_m can be easily converted into moles and hence the specific surface area (Sg, m^2/g) can be derived. Thus in the case of an adsorbed monolayer of N_2, where the molecular area is A= 16.2 $Å^2$ at 77K,

$$Sg = \frac{Vm}{0.0224} \times 6.023 \times 10^{23} \times A \qquad \text{(eq.4)}$$

It is important to notice that the organic functionalization influences the porosity of the material and is observed a gradual decrease in the specific surface followed by a concomitant decrease of the pore size and volume. N_2 adsorption-desorption isotherms were recorded in this work on a Micromeritics ASAP2010 automated sorption analyser.

3.5. Powder X-Ray Diffraction

The organization of hybrid materials can be measured with the powder X-Ray diffraction (pXRD) technique. X-ray measurements were

performed with a Seifert 3000TT diffractometer using Cu Kα radiation. Under irradiation, the interaction of the repeating planes of a sample with an incident beam is described by Bragg's law:

$$\lambda = 2 \cdot d_{hkl} \cdot \sin\theta$$

In this equation, θ stands for the angle between the incident beam and the plane, d_{hkl} represents the distance between two consecutive identical planes, and λ is the incident beam wavelength.

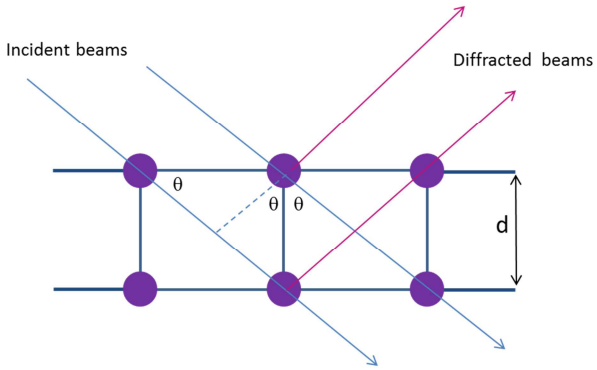

Figure 3.4. Schematic representation of Bragg's law.

The distance between planes can be determined from the incident beam and the measured dispersion angles. Powder X-ray diffractograms (Figure 3.5) reveal several properties about the sample under investigation. One of them is the crystalline degree of the sample, directly related with the peak broadness. Nanoparticles possess very few planes that satisfy the Bragg equation, in consequence the peak broadness increases and the peak height decreases (obtaining lower peak definition). Mesoporous materials, however, are typified by a few low angle diffraction peaks (below 10º 2θ), as shown in the pXRD pattern in Figure 3.5 (left). This is a reflection of the large unit cell dimensions, compared to microporous materials, and of the essentially amorphous frameworks.

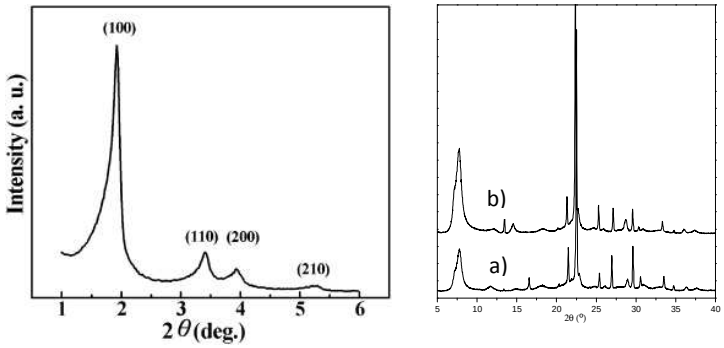

Figure 3.5. pXRD pattern of MCM-41 (left) and Zeolite beta (right) in the as synthesized (a) and SDA-extracted (b) versions for X-ray diffraction.

Exhaustively pXRD analysis and their comparision between the hybrid material and their corresponding pattern is important to ensure that the structural ordering of the channels has not changed after each organic functionalization step.

X-ray measurements were performed with a Seifert 3000TT diffractometer using Cu Kα radiation (Kα1 and Kα2).

3.6. Electron microscopy.

The material morphology can be studied by *Transmission Electron Microscopy* (TEM) and by *Scanning Electron Microscopy* (SEM).

Transmission Electron Microscopy (TEM) is used in material science to understand local structural information of materials and to confirm structural information. TEM technology allows the recording of images obtained when a beam of electrons cross a thin layer of the material. These high energy electrons have wavelengths smaller than the interatomic distances in a crystal lattice. Consequently, diffraction occurs as the electron beam interacts with the atomic electron clouds

contained within the sample. As a result the diffraction angles are small and are concentrated into a narrow cone around the undiffracted beam. In order to focus and magnify the beam through the microscope, a series of lenses are required. Typically a TEM consists of three stages of lensing. The stages are the condenser lenses, the objective lenses, and the projector lenses. The condenser lenses are responsible for primary beam formation, while the objective lenses focus the beam that comes through the sample itself (in STEM scanning mode, there are also objective lenses above the sample to make the incident electron beam convergent). The projector lenses are used to expand the beam onto the phosphor screen or other imaging device, such as film.

With this technique microporous and mesoporous channels located inside the material can be seen in structured materials, as well as their structural organization and their structural stability after their organic functionalization. However TEM must be complement with XRD data in order to gain the necessary information to elucidate the structure.

On the other hand, Scanning Electron Microscopy (SEM) is used to get information about the surface morphology, texture, particle shape and size of materials. In this case, it is not necessary to analyse a thin layer of material, since the microscope only explores the sample surface, which is previously covered with a metallic thin layer. Electrons from the incident beam scanning the sample can be dispersed or they produce secondary electrons. Dispersed and secondary electrons are collected and evaluated by an electronic device, which converts this information into a pixel.

With this technique, realistic tridimensional images of the hybrid surface are obtained. A comparison of the SEM microscopy image between

functionalized and non-functionalized solids should show the same microstructure for both of them indicating high purity and homogeneous crystal size distribution (which suggest a homogeneous composition along every sample).

Scanning Electron Microscopy images were obtained on a Jeol JSM 6300 operated at 30kV. Transmission Electron Microscopy images were obtained on a Philiphs TEM CM10 operating at 100 kV.

3.7. Ultraviolet-visible spectroscopy.

UV-visible diffuse reflectance spectroscopy and Ultraviolet-visible spectroscopy have been recorded also to study the organic functionalization of the materials. The difference between them, is that in UV/Vis spectroscopy one measures the relative change of transmittance of light as it passes through a solution, whereas in diffuse reflectance, one measures the relative change in the amount of reflected light off of a surface.

For the quantitative determination of the organic content UV-visible spectroscopy has been employed by monitoring the organic component band in solution upon dissolving the sample with HF in acetonitrile:water mixtures (Organic compounds, especially those with a high degree of conjugation, also absorb light in the UV or visible regions of the electromagnetic spectrum). The Beer-Lambert law states that the absorbance of a solution is directly proportional to the concentration of the absorbing species in the solution which is determined from a calibration curve. This is also a way to determine the relationship between the amounts of organic molecules introduced in the reaction mixture and the final organic content in the solid obtained.

The differents UV-Vis diffuse reflectance spectrums and UV-vis absorption spectrums have been recorded on a Perkin-Elmer Lambda 35 UV/VIS spectrometer.

To conclude this chapter it should be mentioned that only the combination of several different techniques can allow to fully characterizing a hybrid material. The information brought by the different analyses has been compared in order to better understand the effect of the structure and morphology on the properties of the different hybrid supports obtained.

Chapter 4

Hybrid organic-inorganic porous materials used for optical sensing using the chemodosimeter approach.

4.1. Objectives

In this chapter, different examples of organic-inorganic hybrid materials will be designed for chromogenic sensing using the chemodosimeter approach. In all of the examples that will be describe next, our objective is to demostrate that a hybrid organic-inorganic materials based on a siliceous supports (including zeolites, mesoporous materials and composite polymers) with a pendant aniline subunit could be considered as a starting material in order to anchor different types of dyes using different synthetic procedures.

Different studies will be carried out in order to prove the selectivity and the sensitivity of the prepared materials:

- In a first step, the aniline subunit (organic functionality) will be introduced in the synthesis gel. The co-condensation method with the aniline subunit should prevent organic compound degradation over synthesis conditions. Also, the presence of aniline moieties in the solids could allow subsequent functionalization in order to prepared 3D hybrid structure with selected colorimetric sensors.

- Aniline-functionalized mesoporous solids and aniline-functionalized microporous solids will be prepared in order to test if the inorganic support plays any role in the sensing protocols (related with a possible discrimination by size). Also, in order to tune the polarity of the cavities containing the colorimetric probes, post-grafting organic functionalization will be done. Polymeric matrix and non porous silica materials (silica fumed) will be prepared and its sensing behavior tested in order to compare with the results obtained when using porous supports.

- In order to test the versatility of these aniline-functionalized mesoporous or microporous materials, the aniline functionality will be used for the preparation of several organic dyes by using selected organic reactions.

- In order to improve the applicability in real sensing protocols, the prepared mesoporous materials will be supported in polymeric matrices. This new composite materials will be tested as a sensor and it will be compared with the sensing response for the corresponding components alone.

Advanced Materials, **2004**, 16, 1783-1786

4.2. Chromogenic discrimination of primary aliphatic amines in water with functionalized mesoporous silica.

Chromogenic discrimination of primary aliphatic amines in water with functionalised mesoporous silica.

María Comes,[a] M. Dolores Marcos,[a] Ramón Martínez-Máñez,*[a] Félix Sancenón,[a] Juan Soto,[a] Luis A. Villaescusa,*[a] Pedro Amorós,[b] Daniel Beltrán. [b]

[a] *GDDS, Dpto de Química, Universidad Politécnica de València, Camino de Vera s/n, E-46071 Valencia, Spain.*

[b] *Institut de Ciència dels Materials (ICMUV), Universitat de València, P.O. Box 2085, E-46071 València, Spain*

Advanced Materials, **2004**, 16, 1783-1786

A new approach to the design of chromogenic reagents is described using chromogenic molecules anchored onto modified MCM-41 type nanosized cavities as additional factor to enhance selectivity. Following this approach a remarkable chromogenic detection in water of primary aliphatic amines of a certain length is reported. The picture shows selective colour changes from magenta to yellow of the "sensing solid" **S3** in the presence of n-heptylamine, n-octylamine and n-nonylamine, whereas other longer or shorter primary linear aliphatic amines do not induce significant colour variation.

The field of chromogenic receptors for molecular sensing has grown in interest during the past years and a number of work has been devoted to the design and synthesis of new colorimetric reporters for a number of guests.[1] These designed probes have been primarily applied to the progress of chromogenic receptors for cations and more recently for anions.[2] However, related to this field, selective chromogenic chemosensors for target neutral organic guests are scarce. The relatively few examples reported usually follow a chemodosimeter approach in which the target molecule induces a specific chemical reaction (coupled with a colour change).[3] This chemodosimeter approach normally relies on the specific reactivity of a certain chemical functional group and seems to be one of the most promising routes to selective chromogenic receptors. However, the distinction of organic molecules containing the same functional group is hardly achieved and in general it might be said that, the distinction of a certain member of a family of similar organic molecules is a field barely studied within known sensing concepts.[4]

As a suitable mode to enhance selectivity we have focused our attention on mesoporous materials and in the design of hybrid solids capable of illustrating their ability of contributing to molecular recognition protocols.[5] Thus, although mesoporous solids have received much attention because of their potential use in catalysis, optical devices, nanotechnology, quantum dots, etc,[6] due to their large surface area, mechanical strength and homogeneous distribution of the pores, they have been by far much less studied in molecular or supramolecular recognition events and, as far as we know, have never been used as active systems in the chromogenic selective detection of target guests. The possibility of combining predefined selective chemical binding centres with selected physical properties of these solids (especially bio-

inspired properties such as the control of the hydrophobic properties near the recognition centre) might guide to promising multi-functional materials for new mesoscopic scale-based recognition procedures.[7] This can be achieved by chemically adjusting the pore surface properties to, for example, induce changes in the effective pore diameter or in the hydrophilic/hydrophobic properties of the nanoscopic pores. In this work we present the combination of different research fields such as chromogenic sensing and that of solid state chemistry as a route to develop systems for the enhanced colorimetric discrimination of very similar guests. We will illustrate this idea through the design of a "hybrid sensing solid" capable of discriminating among primary aliphatic amines of different lengths in water.

For this work the reactivity of the 2,4,6-triphenylpyrylium scaffolding[8] was used as chromogenic amine reporter. Specifically we made use of derivatives containing a 4-amino-phenyl group attached to the pyrylium framework.[9] This gave 4-(4-amino-phenyl)-2,6-diphenylpyrylium (see **I** in Scheme 1) groups, which are highly coloured (magenta, λ_{max} = 540 nm in acetonitrile). The reaction of the magenta derivative **I** with primary aliphatic amines in acetonitrile:water led to yellow solutions due to the formation of the corresponding pyridinium salt (see **II** in Scheme 1). This reactivity of **I** to give **II** was confirmed by studying the reactivity in acetonitrile of **I** with 1-butylamine (see Supporting Information).

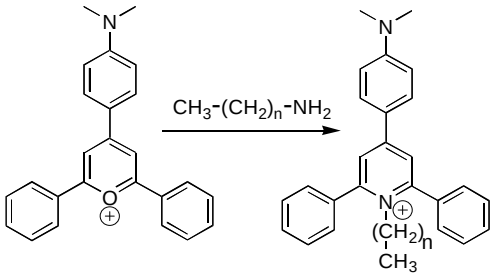

I **II**

Scheme 1. Reactivity of pyrylium derivatives to give pyridinium salts.

As a further step towards a new concept of selective chromogenic systems, the 4-(4-amino-phenyl)-2,6-diphenylpyrylium chromogenic derivative was anchored onto a porous solid. Actually, we have taken advantage of the special characteristics of the UVM-7 material in which mesoporous nanosized MCM-41 type particles are joined together in micrometric conglomerates giving rise to an important textural porosity that may facilitate the movement of the active species through the solid.[10] The synthetic procedure we have followed is depicted in Scheme 2. The trimethoxysilyl aniline derivative **III** was prepared by reaction of methylaniline and 3-iodopropyltrimethoxysilane. Incorporation of this precursor to the mesoporous solid was carried out through the co-condensation approach in order to obtain a highly dispersed organic moiety onto the pore surface. Removal of the surfactant by using well-established methods yielded solid **S1**. As the amount of the aniline derivative **III** loaded on **S1** was relatively small, it may still possess many dangling OH groups. In order to tune the polarity of the surface, hydrophobic moieties were anchored to the surface of **S1** by using hexamethyldisilazane.[11] This functionalisation process yielded solid **S2** (see *Scheme 2*).

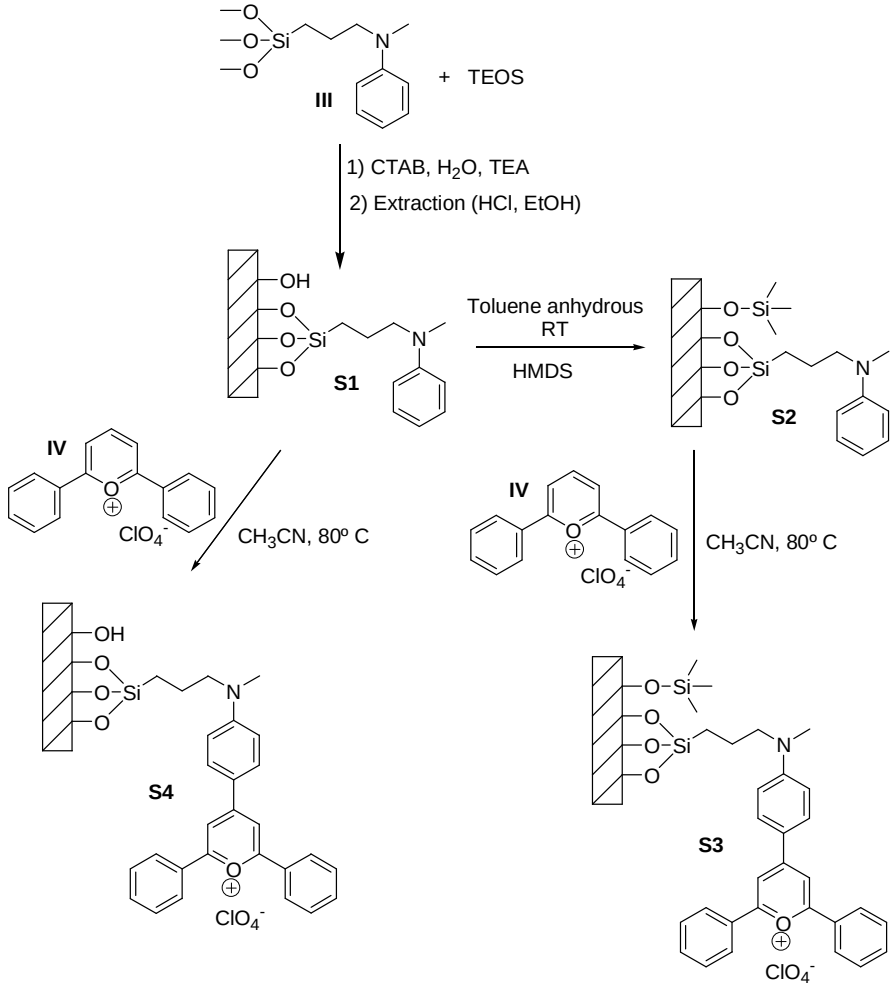

Scheme 2. Synthetic route to the solid sensor **S3.**

Further reaction of **S2** with diphenylpyrylium perchlorate gave the final mesoporous solid sensor **S3** as a red/magenta solid. For the sake of comparison, the solid **S4**, containing a hydrophilic inner pore surface, was also prepared from solid **S1** (see Scheme 2). Also for comparison purposes we prepared solid **S5** which is similar to **S3** (pyrylium-functionalised plus hydrophobic surface) but using a non-porous small particle silica matrix. Final solids were characterised by a number of techniques (see Supporting Information for details). X-ray diffraction

and SEM studies confirmed the presence of the UVM-7 mesostructure of the **S1**-**S4** solids. Aniline and methyl contents were determined by thermogravimetric and elemental analysis whilst UV-vis spectroscopy was used for chromophore determination. N_2 adsorption-desorption isotherms were used for the determination of pore size and specific surface area (see Table 1)

Solid	Aniline/SiO_2[a]	Pyrylium[a] /SiO_2	Methyl/SiO_2[a]	Pore size (nm)	Specific surface (m^2/g)
S3	$8.1x10^{-3}$	$5.2x10^{-4}$	0.59	2.4	668
S4	$1.0x10^{-2}$	$5.5x10^{-4}$	-	2.8	1042
S5	$4.2x10^{-3}$	$1.7x10^{-4}$	0.09	-	-

a: molar ratios

Table 1. Characteristics of solids **S3**, **S4** and **S5.**

Though there is no direct proof for the pyrylium location, the fact that the inner pore surface is larger than the external one and the presumed preferred localization of the aniline groups inside the mesopores strongly supports the idea that the molecular probes suitable for primary amines are confined in highly hydrophobic nanoscopic cavities in **S3**. On the contrary, the molecular reporters in **S4** are confined in hydrophilic cavities. Both **S3** and **S4** solids are optically transparent and highly coloured due to the presence of the 4-(4-amino-phenyl)-2,6-

diphenylpyrylium moiety. A schematic representation of the **S3** solid at nanometric and molecular level is shown in Scheme 3.

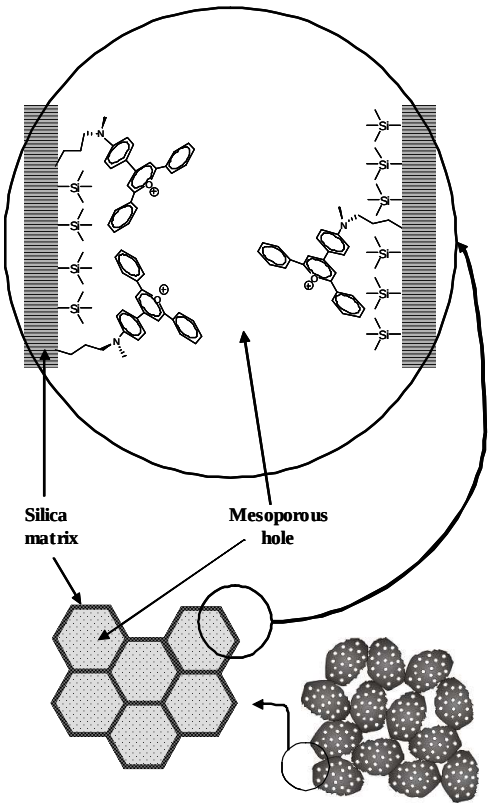

Scheme 3. Representation of the molecular and nanoscopic structure of solid **S3**

Solid **S3** shows some advantages respect to the parent compound **I**. Thus, whereas **I** is unstable at basic pH because of the nucleophilic attack by OH^- (colour change from magenta to yellow), solid **S3** remains magenta at basic pH (11.5) for weeks. Additionally, whereas **I** is not soluble in water, **S3** can be used in aqueous media. The sensing ability of the hydrophobic **S3** solid was studied in water through assays involving the addition of 250 equivalents (with respect to the pyrylium

receptor anchored to **S3**) of the corresponding guest to water suspensions of the essayed solid. The most remarkable result is the high level of selectivity found for **S3**. This is depicted in Figure 1 that shows the selective colour shift at 10 minutes from magenta (λ_{max} = 540 nm) to yellow (λ_{max} = 460 nm) only for "medium" chain amines such as n-heptylamine, n-octylamine and n-nonylamine, whereas no significant colour change is shown for amines with shorter and longer aliphatic chains. The change in colour is clearly ascribed to the formation of the pyridinium salt as shown in Scheme 1. In addition, the selectivity shown by solid **S3** for certain primary amines is quite noteworthy as this solid also remains silent upon addition of usually water-present anions and cations and also upon addition of alcohols, phenols, carboxylates, thiols and secondary, tertiary and aromatic amines.

For comparison, the same sensing assay was performed using **S4**. Remarkably, the response versus amines is strongly dependent upon the pore environment. Thus, **S4** remains silent in the presence of amines under similar conditions to those used with **S3** (see Figure 1). The only reaction observed in **S4** was the typical deterioration of non-hydrophobated silica solids when left under the hydroxyl ion attack during long periods of time. That lower reactivity of solid **S4** versus any amine is feasibly attributed to its hydrophilic character that would impose strong interactions between the amines and the numerous silanol groups at the surface making the diffusion of the amines from water to the pyrylium groups in the pores especially unfavourable. Under similar experimental conditions, the analogous molecular chemodosimeter **I** in acetonitrile:water 80:20 v/v solutions changed to yellow in the presence of primary amines. Figure 1 also shows the behaviour found for **S5**. As it can be seen short amines do not react with **S5**, probably due to their hydrophilic nature, whereas the remaining

amines (much more hydrophobic) gave reaction with the pyrylium reporter. This unspecific reactivity with long-chain amines is an expected behaviour for **S5** under the premise that the porous nature of the solids does actually play a fundamental role in the observed selectivity found for **S3**.

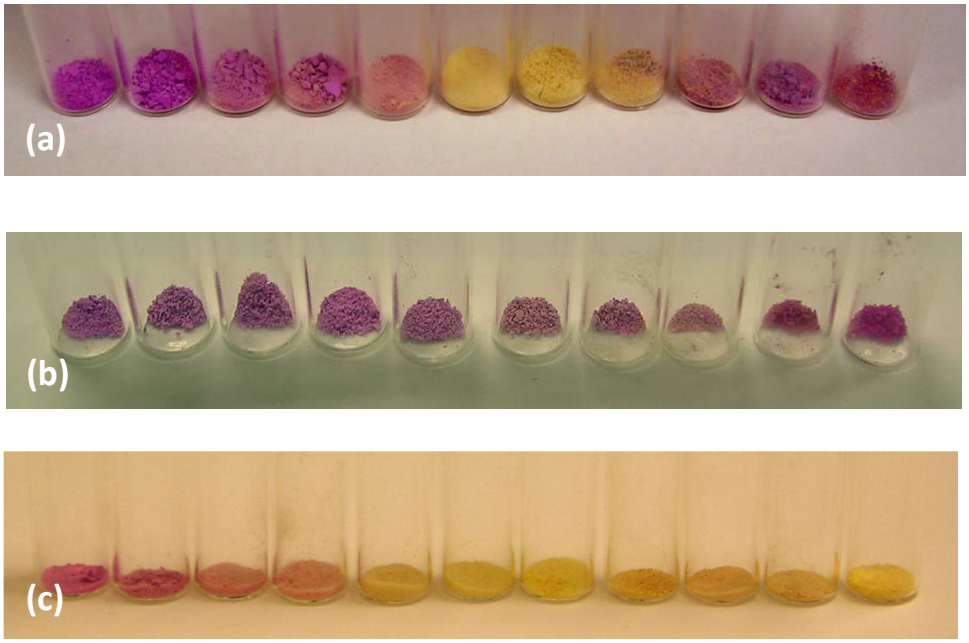

Figure 1. Photographs showing the colour developed by solids **S3** (a), **S4** (b) and **S5** (c) after being ten minutes in contact with linear primary aliphatic amines in water. (a) From left to right, no amine, n-propylamine, n-butylamine, n-pentylamine, n-hexylamine, n-heptylamine, n-octylamine, n-nonylamine, n-decylamine, n-undecylamine and n-dodecylamine. (b) From left to right, n-propylamine, n-butylamine, n-pentylamine, n-hexylamine, n-heptylamine, n-octylamine, n-nonylamine, n-decylamine, n-undecylamine and n-dodecylamine. (c) as in (a).

Solid **S3** displayed a remarkable enhanced selectivity as a consequence of two specific properties of this solid: the hydrophobicity of the inner

surface and the pore system. Thus, whereas the hydrophobic surfaces would favour the docking of large versus small guests to the active centres, the pore system might entail a different trend, favouring the entrance of small amines versus long chain ones. In addition, a "sealing off" effect might be associated with the guest size: the reaction of large amines with the most accessible active centres could hinder the accessibility of additional amines to other active centres placed more deeply into the pores. The stronger interaction of those larger amines with the hydrophobic surface might also reduce their diffusion through the solid and help the mentioned "sealing off" effect. These different tendencies might result in the overall observed behaviour as colour changes in **S3** are only found for relatively short but hydrophobic enough linear "medium" chain amines.

In conclusion, we have shown that the incorporation of organic chromogenic molecules to porous solids is a suitable approach for the design and development of highly selective chromogenic organic-inorganic hybrid solid "receptors" for the discrimination of similar organic guests in aqueous environments. The designed protocol takes advantage of chromogenic ideas but uses nanosized cavities and hydrophobicity as additional factors to enhance selective guest response, mimicking in some aspects the active site cavities found in biological receptors. Discrimination of closely related aliphatic amines by colour changes is not usual and to the best of our knowledge only a very recent example has been reported using molecularly imprinted polymers.[4a] The ideas reported here open the possibility of developing a new generation of tailor-made selective sensing systems built up by the fine control of the properties of both the molecular receptor and the solid. Especially, the anchoring of molecular reporters onto suitable siliceous mesoporous supports can be a promising tuning tool for

selectivity enhancement that might in principle be applied to the design of new chemosensors for a broad range of target species.

References.

[1] a) J.- M. Lehn, *Supramolecular Chemistry*; VCH: Weinheim, **1995**; b) M. Inouye, *Color. Non-Text. Appl.*, **2000**, 238.

[2] a) R. Martínez-Máñez, F. Sancenón, *Chem. Rev.* **2003**, *103*, 4419-4476; b) P. D. Beer, P. A. Gale, *Angew. Chem. Int. Ed.* **2001**, *40*, 486-516; c) P. A. Gale, *Coord. Chem. Rev.*, **2003**, *204*, 191-221.

[3] Some very recent chromoreactands for amines have been described for instance based on (trifluoroacetyl)azobenzene dyes and pyrylium cyanine dyes. a) G. J. Mohr, C. Demuth, U. E. Spichiger-Keller, *Anal. Chem.* **1998**, *70*, 3868-3873; b) R. Yang, K. Li, F. Liu, N. Li, F. Zhao, W. Chan, *Anal Chem.* **2003**, 75, 3908-3914. c) O.M. Kostenko, S.Y. Dmitrieva, O.I. Tolmachev, S.M. Yarmoluk, *J. Fluorescence*, **2002**, *12*, 173-175.

[4] a) E. Mertz, S. C. Zimmerman, *J. Am. Chem. Soc.* **2003**, *125*, 3424-3425; b) V. S.-Y. Lin, C.-Y. Lai, J. Huang, S.-A. Song, S. Xu *J. Am. Chem. Soc.* **2001**, *123*, 11510-11511; c) F. Sancenón, R. Martínez-Máñez, M. A. Miranda, M. J. Seguí, J. Soto, *Angew. Chem. Int. Ed.* **2003**, *42*, 647-650; d) G. J. Mohr, N. Tirelli, C. Lohse, U. E. Spichiger-Keller, *Adv. Mater.* **1998**, *10*, 1353-1357; e) E. K. Feuster, T. E. Glass, *J. Am. Chem. Soc.* **2003**, *125*, 16174-16175.

[5] a) A. B. Descalzo, D. Jiménez, M. D. Marcos, R. Martínez-Máñez, J. Soto, J. El Haskouri, C. Guillém, D. Beltrán, P. Amorós, M. V. Borrachero, *Adv. Mater.* **2002**, *14*, 966-969; b) A. B. Descalzo, D. Jiménez, J. El Haskouri, D. Beltrán, P. Amorós, M. D. Marcos, R. Martínez-Máñez, J. Soto, *Chem. Commun.*, **2002**, 562-563.

[6] a) C.-Y. Lai, B. G. Trewyn, D. M. Jeftinija, K. Jeftinija, S. Xu, S. Jeftinija, V. S.-Y. Lin *J. Am. Chem. Soc.* **2003**, *125*, 4451-4459; b) A. P. Wight, M. E. Davis *Chem. Rev.* **2002**, *103*, 3589-3614.

[7] S. Huh, J. W. Wiench, J. -C. Yoo, M. Pruski, V. S.-Y. Lin *Chem. Mater.* **2003**, *15*, 4247-4256.

[8] J. Staunton, *Compr. Org. Chem.* **1979**, *4*, 607-627.

[9] F. Sancenón, A. B. Descalzo, R. Martínez-Máñez, M. A. Miranda, J. Soto, *Angew. Chem. Int. Ed*. **2001**, *40*, 2640-2643.

[10] UVM-7 consist of soldered small (12–17 nm) mesoporous particles that generate a bimodal pore system of 3.0–3.2 nm surfactant mesopores and 20–70 nm textural pores, see J. El Haskouri, D. Ortiz de Zárate, C. Guillem, J. Latorre, M. Caldés, A. Beltrán, D. Beltrán, A. B. Descalzo, G. Rodríguez-López, R. Martínez-Máñez, M. D. Marcos, P. Amorós *Chem. Commun*. **2002**, 330–331.

[11] R. Anwander, I. Nagel, M. Widenmeyer, G. Engelhardt, O. Groeger, C. Palm, T. Röser *J. Phys. Chem. B.* **2000**, *104*, 3532-3544.

Advanced Materials, **2004**, 16, 1783-1786

Supporting Information

Chromogenic discrimination of primary aliphatic amines in water with functionalised mesoporous silica.

María Comes, M. Dolores Marcos, Ramón Martínez-Máñez, Félix Sancenón, Juan Soto, Luis A. Villaescusa, Pedro Amorós, Daniel Beltrán.

Study of the reactivity of I with amines.

Synthesis of **I** is straightforward and was achieved by reaction of 2,6-diphenylpyrylium perchlorate with N,N-dimethylaniline in DMF at 140ºC. Subsequent addition to the reaction crude of diethyleter afforded the desired receptor in 50% yield as a red-magenta solid. The utility of L^1 as chromogenic reagent was tested in water:acetonitrile 80:20 v/v in the presence of equimolar amounts of thiols, primary, secondary and tertiary aliphatic amines, aromatic amines, alcohols and phenols. Colour changes from magenta to yellow were only observed in the presence of primary aliphatic amines. The reaction is complete in some few minutes. Additionally to the color change, **I** can also act as a fluorogenic reagent. Thus, whereas the pyrylium derivative is not fluorescent the final pyridinium gave, upon excitation at 440 nm, an emission fluorescence band centered at 468 nm.

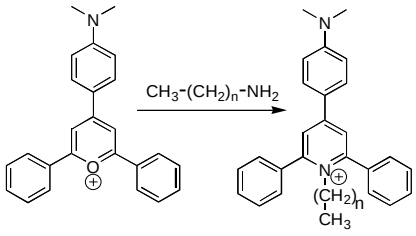

I **II**

Scheme 1. Reactivity of **I** with primary aliphatic amines.

^{1}H-NMR (CD_3CN) of **I** upon addition of 1-butylamine confirmed the formation of **II**. ^{1}H-NMR of 4-(4-dimethylamino-phenyl)-2,6-diphenylpyrylium perchlorate consists of a singlet centred at 3.31 ppm ascribed to the dimethylamino group and three groups of signals in the aromatic zone; two doublets centred at 7.05 and 8.37 ppm attributed to the 1,4-disubstitiuted aromatic ring, and a singlet centred at 8.35 ppm ascribed to the trisubstituted pyrylium ring. Upon 1-butylamine addition new resonances appeared being the most significant one triplet centred at 4.22 ppm attributed to the methylene directly attached to the quaternary ammonium nitrogen. The mass spectrum also confirmed that **II** is obtained upon addition of 1-butylamine to **I**.

Compound I: ^{1}H NMR (CD_3CN): δ = 3.30 (s, 6H, N*(CH$_3$)$_2$*), 7.05 (d, 2H, C_6H_4), 7.80 (m, 10H, C_6H_5), 8.33 (d, 2H, C_6H_4), 8.35 (s, 2H, C_5H_2O).

Compound II: ^{1}H NMR (CD_3CN): δ = 0.48 (t, 3H, N-CH_2-CH_2-CH_2-*CH$_3$*), 0.82 (q, 2H, N-CH_2-CH_2-*CH$_2$*-CH_3), 1.40 (q, 2H, N-CH_2-*CH$_2$*-CH_2-CH_3), 3.13 (s, 6H, N*(CH$_3$)$_2$*), 4.22 (t, 2H, N-*CH$_2$*-CH_2-CH_2-CH_3), 6.90 (d, 2H, C_6H_4), 7.73 (m, 10H, C_6H_5), 7.95 (d, 2H, C_6H_4), 8.03 (s, 2H, C_5H_2N). Mass spectrum m/z : 407.

Synthesis of materials S1, S2, S3 and S4.

The solids **S1**, **S2**, **S3** and **S4** were prepared following the route shown in Scheme 2.

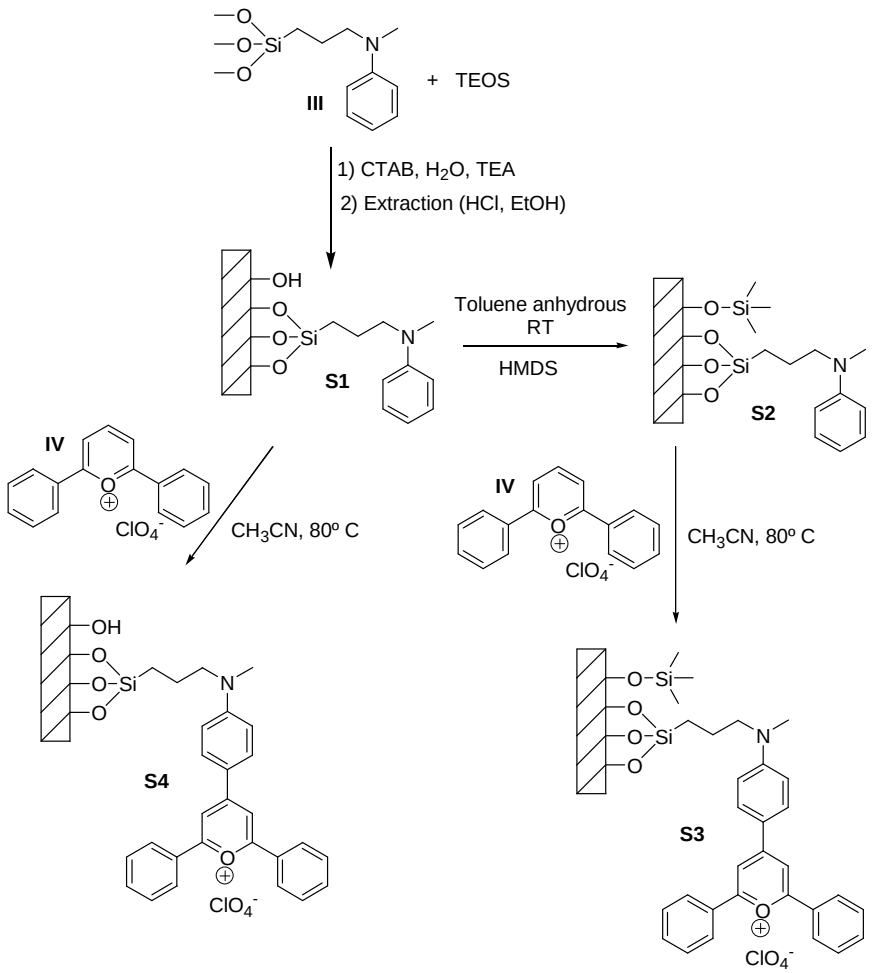

Scheme 2: Synthetic scheme for the preparation of the sensor materials **S1**, **S2**, **S3** and **S4**.

Synthesis of S1.

Compound **III** was quantitatively obtained as an oil by reaction of *N*-methylaniline with (3-iodopropyl)trimethoxysilane (unpublished results). Compound **III** was incorporated to a MCM-41 type solid following a co-

condensation procedure. The method is based on the use of a simple structural directing agent (CTAB:cetyltrimethylammonium bromide) and a complexing polyalcohol (2,2',2''-nitrilotriethanol, $TEAH_3$). Compound **III** was added to the $TEAH_3$ under stirring and heating at 120 ºC. Then, the mixture was cooled to 90 ºC and TEOS added. The mixture was again heated to 120 ºC and then CTAB and water was added at 80 ºC. The molar ratio of the reagents was adjusted to 3.5 $TEAH_3$: 0.985 TEOS: 0.015 A: 0.26 CTAB: 90 H_2O. The mixture was aged at room temperature for 24h. The resulting powder was collected by filtration, washed with water and ethanol and air-dried. The surfactant was extracted with a solution of HCl 1M in ethanol.

Synthesis of S2.

0.60 g of **S1** was dehydrated through azeotropic distillation using Dean-Stark trap. Then, 2.61 mL of $Me_3SiNSiMe_3$ (0.0124 mol) were added. After stirring the reaction mixture for 24 h at room temperature, the resulting powder (**S2**) was collected by filtration, exhaustively washed with toluene and acetone and air-dried.

Synthesis of S3.

To a suspension of the 0.35 g of the solid **S2** in acetonitrile, 0.63 mg of 2,6-diphenylpyrylium perchlorate (**IV**) (1.90 mmol) were added and the mixture heated at 80 ºC for 16 h. The resulting magenta/pink powder was collected by filtration, exhaustively washed with acetone and dried.

Synthesis of S4.

To a suspension of **S1** in acetonitrile (2 g), 2.14 mg of 2,6-diphenylpyrylium perchlorate (**IV**) (6.4 mmol) were added and the mixture heated at 80 ºC for 16 h. The resulting magenta/pink powder was collected by filtration, exhaustively washed with acetone and dried.

Synthesis of S5.

The same procedure as for **S3** but using silica fumed as supporting material.

Materials characterization.

X-ray measurements were performed with a Seifert 3000TT diffractometer using Cu Kα radiation. Thermo-gravimetric analysis of **S1**, **S2**, **S3** and **S4** materials were carried out with a TGA/SDTA 851e Mettler Toledo balance, with a heating program consisting in a first heating ramp of 10 °C per minute from 393 K to 1273 K, and then a plate at 1273 during 30 minutes. UV-Vis diffuse reflectance absorption spectra were recorded on a Perkin-Elmer Lambda 35 UV/VIS spectrometer. IR spectra were recorded on a Jasco FT/IR-460 Plus between 400 and 4000 cm^{-1} diluting the solids in KBr pellets. Scanning Electron Microscopy images were obtained on a Jeol JSM 6300 operated at 30kV. N_2 adsorption-desorption isotherms were recorded on a Micromeritics ASAP2010 automated sorption analyser.

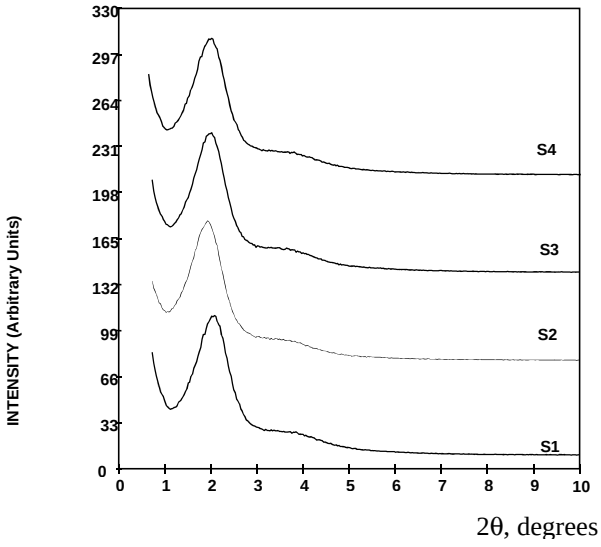

Figure I. X ray powder diffraction patterns for the solids **S1**, **S2**, **S3** and **S4**.

Elemental Analysis. **S1**: nitrogen 1.83%, carbon 3.18%, hydrogen 1.60%; **S2**: nitrogen 0.25%, carbon 12.71%, hydrogen 3.17%; **S3**: nitrogen 0.25%, carbon 12.02%, hydrogen 2.89%; **S4**: nitrogen 0.25%, carbon 3.69%, hydrogen 1.69%; **S5**: nitrogen 0.15%, carbon 3.82%, hydrogen 0.66%.

Figure I shows the powder X ray patterns of the four solids. The main features of a disordered MCM-41 phase typical for the UVM-7 material are clearly shown in the first **S1** material and remain in **S2, S3** and **S4** solids, suggesting that the structural ordering of the channels has not changed after each functionalization step. Thermo-gravimetric analysis curves for **S1**, show a weight loss of 24.17 % corresponding to solvents (T < 180 °C) and another weight loss of 5.40 % due to the decomposition of the organic groups (180 °C < T < 680 °C). For **S2**, a weight loss of 11.67 % due to the decomposition of the organic groups (180 °C < T < 680 °C) were recorded. TG analysis of the **S3** solid resulted in a decomposition curve from which a weight loss of 0.58 % corresponding to solvents (T < 180 °C) and another one of 11.32 % due to the decomposition of the organic groups (180 °C < T < 680 °C) were found. For **S4** solid TG analysis resulted in a decomposition curve from which a weight loss of 26.63 % corresponding to solvents (T < 180 °C) and another one of 7.00 % due to the decomposition of the organic groups (180 °C < T < 680 °C) were calculated. And finally, for **S5** solid TG analysis resulted in a decomposition curve from which a weight loss of 0.47 % corresponding to solvents (T < 180 °C) and another one of 7.02 % due to the decomposition of the organic groups (180 °C < T < 680 °C) were calculated.

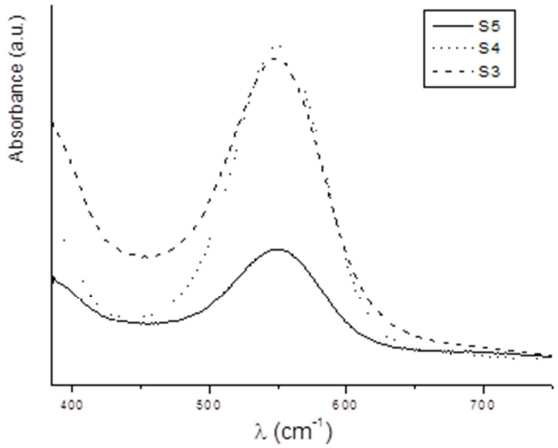

Figure II. UV-vis diffuse reflectance spectra of **S3, S4** and **S5** materials (ethylenglycol suspension).

In **Figure II**, the diffuse reflectance on an ethylenglycol suspension of **S3**, **S4** and **S5** solids are shown. Spectra were normalised to the same amount of residual SiO_2. Every solid presents a similar band centred at 540 nm related with the absorption of the pyrylium moiety indicating that both materials have been chromophore-functionalised in a similar extension. In order to get a quantitative analysis of the samples the pyrylium content was determined by dissolving 0.0035 g of the corresponding solid in acetonitrile where 15 μL of HF (48%wt in water) had been added. The UV-visible spectra of this mixture were registered and their pyrylium content was calculated by interpolation in a suitable calibration curve. From these data and the aniline, methyl and SiO_2 content obtained from TGA and EA, the overall composition of the solids was determined (see Table 1).

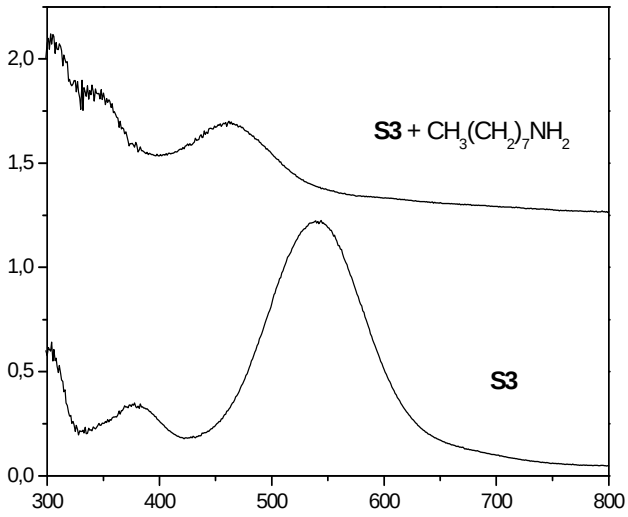

Figure III. UV-Visible diffuse reflectance spectra of solid **S3** after and before reaction with n-octylamine in water.

Figure III shows the UV-visible diffuse reflectance spectra of **S3** before and after mixing in water with 250 equivalents of n-octylamine. Upon addition of n-octylamine, the band at 540 nm, related with the absorption of the pyrylium moiety, disappears and a new absorption at 463 nm is observed. These colour transformations are similar to those found upon addition of primary aliphatic amines to solutions of **I** (magenta) in order to give **II** (yellow).

The most important differences in the infrared spectra are found from **S1** to **S2** solid, while **S2** and **S3** solids gave a quite similar spectrum. The infrared spectra showed an intensity decrease of the silanols band at 1080cm^{-1} in the spectra of the **S2** and **S3** materials and the appearance of new bands related to the functionalisation with CH_3 groups; stretching C-H vibrations at 2964cm^{-1} and bands between 850

and 600 cm^{-1} probably due to the stretching vibrations of the $Si(CH_3)_3$ moieties. Bands related to the pyrylium group have not been detected surely due to its low relative amount in the final solid **S3**. In the same way, **S4** spectrum is very close to that of **S1** as only a small amount of diphenylpyrylium has been anchored onto **S4**.

S1, **S2**, **S3** and **S4** gave SEM images of typical UVM-7 materials: nanometric particles joined together into micrometric conglomerates giving rise to its characteristic textural porosity. **S1, S2** and **S4** also show the same type of microstructure (see *Chem. Commun*. **2002**, 330 for a representative SEM image of UVM-7 materials).

S3 (**Figure IV**) and **S4** (**Figure V**) solids show N_2 adsorption-desorption isotherms similar to those of the parent UVM-7 material: curves with two adsorption steps (at intermediate and high P/P_0 values) related to their bimodal pore system. The first step corresponds to the nitrogen condensation inside the intra-nanoparticle mesopores (disordered MCM-41 type) and the second one to the condensation inside the interparticle large pores (textural porosity). The values of the pore size (BJH method) and the specific surface (BET model) are summarised in **Table 1** in the manuscript. The pore size distribution is shown as inset in the corresponding figures.

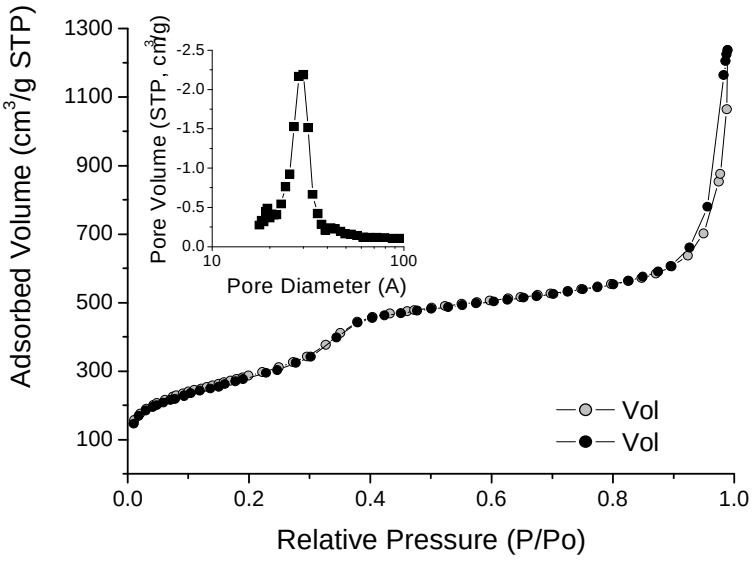

Figure IV. N_2 adsorption-desorption isotherms and pore size distribution (in the inset) for **S3** material.

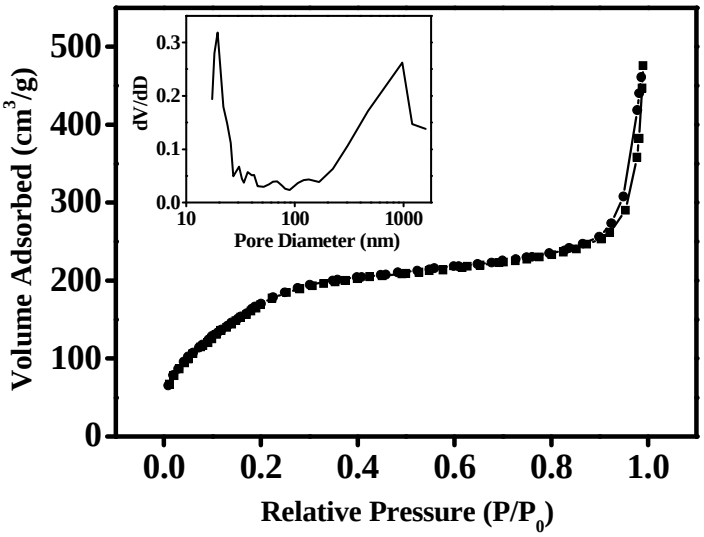

Figure V. N_2 adsorption-desorption isotherms and pore size distribution (in the inset) for **S4** material.

Chem. Commun. **2006**, 2239-2241

4.3. Sensory hybrid host materials for the selective chromo-fluorogenic detection of biogenic amines.

Chapter 4

Sensory hybrid host materials for the selective chromo-fluorogenic detection of biogenic amines.

Beatriz García-Acosta,[a] María Comes,[a] Julia L. Bricks,*[,b] Margarita A. Kudinova,[b] Vladimir V. Kurdyukov,[b] Alexei I. Tolmachev,[b] Ana B. Descalzo,[a,c] M. Dolores Marcos,[a] Ramón Martínez-Máñez,*[,a] Ana Moreno,[a] Félix Sancenón,[a] Juan Soto,[a] Luis A. Villaescusa,[a] Knut Rurack,*[,c] José M. Barat,[d] Isabel Escriche,[d] and Pedro Amorós [e]

[a] Instituto de Química Molecular Aplicada, Departamento de Química Universidad Politécnica de Valencia, Camino de Vera s/n, E-46071 Valencia, Spain. E-mail: rmaez@qim.upv.es

[b] Institute of Organic Chemistry, National Academy of Sciences 5 Murmanskaya St. Kiev-94, UKR-253660, Ukraine. E-mail: timophei@bricks.kiev.ua

[c] Div. I.5, Bundesanstalt für Materialforschung und –prüfung (BAM) Richard-Willstätter-Strasse 11, D-12489 Berlin, Germany. E-mail: knut.rurack@bam.de

[d] Departamento de Tecnología de Alimentos, Universidad Politécnica de Valencia Camino de Vera s/n, E-46022 Valencia, Spain.

[e] Institut de Ciència del Materials (ICMUV, Universitat de València P.O. Box 2085, E-46071 València, Spain.

Chem. Commun. **2006**, 2239-2241

Pyrylium-containing mesoporous materials have been used for the chromo-fluorogenic sensing of biogenic amines in aqueous environment.

Biologically active amines are ubiquitous chemical compounds that play an important role in many different areas. Depending on their chemical composition and origin, basically two different groups can be found. A major group are the so-called biogenic amines that are formed in the normal metabolism of animals, plants and micro-organisms via decarboxylation of the respective amino acid through substrate-specific enzymatic reactions. The formation of these biogenic amines is undesirable in foods and beverages because they can induce headaches, respiratory distress, heart palpitation and several allergenic disorders.[1] Histamine is the most toxic of the biogenic amines and the main cause of scombroid poisoning by acting synergistically with other amines. Thus, the level of biogenic amines in a food product is a quality index and the development of easy-to-use determination protocols of interest. The second group are fatty amines such as shingosine (a fatty amine that carries two additional hydroxyl groups in the polar head region) and its close metabolites that are important cellular messengers and have a profound impact on e.g. mitosis and apoptosis.[2] Other fatty amines, that usually stem form anthropogenic sources, are simple amines with chain length > C_{10} that find wide-spread application in corrosion inhibition, asphalt emulsions or as petroleum additives and are well known for their antifungal and disinfectant properties.[3] Accordingly, the toxicological role of the latter compounds has the largest impact on aquatic organisms and for instance in marine foodstuff, a combination of all these amines can be encountered.

All these amines are usually determined by chromatographic methods. However, these techniques are costly and not suitable for in-situ sensing or rapid screening applications. An appealing alternative is the use of selective chromo- or fluorogenic chemosensors.[4] In fact the development of highly selective probes or indicators for small bio-molecules is still a barely studied field.

One such advanced goal is the development of selective probes for real samples that would sense biogenic amines (first group, see above) via a simple chromo-fluorogenic test but would ideally remain silent in the presence of fatty amines (second group) and amino acids (another prominent source of amino moieties).

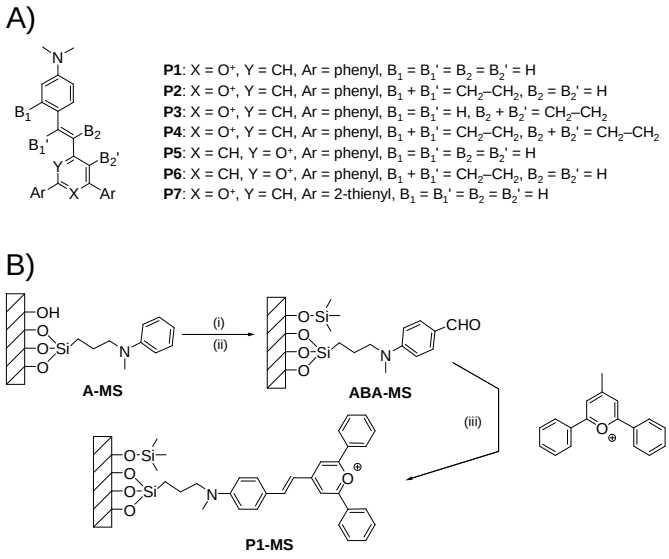

Scheme 1. A) Compound library of pyrylium dyes spectroscopically studied and tested as sensor molecules for biologically active amines. The corresponding methylpyridinium derivatives M1–M7 with $N^+–CH_3$ instead of O^+ have been also studied spectroscopically. B) Synthesis of solid P1-MS. (i) hexamethyldisilizane, toluene, room temperature, 16 h (ii) $POCl_3$ in DMF 1 h at 0 ^oC and then 3 h at 100 ^oC, (iii) 4-methyl-2,6-diphenylpyrylium, MeCN, 80 ^oC, 16 h.

To achieve this goal we focused our attention on pyrylium compounds. As others and we have shown previously, such heterocyclic ring systems react with amines to the corresponding pyridinium derivatives.[5] Furthermore, pyrylium and the respective pyridinium salts are strong electron acceptors so that appropriate integration into a charge-transfer chromophore yields deeply coloured dyes that absorb and emit in the red spectral range.[6]

The compounds **P1–P7** (pyrylium dyes) and **M1–M7** (methylpyridinium derivatives) (see Scheme 1) were prepared7 and investigated to select the optimum combination of pyrylium/methylpyridinium dye for the selective and sensitive detection of the target analytes. While all the P dyes absorb at ca. 640 nm in highly polar solvents, their different bridging patterns and positions of the reactive oxygen atom were assumed to influence selectivity. The decisive criterion for the **M** dyes, that serve as models for the product of the sensing reaction between amine and **P** dye, lies with signal output. Whereas the emission of differently rigidized styryl dyes is commonly found at similar wavelengths, their fluorescence yields often depend dramatically on the flexibility of the λ system.[8] Spectroscopic studies of the dyes revealed that three of the methylpyridinium dyes (**M1**, **M2**, **M4**) show reasonable fluorescence of $0.05 > \lambda_f > 5 \times 10^{-3}$ in MeCN in the red spectral range, at $\lambda_{max} \sim 660$ nm.

However, concerning a unique preference for biologically active amines, all the **P** dyes are rather unselective and thus not suitable as molecular sensors. At room temperature, they react with biogenic amines such as histamine, putrescine and cadaverine as well as with decylamine (as a representative of large lipophilic fatty amines) in mixed aqueous organic solutions (H_2O:MeCN 90:10 v/v) at basic pH, but also with a number of

natural amino acids, especially glycine, tyrosine, histidine, cysteine and lysine. As the best performance in this respect was found for **P1** and since **M1** is among the most fluorescent **M** derivatives, the pair **P1**/**M1** was selected for further improvement of the system.

Figure 1. Photograph showing the colour change in **P1**-**MS** in the presence of amino acids and biogenic amines. From left to right: no guest, glycine, valine, leucine, phenylalanine, proline, tyrosine, arginine, tryptophan, cysteine, lysine, histidine, histamine, putrescine and cadaverine. The final solids filtered and suspended in ethylene glycol are shown.

A way to overcome a lack of selectivity is to enhance host–guest interactions for the particular target analyte. Apart from the traditional design of complex hosts with multiple binding sites, enhanced selectivity can be obtained by coupling the probe to nanoscopic inorganic solids. Here, the use of mesoporous solids is highly suitable because, if properly functionalised, their rigid 3D nanoscopic scaffold can behave as a biomimetic prototype of "binding pockets" of bio-molecules.[9] Thus, to improve the analytical performance of the couple **P1**/**M1** we anchored **P1** covalently to the inner walls of the hydrophobically functionalised mesopores of a disordered MCM-41 type [10] hybrid material (Scheme 1).[11]

For comparison and to demonstrate the effect of the functionalised "binding pockets" on the final selectivity observed, two more systems were prepared; (i) the **P1**-**FS** solid containing **P1** probes anchored onto hydrophobized fumed silica (similar to **P1**-**MS** but without the presence of

mesopores) and (ii) a sensory PVC-membrane containing the dye **P1** and NPOE as plasticizer (**P1**-**PVC**).[12]

The performance of these materials was tested in water at pH 10.5 in the presence of biogenic amines and natural amino acids as potential competitors. The reaction of the blue materials (λ_{max} = 650 nm) with histamine, putrescine and cadaverine resulted in the evolution of a new band at 521 nm due to the formation of the corresponding pyridinium derivative (colour modulation from blue to red) within a few minutes for upper millimolar concentrations. Although lower concentrations require longer reaction times, the latter can be satisfactorily shortened by heating.

As an example, Figure 1 shows a photograph of solid **P1-MS** in the presence of amino acids and biogenic amines, whereas Figure 2 shows the fluorometric sensing features that allow, using relatively simple devices, a sensitive detection even at low biogenic amines concentration when the chromo-fluorogenic reaction is only partially completed. The emission of the reaction product can be conveniently monitored in the red visible range, the relationship between analyte concentration and response is linear, and the combination of the sensory materials (here **P1-MS**) with fluorometric detection is sufficiently sensitive to yield a limit of detection of 5×10^{-4} M of histamine.

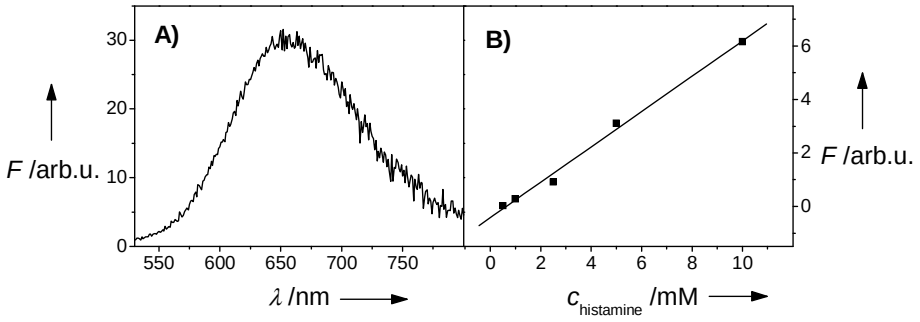

Figure 2. A) Emission spectrum of the P1-MS–histamine reaction product as measured for 0.01 mg mL^{-1} solid suspended in ethylene glycol; λ_{exc} = 490 nm. B) Corresponding calibration curve.

As it is shown exemplarily in Figure 1, there is a remarkably selective response to biogenic amines, whereas **P1-FS**, **P1-MS** and **P1-PVC** remain completely silent even in the presence of a very large excess of amino acids. Especially the discrimination of histamine over its closely related parent amino acid histidine and other amino acids with nucleophilic residues (e.g. lysine and cysteine) is a striking feature and clearly shows the improved response of the prepared sensory materials when compared to that of **P1** in solution under similar conditions (see above). Apparently, the confinement of the probe into hydrophobic systems prevents the anchored **P1** molecules from a nucleophilic attack of charged amino acids, i.e. hinders the amino acids to enter or approach the hydrophobic environments, while the neutral amines can still react.

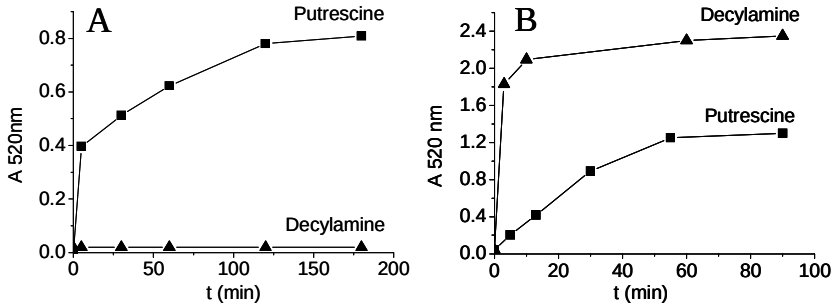

Figure 3. Absorbance vs. time at 520 nm in the presence of 300 ppm of putrescine or *n*-decylamine in water at 60 °C for the sensory materials A) **P1-MS** and B) **P1-PVC.**

This discrimination of biogenic amines vs. amino acids is very similar for the three sensory materials **P1-FS**, **P1-MS** and **P1-PVC**. However, they behave differently if discrimination by size and lipophilicity is considered. For instance, this differentiation is evident from a comparison of the reactivity of the solids with putrescine and a fatty amine such as *n*-decylamine. Here, **P1-PVC** reacts faster with *n*-decylamine than with putrescine, whereas in remarkable conrast the solid **P1-MS** displays a much faster reactivity for putrescine than for *n*-decylamine (similar results were obtained with histamine). This control in the selectivity can be seen in Figure 3 that shows the colour change (absorbance at 520 nm) in the presence of 300 ppm of putrescine or *n*-decylamine in water for the sensory materials **P1-MS** and **P1-PVC**. Finally, **P1-FS** display a rather similar reactivity for both amines (not shown).

This behaviour is tentatively attributed to the individual features of the different solids. **P1-PVC**, a highly disordered material with a large distribution of pore sizes, is clearly preferred by the fatty amines due to the highest lipophilic character of the three hybrids. **P1-FS**, conglomerates

of high-surface nanoparticles with a textural porosity, is largely indifferent toward the lipophilicity of the guest. On the other hand, the size discrimination observed for the MCM41-type **P1-MS** solid is based on the interplay between the passivated surface that tends to prefer more hydrophobic guests and the size of the ordered and rather uniform pores that tends to discriminate by size. Furthermore, during the course of an analysis, increasing reaction events will block the entrances of the channels more effectively for long-chain amines. These trends lead to the fact that amines with a medium-sized alkylic or alkylarylic end group exhibit a much faster response than the fatty amines. The combination of molecular concepts and pre-organized 3D solid state features thus display synergistic effects that allow to modulate simple hydrophobic discrimination toward a more sophisticated differentiation by polarity and size.[13]

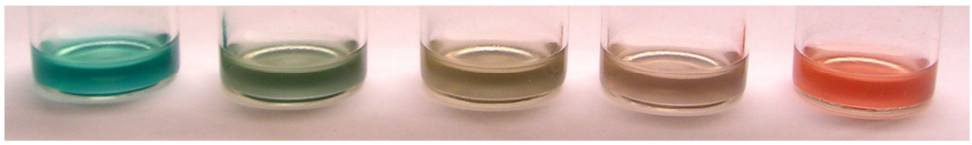

Figure 4. Photograph of a suspension of solid **P1-MS** in contact with aqueous extracts of gilthead bream (*sparus aurata)* at pH 10 with increasing amounts of histamine after 30 min of reaction at 50 °C. From left to right: $c_{\text{histamine}}$ = 0, 3.75 × 10^{-3}, 6.25 × 10^{-3}, 1.25 × 10^{-2} and 2.50 × 10^{-2} M.

Motivated by the favourable response features of the sensory materials, we tested the potential of **P1-MS** for the determination of biogenic amines in realistic media, extracts of fish (*sparus aurata*) spiked with increasing amounts of histamine. In a typical assay, 0.35 mL of an aqueous extract of *sparus aurata* (obtained from 10 g of the fish grinded up with 50 mL of water, heated and filtered or centrifuged) at pH 10 were mixed with known amounts of histamine and 1 mg of **P1-MS**. The gradual colorimetric

modulation was observed as a function of histamine concentration (Figure 4). This response, visible by the naked eye from blue to red-orange, in a complex realistic sample medium suggests that **P1-MS**, or similar systems, are promising optical sensors for the rapid screening of toxic biogenic amines in target foods.

In summary, we have shown the rational development of sensory materials for the chromo- and fluorogenic detection of biogenic amines in complex liquid samples. The probe molecule is a reactive pyrylium chromophore that is anchored into the inner hydrophobic pores of a mesoporous siliceous support. The solid **P1-MS** demonstrates that the combination of molecular concepts and 3D solid state preorganized features (for instance confinement in nanometric pores and hydrophobicity) might open new attractive and synergistic hetero-supramolecular routes to enhanced recognition/sensing protocols for species of interest.

Notes and references

[1] C. Ruiz-Capillas, F. Jiménez-Colmenero, *Crit. Rev. Food. Sci*. **2004**, 44, 489. M.H.

[2] M. Maceyka, S.G. Payne, S. Milstien, S. Spiegel, *Biochim. Biophys. Acta* **2002**, 1585, 193.

[3] J.A. Finlay, M.E. Callow, *Biofouling* **1996**, 9, 257.

[4] R. Martínez-Máñez, F. Sancenón, *Chem. Rev.* **2003**, 104, 4419.

[5] A.I. Tolmachev, N.A. Derevyanko, E.F. Karaban, M.A. Kudinova, *Khim. Geterotsikl. Soedin.* **1975**, 612. A.R. Katritzky, *Tetrahedron* **1980**, 36, 679. A.T. Balaban, A. Dinculescu, G.N. Dorofeenko, G.W. Fischer, A.V. Koblik, V.V. Mezheritskii, W. Schroth *Adv. Heterocycl. Chem.* **1982**, Suppl. 2, 1–404.

[6] J.L. Bricks, J.L. Slominskii, M.A. Kudinova, A.I. Tolmachev, K. Rurack, U. Resch-Genger, W. Rettig, *J. Photochem. Photobiol., A Chem.* **2000**, 132, 193.

[7] For general synthesis details see: ref 6; M Sczepan, W. Rettig, A.I. Tolmachev, V.V. Kurdyukov, *Phys. Chem. Chem. Phys.* **2001**, 3, 3555. R. Wizinger, P. Ulrich, *Helv. Chim. Acta* **1956**, 39, 207. M.A. Kudinova, V.V Kurdyukov, A.D. Kachkovskii, *Khim. Heterocycl. Soed.* **1998**, 494. Additionally compounds **P6** and **P8** were prepared by reaction of 2-methyl-4,6-diphenylpyrylium tetrafluoroborate or 2,3-trimethylene-4,6-diphenylpyrylium tetrafluoroborate, and 5-dimethylamino-1-indanone (cf. A.T. Brown, G. Hallas, R. Lawson, *Chem. Ind.* 1981, **7**, 248) in acetic anhydride at 125–130°C for 1 h.

[8] M. Sczepan, W. Rettig, A.I. Tolmachev, *Photochem. Photobiol. Sci*. **2003**, *2*, 1264.

[9] A.B. Descalzo, K. Rurack, H. Weisshoff, R. Martínez-Máñez, M.D. Marcos, P. Amorós, K. Hoffman, J. Soto, *J. Am. Chem. Soc.* **2005**, 127, 184. M. Comes, G. Rodríguez-López, M.D. Marcos, R. Martínez-Máñez, F. Sancenón, J. Soto, L.A. Villaescusa, P. Amorós, D. Beltrán, *Angew. Chem. Int. Ed*. **2005**, 44, 2918. D.R. Radu, C.-Y. Lai, J.W. Wiench, M. Pruski, V.S.-Y. Lin, *J. Am. Chem. Soc.* **2004**, 126, 1640. V.S.-Y. Lin, C.-Y. Lai, J. Huang, S.-A. Song, S. Xu, *J. Am. Chem. Soc.* **2001**, 123, 11510. M. Comes, M.D. Marcos, R. Martínez-Máñez, F. Sancenón, J. Soto, L.A. Villaescusa, P. Amorós, D. Beltrán, *Adv. Mater.* **2004**, 16, 1783,

[10] J. El Haskouri, D. Ortíz de Zárate, C. Guillém, J. Latorre, M. Caldés, A. Beltrán, D. Beltrán, A.B. Descalzo, G. Rodriguez-López, R. Martínez-Máñez, M.D. Marcos, P. Amorós, *Chem. Commun.*, **2002**, 330.

P1-MS and **P1-FS** possess a hydrophobic surface with a molar ratio of CH_3/SiO_2 = 0.33 and 0.25, respectively, and **P1** is incorporated with a molar ratio of pyrylium/SiO_2 = 6.38×10^{-4} and 2.28×10^{-4} into **P1-MS** and **P1-FS**, respectively. Additional characterization for **P1-MS**: Powder X-ray patterns show the presence of a disordered MCM-41 phase indicating that no changed after the functionalization process. IR spectra of **P1-MS** showed silanol bands at 1080 cm^{-1} and stretching C-H vibrations (from CH_3 groups) at 2964 cm^{-1} and bands in the 850-600

cm^{-1} range due to stretching vibrations of $Si(CH_3)_3$ moieties. Due to its low relative amount in the final solid, bands of the pyrylium group were not detected. N_2 adsorption-desorption isotherms showed a characteristic behaviour for a mesoporous material with a specific surface (BET model) of 753 $m^2\ g^{-1}$, a volume of 0.56 cc g^{-1} and a pore diameter (BJH method) of 2.51 nm.

P1-PVC was prepared by mixing **P1** (2 %wt.), poly(vinyl chloride) (49 %wt.) and nitrophenyl octyl ether (49 %wt.) in 5 mL of THF. The solvent was evaporated to give a blue-greenish membrane.

In preliminary studies we have observed that the sensory material **P1-FS**, **P1-MS** and **P1-PVC** can in part regenerated after their use by treatment with an acidic aqueous solution that partially liberates the original blue pyrylium probe. We will address this reactivity in the future, based on the detailed reaction mechanisms of pyrylium-pyridinium interconversion [see for instance A.T. Balaban et al, Pyrylium Salts: Syntheses, Reactions, and Physical Properties, in Advances in Heterocyclic Chemistry, **1982**, Suppl. 2, p. 114-115]. This reversible process points towards the possibility of using the sensory materials for repetitive cycles for qualitative purposes.

J. Mater. Chem., **2008**, 18, 5815-5823

4.4. Hybrid functionalized mesoporous silica-polymer composites for enhanced analyte monitoring using optical sensors.

Chapter 4

Hybrid functionalised mesoporous silica-polymer composites for enhanced analyte monitoring using optical sensors

María Comes,[a] M. Dolores Marcos,[a] Ramón Martínez-Máñez,*[a] Félix Sancenón[a], Luis A. Villaescusa[a] , Anja Graefe[b] and J. Gerhard Mohr*[b]

[a] Instituto de Química Molecular Aplicada, Departamento de Química, Universidad Politécnica de Valencia, Camino de Vera s/n, 46071, Valencia, Spain. rmaez@quim.upv.es

[b] Institute of Physical Chemistry, Friedrich-Schiller University Jena, Lessingstrasse 10, D-07743 Jena, Germany. gerhard.mohr@uni-jena.de

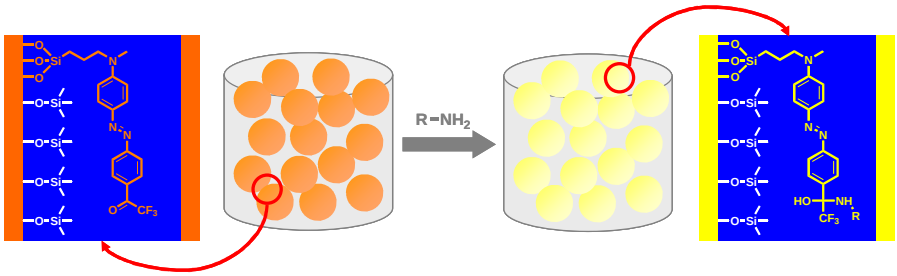

We report herein a new optical sensor for the colorimetric monitoring of aqueous amines designed by anchoring a suitable reactand on a 3D hybrid material that was further imbibed on a polymeric matrix. An azo chromophore containing a trifluoroacetophenone moiety was used as signaling reporter. In this system colour modulation is consequence of the reversible reaction of the amine with the trifluoroacetyl group that results in the formation of a hemiaminal. Based on this chemodosimeter approach but at the same time trying to enhance selectivity the chromoreactand was anchored in a first step onto suitable mesoporous nanoscopic hydrophobic pockets. As mesoporous system we selected an UVM-7 solid (a MCM41-type material) containing a homogeneous distribution of pores of about 3 nm and a specific surface of over 1000 m^2/g. For the preparation of the sensory material, in a first step, the dye precursor *N*-methyl-*N*-propyl-3-(trimethoxysilyl)aniline (**I**, MPTMSA) was mixed together with 2,2′,2′′-nitrilotriethanol, cetyltrimethylammonium bromide and TEOS to prepare the UVM-7 mesoporous functionalized solid **S1**. In a second step, and in order to tune the pore polarity, **S1** was further reacted with hexamethyldisilazane by blocking the dangling –OH groups introducing $–CH_3$ moieties. This second reaction yields **S2** that was, in a further step, reacted with trifluoroacetylaniline (TFAA) and sodium nitrite to yield the final mesoporous sensory solid **S3**. Whereas **S2** is colourless, **S3** shows an intense band centred at 510 nm that was assigned to the anchored azo dye. Prior to the immobilisation of the sensor particles **S3** in a polymer layer, the optical properties of **S3** were determined in the presence of aqueous amines. It was found that whereas the analogous molecular probe in solution gives an unspecific response, the hybrid sensory materials **S3** shows enhanced features in terms of selectivity only reacting with the not-too-large but lipophilic enough amines *n*-octylamine and *n*-decylamine. The material **S3** neither reacts with small hydrophilic amines (due to the hybrophobicity of the

inner pores in **S3**) nor with very large aliphatic amines (due to the size of the pore). In the second part of this work a composite material (**P-S3**) was prepared by mixing hydrophilic polyurethane polymer and **S3**. The X-ray diffraction patterns of **P-S3** displays the characteristic intense peak of the MCM-41 type mesoporous material and TEM images show a homogeneous dispersion of the nanometric mesoporous particles into the polymeric matrix. The measurements were carried out in a flow-through module connected to an optical fiber via a Y-probe at pH 9.5 (borax buffer). The **P-S3** composite retains the favourable features in terms of selectivity shown by **S3** and only displays a clear change in colour for *n*-octylamine, *n*-decylamine but no response to the remaining lineal primary amines. The response time of the sensor **P-S3** to solutions of these amines was in the range of few seconds, the regeneration time was between 5 to 10 min and the detection limit was $6x10^{-4}$ mol dm^{-3}. The sensor response was reproducible and reversible.

Introduction

One of the most appealing and promising fields within supramolecular chemistry is related with the preparation of receptors for the optical detection of target analytes. In this area chromogenic and fluorogenic sensors for metal cations[1] and anions[2] have been developed in the last twenty years, and there is a timely increasing interest in the design of chemosensors for neutral species[3]. In fact, the detection of electrically neutral guests is still a demanding task. Optical sensing using chemosensors is based on molecular entities built up by two components, namely the binding site and the signaling subunit. The binding site is designed to selectively coordinate target species whereas the signaling entity allows the visualization of the coordination event through colour changes or enhancement/quenching processes of the emission band. When changes in colour are based on a chemical reaction (reversible or irreversible) rather than the formation of non-covalent interactions (hydrogen bonding or/and electrostatic interactions) usually the terms "reactand" or "chemodosimeter" are applied[4].

Among different neutral analytes, the accurate determination of toxic substances such as amines has become significantly relevant in recent years.[5] Amines are ubiquitous biologically active compounds. For instance, amines are used in fertilizers, or can also be found in wastewater from the surfactant, pharmaceutical and dye manufacturing industries. Additionally, the concentration of amines is a quality criterion for food and beverages Common analytical methods for the determination of amines include chromatographic methods[6] and amperometric or potentiometric techniques,[7] polymer-coated piezoelectric sensors[8], or quartz crystal microbalances.[9] However some

of these techniques are high-cost and not suitable for *in situ* or *at site* determination or for rapid screening applications. In the latter case, optical and electrochemical sensing devices are mostly employed. In particular optical sensors[10] for the detection of amines where an indicator dye responds to the analyte by a change in color or fluorescence have been recently applied.[11] Some of these systems are based on the use of the trifluoroacetyl function in azobenzene[12] or stilbene[13] dyes.

With the aim to improve the use of optically active dyes for amine detection, chromogenic and fluorogenic molecules have traditionally been incorporated into polymeric matrices. In fact polymer materials have been widely used as suitable supports in the fabrication of ion-selective electrodes and optodes.[14] This is because polymers are usually chemically and physically stable materials able to achieve good operational lifetime and shelf-life. Polymers can be stable even at elevated temperatures, against ambient light and chemicals and it is not difficult to select non-toxic and biocompatible polymers especially for use in clinical and biochemical applications. Additionally, it is well-known that a suitable combination of polymers and plasticizers can play a remarkable role in the response of optical and electrochemical sensors.[15] However polymeric supports have certain limitations in relation to the sensing behaviour and usually they can only tune the response to certain analytes in terms of polarity and lipophilicity. Furthermore, a study with trifluoroacetyl dyes in different polymer matrices has shown that the matrix does not enhance or modify the selectivity in the recognition amines.[16] In addition, the used dye-receptors often show limited sensing features and it is not uncommon that they display optical changes in response to a wide range of compounds and are not able to discriminate similar guests from a family of related compounds.

From a different field, in the last years there has been increasing interest in the blending of supramolecular concepts with porous inorganic solids in order to obtain hybrid organic-inorganic materials with enhanced patterns of selectivity and new functional chemical properties.[17] For instance, it has been reported that the anchoring of suitable binding sites on the surface of certain preorganized solids leads to the formation of nanometer-sized binding pockets that mimic the behaviour of certain complex biological superstructures.[18,19] Although mesoporous solids have received much attention because of their potential use in catalytic processes or nanotechnology due to their large surface area, mechanical strength, and homogeneous pore distributions,[20] they still have scarcely been used for supramolecular recognition or sensing protocols.[21] Yet the combination of chemical binding centers with selected physical properties of mesoporous solids (especially bio-inspired properties such as the control of the hydrophobic properties near the recognition centre) is an appealing mode of modulate selectivity. However, these solid systems have traditionally been far from becoming optical sensors as they are usually obtained in the form of fine powder.

With the background of these three distant fields (i.e. solid state chemistry, supramolecular concepts and optical sensors design) we became interested in combining, as far as we know for the first time, the use of reactands for optical amine detection with hybrid materials and polymeric supports in order to prepare composite amine sensors. It was in our aim to demonstrate that the suitable blending of timely inorganic and polymeric materials with supramolecular concepts can lead to the design of final sensing devices showing enhanced features in terms of selectivity and reversibility.

Results and discussion.

Preparation of functionalised mesoporous material and preliminary reactivity studies

The chemodosimeter approach is one of the methods used for the development of optical probes for neutral analytes. These chemodosimeters are based on specific chemical reactions (usually irreversible, although they can also be reversible) induced by the presence of target species coupled with significant colour or emission changes. Several reactands have been recently reported for the colorimetric detection of amines. In this line it has been shown that the anchoring of a trifluoroacetophenone moiety into certain dye scaffolds is a suitable approach for the preparation of chemodosimeters for amine sensing.[22] In these systems the sensing principle for the colour modulation is the consequence of two chemical reactions, i.e. conversion of the trifluoroacetyl group into a diol upon interaction with water (during conditioning of the chemosensor), and further conversion of the diol into a hemiaminal upon interaction with amines (see Scheme 1).[23]

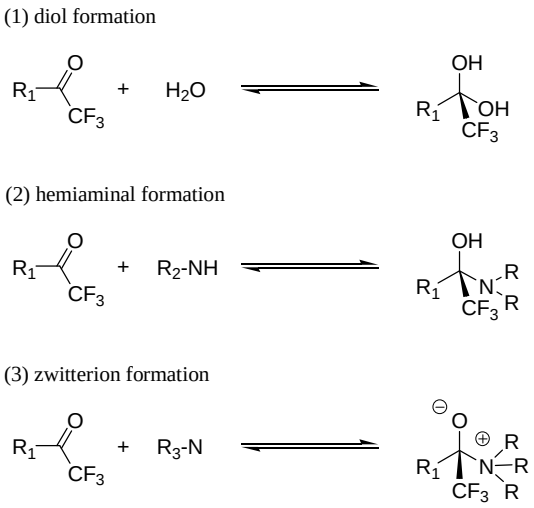

Scheme 1. Reactions of 4-trifluoroacetyl derivatives with (1) water and (2) primary and secondary amines.

In the work we show herein we have chosen as dye an azo chromophore (see Scheme 2). In this scaffold, the dialkylamino group acts as electron donor, whereas the acceptor part of the molecule is the trifluoroacetyl moiety. This class of compounds, upon interactions with amines, shows a decrease of the wavelength at around 500 nm and an increase of a new band at 420 nm. The change in colour is due to the modification of the acceptor ability of the trifluoroacetyl group after conversion into the corresponding hemiaminal.

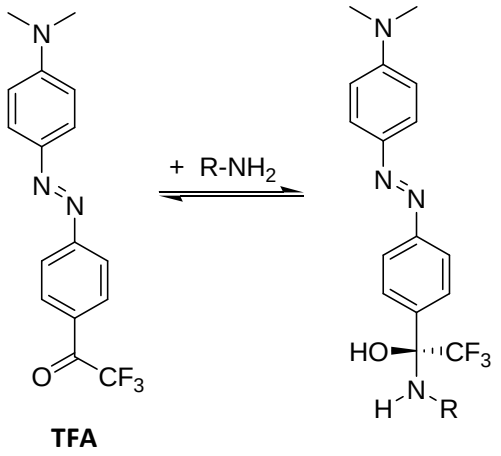

TFA

Scheme 2. Reaction of primary amine with 4-trifluoroacetylazobenzene (TFA).

Based on this chemodosimeter approach but at the same time trying to develop advanced materials showing enhanced optical features for monitoring primary amines, we have designed in a first step a suitable route for the anchoring of the chromoreactand onto mesoporous nanoscopic hydrophobic pockets. This was carried out with the aim of increasing selectivity (see below). As stated in the introduction, among different inorganic support, scaffolds containing pre-organised structural features are especially appealing. Among them, mesoporous MCM41-type materials are very promising supports containing a homogeneous distribution of pores of *ca*. 2-3 nm and a very large specific surface of

over 1000 m^2/g.[24] These supports can easily derivatised with a large range of functional groups. Within the family of MCM41-type mesoporous materials we have used UVM-7 solids which consists of MCM-41 mesoporous nanosized particles joined together in micrometric conglomerates resulting in an important textural porosity in the range of the 40 to 70 nm that facilitate the movement of the active species through the solid.[25] The route for the preparation of the sensory material **S3** is shown in Scheme 3. A protocol based on the inclusion of an organic dye precursor in the synthesis gel for the preparation of the mesoporous UVM-7 phase was employed. This method was selected because it is generally admitted that co-condensation procedures place the organosilane moiety preferentially inside the mesoporous channels rather than on the external surface. N-Methyl-N-(propyl-3-trimethoxysilyl)aniline (**I**, MPTMSA) was employed as the dye precursor. **I** is stable under the severe conditions employed for the surfactant extraction in order to create the mesoporosity. In a first step MPTMSA was mixed together with 2,2',2''-nitrilotriethanol ($TEAH_3$), cetyltrimethyl-ammonium bromide, (CTAB), tetraethoxysilane (TEOS) and H_2O to prepare the UVM-7 mesoporous functionalised solid **S1**. After the surfactant extraction, in a second step, and in order to tune the polarity of the surface, **S1** was further reacted with hexamethyldisilazane (HMDS) in order to "block" the dangling –OH groups introducing $-CH_3$ moieties. Reaction with the hexametyldisilazane must be carried out in this stage before the dye (TFA) is prepared because of the reactivity of HMDS and the TFA derivative. The second reaction yields the highly hydrophobic **S2** material (see Scheme 3). In the final step the solid **S2** was reacted with trifluoroacetylaniline (TFAA) and sodium nitrite to yield the final mesoporous sensory solid **S3** as an orange powder.

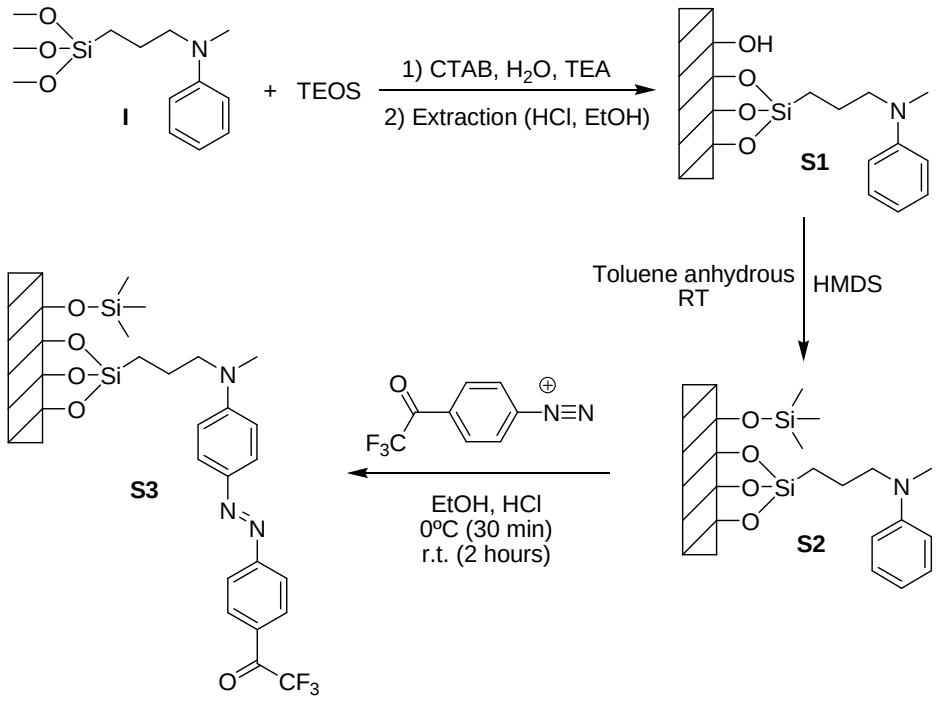

Scheme 3. Synthesis of the azo dye covalently anchored to the mesoporous silica.

Solids were characterised using standard procedures. X-Ray diffraction patterns of the hybrid materials **S1**, **S2** and **S3** are shown in Figure 1. For all the solids, the characteristic intense peak of a surfactant-assisted mesoporous material at *ca*. 2θ = 2º can be observed, indicating that the different synthesis steps have no significant effect on the mesoporous structure of the silica matrix. Additionally to the expected mesoporous system, the bimodal pore array characteristic of the UVM-7-like solids can be appreciated through TEM and porosimetry measurements. Figure 2 shows a representative TEM image of **S3** showing the nanoparticle architecture and the bimodal hierarchic pore organization typical of UVM-7 silicas. The hybrid material **S1** and **S2** display similar TEM images

(not shown). The solid **S3** has also been studied *via* N_2 adsorption-desorption isotherms. The isotherm for **S3** shows two steps. The first, at $0.2 < P/P_0 < 0.6$ originates from the capillary condensation of N_2 into the mesopores. There is no hysteresis loop in this interval and the pore distribution is very narrow suggesting the presence of uniform cylindrical mesopores. For this step a pore diameter of 2.71 nm and a pore volume of 0.32 $cm^3\ g^{-1}$ were calculated. The second step, at higher relative pressures, is related with the filling of textural inter-particle pores typical of the UVM-7 scaffolding. In this case, the curves show hysteresis and a broader pore distribution. A volume of 0.60 $cm^3\ g^{-1}$ and a diameter of 42.8 nm for the textural pore were determined. The specific surface area was calculated from a BET[26] treatment of the isotherm, and volume of the pore size was estimated from the BJH method[27] (see Table 1).

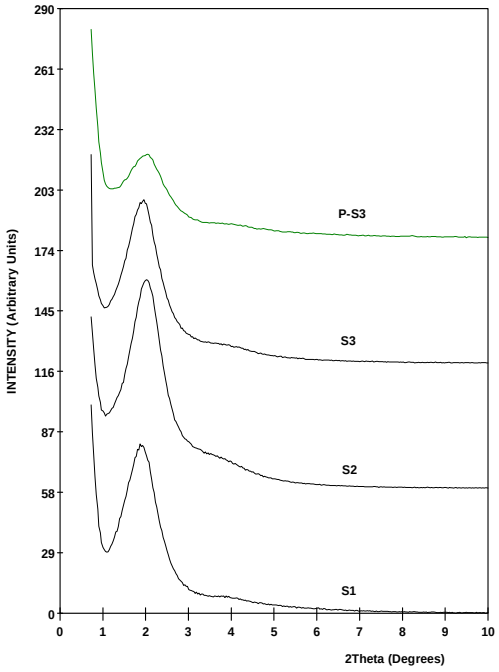

Figure 1. Powder X-ray diffraction patterns of solids **S1**, **S2**, **S3** and the polymeric composite **P-S3.**

Table 1. BET specific surface values, pore volume and pore size calculated from the N_2 adsorption-desorption isotherms for some of the materials.

	S_{BET} ($m^2\ g^{-1}$)	V_{text} [a] ($cm^3\ g^{-1}$)	D_{text} [a] (nm)	V_{meso} [b] ($cm^3\ g^{-1}$)	D_{meso} [b] (nm)
UVM-7[c]	1075	1.42	66.5	0.98	2.97
S3	451.9	0.60	42.8	0.32	2.71

[a] Volume (V) and diameter (D) of textural pore. [b] Volume (V) and diameter (D) of mesopore. [c] Values taken from ref. 25.

When comparing these data with those for the non-functionalised solid UVM-7 (mesoporous pore diameter and pore volume: 2.97 nm, 0.98 $cm^3\ g^{-1}$; textural pore diameter and pore volume: 66.5 nm, 1.42 $cm^3\ g^{-1}$) it is evident that the higher degree of functionalization in **S1-S3** results in a reduction of both mesoporous and textural pores, which indicates the presence of the active sites on the inner surfaces of the solid.

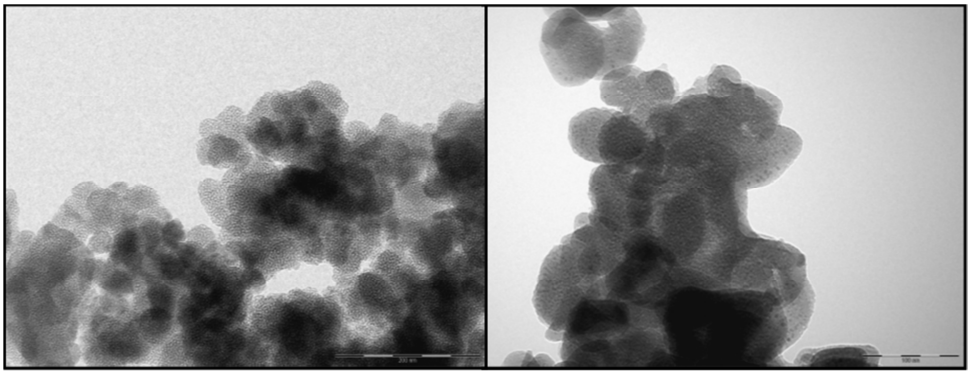

Figure 2. TEM images of solid **S3** (left, the bar corresponds to 200 nm) and the composite **P-S3** (right, the bar corresponds to 100 nm).

IR spectra were recorded between 400 and 4000 cm^{-1} by diluting the solids in KBr pellets. The most important feature is an intensity decrease of the silanol band at 950cm^{-1} in **S2** and **S3** when compared with **S1** and the appearance of a new bands related to the functionalisation with CH_3 groups; i.e. stretching C-H vibrations at 2964 cm^{-1} and bands between 850 and 600 cm^{-1} probably due to Si-C vibrations of the $Si(CH_3)_3$ moieties. Bands related to the azo group have not been detected surely due to the relatively low amount in the final solid **S3**. The loading for **S1**, **S2** and **S3** was determined by elemental analysis and thermo-gravimetric (TGA) studies. From the elemental contents (C, H, N), the loading of the aniline moiety in **S1**, the CH_3 content in **S2** and **S3** and the amount of azo dye in **S3** were calculated (see Table 2).

	Aniline [a] mmol g^{-1}	*CH_3* [a] mmol g^{-1}	*Azo dye* [a] mmol g^{-1}	*$Si(CH_3)_3$* [b] groups nm^{-2}	*Azo dye* [b] groups nm^{-2}
S1	0.16	-		-	-
S2	0.14	9.82		3.0	-
S3	0.14	9.82	0.087	3.0	0.078

[a] Aniline, CH_3 and azo dye groups in mmol per gram of SiO_2 in solid **S3**.
[b] $Si(CH_3)_3$ and azo dye groups per nm^2 in solid **S3**.

Table 2. Aniline, CH_3 and azo dye moles per SiO_2 gram and estimated inter-group distances for the prepared materials.

From these studies a clear increase of the organic material from **S1** to **S3** is observed. **S1** has a content of 0.16 mmol of aniline groups per gram of SiO_2. This content approximately remains in the methyl-functionalised solid **S2** (0.14 mmol/g SiO_2). The reaction of **S1** with the hexamethyldisilazane to give **S2** results in the formation of the hydrophobic solid for which a content of 9.82 mmol of CH_3 groups per gram of SiO_2 was found. The reaction of **S2** with TFAA and sodium nitrite yields solid S3 that contains the trifluoroacetylazobenzene-derivative dye anchored on the mesoporous surface (see Shceme 3). From TGA

and elemental analysis a content of 0.09 mmol of dye/g SiO_2 in **S3** was determined.

Taking into account these data and the value of the specific surface of the UVM-7 scaffolding, the average coverage (β_A in groups per nm^2) of the surface by the azo derivative in **S3** solids and the $Si(CH_3)_3$ groups in **S2** and **S3** was calculated (see Table 2) using equation (1).

$$(1) \qquad \beta_A = \alpha_A \times 10^{-3} \times S^{-1} \times 10^{-18} \times N_A = \alpha_A \times S^{-1} \times 602.3$$

where α_A is the dye content (mmol/g SiO_2) and S is the specific surface ($m^2\ g^{-1}$) of the **UVM-7** material and N_A is the Avogadro's number. From equation (1) a surface coverage of *c.a.* 0.078 azo dyes per nm^2 was calculated for solid **S3** and a surface coverage of *ca.* 3.0 $Si(CH_3)_3$ groups per nm^2 was found for **S2** and **S3**. The formation of the azo dye inside the mesoporous scaffolding when **S2** is transformed to **S3** was clearly assessed by recording the UV-Vis spectra of solid **S3** (suspended in ethylene glycol) by diffuse reflectance. Thus, whereas **S2** is colourless, **S3** shows an intense band centred at 510 nm that was assigned to the anchored azo dye. This band is bathochromically shifted by 30 nm when compared with the band shown by the parent dye TFA in acetonitrile solutions most likely due confinement effects related to the highly hydrophobic environment around the dye on the pore voids.

The reactivity and optical properties of 4-(N,N-dimethyl-amino)-4'-trifluoroacetylazobenzene (see TFA in Scheme 2) have been recently studied and described in detail elsewhere.[28] As stated above the reaction of TFA with amines results in the conversion of the trifluoroacetyl form into the hemiaminal and the corresponding shift of the maximum in the

spectrum from *ca*. 490 nm to *ca*. 420 nm. The absorbances of TFA-like derivatives with aliphatic primary, secondary and tertiary amines are comparable, although the reaction rate of the dye with primary amines (few minutes) is much faster than with secondary or tertiary amines (several hours). Also the reactivity of TFA-like derivatives is slower with alcohols, this behavior being most likely due to the higher nucleophilicity of amines. Less nucleophilic amines such as aniline and pyridine do not react with TFA. However, although TFA is able to colorimetrically discriminate between amines of different nucleophilicity it is unable to distinguish from similar nucleophilic amines. Thus, for instance TFA-like derivatives respond in a similar manner to different linear primary amines.[29] The increase of selectivity in these TFA-like structures would require an extraordinary synthesis effort, for instance by creating host structures that could additionally control the reactivity of the trifluoroacetyl group as a function of the shape of the amines.

CH_3-$(CH_2)_n$-NH_2					
	n=2	5	7	9	11
S3	-	-	x	x	-
TFA	x	x	x	x	x

[a] x = strong response; - = no response

Table 3. Chromogenic response of **S3** to aqueous amines[a].

S3 is a hybrid material containing the signaling amine indicator dye anchored on hydrophobic 2.3 nm sized nanoscopic pockets. In preliminary studies, in order to show the enhanced selectivity of **S3** when compared with the analogous molecular based receptor, and prior to the incorporation of the sensory material into the polymeric membrane, the optical properties of **S3** were determined using a variety of aqueous amine solutions. In a typical assay 5 mg of **S3** were exposed to different aqueous solutions of lineal amines at pH 9.5 (C_{amine} = $1 \cdot 10^{-3}$

mol L^{-1}). Then the solid was filtered and its UV-vis spectrum recorded. The results are summarized in Table 3. It was clearly shown that only *n*-octylamine and *n*-decylamine are able to induce a colour modulation in **S3**, whereas the solid remained silent in the presence of shorter (*n*-propylamine, *n*-hexylamine) and larger (*n*-dodecylamine) amines.

There is a very remarkable difference between the response of the solid **S3** and that found for TFA both in solution and in organic polymer sensor layers. The selectivity of polymer sensor layers based on TFA for amines is governed by both the chemical reactivity of the amine (i.e. the amine's nucleophility and the steric hindrance of bulky alkyl chains to allow interaction with the trifluoroacetyl group) and by the amine's lipophilicity that affects its extraction into the liphophilic polymer layer (described by the 1-octanol/water partition coefficient).[30] Consequently, the observed sensitivity within primary amines is higher for more lipophilic 1-hexylamine (log K_{OW}=2.06, K^{opt}= 600 M^{-1}) than for 1-propylamine (log K_{OW}=0.48, K^{opt}= 20 M^{-1}) although both show similar chemical reactivity with TFA in acetonitrile (comparable association constants K_{assoc} of 280 M^{-1}). Diethylamine is sterically hindered in its chemical reaction, and consequently the K_{assoc} value is lower than for primary amines (namely 11 M^{-1}). As a result, the K^{opt} value for diethylamine (log K_{OW}=0.58, K^{opt}= 1.7 M^{-1}) is lower by a factor of 10 compared to 1-propylamine, although both have comparable lipophilicity. This pattern of TFA with respect to selectivity can not be modified, neither by changing the organic solvent for TFA nor by changing the polymer matrix which TFA is immobilized.[16] In contrast, the hybrid material **S3** shows enhanced selectivity preferentially reacting with the not-too-large but lipophilic enough amines *n*-octylamine and *n*-decylamine. **S3** reacts neither with small hydrophilic amines (due to the hybrophobicity of the inner pores in **S3**) nor with very large aliphatic

amines (due to the size of the pores). Figure 3 shows the diffuse reflectance spectra of solid **S3** before and after reaction with *n*-octylamine. **S3** exhibits the characteristic charge-transfer band centered at 510 nm that undergoes a blue shift to 458 nm upon reaction with the amine.

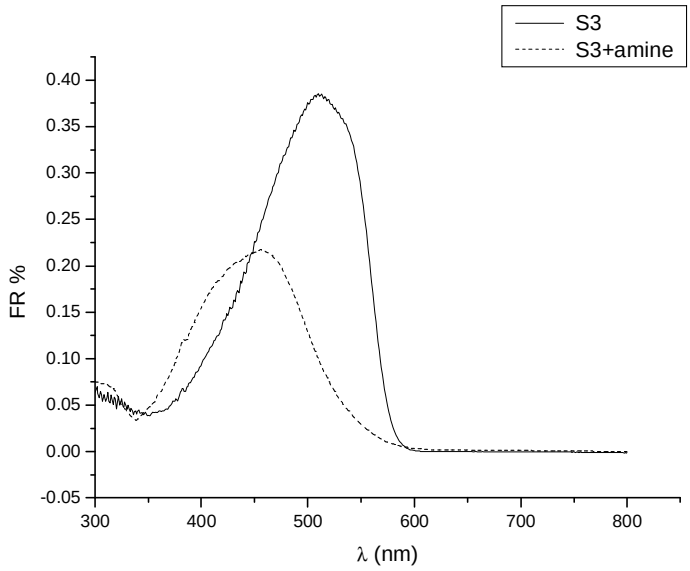

Figure 3. Diffuse reflectance spectra in water suspension of solid **S3**, before and after the addition of *n*-octylamine (C=2 x 10^{-3} mol L^{-1}).

In summary, as a result of the probe confinement onto nanopores an enhanced selective chromogenic response is found and solid **S3** is capable of chromogenically discriminating certain analyte within a set of similar organic molecules having the same functional group. Despite these favourable features, solid **S3** is obtained as a powder and in this form is poorly applicable in real samples and is not suitable for calibration and for continuous monitoring of amines. Thus, in the second part of this work we have explored studied the possibility of incorporating the material **S3** into a polymeric matrix in order to prepare

hybrid mesoporous silica-polymer composites for the development of an optical amine sensor having a synergic combination of the favourable features of the polymeric matrix and the mesoporous solid.

Preparation of the polymer-mesoporous composite as optical sensors for amines

In the design of the polymer-mesoporous composite it is possible to select different polymeric matrices. However, it has to be taken into account that part of the selective behaviour shown by **S3** is due to the hydrophobic nature of the pores. Therefore, the use of hydrophobic polymers that could compete with the selectivity trend of **S3** is not advisable. In fact, preliminary studies demonstrated that **S3** does not display selective sensing features when placed in lipophilic polymers such as poly(vinyl acetate), poly(methyl methacrylate) or polystyrene derivatives. For this reason, the composite material was prepared by mixing a hydrophilic polyurethane polymer (Hydromed D4) and the mesoporous material **S3**. The mixture was stirred for 1 hour in chloroform and then an aliquot of the suspension was transferred onto the polyester layer which acts as the mechanical support for the sensor. The final sensor membrane, **P-S3**, was placed in ambient air for drying. XRD, and TEM microscopy techniques were employed to characterize the composite. The X-ray diffraction patterns of **P-S3** displays the characteristic intense peak of the MCM-41 type mesoporous material at *ca*. 2θ = 2º (see Figure 1), whereas the TEM images (see Figure 2) shows the characteristic bimodal pore array of the UVM-7-like solids. TEM images also show a homogeneous dispersion of the nanometric mesoporous particles within the polymeric matrix. Both, X-ray patterns and TEM images are very similar to those found for **S3** alone indicating that the incorporation into the polyurethane polymer has not effect in

the characteristics of the mesoporous phase. A representation of the **P-S3** composite is shown in Figure 4.

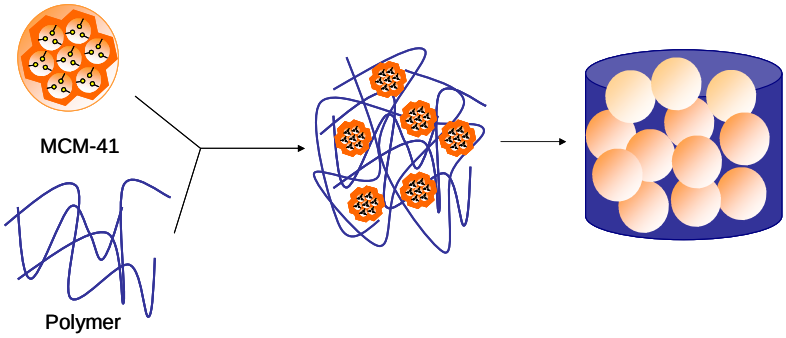

Figure 4. Graphical representation of the synthesis of the **P-S3** composite.

The corresponding solids **S1** and **S2** did not show amine sensing features and therefore were not incorporated into the polymeric matrix. The measurements with the sensor layer were carried out in a flow-through module connected to an optical fiber *via* a Y-probe. A schematic representation of the measuring system used in shown in Figure 5.

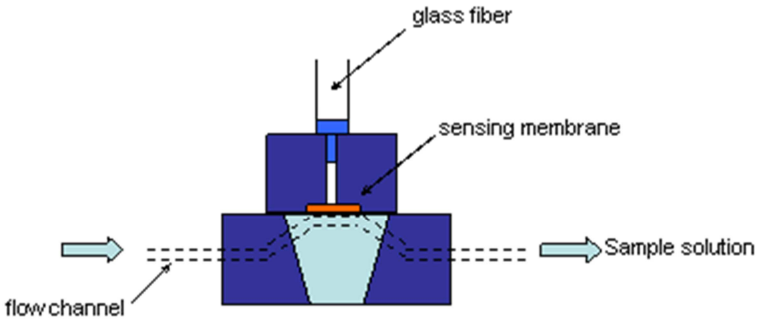

Figure 5. Schematic set-up of the transflectance probe, a fibre-optical Y-probe in contact with the optode membrane within the continuous-flow module.

The pH of the amine solutions was controlled with a borax buffer at 9.5. At this pH it was confirmed that both the polymeric matrix and the hydrophobic mesoporous solid were stable. Thus, although it has been

reported that silica matrices are not stable at basic pH, we confirmed that solid **S3** remained without decomposition in this media most likely due to its high hydrophobicity. Previously to the measurements with **P-S3**, the film is introduced into the buffer solution overnight, to ensure an appropriate degree of humidity inside the membrane which, in addition, avoids swelling of the polymer during the measurements.

The membrane shows significant absorbance modulations on exposure to certain aqueous amine solutions (vide infra). For the sake of simplicity, the spectrum of the reflecting sensor layer after conditioning in water was set to zero (baseline). Therefore, the recorded spectral changes are referred to the difference between the reflectance of the water-conditioned membrane and the membrane after exposure to aqueous amine.[31] This difference is the so-called "relative transflectance". As the amine concentration increased, the absorbance around 500 nm decreased while the absorbance at around 400 nm increased. Consequently, more light was reflected around 500 nm with increasing amine concentration and less around 400 nm. As explained above this change in absorbance is caused by a conversion of the trifluoroacetyl group of the chromoreactand into the corresponding hemiaminal form. For evaluating the optical sensor performance, *n*-propylamine, *n*-hexylamine, *n*-octylamine, *n*-decylamine and *n*-dodecylamine primary amines were chosen as the analytes.

Figure 6 shows the response of the composite **P-S3** measured in transflectance mode on exposure to aqueous amines at pH 9.5 and at wavelength of 520 nm. A very similar, albeit now quantifiable response, can be seen compared to solid **S3** with a clear change in colour for *n*-octylamine and *n*-decylamine, whereas no response to the other primary amines was observed. A linear sensitive range of the composite **P-S3** for

aqueous solutions of *n*-octylamine and *n*-decylamine was found to be from 1.0-100 mM, and the detection limit was 6 x 10^{-4} mM (Table 4). The forward response time of **P-S3** for the amines was 10 s while the reverse response was significantly slower and was in the range of 300-600 s, especially in the case of the hydrophobic amines. In these cases, the use of dilute acetic acid solutions favoured the reversibility.

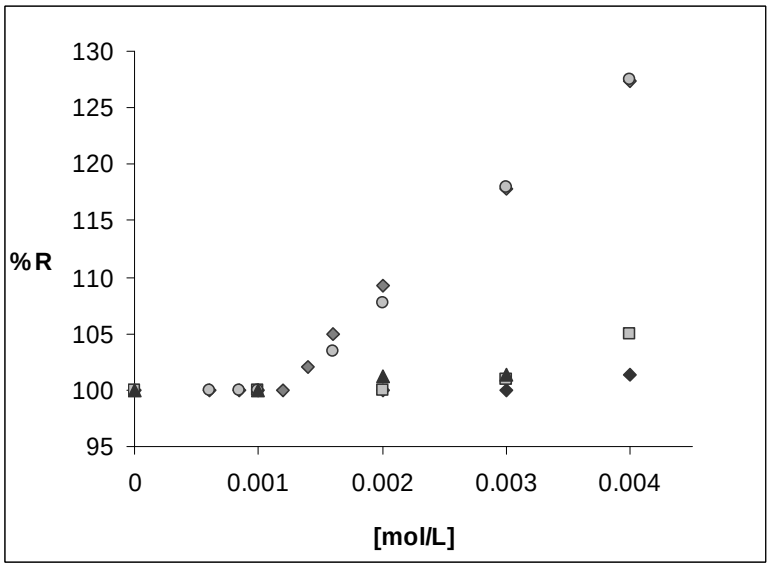

Figure 6. Calibration graph for **P-S3** versus different amine concentration of *n*-propylamine, *n*-hexylamine, *n*-octylamine, *n*-decylamine and *n*-dodecylamine, measured in transflectance mode at 520 nm on exposure to aqueous amine solution at pH 9.5.

	P-S3
Response time/s	10
Regeneration time/min	5
Detection limit/mol dm^{-3}	6 x 10^{-4}
Dynamic range/mol dm^{-3}	0,1

Table 4. Response characteristics of composite **P-S3** to aqueous *n*-octylamine.

The **P-S3** composite material displayed tailored selectivity which was governed by (a) the lipophilicity that determines the distribution of the amine between the composite and the aqueous phase, and (b) the relation between amine and pore size that controls the entrance of the amine into the pore voids where the colorimetric probe is anchored. The sensor material **P-S3** shows enhanced selective response (as a consequence of the inclusion of the chromogenic probe into hydrophobic nanoscopic pockets on mesoporous materials) that would hardly be achieved using similar molecular-based reactands in conventional polymer matrices. Additionally, the **P-S3** material shows large resistance to leaching and, therefore, fulfils one of the basic requirements for the design of real optical sensors. Moreover, the combination of the sensing features of **S3** with polymer materials widely used for the preparation of optodes resulted in a suitable combination for the production of sensors for aliphatic amines of potential application in certain fields such as food industry. This system gives multiple possibilities for modification *via* the use of different mesoporous materials with tailor-made pore openings, or by using polymeric matrices with different polarity. In addition, the new system shows a good dispersion of the mesoporous solid into the polymeric matrix that ensures the homogeneity of the final composite material and the homogeneity in their response. The relatively easy preparation of the composite combined with its inertness makes it suitable for a wide range of applications in sensing protocols.

Conclusions

In conclusion, we have reported a new optical material prepared by anchoring a suitable reactand on a hybrid material that was further incorporated on a polymeric support to yield a composite with enhanced selectivity for amine detection. An azo chromophore containing a

trifluoroacetophenone moiety was used as signaling reporter and a mesoporous system (UVM-7) was selected as inorganic support. The final hybrid material (**S3**) contains signaling amine indicator dyes anchored on hydrophobic 2.3 nm sized nanoscopic pockets. **S3** shows an enhanced response in terms of selectivity reacting "medium-length" amines but giving no response in the presence of small hydrophilic amines or large aliphatic amines. These favourable features in terms of selectivity remain the composite **P-S3** prepared by combining a hydrophilic polyurethane polymer and **S3**. The response time of the sensor **P-S3** to solutions of these amines was of the order of seconds, the regeneration time was between 5 to 10 min and the detection limit was $6 \cdot 10^{-4}$ mol L^{-1}. The sensor response was reproducible and reversible.

In a wider perspective we have shown here that favourable characteristics using mesoporous supports in combination with polymeric matrices can be a suitable method for the fabrication of optical materials with enhanced selectivity. What makes this system attractive is that several building blocks, i.e. mesoporous solids, hybrophobic binding pockets, reversibly-responding amine indicator dyes, polymeric materials, etc., can be combined in a predetermined fashion for the design of tailor-made optical sensors showing improved features that would be hardly achievable using the corresponding components alone. Furthermore, these selective sensor materials demand less calibration than unselective senor arrays which require chemometric approaches. While such arrays rather yield qualitative information and patterns, selective sensors enable reproducible quantification of analytes.

Experimental

Reagents.

For the preparation of the mesoporous material, tetraethoxysilane (TEOS), 2,2′,2′′-nitrilotriethanol ($TEAH_3$) and cetyltrimethylammonium bromide (CTAB) were obtained from Aldrich. For standard solutions, primary aliphatic amines solutions were prepared by dissolving the appropriate amount of each amine in 0.1M borate buffer solution. The pH was adjusted to 9.5, and the amount of the chemically reactive (i.e. nucleophilic) neutral form of the respective amine was calculated with the help of the Henderson-Hasselbalch equation; the pK_a of the amines being typically around 10.6.

Apparatus.

For spectral characterization of the sensor layers a modular diode array spectrometer (Carl Zeiss Jena Germany) was used, with a halogen lamp CLH 500 as the light source and a MCS 521 VIS spectrometer for optical detection. The measurements were performed in a flow-through module connected to the optical fibre *via* a Y-probe. The Y-probe was inserted into the head part of a sensor module. It was in direct contact with the inner boundary of the membrane support. Using Zeiss Aspect Plus software, the data was interpreted and evaluated and the parameters for the measurements were set. The sample solutions were pumped at a flow rate of 1.5 mL min^{-1} using a peristaltic pump (Perimax 12) and silicone tubes of 1 mm inner diameter ("Sikolit" by Angst and Pfister, Zürich, Switzerland).

Synthesis of S3.

The N-methyl,N-(propyl-3-trimethosysilyl)aniline (MPTMSA) was incorporated into the mesoporous solid *via* the co-condensation

approach in order to obtain a highly dispersed organic moiety on the pore surface. The synthesis strategy we used to prepare UVM-7 silicas and hybrid related organosilicas is an application of the so-called "atrane route". The procedure is based on the use of a simple structural directing agent (CTAB) as a porogen species and a complexing polyalcohol ($TEAH_3$) as hydrolitic precursor. MPTMSA (**I**) was added to the $TEAH_3$ under stirring and heating at 120 ºC. Then, the mixture was cooled to 90ºC and TEOS added. The mixture was again heated to 120 ºC to form the corresponding atrane. The mixture was allowed to cool down until 80 ºC and then CTAB and water were added. The molar ratio of the reagents was adjusted to 3.5 $TEAH_3$: 0.985 TEOS: 0.015 MPTMSA: 0.26 CTAB: 90 H_2O. The mixture was aged at room temperature for 24h. The resulting powder was collected by filtration, washed with water and ethanol and air-dried. Removal of the surfactant by a hydrochloric acid ethanol solution (1 g of solid per 100 mL HCl-EtOH, 16h at 80 ºC) yielded solid **S1**. In order to tune the polarity of the surface hexamethyldisilazane ($Me_3SiNSiMe_3$, HMDS) was used to the dangling –OH groups, introducint highly hydrophobic $–CH_3$ moieties in solid **S2**. 0.60 g of **S1** was firstly dehydrated through azeotropic distillation using a Dean-Stark trap. Then, 2.61 mL of HMDS (12,4 mmol) were added. After stirring the reaction mixture for 24h at room temperature, the resulting powder (**S2**) was collected by filtration, exhaustively washed with toluene and acetone and air-dried. Finally, 0.5 g **S2,** 27,8 g $NaNO_2$ (in water) and 75,6 g of TFAA (dissolved in DMF and HCl 6 N (10 mL)) were mixed and reacted at 0 ºC for 30 min and 120 min at room temperature yielding the mesoporous sensory solid **S3** that was washed with water and acetone and air-dried.

Preparation of P-S3.

The polyurethane polymeric material Hydromed D4 (Cardiotech Inc., Woburn, MA, USA) was used for embedding the mesoporous material, **S3**. 15 mg of Hydromed D4 was mixed with 25 mg of solid **S3** and with 300 μL of chloroform. The mixture was stirred for 1 hour. Within a chloroform atmosphere, a 0.3 mL aliquot of the suspension was transferred onto the polyester film. The final membrane **P-S3** was placed in ambient air for drying.

Chem. Eur. J. **2006**, 12, 2162-2170

4.5. Anchoring dyes into multidimensional large-pore zeolites: A prospective use as chromogenic sensing materials.

Chapter 4

Dye anchoring into multidimensional large pore zeolites. A prospective use as chromogenic sensory materials.

María Comes[a], Mª Dolores Marcos[a], Ramón Martínez-Máñez[a], Mª Carmen Millán[b], José Vicente Ros-Lis[a], Félix Sancenón[a], Juan Soto[a], Luis A. Villaescusa[a]*

[a] Centro de Investigación en Química Molecular Aplicada, Departamento de Química, Universidad Politécnica de Valencia, Camino de Vera s/n, E-46071 Valencia (Spain). Fax: (+34) 96-387-9349. e-mail: lvillaes@qim.upv.es

[b] Departamento de Física Aplicada, Universidad Politécnica de Valencia, Camino de Vera s/n, E-46071 Valencia (Spain).

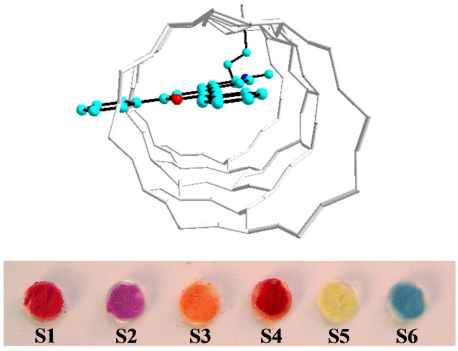

Chem. Eur. J. **2006**, 12, 2162-2170

A tunable, undemanding and versatile procedure for dye-anchoring into the pores of multidimensional zeolites has been developed based on the inclusion of organic dye-precursors in the synthesis gel. As a proof of the concept an aniline-functionalised zeolite beta was obtained by reaction of triethylorthosilicate (TEOS), tetraethylammonium hydroxide and MPTMSA (N-methyl,N-(propyl-3-trimethoxysilyl) aniline) in the presence of HF. Further extraction of the structure directing agents resulted in a highly crystalline white functionalised zeolite beta containing anchored aniline groups. Similar organic functionalised molecular sieves (OFMS) have been explored as novel catalysts, but, as far as we know, OFMS have never been used as precursors for dye immobilisation or to design new solid-based host systems for selective molecular sensing processes as it is reported here. In a second step the dye-containing solids were prepared by reaction of the hybrid material with the appropriate reactives to obtain tricyanovinylbenzene, triphenylpyrylium, azoic and squarine derivatives. All these reactions are straightforward and involve electrophilic aromatic substitution or diazotisation reactions on the electron-rich aniline ring. The final dye functionalised solid materials were isolated by simple filtration and washing procedures, which have been characterised by a number of techniques. In all cases the beta structure of the solid remains unaltered. Among the large number of areas where dye-containing zeolites might be of importance, we were interested in testing their unconventional use as hetero-supramolecular hosts in chromogenic protocols. In order to check their potential use as chemosensors solids, anchored triphenylpyrilium and squarine microporous solids were selected and used as chemodosimeters for the chromogenic discrimination of amines. It was found that the response of both solids to amines is basically governed by the 3D solid architecture that adequately tunes the intrinsic unselective reactivity of the pyrylium dye.

We believe that these, and similar future dye-zeolite hosts, might be promising new sensory materials capable of discriminate and sense, to the naked eye, selected target guests by size and/or polarity within families or closely related molecules via new solid state-supramolecular chemistry protocols.

Introduction.

For years, considered amount of work has been devoted to the study of the inclusion of organic dyes into porous solids.[1] Since solids provide large surface area, optical transparency and mechanical stability, these organic-inorganic hybrid composites have been extensively studied for applications in second harmonic generation[2], solid state lasers[3], photocatalysis[4], photonic antenna devices[5], etc. Additionally, examples have recently been reported related to their use in less conventional fields such of that of sensing.[6] Dyes have been extensively immobilised in amorphous silica through a sol-gel process[7], in contrast, the confinement of dyes in crystalline microporous solids such as zeolites has not been exhaustively explored, despite their well-defined structural properties, for example regular cages and channels, that make them ideal hosts for dye-inclusion compounds.[8] In fact, as far as we know, the covalent attachment of dyes into the microporous voids of a zeolite has never been used as a method for dyes immobilisation, although dyes have been selectively anchored on the outer surface[9]. This is probably due to the relative small openings of zeolites and the lack of abundant dangling ≡SiOH groups, which preclude immobilisation through grafting in the way that it is usually carried out in amorphous or mesoporous solids.[10]

There are basically three strategies for dye encapsulation into silica based microporous solids: (1) inclusion of the dye into the synthesis gel,[11] (2) simple surface adsorption[12] and (3) the ship-in-bottle approach.[13] The former approach is quite restrictive because of the inherent difficulties in making crystallising the desired microporous phase as well as the usual low stability of the organic dyes under the synthesis conditions for microporous materials. Additionally, following this strategy it is not easy to incorporate some of the dye molecules into

the crystalline framework. A possible serious drawback of the adsorption strategy is the usually uncontrollable formation of dye aggregates.[14] This can be circumvented by selecting the appropriate host avoiding the formation of dye aggregates, for instance by using low-silica zeolites (zeolites with a large aluminium content and highly charged framework) as hosts for positively charged dyes.[15,5] The ship-in-the-bottle approach interestingly makes use of host frameworks possessing cavities that are larger than the entrance opening; in these systems, reactants are allowed to diffuse in, but the products are prevented from exiting. Following this approach, the zeolite faujasite has been used almost exclusively and beautiful examples have been reported, most of them related to the presence of transition-metal atoms [16]. Moreover, the fact that in some cases the same reaction can occur in both within and outside of the solid makes it difficult to determine whether the product is really within the microporous voids. [17]

However, the inclusion of dyes into microporous materials has been used in a large number of research and applied fields and therefore, new protocols for controlled dye-immobilization in microporous solids is a field of interest. Our proposed approach widens the possibilities for dye-immobilisation through inclusion of organic dye precursors containing trialcoxysilanes in the synthesis gel. Thus, after the extraction of the pore-filling agents, the dye precursor remains covalently bonded to the microporous framework. As a proof-of-the-concept we show here a rather simple route to anchor selected dyes into the inner surface of zeolite Beta. This synthesis procedure is tunable, undemanding and versatile for ubiquitous anchoring of dyes into the pores of multidimensional zeolites. With regard to the possible large number of different applications of these solids containing anchored dyes we have

tested their prospective use as molecular-selective, chromogenic sensor materials.

Results and discussion.

The protocol we have developed to anchor dyes is based on the inclusion of organic dye precursors in the synthesis gel to obtain, after the extraction of the structure directing agents (SDA), zeolite derivatives containing covalently bonded organic groups on the pore walls.[18] This is a general method that is operative as long as the organic moiety to be anchored is stable in the synthesis media. These organic, functionalised molecular sieves (OFMS) were formerly developed by the pioneering work of Davis.[18] These have been explored as novel catalysts, but OFMS have never been used as precursors for dye-immobilisation or to design new solid-based host systems for selective molecular sensing processes as we will see below. The framework zeolite beta was selected, the synthesis of which has been carried out by using tetraethylammonium (TEA) and fluoride anions as the structure-directing agents and mineralisers, following the procedure of Cámblor.[19] One of the properties of pure silica zeolites prepared through the fluoride route is their lack of connectivity defects, related to the fact that charges arising from TEA cations are counterbalanced by fluoride anions and there is no need for the presence of pairs $\equiv SiO^-$ $HOSi\equiv$, giving rise to hydrophobic molecular-sieves.[20] Zeolite beta consists of the intergrowth of several polymorphs, all characterised by a 3D channel system with access to the microporous void that is limited by windows (ca. 6.8Å in diameter) composed of 12 silicon atoms[8]. Most applications require multidimensionality and no pore-block-ages of the structure. As the dye precursor to be anchored to the zeolite walls we have chosen N-methyl,N-(propyl-3-trimethoxysilyl) aniline (MPTMSA).[21]

The hybrid material was synthesised by reaction of triethylorthosilicate (TEOS), tetraethylammonium hydroxide and the aniline derivative MPTMSA in the presence of HF. Three different amounts of the aniline derivative MPTMSA were introduced into the synthesis mixture. The starting composition was taken from that proved to be efficient for the synthesis of zeolite beta and other pure silica polymorphs in fluoride media at near neutral pH.[20] Gel compositions can be expressed as SiO_2:***n*** MPTMSA:0.5TEAF:4H_2O, where ***n*** is 0.005, 0.022 and 0.046 respectively. Each of the mixtures was allowed to react in 23-mL Teflon-lined Parr autoclave at 150 ºC for 12 days. After this time, the fully crystalline derivatives of zeolite Beta were obtained for all the aniline contents tested. Yields were in the range of 33-36 % (higher than 90 % of the silica was transformed into crystalline Beta framework). XRD patterns and SEM images of the white solids indicate high purity and a homogeneous composition throughout every sample (i.e., all the crystals present were of the same composition). Extraction of the pore-filling agents with aqueous acetic acid was carried out twice to ensure complete removal of SDA. This resulted in a highly crystalline, white, functionalised zeolite Beta containing anchored aniline groups (see solid **I** in Scheme 1). The determination of the amount of the organic aniline functionalisation was carried out by monitoring the aniline band in solution at 254 nm after dissolution of the sample with HF in acetonitrile/water mixtures. The values of the aniline content obtained were in agreement with thouse found from thermogravimetric analysis (TGA). Figure 1 shows the relationship between the amounts of the aniline derivative MPTMSA introduced in the reaction mixture and the final aniline content in solid **I**. As can be seen, when the MPTMSA-doping is small, the incorporation is near quantitative; however, there is a limit for aniline incorporation (around 1.35 %) which must be related to the

destabilising effect that the substitution of aniline for TEA cations has on the zeolite crystallisation. This general behaviour has also been observed when pure silica zeolites are doped with aluminium.[20] This destabilising effect is probably enhanced by the formation of connectivity-defects arising from the presence of the ≡Si-C-R groups, which must force the appearance of one dangling groups per ≡Si-C substituted (≡Si-O^- or ≡Si-OH, probably dependent on the pH). On the other hand, zeolite Beta can be synthesised using about 25 different SDA[22] when the fluoride route is employed, then, anchored aniline might be behaving as a suitable pore-filling agent and should counterbalance the above mentioned detrimental effects. This is another reason why zeolite Beta is a good candidate for use as a host for OFMS design.

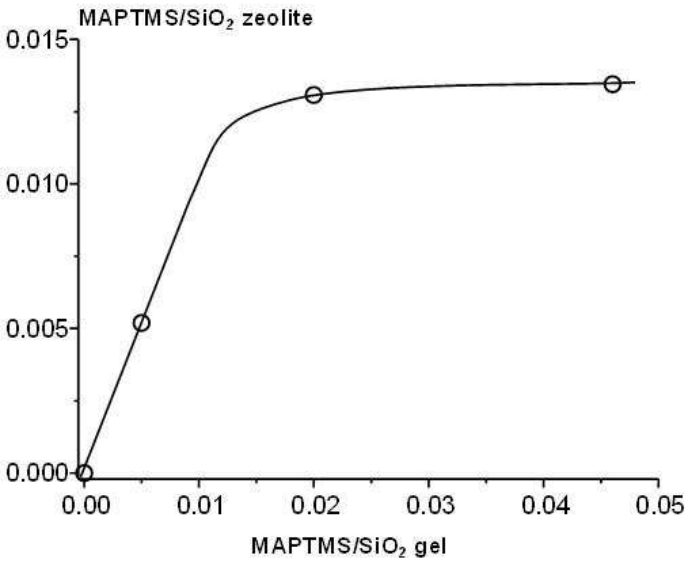

Figure 1. Aniline derivative/SiO_2 molar ratio in the zeolite as a function of that in the synthesis mixture.

The final ideal unit cell (u.c.)composition of solid **I** (for polymorph A, 64 SiO_2/u.c.) can be described as

$(SiO_2)_{64-2n}(SiO_{3/2}OH)_n(SiO_{3/2}(CH_2)_3CH_3N(C_6H_5))_n$ where *n* can vary up to 0.86. Thus, the amount of aniline incorporated can be readily obtained by simply controlling the MPTMSA introduced into the synthesis mixture. The ^1H and ^{13}C NMR spectra of the solid dissolved in NaOH confirm the presence of the Si-C bond as well as the aromatic aniline moiety, which appears to be intact even after the demanding synthesis conditions. Figure 2 shows the XRD patterns and SEM images of the aniline-functionalised zeolite Beta as-synthesised and after the removal of the SDA (solid **I**, *n*=0.0022). The synthetic route appeared to be quite versatile and in preliminary assays we have also obtained structures based on the zeolite silicalite (2D, pore diameter ca. 5.5 Å) containing anchored aniline groups.

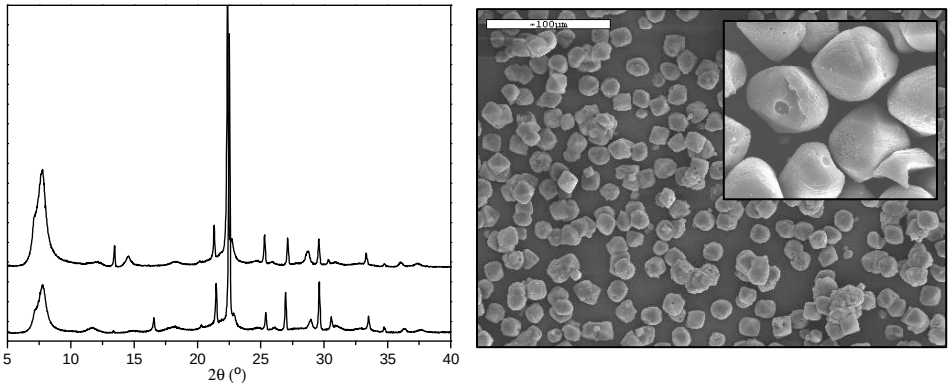

Figure 2. XRD patterns and SEM images of the aniline functionalised beta zeolite. a) as-synthesised b) sample extracted.

At this stage, the hybrid microporous materials **I** containing dangling aromatic N,N-dialkyl-substituted aniline rings is available as a starting material to synthesize dyes of different nature. Solid **I** containing an aniline/SiO_2 ratio of 0.0135 was selected for this purpose. To show the flexibility of the approach we have prepared solids **S1- S6** by reaction of solid **I** with tetracyanoethylene (**S1**), 2,6-diphenylpyrylium (**S2** and **S5**),

4-aminobenzenesulfonic acid (**S3**), 4-nitroaniline (**S4**) or 3,4-dihydroxy-3-cyclobutene-1,2-dione (**S6**) (see Scheme 1).[23] All these reactions are straightforward and involve electrophilic aromatic substitution or diazotisation reactions on the electron-rich aniline ring. The final dye-functionalised solid materials were isolated by simple filtration and exhaustive washing procedures. The **S1**-**S6** solids have been characterised by X-ray diffraction, TGA, elemental analysis and UV/Vis spectroscopy. In all cases the Beta structure of the solid remains unaltered. The solids are brightly coloured ranging from yellow (for solid **S5**) to those absorbing at the far end of the visible window (solid **S6**). Figure 3 shows the visible spectra of the solids.

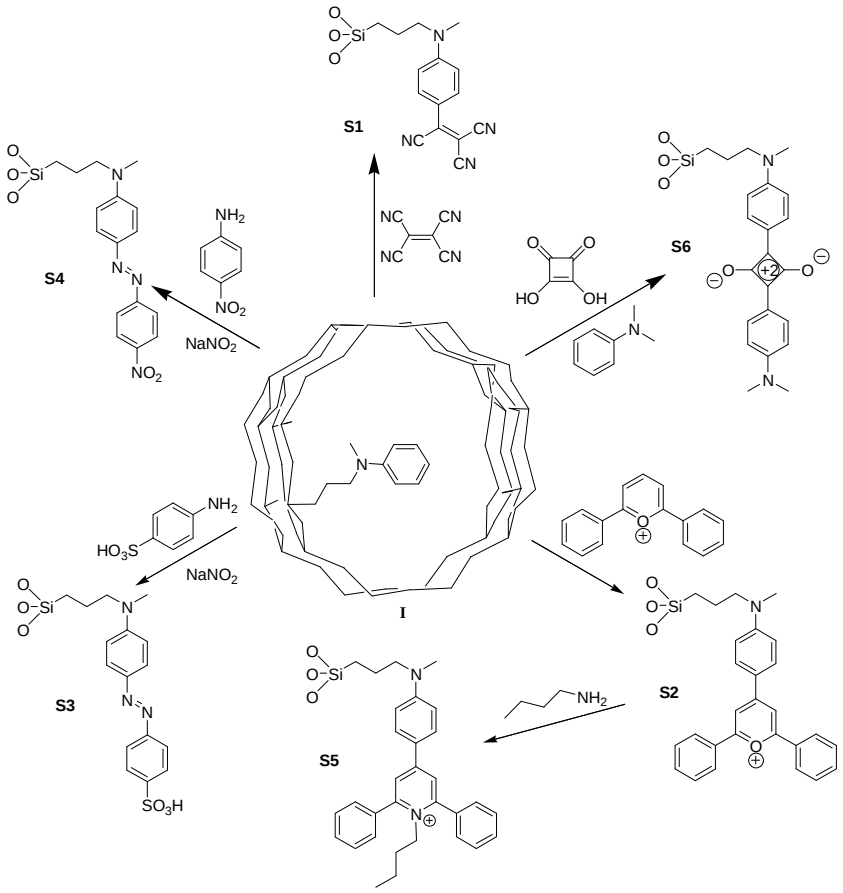

Scheme 1. A schematic representation of solids **I**, **S1**-**S6.**

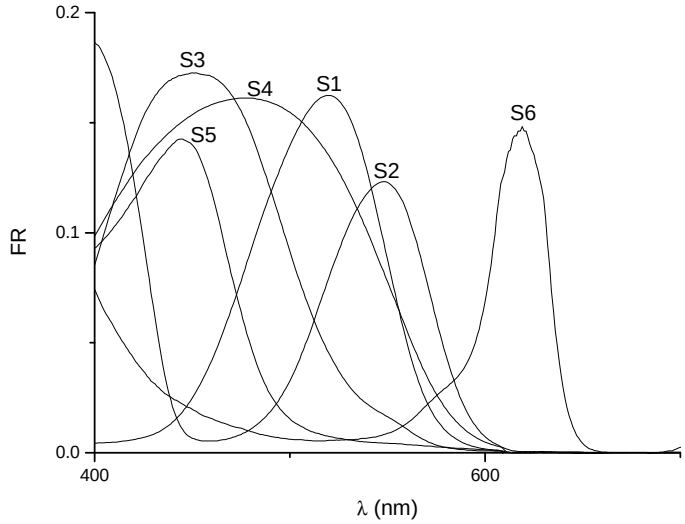

Figure 3. Visible spectra of solids **S1** to **S6** suspended in ethylenglycol.

Typical final solids were obtained with dye content ranging from 4.13 x 10^{-4} mol of dye/mol of SiO_2 for solid **S4** to 1.12 x 10^{-5} mol of dye/mol of SiO_2 for solid **S6** (see Experimental Section). Despite the partial functionalisation of the aniline in the synthesis procedure of materials **S1**-**S6** from solid **I**, the final solids are brightly coloured (see Graphical Abstract) and the final dye content should be adequate for many applications. More importantly, the grafting protocol through covalent bonding of organic dyes to the framework of a zeolite shows some remarkable advantages when compared to the other strategies of inclusion of organic dyes into microporous silica-based materials. The necessary condition in the common ship-in-bottle approach in which the formed product has to be bulkier than the cavity to avoid leaching is not applicable in the protocol that we have followed, since the final dye is covalently bonded to the silica framework. An additional advantage is related to the enhanced chemical stability presented by the covalently

anchored chromophores when compared to that in solution; that is, squaraine and tricyanovinyl derivatives are known to undergo a rapid and effective attack by nucleophiles such as R-SH, CN^- and OH^- in aqueous environments, whereas the corresponding solids **S1** and **S6** that have anchored dyes do not react with these species even after weeks.[24]

Among the large number of areas where coloured solids might be of importance, we are especially interested in their unconventional use as sensory materials in chromogenic protocols.[25] In relation to the design of new chemical sensors, those relying on the construction of "binding structures" using 3D solid architectures are especially appealing. Here, the selectivity is not related to the production of a complicated host but imposed by the solid structure itself that is capable of discriminating the shape-selectivity, polarity, and size of the guest. Besides, sensing response by microporous solids might use pre-concentration effects provided by the adsorption properties of zeolites. Thus, it is unexpected that despite the number of fields where zeolites have been used, their use in chromogenic sensing procedures has been very limited.[26] As it has been suggested above, this might have been a consequence, among other factors, to the lack of convenient routes to unambiguously anchor dyes into the pore voids.

To check their potential use as sensory materials we have selected solids **S2** and **S6** and tested their capability towards the chromogenic discrimination of amines. Preliminary experiments to find sensory properties in the rest of the solids **S1**, **S3**, **S4** and **S5** did not show any remarkable result and will be more exhaustively studied in due course.
As has been reported, 4-(4-aminophenyl)-2,6-diphenylpyrylium dye derivatives displays a red-magenta colour that changes to yellow by

reaction with primary amines due to transformation into pyridinium derivatives. In addition to the colour change, the pyrylium derivative is not fluorescent, whereas the obtained pyridinium fluoresces at about 470 nm upon excitation to give the yellow band at aproximately 440 nm.[27] However, this chromo-fluorogenic pyrylium response to primary amines is rather unspecific in solution and we have found that it can be conveniently modulated when incorporated to the zeolite framework (see below). A representation of the dye anchored within the zeolite Beta pores (solid **S2**) is shown in Figure 4.

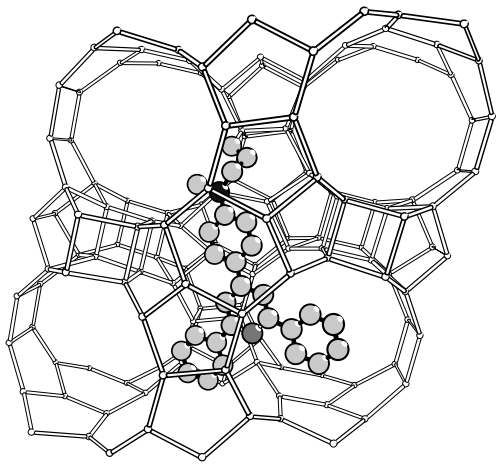

Figure 4. Representation of solid **S2** containing a pyrylium dye anchored on the zeolite beta walls.

The response of this dye-containing solid **S2** to a number of amines was tested and it was found that it can act as suitable selective heterosupramolecular host in selective chromofluorogenic-sensing protocols. The response of **S2** to amines is basically modulated by three factors (i) the reactivity of the 4-(4-aminophenyl)-2,6-diphenylpyrylium dye, (ii) the polarity and (iii) the dimensions of the openings of the zeolite Beta scaffolding. Chromogenic amine discrimination has been studied in two solvents of different polarity, ethanol and water. The

results are summarised in Figure 5 that shows the response to a number of amines of the functionalised- zeolite **S2**. The chromogenic sensing response was monitored in water at basic pH (pH ~ 10) except for the amines 9-methylaminoanthracene, 1-methylaminopyrene, 3,3-diphenylpropylamine, and benzylamine, that were water insoluble and were only tested in ethanol. In all cases the colour changes were measured after a long time to assure equilibrium conditions and minimize possible discrimination due to kinetic effects. As stated above the reactivity of the dye is governed by a nucleophiplic attack of primary aliphatic amines to the pyrylium ring. This response is also conserved into the zeolite framework and **S2** reacts with certain aliphatic amines (see below) but remains a magenta colour in the presence of other amines. In less-polar media (ethanol), the size discrimination is clearly observed and only "small" amines such as *n*-propylamine, *n*-butylamine, *n*-heptylamine, and "medium" amines such as 3,3-diphenylpropylamine, and benzylamine are capable of reaching the pyrylium signaling units into the inner pores inducing inducing magenta-to-yellow colour transformations. All those amines have one longitudinal section smaller in size (at least in one direction) than the dimensions of the opening in zeolite Beta. In contrast, solid **S2** in contact with an ethanol solution of bulky primary amines such as 9-methylaminoanthracene, 1-methylaminopyrene, and the amine containing dendrimer PAMAM-0 remained completely inactive for weeks. This test also proves that dyes are on the inner-pore surface of the microporous zeolitic framework.

We observe notable polarity discrimination in water. Thus, the increase in strength of hydrogen bonding to the solvent can cause significant decrease in the removal of highly hydrophilic amines from water to the hydrophobic zeolite pores. This effect can be observed when comparing, for instance, the reactivity of the amines *n*-propylamine, *n*-butylamine

and *n*-heptylamine (see Figure 5). Whereas the "small" but hydrophobic amine *n*-heptylamine is able to transform the pyrylium to the pyridinium group in **S2** quantitatively, other less hydrophobic amines such as *n*-propylamine and *n*-butylamine only induce a partial colour change. Additionally, the somewhat similar but highly hydrophilic amine lysine or dopamine did not induce any chromogenic response after weeks. In fact there is a clear correlation between the hydrophobicity of these amines (*n*-heptylamine > *n*-butylamine > *n*-propylamine > lysine ≅ dopamine) and the ability of the amine to induce pyrylium-to-pyridinium transformation in the sensor zeolite **S2**. A similar effect can be found in the related amines, *n*-heptylamine and the less hydrophobic derivatives 6-hydroxyhexylamine and 5-hydroxypentylamine. For instance, *n*-heptylamine and 6-hydroxyhexylamine are primary amines with the same chain length but show a different polarity due to the presence of the OH group in the latter. The addition of an aqueous solution of *n*-heptylamine to **S2** resulted in a remarkable colour variation in less than four minutes. On the contrary, **S2** remained magenta for at least 30 minutes upon addition of 6-hydroxyhexylamine as expected from the hydrophobic nature of the pure silica microporous framework. This different reactivity was also observed for longer time (see Figure 5). As an example of size and polarity discrimination, Figure 6 shows the colour changes observed with solid **S2** upon addition of the amines 3,3-diphenylpropylamine, 1-methylaminopyrene in ethanol, and *n*-heptylamine and 6-hydroxyhexylamine in water after a reaction time of 20 min.

The hydrophobic effect in the inner pores of the zeolite framework is also indicated from the additional stability of the anchored dye against nucleophilic attack of OH^- from water. Thus, whereas basic aqueous solutions of pyrylium derivatives readily became yellow due to formation

of the corresponding 1,5-dienone, the magenta colouration of solid **S2** remained unaltered for weeks even at very high pH values.

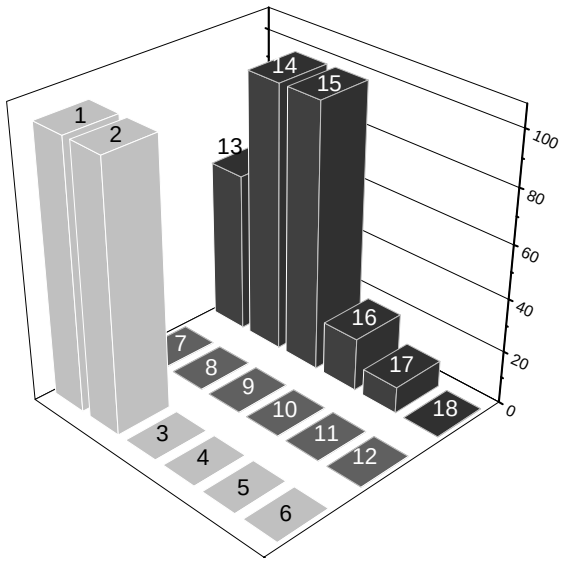

Figure 5. Schematic representation of the relative response of pyrylium functionalised zeolite beta (**S2**) to different amines. From 1 to 18: 3,3-diphenylpropylamine, benzylamine, PAMAM-0, dopamine, 1-aminomethylpyrene, 9-aminomethylantracene, aniline, diethanolamine, tripropylamine, 4-(dimethylamino)benzoic acid, 4-bromoaniline, 2-aminobenzothiazole, 5-amino-1-pentanol, 6-amino-1-hexanol, n-heptylamine, n-butylamine, n-propylamine and lysine.

Figure 6. Colour changes observed on solid **S2** upon addition of several amines. From left to right: no amine, 3,3-diphenylpropylamine, 1-methylaminopyrene, n-heptylamine and 6-amino-1-hexanol.

Solid **S6** was also studied as a potential sensory material for chromofluorogenic sensing of amines. Squaraine dyes have been reported to react with amines through an addition reaction with the four-membered ring leading to the rupture of the extended π system in the squaraine framework and subsequent decolouration. Studies with **S6** were carried out under the same conditions as those for solid **S2** and showed a similar reactivity. This similar response of solids **S2** and **S6** strongly indicates that the observed reactivity, and therefore the sensory ability of these materials, is governed by the 3-D solid architecture that adequately tunes the reactivity of the squaraine and pyrylium dyes. This led to new solid-state, supramolecular sensor materials with enhanced sensing abilities.

Conclusions.

In summary, we have reported a suitable route to anchor dyes into the inner voids of the siliceous frameworks of zeolites. The protocol developed that promotes the anchoring of the dyes is based on the inclusion of organic dye precursors in the synthesis gel. This procedure is easily tunable and versatile, and allows us to obtain novel dye-containing hybrid materials with promising applications in a number of different fields. The versatility of this approach has been demonstrated by preparing solids **S1**-**S6** by straightforward reaction of the organic, functionalised molecular sieve **I** with tetracyanoethylene (to give solid **S1**), 2,6-diphenylpyrylium (yielding solids **S2** and **S5**), 4-aminobenzenesulfonic acid (to give solid **S3**), 4-nitroaniline (giving solid **S4**) or 3,4-dihydroxy-3-cyclobutene-1,2-dione (resulting in solid **S6**). The anchoring of dyes through covalent bonds into the zeolite framework shows certain advantages when compared to other strategies of inclusion of organic dyes into microporous silica solids. We believe

that this work might open up new possibilities for the synthesis of dye-containing microporous solids by applying similar synthesis protocols to some of the more than 150 known zeolitic topologies. Additionally, we have also shown the potential applicability of these zeolites containing dyes as sensors in chromogenic sensing protocols. By using new solid-state supramolecular chemistry protocols, we have demonstrated that employing multidimensional channel systems as solid hosts enclosing suitable binding structures and/or signaling units might lead to new sensor materials that allow to visibly discriminate selected target guests by size and polarity within families or closely related molecules.

Experimental section

General remarks.

All commercially available reagents were used without further purification. Air/water-sensitive reactions were performed in flame-dried glassware under argon. Acetonitrile was dried with CaH_2 and distilled prior to use.

Materials characterization.

X-ray measurements were performed with a Seifert 3000TT diffractometer using $Cu_{K\alpha}$ radiation. Thermogravimetric analysis of solids **I**, **S1**, **S2**, **S3**, **S4**, **S5** and **S6** solids was carried out with a TGA/SDTA 851e Mettler Toledo balance, by using a heating program consisting of a first heating ramp of 10 °C per minute from 393-1273 K, and then a plateau at 1273 K for 30 min. UV/Vis diffuse-reflectance absorption spectra were recorded on a Perkin-Elmer Lambda 35 UV/VIS spectrometer (suspension of 0.002 g of the corresponding solid in ethyleneglycol (2.7mL)). Scanning electron microscopy images were obtained with a Jeol JSM 6300 microscope operated at 30kV.

Determination of organic content.

The determination of the contents of the organic functionalisation was carried out by means of UV/visible spectroscopy by using calibration curves. These curves were obtained by dissolving increasing quantities of N,N-dimethylaniline or the correspondent dye (final concentrations in the range 1.0×10^{-5} to 1.0×10^{-7} mol·dm^{-3}) with a fixed quantity of pure inorganic matrix (0.01 g) and HF (48% in water, 0.023 mL) in acetonitrile (0.5 mL) mixtures. Next, the absorbance of aniline band (254 nm) or the visible band was plotted against organic concentration. Finally, the functionalised solids were subjected to the same treatment

and the absorbances at 254 nm for solid **I,** or the visible bands in the case of solids **S1**-**S5,** were measured and employed to estimate organic contents.

A slightly modified procedure was employed with solid **S6.** The calibration curve was obtained by dissolving increasing quantities of the squaridine dye in diethyl ether. The functionalised **S6** material was suspended in ethyleneglycol and the absorbance measured. The dye content was estimated by interpolation in the calibration curve.

Synthesis procedures.

The synthesis of N-methyl,N-(propyl-3-trimethoxysilyl) aniline has been previously published.[21] Also, the synthesis of the corresponding dyes in the experiments to determine organic content were straightforward and published elsewhere.[24]

Syntheses of precursor solid were carried out by reaction of triethylorthosilicate (TEOS), tetraethylammonium hydroxide and MPTMSA (N-methyl,N-(propyl-3-trimethoxysilyl) aniline) in the presence of HF for several organosilane contents. The overall molar composition can be described as SiO_2:*n*MPTMSA:0.5TEAF:4H_2O. A detailed synthesis procedure for the sample used to generate the rest of colored derivatives is as follows: A solution of MPTMSA (N-methyl,N-(propyl-3-trimethoxysilyl) aniline, 0.80 g) in TEOS (triethylorthosilicate, 27.08 g, 0.129 mol) was added to a vessel containing a solution of tetraethylammonium hydroxide (35% wt, 28.02 g, 0.066 mol) and water (52.84 g, 2.93 mol). The alcoxides were allowed to hydrolyse at room temperature. Then, the temperature was increased to 50 ºC to evaporate alcohols and water until 25.27 grams of gel are obtained. HF

(2.71 g, 0.065, 48%) was added to the mixture that was stirred by hand. The overall molar composition was SiO_2:0.022MPTMSA:0.5TEAF:4H_2O. The paste was distributed in 23-mL Teflon-lined Parr autoclaves and allowed to react at 150 ºC for 12 days under static conditions. After this time, the paste (pH= 8.2) was recovered by filtration and washed with plenty of water, yielding (33.5 % wt) fully crystalline zeolite Beta. Extraction with aqueous acetic acid (50 % wt) was carried out twice to ensure complete SDA removal (losses were kept constant form one sample to another as mesasured by TGA, which was used for organic content determination). This resulted in a highly crystalline, white, functionalised zeolite Beta containing anchored aniline groups (solid **I**). ^{1}H and ^{13}C NMR spectroscopy was carried out on samples that had been previously dissolved in NaOH (D_2O, 2.5 mol·dm^{-3}).

S1-**S6** materials were obtained by straightforward reaction of solid **I** with tetracyanoethylene (**S1**), 2,6-diphenylpyrylium perchlorate (**S2** and **S5**), 4-aminobenzenesulfonic acid (**S3**), 4-nitroaniline (**S4**), or 3,4-dihydroxy-3-cyclobutene-1,2-dione (**S6**). The **S1**-**S6** solids were characterised by X-ray diffraction, TGA, and UV/Vis spectra. In all cases the Beta structure of the solid remained unaltered. These were obtained as brightly coloured solids that ranged from yellow (for **S5**) to those absorbing at the far end of the visible window (**S6**).

Solid *S1*: Solid **I** (1.0 g containing 0.16 mmol of aniline) was suspended in acetonitrile (10 mL) and then tetracyanoethylene (0.1 g, 0.78 mmol) was added. The mixture was allowed to react at 80 ºC for 16h. The solid material was exhaustively washed with acetonitrile and acetone until no colour in the washing layers was observed and was then air-dried. The final **S1** material was an intense red colour and gave an absorption band

centred at 517 nm. The amount of dye was 1.5 mmol of dye/mol of SiO2. **CAUTION***:* HCN is evolved in the synthetic procedure.

Solid *S2*: Solid **I** (1.0 g containing 0.16 mmol of aniline) was suspended in ethanol (80 mL) and then 2,4-diphenylpyrylium perchlorate (0.52 g, 1.57 mmol) was added. The mixture was refluxed for 24 h and was then filtered. The solid material was exhaustively washed with ethanol and acetone until no colour in the washing layers was observed and was then air-dried. The final **S2** material was an intense magenta colour and gave an absorption band centred at 550 nm. The amount of dye was 0.06 mmol of dye/mol of SiO_2.

Solid *S3*: 4-aminobenzenesulfonic acid (0.12 g, 0.70 mmol) was dissolved in a mixture containing ethanol (7.2 mL) and hydrochloric acid (0.2 mL, 35%). Then a solution of $NaNO_2$ (0.05 g, 0.73 mmol) in water (0.6 mL) was added and allowed to react for 30 min. The diazonium salt solution formed was added dropwise to a cooled (0-5 ºC) suspension of solid **I** (1.0 g containing 0.16 mmol of aniline) in 1:1 (v/v) water/ethanol mixture (40 mL) and was allowed to react for 3 h at 0-5 ºC, and for 16 h at room temperature. The solid material was filtered, exhaustively washed with ethanol and acetone until no colour in the washing layers was observed and was then air-dried. The final **S3** material was obtained as an orange solid (absorption band centred at 521 nm). The amount of dye was 0.46 mmol of dye/mol of SiO_2.

Solid *S4*: 4-nitroaniline (0.11 g, 0.80 mmol) was dissolved in a mixture containing ethanol (7.2 mL) and hydrochloric acid (0.2 mL, 35%). Then a solution of $NaNO_2$ (0.055 g, 0.80 mmol) in water (0.6 mL) was added and allowed to react for 30 min. The diazonium salt solution formed was added dropwise to a cooled (0-5 ºC) suspension of solid **I** (1.0 g

containing 0.16 mmol of aniline) in 1:1 (v/v) water/ethanol mixture (40 mL) and was allowed to react for 3 h at 0-5 ºC and for 16 h at room temperature. The solid material was filtered, exhaustively washed with ethanol and acetone until no colour in the washing layers was observed and then air-dried. The final **S4** material was obtained as dark-red solid (absorption band centred at 511 nm). The amount of dye was 4.13 mmols of dye/mol of SiO_2.

Solid *S5:* Solid **S2** (1.0 g, containing $9.19x10^{-4}$ mmol of pyrylium dye) was suspended in aqueous ammonium hydroxide (1.0 mL). The mixture was allowed to react at room temperature for 15 min. The solid material was exhaustively washed with water and with acetone and was then air-dried. The final **S5** material was obtained as a yellow solid (absorption band centred at 440 nm). The amount of dye was 0.06 mmol of dye/mol of SiO_2.

Solid *S6:* In a round-bottomed flask fitted with a Dean-Stark system, solid **I** (1.0 g containing 0.16 mmol of aniline) was suspended in anhydrous toluene (100 mL) and was refluxed for 2 h. Then 3,4-dihydroxy-3-cyclobutene-1,2-dione (0.12 g, 1.07 mmol) was added and the mixture was refluxed for one more hour. After that, N,N-dibutylaniline (1.80 ml, 13 mmol) was added and the reflux was continued. Triethylorthoformiate (15 mL, 78.16 mmol) was added 30 min later and the crude was refluxed for another 16 h. The crude reaction mixture was filtered and the solid was exhaustively washed with toluene and acetone until no colour in the washing layers was observed and was then air-dried. The final **S6** material exhibited an intense blue colour and displayed an absorption band centred at 620 nm. The amount of dye was 0.011 mmol of dye/mol of SiO_2.

Sensing studies: Sensing studies were carried out with solid **S2** in the presence of amines with different substitution patterns, size and polarity (lysine, *n*-propylamine, *n*-butylamine, *n*-heptylamine, 6-amino-1-hexanol, 5-amino-1-pentanol, aniline, diethanolamine, tripropylamine, 4-(dimethylamino)benzoic acid, 4-bromoaniline, 2-aminobenzothiazole, 1-methylaminopyrene, 9-methylaminoanthracene, 3,3-diphenylpropylamine, benzylamine, dopamine and PAMAM-0). Solutions of amine (c = 0.01 mol·dm^{-3}) were prepared by dissolution in ethanol or water (depending on its solubility). The solution of amine (2 mL) was added to solid **S2** (0.003 g) and the mixture was allowed to react for 24 h. The liquid was separated by centrifugation and the remaining solid was suspended in ethylene glycol. The absorbance of the final solid was measured by the diffuse reflectance technique. Upon addition of certain amines with the appropiate substitution, size, or polarity, the band at 540 nm (related to the absorption of the pyrylium moiety) disappears and a new absorption band centred at 463 nm (related to the pyridinium moiety) was observed. This change in colour was ascribed to transformation of the pyrylium ring to the pyridinium ring by nucleophilic attack of the corresponding amine.

References.

[1] a) G. Schulz-Ekloff, D. Wöhrle, B. van Duffel, R. A. Schoonheydt, *Micropor. Mesopor. Mater.*, **2002**, *51*, 91-138; b) D. Bruhwiler, G. Calzaferri, *Micropor. Mesopor. Mater.*, **2004**, *72*, 1-23; c) D. Wöhre, G. Schulz-Ekloff, *Adv. Mater.*, **1994**, 6, 875-880.

[2] a) H. S. Kim, S. M. Lee, K.. Ha, C. Jung, Y.-J. Lee, Y. S. Chun, D. Kim, B. K. Rhee, K. B. Yoon, *J. Am. Chem. Soc.,* **2004**, 126, 673 -682; b) G. Schulz-Ekloff, *Stu. Surf. Sci. Catal.*, **1994**, 85, 145-175.

[3] R. Reisfeld, *Opt. Mater.*, **1994**, 4, 1-3; F. Marlow, M. D. McGehee, D. Zhao, B. F. Chmelka, G. D. Stucky, *Adv. Mater.*, **1999**, 11, 632-636.

[4] Solid state and surface photochemistry in "molecular and supramolecular photochemistry", vol 5. Edited by V. Ramamurthy and K.S. Schanze. Editorial: Marcel Dekker inc. N.Y. **2003**.

[5] H. Maas, S. Huber, A. Khatyr, M. Pfenniger, M. Meyer, G. Calzaferri, "Organic-Inorganic composites as photonic antenna" in "molecular and supramolecular photochemistry", vol 9, edited by V. Ramamurthy and K.S. Schanze. Editorial: Marcel Dekker inc. N.Y. **2003**.

[6] a) A.B. Descalzo, K. Rurack, H. Weisshoff, R. Martínez-Máñez, M.D. Marcos, P. Amorós, K. Hoffman, J. Soto, *J. Am. Chem. Soc.*, **2005**, *127*, 184-200; b) M. Comes, G. Rodríguez-López, M.D. Marcos, R. Martínez-Máñez, F. Sancenón, J. Soto, L. A. Villaescusa, P. Amorós, D. Beltrán, *Angew. Chem. Int. Ed.*, **2005**, *44*, 2918-2922; c) S. Huh, J.W. Wiench, B.G. Trewyn, S. Song, M. Pruski, V.S.-Y. Lin, *Chem. Commun.*, **2003**, 2364-2365 ; d) V.S.-Y. Lin, C.-Y. Lai, J. Huang, S.-A. Song, S. Xu, *J. Am. Chem. Soc.* **2001**, *123*, 11510–11511; e) D. R. Radu, C. -Y. Lai, J. W. Wiench, M. Pruski, V. S. -Y. Lin, *J. Am. Chem. Soc.* **2004**, *126*, 1640–1641 ; f) M. Comes, M. D. Marcos, R. Martínez-Máñez, F. Sancenón, J. Soto, L. A. Villaescusa, P. Amorós, J. Beltrán, *Adv. Mater.*, **2004**, 16, 1783-1786.

[7] a) M. Ganschow, M. Wark, D. Wöhrle, G. Schulz-Ekloff, *Angew. Chem. Int. Ed.*, **2000**, *39*, 160-163; b) G. E. Badini, K. T. V. Grattan, A. C. C. Tseung, *Rev. Sci. Instrum.*, **1995**, *66*, 4034-4040; c) J. L. Meinershagen, T. Bein, *Stu. Surf. Sci. Catal.*, **2001**, *135*, 3518-3525.

[8] http://www.iza-structure.org

[9] a) S. Huber, G. Calzaferri, *Angew. Chem.* **2004**, 116, 6906-6910; *Angew. Chem. Int. Ed.* **2004**, 43, 6738-6742; b) T. Ban, D. Brühwiler, G. Calzaferri, *J. Phys. Chem. B* **2004**, 108, 16348-16352.

[10] a) P. Sutra, D. Brunel, *Chem. Commun.*, **1996**, 2485-2486; b) Y. V. S. Rao, D. E. Vos, T. Bein, P. A. Jakobs, *Chem. Commun.,* **1997**, 355-356.

[11] a) K. J. Balkus Jr., S. Kowalak, K.T. Ly, D. C. Hargis, *Stu. Surf. Sci. Catal.*, **1991**, *69*, 93-99; b) S. Wohlrab, R. Hoppe, G. Schulz-Ekloff, D. Wöhrle, *Zeolites*, **1992**, *12*, 862-865; c) R. Hoppe, G. Schulz-Ekloff, D. Wöhrle, C. Kirschhock, H. Fuess, L. Uytterhoeven, R. Schoonheydt, *Adv. Mater.*, **1995**, *7*, 61-64.

[12] a) K. Hoffmann, F. Marlow, J. Caro, *Adv. Mater.*, **1997**, *9*, 567-570; b) G. Calzaferri, N. Gfeller, *J. Phys. Chem.*, **1992**, *96*, 3428-35; c) N. Gfeller, S. Megelski, G. Calzaferri, *J. Phys. Chem. B*, **1998**, 102, 2433-2436; d) S. Ernst, M. Selle, *Micropor. Mesopor. Mater.*, **1999**, *27*, 355-363; e) C. J. Liu, S. –G. Li, W. –Q. Pang, C. –M. Che, *Chem. Commun.*, **1997**, 65-66; f) K. Hoffman, F. Marlow, J. Caro, *Zeolites*, **1996**, 16, 281-286; g) K. Hoffman, F. Marlow, J. Caro, S. Dähne, *Zeolites*, **1996**, *16*, 138-141.

[13] a) C. Schomburg, M. Wark, Y. Rohlfing, G. Schulz-Ekloff, D. Wohrle, *J. Mater. Chem.*, **2001**, *11*, 2014-2021; b) A. Corma, H. García, *Eur. J. Inorg. Chem.*, **2004**, 1143-1164.

[14] a) D. Brusilovsky, R. Reisfeld, *Chem. Phys. Lett.*, **1987**, 141, 119-121; b) R. Hoppe, G. Schulz-Ekloff, D.Wöhrle, E.S. Shpiro, O.P. Tkachenko, *Zeolites*, **1993**, 13, 222-228; c) R. Hoppe, G. Schulz-Ekloff, D. Wöhrle, M. Ehrl, C. Brauchle, *Stu. Surf. Sci. Catal.*, **1991**, 69, 199-206; d) M. Wark, A. Ortlam, M. Ganschow, G. Schulz-Ekloff, D. Wöhrle, *Ber. Bunsenges. Phys. Chem.*, **1998**, 102, 1548-1553.

[15] a) G. Calzaferri, D. Brühwiler, S. Megelski, M. Pfenniger, M. Pauchard, B. Hennessy, H. Maas, A. Devaux, U. Graf, *Solid State Sciences*, **2000**, *2*, 421–447; b) H. Maas, A. Khatyr, G. Calzaferri, *Micropor. Mesopor. Mater.*, **2003**, 65, 233–242.

[16] a) N. Herron, *Inorg. Chem.* **1986**, *25*, 4714-4717; b) K. J. Balkus Jr., A. A. Welch, B. E. Gnade, *Zeolites* **1990**, *10*, 722-729; c) M. Ichikawa, T. Kimura, A. Fukuoka, *Stud. Surf. Sci. Catal.* **1991**, *60*, 335-342; d) M. Alvaro, B. Ferrer, V. Fornes, H. Garcia, J. C. Scaiano, *J. Phys. Chem. B* **2002**, *106*, 6815-6820; e) I.

Casades, S. Constantine, D. Cardin, H. Garcia, A. Gilbert, F. Marquez, *Tetrahedron* **2000**, *56*, 6951-6956.

[17] C. Schomburg, D. Wohrle, G. Schulz-Ekloff, *Zeolites*, **1996**, *16*, 232-236.

[18] a) C.W. Jones, K. Tsuji, M.E. Davis, *Nature*, **1998**, *393*, 52; b) K. Tsuji, C. W. Jones, M. E. Davis, *Micropor. Mesopor. Mater.*, **1999**, *29*, 339-349; c) C. W. Jones, K. Tsuji, M. E. Davis, *Micropor. Mesopor. Mater.*, **1999**, *33*, 223-240.

[19] M. A. Camblor, A. Corma and S. Valencia, *Chem. Commun.*, **1996**, 2365-2366.

[20] a) L. A. Villaescusa, M. A. Camblor, *Recent Res. Devel. Chem.*, **2003**, 1, 93-141; b) M. A. Camblor, L.A. Villaescusa, M. J. Díaz-Cabañas, *Top. Catal.*, **1999**, 9, 59-76.

[21] M. Comes, L. A. Villaescusa, M. D. Marcos, R. Martínez-Máñez, F. Sancenón, J. Soto, *Synth. Commun.*, **2005**, 35, 1511-1516.

[22] M. A. Camblor, P. A. Barrett, M. J. Díaz-Cabañas, L. A. Villaescusa, M. Puche, T. Boix, E. Pérez and H. Koller, *Micropor. Mesopor. Mater.*, **2001**, 13, 2332-2341.

[23] a) D. Jiménez, R. Martínez-Máñez, F. Sancenón, J, Soto, *Tetrahedron Lett.*, **2004**, *45*, 1257-1259; b) D. Markovitsi, C. Jallabert, H. Strzelecka, M. Veber, *J. Chem. Soc., Faraday Trans.*, **1990**, *86*, 2819-2822; c) J. P. Dix, F. Vogtle, *Chem. Ber.*, 1981, 114, 638-651; d) U. Oguz, E. U. Akkaya, *J. Org. Chem.*, **1998**, *63*, 6059-6060.

[24] a) C. Uncuta, A. Tudose, M. T. Caproiu, C. Stavarache, A. T. Balaban, *J. Chem. Res. Synopses*, **2001**, 170-171, 523-535; b) C. Uncuta, M. T. Caproiu, V. Campeanu, A. Petride, M. G. Danila, M. Plaveti, A. T. Balaban, *Tetrahedron*, **1998**, 54, 9747-9764; c) T. Zimmermann, *J. Heterocyclic Chem.*, **1995**, 32, 563-567; d) A. R. Katritzky, B. J. Agha, R. Awartani, R. C. Patel, *J. Chem. Soc., Perkin Trans. 1*, **1983**, 2617-21; e) C. Toma, A. T. Balaban, *Tetrahedron*, **1966**, 7, 27-34; f) C. Toma, A. T. Balaban, *Tetrahedron*, **1966**, 7, 9-25; g) J. V. Ros-Lis, B. García, D. Jiménez, R. Martínez-Máñez, F. Sancenón, J. Soto, F. Gonzalvo, M. C. Valldecabres, *J. Am. Chem. Soc.*, **2004**, 126, 4064-4065; h) J. V. Ros-Lis, R. Martínez-Máñez, J. Soto, *Chem. Commun.*, **2002**, 2248-2249.

[25] R. Martínez-Máñez, F. Sancenón, *Chem. Rev.* **2003**, *104*, 4419-4476.

[26] a) J. L. Meinershagen, T. Bein, *J. Am. Chem. Soc.*, **1999**, *121*, 448-449; b) J.L. Meinershagen, T. Bein, *Adv. Mater.*, **2001**, 13, 208-221; c) M. A. Zanjanchi,

S. H.. Sohrabnezhad, *Sensors Act. B*, **2005**, 105, 502–507; d) M. Ibe, M. Ohara, M. Sadakata, O. Masayoshi, T. Okubo, *Trans. Mater. Res. Soc. Japan*, **2000**, 25, 457-460; e) Y. Komori, S. Hayashi, *Chem. Mater.*, **2003,** *15,* 4598-4603.

Chapter 5

Biomimetic "binding pockets" in hybrid organic-inorganic materials for displacement assays.

5.1. Objectives

In the present chapter will be developed different hybrid organic-inorganic systems that will be employed in selective colorimetric indicator by displacement assays.

In general, the design of sensing materials for anions involves a selection of suitable recognition sites that will be incorporated in the solid support in order to bind the target analyte. In the case of anion coordination, interactions with the receptors will mainly involve

electrostatic forces or formation of hydrogen bonds. Generally, it should be considered different features of the target anions:

- The shape and geometry of the anion to coordinate,
- Its charge, which can be varied as a function of the pH,
- And its hydrophobicity.

The objectives of this chapter are:

- To choose specific anion-binding groups able to interact with anions through electrostatic attractive forces or hydrogen-bonding interactions. Electrostatic interactions with anions are found when using positively charged receptors having for instance guanidinium or ammonium groups (these two groups have a positive charge that basically does not depend on the pH of the medium) or amines (they are usually protonated and therefore charged at neutral and acidic aqueous solutions). Moreover typical receptors for hydrogen bonding interactions are ureas, thioureas, calyx[4]pyrroles, sapphyrins, porphyrins, amides, polyamines and guanidinium groups.

- To prepare different hybrid organic-inorganic mesoporous supports containing anion binding sites.

- To select suitable dyes for loading the hybrid organic-inorganic materials.

- To test the displacement of the dyes in the presence of a target anions in solution.

Chem. Commun., **2008**, 3639-3641

5.2. Hybrid materials with nanoscopic anion binding pockets for the colorimetric sensing of phosphate in water using displacement assays.

Chapter 5

Hybrid materials with nanoscopic anion-binding pockets for the colorimetric sensing of phosphate in water using displacement assays

María Comes,[a] María D. Marcos,[a] Ramón Martínez-Máñez, [a,*] Félix Sancenón,[a] Juan Soto,[a] Luis A. Villaescusa [a] and Pedro Amorós.[b]

[a] Instituto de Química Molecular Aplicada, Universidad Politécnica de Valencia, Camino de Vera s/n, 46022, Valencia, Spain. E-mail: rmaez@qim.upv.es

[b] Institut de Ciència del Materials (ICMUV, Universitat de València. P.O. Box 2085, E-46071 València, Spain.

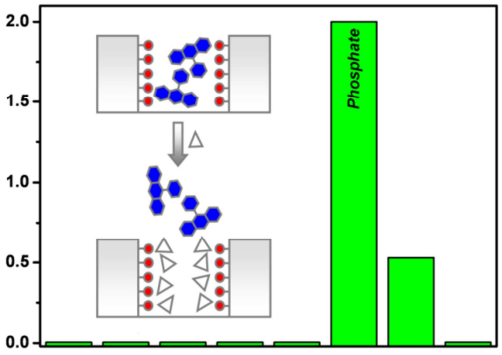

Chem. Commun., **2008**, 3639-3641

Mesoporous amino-functionalised solids containing certain dyes have been used as suitable anion hosts in displacement assays for the colorimetric signaling of phosphate in water.

Introduction

One recently suggested procedure to develop new supramolecular concepts is to attach molecular/supramolecular entities to pre-organised nanoscopic structures. These hybrid systems show cooperative functional behaviours that result in chemical amplification processes.[1] In this field, recent research for the development of smart sensory materials has been reported.[2] This approach allows in a simple way to create hybrid sensing ensembles that can signal analytes for whose selectivity is hard to achieve by conventional methods or may require extensive synthetic chemistry in order to prepare selective receptors. Also the design of hybrid solids with certain surface features (e.g. the presence of mesopores) has been reported to provide new unpredicted functional synergic effects.[3] Following our interest in the development of sensing systems using hybrid materials[4] we report herein how the combination of supramolecular and nanoscopic solid state concepts allows the development of a simple signaling protocol for chromogenic detection of phosphate in aqueous solutions.

Selective chromogenic phosphate receptors are very rare and very few examples displaying colorimetric sensing features for this anion in pure water based on coordination/supramolecular ideas have been described. In one of them a dinuclear Zn(II) complex with H-bpmp (2,6-bis(bis(2-pyridylmethyl)aminomethyl)-4-methylphenol) forms an ensemble with Pyrocatechol Violet (1:1 stoichiometry) that changes its colour selectively in the presence of phosphate *via* phosphate coordination with the Zn

complex and release of the pyrocatechol dye.[5] The other reported example uses a sensing ensemble formed between Pyrocatechol Violet with $YbCl_3$.[6] Addition of phosphate to the formed complex results in a yellow coloration of the solution due to $YbCl_3$-phosphate coordination and release of the dye. Also very recently and following a remarkable approach, the effective sensing of phosphate and other biologically important phosphate-derivatives in water has been successfully achieved by the use of arrays of relatively simple chromogenic receptors embedded in polyurethane membranes.[7]

These examples are all molecular-based. In contrast, we have followed here a different protocol relying on the use of nanoscopic hybrid "binding pockets" as mimicking systems of active-site cavities in biological systems. In fact recent interesting examples dealing with the functionalization of nanoscopic pockets on solid supports with suitable dyes have been used for the development of colorimetric probes in water for certain metal cations[8] and anions[9] with very fine results. We believed that this biomimetic approach may allow us to design probes for the development of simple displacement assays[10] for optical signaling of target guests.

The designed protocol for the colorimetric signaling of phosphate is shown in Scheme 1. Suitable nano-sized pores from a MCM41-type material are functionalized with simple amine binding sites in one step. Then the functionalized solid is loaded with a certain dye able to give binding interactions with the coordination sites. This is the signaling reporter. In the sensing protocol, the target analyte is preferentially bonded by the nanoscopic hybrid binding pocket, inducing the delivery of the dye to the solution resulting in the colorimetric detection of the guest.

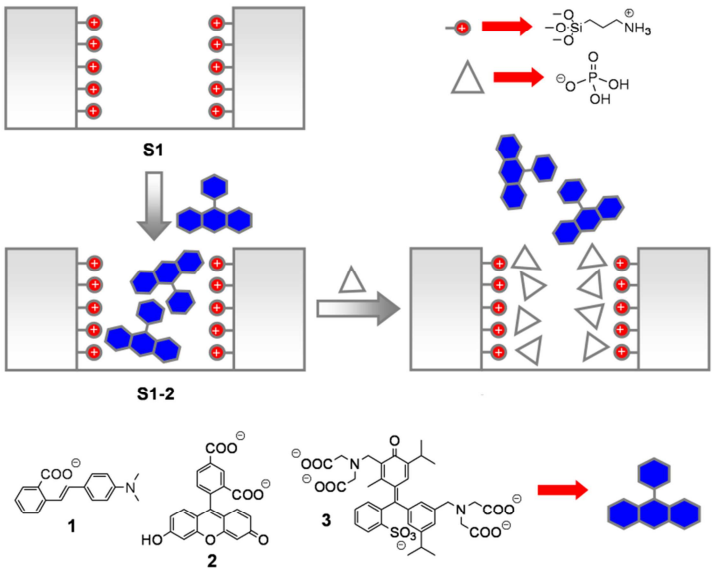

Scheme 1 Protocol for phosphate signaling in water using mesoporous solids containing nanoscopic binding pockets and suitable dyes.

Inspired by this concept the "host" 2.4 nm pore diameter mesoporous solid **S1** containing nanoscale cavities was prepared and loaded with suitable dyes as signaling reporters. In order to enhance accessibility onto the pores we used as starting material the mesoporous MCM41-type UVM-7 derivative which is characterized by their nanometric particle size and bimodal pore system.[11] This mesoporous material was first made react with 3-aminopropyltrietoxysilane to yield solid **S1**. To introduce the signaling units into the pores, solid **S1** was further loaded with three different dyes (*i.e.* Methyl red, **1**, Carboxyfluorescein, **2** and Methylthymol Blue, **3**) at room temperature in water at pH 7.5 for 24 h to yield solids **S1-1**, **S1-2** and **S1-3** (see Scheme 1) that were isolated by filtration and washed until no elimination of the dye to the naked eye was observed. The amines in solid **S1** at neutral pH in water are

expected to be partially protonated and therefore binding with the anionic carboxylate-containing dyes **1**-**3** occurs *via* hydrogen bonding and electrostatic interactions. The final **S1** solid has an amine content of 0.175 mol amine per mol of SiO_2, whereas typical dye loading for different prepared solids was in the 0.02 - 0.1 dye/SiO_2 mol/mol range.

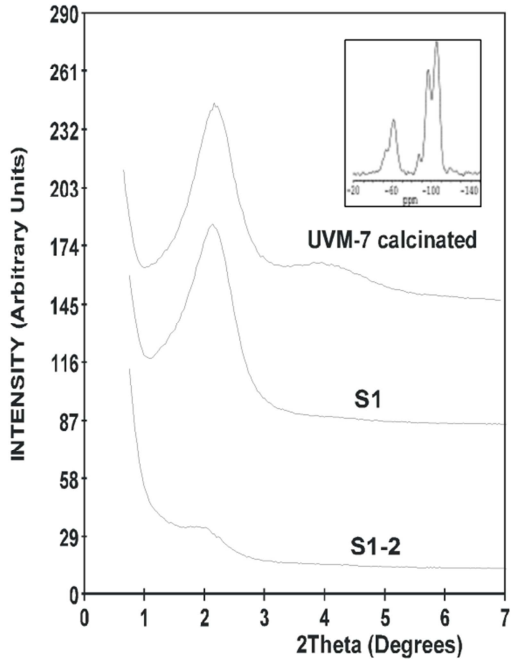

Figure 1. X-ray powder diffraction for the calcinated **UVM-7**, **S1** and **S1-2** materials. The inset shows the ^{29}Si MAS NMR spectrum of the amine-functionalised solid **S1**.

Characterization of the materials by XRD and TEM techniques has been carried out. Figure 1 shows the XRD patterns for the UVM-7, the amine-functionalised solid **S1** and the final carboxyfluorescein-loaded **S1-2** sensory material. The X-ray powder pattern of UVM-1 and **S1** are very similar whereas the low-angle *(100)* reflexion decreases in intensity for **S1-2** due to a decrease in contrast as a consequence of the larger filling

of the pores by the organic dye. Moreover, the existence of the d_{100} peak and the presence in the TEM images of the typical mesoporous structure (see Figure 2) strongly evidence that the functionalization with the amine and the further loading with the dye does not affect the mesoporous UVM-7 type scaffolding. The ^{29}Si MAS NMR spectrum of functionalised **S1-2** solid is shown in the inset. It displays the presence of two groups of signals that correspond to T-silicon (-61 and -53 ppm) and Q-silicon (-105, -97 and -87 ppm) centres, indicative of the condensation of the aminosilane derivative with the silanol groups on of the silica surface in the preparation of **S1**. Spectrum deconvolution gave an approximate relation between Q and T centres of 3:1 in good accordance with chemical analysis data (see Supporting Information for further characterization details).

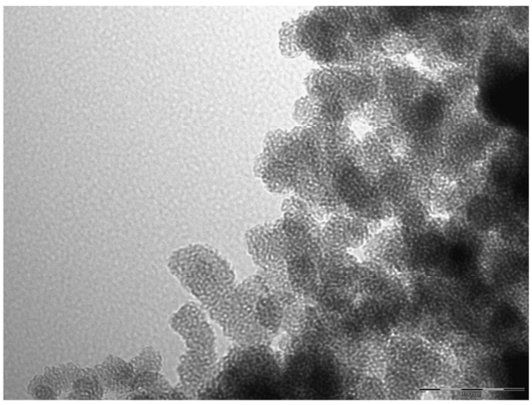

Figure 2. TEM image of solid **S1-2** showing the nanometric particle size.

Amines have been extensively used as suitable groups for the design of receptors able to bind anionic guests. Solids **S1-1**, **S1-2** and **S1-3** contain nanoscopic binding pockets functionalised with anion coordination sites (amines) and different dyes. In a typical experiment 30 mg of the corresponding solid were suspended in water at pH 7.5 (HEPES 0.01 mol

dm^{-3}) in the presence of a certain anion and after 10 minutes the mixture was filtered and the absorbance at the corresponding visible band measured (426, 490 and 605 nm for Methyl Red (solid **S1-1**), Carboxyfluorescein (solid **S1-2**) and Methylthymol Blue (solid **S1-3**), respectively). The anions fluoride, chloride, bromide, iodide, phosphate, sulfate, acetate and nitrate were studied as sodium or potassium salts. The results are summarized in Figure 3.

Addition of phosphate to the functionalised solid suspension resulted in a remarkable development of colour, especially for **S1-2**. Addition of similar anions such as sulfate also induced some colour but in a remarkable lesser extension than phosphate. The solutions remained completely colourless for the **S1-2** and **S1-3** sensory ensembles in the presence of fluoride, chloride, bromide, iodide, acetate and nitrate, whereas **S1-1** also shows some response to acetate.

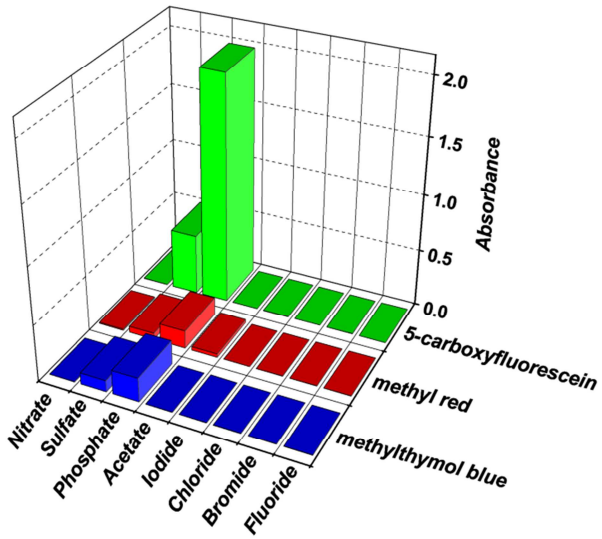

Figure 3. Colorimetric response of solids **S1-1**, **S1-2** and **S1-3** to the presence of certain anion sin pure water at pH 7.5 (HEPES 0.01 mol dm^{-3}), C_{anion} = 1 x 10^{-3} mol dm^{-3}.

A phosphate-selective response was found indicating that the binding pockets in **S1-2** and **S1-3** are capable of recognising phosphate due to favourable coordination when compared with other anions typically present in water. The remarkable phosphate selective behaviour can be explained in terms of preferential formation of phosphate complexes with the tethered amines in the pores. The observed conduct is in agreement with the polyammonium-anion complex formation trend in water that usually follows the order phosphate > sulfate >> nitrate ~ halide ions.[12] Thus, a suitable design of the solid coupled with these phosphate binding favourable feature results in a colorimetric selective response to this anion in pure water. Additionally, **S1-2** shows the better response among the solids tested in terms of sensitivity. Thus absorbances up to values of *ca*. 2 can be easily be observed using **S1-2** in the presence of phosphate. By contrast, under similar conditions **S1-3** shows a poorer response most likely because the Methylthymol Blue dye (a trianion) in **S1-3** forms quite strong complexes with the anchored amines. Consequently, as phosphate must be present as a mixture of mono- and di-anionic species (HPO_4^{2-} and H_2PO^{4-}) at neutral pH, the trianion is poorly displaced. In fact we have observed under competitive conditions that Methylthymol Blue is preferentially included with respect to 5-Carboxyfluorescein in the nanoscopic pockets of **S1** indicating that the former dye binds more tightly with the ammonium groups (see Supporting Information for details). The solid **S1-1** shows a poor response presumably because the monocarboxylate dye Methyl Red is weakly adsorbed at the mesopores and it is released in the washing stage during its preparation.

An additional important aspect in this research was to find out the effect that the nanoscopic pockets have in the sensing behaviour of these hybrid materials. Therefore as an additional study, we prepared a material similar to **S1-2** but using non porous silica (silica gel) as solid support.

This new solid (**SG-2**) contains anchored amine groups and a certain amount of adsorbed Carboxyfluorescein, *via* interaction with the amines at the surface, but lacks the 3D mesoporous structure in **S1-2**. Studies of the interaction of **SG-2** with phosphate and other anions showed no response (see Figure 4). This result shows the effect that the mesoproous 3D organized surface has in the sensing protocol. The presence of nanoscopic binding pockets in **S1** most likely induces some spatial proximity between several ammonium subunits forming a suitable "binding pocket" within the pores that favours coordination with the dye and then with phosphate. This synergic effect is not apparently observed when using locally flat surfaces (**SG-2** material).

The response of the sensing material **S1-2** and **SG-2** as a function of the phosphate concentration in water at neutral pH is illustrated in Figure 4 which plots the absorbance at 490 nm after the displacement protocol described above. The results reveal that the delivery of the dye from **S1-2** to the solution is related with the phosphate – solid interaction and therefore proportional to the amount of phosphate in water. A detection limit lower than $1x10^{-4}$ mol dm^{-3} was calculated.

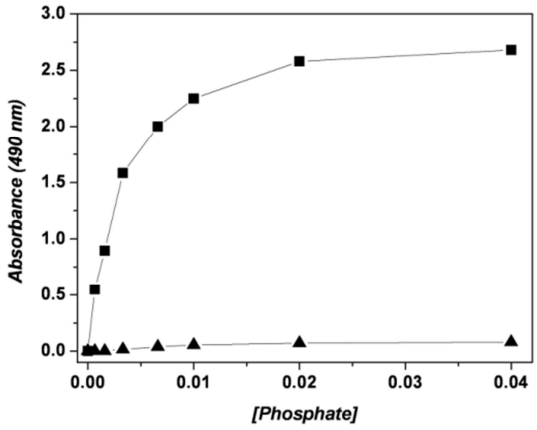

Figure 4. Calibration curve for solids S1-2 (■) and SG-2 (▲) at pH 7.5 (HEPES 0.01 mol dm^{-3}) in the presence of phosphate.

In summary, we have shown that simple functionalised mesoporous solids containing nanosized coordinating pockets also containing commercially available dyes can act as suitable sensory materials for the chromo-fluorogenic detection of anions of environmental importance such as phosphate. The approach allows with a minimum effort to test a large number of combinations and may be of application to a wide range of different guests. The sensing protocol is undemanding and opens the possibility of developing new selective signaling systems by combination of simple coordinating groups and the non-covalent anchoring of suitable dyes in similar hybrid systems.

Notes and references

[1] A.B. Descalzo, R. Martínez-Máñez, F. Sancenón, K. Hoffmann, K. Rurack, *Angew. Chem. Int. Ed.*, **2006**, 45, 5924. K. Ariga, A. Vinu, J.P. Hill, T. Mori, *Coord. Chem. Rev.*, **2007**, 251, 2562.

[2] E. Rampazzo, E. Brasola, S. Marcuz, F. Mancin, P. Tecilla, U. Tonellato, *J. Mater. Chem.*, **2005**, 15, 2687. C.–C. Huang, Z. Yang, K.–H. Lee, H.–T. Chang, *Angew. Chem. Int. Ed.*, **2007**, 46, 6824.

[3] V. S.–Y. Lin, C.–Y. Lai, J. Huang, S.–A. Song, S. Xu, *J. Am. Chem. Soc.*, **2001**, 123, 11510. R. Casasús, E. Climent, M.D. Marcos, R. Martínez-Máñez, F. Sancenón, J. Soto, P. Amorós, J. Cano, E. Ruiz, *J. Am. Chen. Soc.*, **2008**, 130, 1903-1917.

[4] M. Comes, M.D. Marcos, R. Martínez-Máñez, F. Sancenón, J. Soto, L.A: Villaescusa, P. Amorós, D. Beltrán, *Adv. Mater*. **2004**, 16, 1783. A.B. Descalzo, K Rurack, H. Weisshoff, R. Martínez-Máñez, M.D: Marcos, P. Amorós, K. Hoffmann, J. Soto, *J. Am. Chem. Soc.*, **2005**, 127, 184. R. Casasús, E. Aznar, M.D: Marcos, R. Martínez-Máñez, F. Sancenón, J. Soto, P. Amorós, *Angew. Chem. Int. Ed.*, **2006**, 45, 6661. C. Coll, R. Martínez-Máñez, M.D. Marcos, F. Sancenón, J. Soto, *Angew. Chem. Int Ed.*, **2007**, 46, 1675. C. Coll, R. Casasús, E. Aznar, M.D. Marcos, R. Martínez-Máñez, F. Sancenón, J. Soto, P. Amorós, *Chem. Commun.*, **2007**, 1957. A.B. Descalzo, M.D.

Marcos, C. Monte, R. Martínez-Máñez, K. Rurack, *J. Mater. Chem.*, **2007**, 17, 4716.

[5] M. H. Han, D. H. Kim, *Angew. Chem. Int. Ed.*, **2002**, 41, 3809.

[6] C. Yin, F. Gao, F. Huo, P. Yang, *Chem. Commun.*, **2004**, 934.

[7] (a) M. A. Palacios, R. Nishiyabu, M. Marquez, P. Anzenbacher Jr., *J. Am. Chem. Soc.*, **2007**, 129, 7538. (b) G. V. Zyryanov, M. A. Palácios, P. Anzenbacher Jr., *Angew. Chem. Int. Ed.*, **2007**, 46, 7849.

[8] T. Balaji, M. Sasidharan, H. Matsunaga, *Anal. Bioanal. Chem*. **2006**, 384, 488. T. Balaji, S.A. El-Safty, H. Matsunaga, T. Hanaoka, F. Mizukami, *Angew. Chem. Int. Ed.*, **2006**, 45, 7201. S.A. El-Safty, A.A. Ismail, H. Matsunaga, F. Mizukami, *Chem. Eur. J.*, **2007**, 13, 9245.

[9] M. Comes, G. Rodríguez-López, M.D. Marcos, R. Martínez-Máñez, F. Sancenón, J. Soto, L.A. Villaescusa, P. Amorós, D. Beltrán, *Angew. Chem. Int. Ed.*, **2005**, 44, 2918.

[10] For information about displacement assays see for instance: R. Martínez-Máñez, F. Sancenón, *Chem. Rev.*, **2003**, 103, 4419. S. L. Wiskur, H. Aït-Haddou, J. J. Lavigne, E. V. Anslyn, *Acc. Chem. Res.*, **2001**, 34, 963. B. T. Nguyen, E. V. Anslyn, *Coord. Chem. Rev.*, **2006**, 250, 3118. L. Fabbrizzi, N. Marcotte, F. Stomeo, A. Taglietti, *Angew. Chem. Int. Ed.*, **2002**, 41, 3811.

[11] J. El Haskouri, D. Ortiz, C. Guillem, J. Latorre, M. Caldés, A. Beltrán, D. Beltrán, A.B. Descalzo, G. Rodríguz-López, R. Martínez-Máñez, M.D. Marcos, P. Amorós, *Chem. Commun.*, **2002**, 330.

[12] The particular strong interaction of phosphate with amines is reported to be a consequence of the ability of phosphate species to behave as both acceptor and donor in hydrogen bonds. For a detailed discussion see for instance: E. García-España, P. Diez, J.M. Llinares, A. Bianchi, *Coord. Chem. Rev.*, **2006**, 250, 2952. E.A. Katayev, Y.A. Ustynyuk, J.L. Sessler, *Coord. Chem. Rev.*, **2006**, 250, 3004.

Chem. Commun., **2008**, 3639-3641

Supporting Information

Hybrid materials with nanoscopic anion-binding pockets for the colorimetric sensing of phosphate in water using displacement assays.

María Comes, María D. Marcos, Ramón Martínez-Máñez,* Félix Sancenón, Juan Soto, Luis A. Villaescusa and Pedro Amorós.

Chemicals

The products tetraethylorthosilicate (TEOS), *n*-cetyltrimethylammonium bromide (CTAB), sodium hydroxide (NaOH), triethanolamine ($TEAH_3$) and all the anions used in this manuscript were provided by Aldrich and used as received.

Synthesis of the mesoporous UVM-7 support (MCM41-type material).

The synthesis strategy we have used to prepare UVM-7 and hybrid related organosilicas is an application of the so-called "atrane route", a simple preparative technique based on the use of complexes that include triethanolamine($TEAH_3$)-related ligands (i.e. in general "atranes" and silatranes for the silicon containing complexes) as hydrolytic inorganic precursors and surfactants as porogen species. Then, the molar ratio of the reagents in the mother liquor was fixed to 7 $TEAH_3$:2 TEOS:0.52 CTAB:180 H_2O for the synthesis of UVM-7. The mixture was heated to

140 °C to remove ethanol formed during the formation of the atrane complexes by distillation. Then the mixture was cooled to 90 °C and cetyltrimethylammonum bromide (CTAB)) was slowly added. Finally the corresponding amount of water was added and the mixture was subsequently aged at room temperature for 24 h. The resulting powder was collected by filtration, washed with water and ethanol and dried in air. The surfactant was removed by calcination at 550^{o}C for 5 hours.

Synthesis of the amine derivative S1.

The calcinated material (UVM-7) was first activated in a ethanol/HCl 1M solution.

3 g of templated-free **UVM-7** activated material was suspended in 300 ml of anhydrous toluene and heated at 110 ºC in a Dean-Stark in order to remove the adsorbed water by azeotropic distillation under inert atmosphere (Ar atmosphere). Then a large excess of 3-(aminopropyl)triethoxysilane (10-5 ml, 44.7 mmol) was added to the suspension at room temperature and stirred for 16 hours at 100 ºC in reflux system. The final solid (**S1**) was filtered off, meticulously washed with toluene and acetone and dried at 60 ºC for at least 12 hours.

Synthesis of the dye-containing solids S1-2, S1-2 and S1-3.

The amine-functionalised solid **S1** (1 g) was suspended in 100 ml of water at pH 7.5 and the corresponding dye added (0.69 g, 0.4 g or 0.67 g of methyl red, carboxyfluorescein, or methylthymol blue, respectively) at room temperature. The mixture was stirred for 24 hours to yield the corresponding solids **S1-1**, **S1-2** and **S1-3** that were isolated by filtration and exhaustively washed with water until no elimination of the dye was

observed. The solids remained stable for at least two months without apparent degradation of the dyes.

For the sake of comparison, and as a control solid, a similar material was prepared using as support a non-mesoporous silica (fumed silica). The procedure was the same as described above but using in this case silica gel and carboxyfluorescein as dye. The final product (**SG-2**) was filtered, washed and dried at 70 ºC for 12 hours. This solid consists of a "flat" surface (i.e. without the presence of mesopores) with anchored amine groups and a certain amount of adsorbed dye.

General Techniques and characterization

XRD, TG analysis, IR spectroscopy, elemental analysis, TEM microscopy, N_2 adsorption-desorption, UV-visible spectrophotometer techniques were employed to characterize the materials. X-ray measurements were performed on a Seifert 3000TT difractometer using Cu Kα radiation. Thermo-gravimetric analysis were carried out on a TGA/SDTA 851e Mettler Toledo balance, using an oxidant atmosphere (Air, 80 mL/min) with a heating program consisting on a heating ramp of 10 °C per minute from 393 K to 1273 K and an isothermal heating step at this temperature during 30 minutes. IR spectra were recorded on a Jasco FT/IR-460 Plus between 400 and 4000 (cm^{-1}) diluting the solids in KBr pellets. N_2 adsorption-desorption isotherms were recorded on a Micromeritics ASAP2010 automated sorption analyser. The samples were degassed at 120 ºC in vacuum overnight. The specific surfaces areas were calculated from the adsorption data in the low pressures range using the BET model. Pore sized was determined following the BJH method. UV-visible spectroscopy was carried out with a Lambda 35 UV/Vis Spectrometer Perkin Elmer Instruments.

The thermal analysis of the **S1-1**, **S1-2** and **S1-3** solids showed three well defined steps; (i) a first weight loss between 25 and 150 ºC related with the elimination of solvent molecules, (ii) a second step, between 150 and 800 ºC due to the combustion of the organics groups (the propyl-amino groups and the corresponding dye) and (iii) a final weight loss in the ca. 800 - 1000 ºC range attributed to the condensation of the silanol groups.

The powder X-ray diffraction patterns of the obtained for these solids (see Figure 1 in the paper) show the characteristic intense peak at ca. 2θ = 2º (indexed to the (100) reflection assuming the existence of a MCM-41-like hexagonal cell) of a surfactant-assisted mesoporous material, indicating that the different synthetic steps did not affect to a large extent the structure of the silica matrix. In addition to this intense peak, we can observe in those structures with better contrast (lower amount of organics) a wide and small signal that could be assigned to the overlapped (110) and (200) reflections of the typical hexagonal cell. This feature can be associated to an intraparticle porous topology characteristic of MCM-41-like disordered hexagonal silicas. The bimodal pore array of **UVM-7**-like solids is additionally appreciated through TEM images (see Figure 2 in the paper) and porosimetry measurements (see below).

The N_2 adsorption-desorption isotherm of the **S1** material shows a typical curve for these mesoporous solids and it is similar to the curve observed for the parent UVM-7 material. The isotherm is characterised by two adsorption steps at intermediate and high P/P_0 values related with the bimodal pore system. The first step corresponds to the nitrogen condensation inside the mesopores by capillarity (pore size: 2.4 nm and pore volume 0.72 cc/g), whereas the second one corresponds to the

nitrogen condensation inside the interparticle pores (textural porosity, pore size: 41.1 nm and ore volume 0.68 cc/g). The application of the BET model resulted in a value for the total specific surface of 870 m^2/g for **S1**. Additionally, the interaction of the dyes with **S1** to yield the sensory materials **S1-1**, **S1-2** and **S1-3** resulted in a considerable reduction of the total specific surface to ca. 300 m^2/g as consequence of the inclusion of the dyes into the pores.

The infrared spectrum of **S1-1**, **S1-2** and **S1-3** solids show strong bands due to the silica matrix (c.a. at 1250, 1087, 802 and 462 cm^{-1}) and relatively medium and small bands due to the organic loaded molecules (the methyl red, carboxyfluorescein, or methylthymol blue dyes) such as for instance at ca. 1620 and 1400 cm^{-1} assignable to the carboxylate groups.

Several **S1** and **S1-1**, **S1-2**, **S1-3** materials were prepared and their content in amine groups and imidazolium groups and methyl red, carboxyfluorescein, or methylthymol blue dyes were determined from elemental analysis and thermal analysis. From the different prepared solids an average value of 0.175 mol amine/mol SiO_2 and dye contents in the 0.05 - 0.1 dye/SiO_2 mol/mol range were determined.

Competitive adsorption of dyes on S1

In order to better understand the different displacement observed for 5-carboxyfluorescein and methylthymol blue (see article), competitive assays of adsorption of these dyes on the amine-functionalised material **S1** were carried out. In a typical assay, 100 mg of solid **S1** were suspended in 100 mL of an aqueous solution at pH 7.5 (HEPES 0.01 mol dm^3) containing a mixture of both dyes; 5-carboxyfluorescein and

methylthymol blue at a concentration of 2 x 10^{-5} mol dm^3. Adsorption of the dyes on **S1** was followed by simple monitorization of the corresponding visible band of the dyes in the solution. Under these experimental conditions, the percentages of adsorption on **S1** of 5-carboxyfluorescein and methylthymol blue were 21 % and 55 % respectively. This shows that methylthymol blue is preferentially adsorbed on the amine-functionalised **S1** material. In additional experiments (not shown) the adsorption constants (K) for 5-carboxyfluorescein and methylthymol blue were determined using a Langmuir adsorption model and values of log K of 3.57 and 4.74 were obtained respectively. The stronger interaction of methylthymol blue with the mesoporous-functionalised surface is in agreement with the experimental data that shows that 5-carboxyfluorescein (solid **S1-2**) is displaced more efficiently than methylthymol blue (solid **S1-3**) in the presence of phosphate.

Chem. Eur. J. **2009**, 15, 9024-9033

5.3. Mesoporous hybrid materials containing nanoscopic binding pockets for colorimetric anion signaling in water by using displacement assays.

Chapter 5

Mesoporous hybrid materials containing nanoscopic "binding pockets" for colorimetric anion signaling in water using displacement assays

María Comes,[a,b,c] Elena Aznar,[a,b,c] M. Dolores Marcos,[a,b,c] Ramón Martínez-Máñez,[a,b,c]* Félix Sancenón,[a,b,c] Juan Soto,[a,b] Luis A. Villaescusa,[a,b,c] Luis Gil, [a,d] Pedro Amorós.[e]

[a] Instituto de Reconocimiento Molecular y Desarrollo Tecnológico, Centro Mixto Universidad Politécnica de Valencia – Universidad de Valencia, Spain.

[b] Departamento de Química. Universidad Politécnica de Valencia. Camino de Vera s/n. E-46022, Valencia, Spain.

[c] CIBER de Bioingeniería, Biomateriales y Nanomedicina (CIBER-BBN).

[d] Departamento de Ingeniería Electrónica, Universidad Politécnica de Valencia, Camino de Vera s/n, 46071, Valencia, Spain.

[e] Institut de Ciència del Materials (ICMUV), Universitat de Valencia. P.O. Box 2085, E-46071 Valencia, Spain.

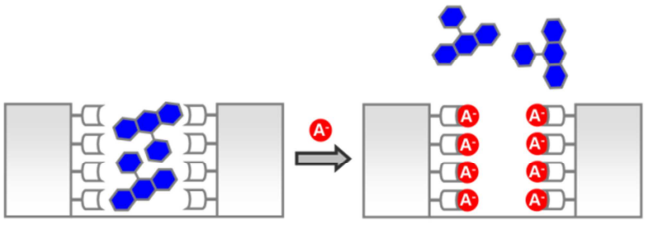

Mesoporous solids functionalized with anion binding groups have proved to be suitable anion hosts and have been used in selective colorimetric displacement assays. As inorganic scaffolding the material UVM-7 was selected. This is a mesoporous MCM41-type support that is characterized by the presence of nanometric mesoporous particles conglomerates. The template-free UVM-7 solid was reacted with 3-aminopropyltrietoxysilane (**1**) to yield solid **S1**. From **S1**, the derivatives **S2** and **S3** were obtained by reaction with 2-methylthio-2-imidazoline hydroiodide (**2**) and butyl isocyanate (**3**), respectively. Additionally, solid **S4** and **S5** were prepared by reaction of the starting mesoporous UVM-7 scaffolding with *N*-methyl-*N´*-propyltrimethoxysilyl imidazolium chloride (**4**) and with 3-(trimethoxysilyl)propyl-*N*,*N*,*N*-trimethylammonium chloride (**5**), respectively. This synthetic procedure results in final solids containing mesoporous binding pockets able to give interactions with anions via electrostatic attractive forces (**S1**, **S2**, **S4**, **S5**) and hydrogen bonding interactions (**S1**, **S2**, **S3**, **S4**). The functionalized solid were then loaded with a dye capable of giving coordinative interactions with the anchored binding sites, in our case 5-carboxyfluorescein to yield the hybrid materials **S1d, S2d**, **S3d**, **S4d** and **S5d**. These solids are the signaling reporters. The sensing ability of these dye-containing solids towards a family of carboxylates namely acetate, citrate, lactate, succinate, oxalate, tartrate, malate, mandelate, glutamate and certain nucleotides has been studied in pure water at pH 7.5 (HEPES 0.01 mol dm^{-3}). In the sensing protocol, a certain analyte may preferentially be bonded by the nanoscopic functionalised pocket, leading to the delivery of the dye to the solution resulting in the colorimetric detection of the guest. The response to a certain anion depends on the characteristics of the binding pockets and the specific interaction of the anion with the binding groups into the mesopores. We believe that the possibility of using a wide variety of mesoporous supports that can be easily

functionalized with anion binding sites, combined with suitable dyes as indicators, makes this approach significant for the opening of new perspectives in the design of chromogenic assays for anion detection in pure water.

Introduction

The recognition of chemical species of varying complexity has been for years one of the most intensively studied areas of supramolecular chemistry. There are many examples in the literature devoted to the synthesis of sophisticated coordination subunits arranged in certain topologies dedicated to achieve high degree of complementarity with the target guests.[1] Once the basis for the design of receptors was established, supramolecular chemists have become interested in recent years in the use of coordination subunits for the preparation of molecules in such a way that the presence of target guests is transformed into a change in colour,[2] fluorescence[3] or redox potential.[4] In fact, the recognition and signaling of chemical species is one of the most fruitful areas of contemporary supramolecular chemistry. In this area chromogenic and fluorogenic sensors for metal cations[5] and anions[6] have been developed whereas there is a timely increasing interest in the design of chemosensors for neutral species.[7] In general the supramolecular signaling process comprises two steps; (i) the selective coordination of the target guest using selective coordinating groups and (ii) a transduction of the coordination event via modulation of the optical or electrochemical signal. This two-step process requires an adequate interaction, generally into a superstructure of both components, the signaling unit and the coordination or binding sites. Additionally, besides fluorescence or electrochemical outputs, colorimetric recognition is especially attractive because it offers the possibility to the so-called "naked eye detection" and are usually systems easy-to-handle that can be applied for instance to the design of rapid screening semi-quantitative determinations. Most of the examples reported in the field of chemosensing are based on relatively simple molecular systems. In fact, receptors displaying sensing features only in organic solvents are

relatively common. Moreover, the milestone of selectivity in water usually finds the counterpart of extensive synthetic chemistry in order to prepare multitopic highly pre-organised systems.

Despite the use of indication formats such as the coordination site - signaling subunit and chemodosimeter, the so-called displacement assay has gained attention in the last years.[8] The displacement approach relies in the formation of binding site - signaling subunit "molecular ensembles" and in the displacement of the signaling subunit (usually a dye) in the presence of a target guest. Receptors for the displacement protocol usually contain multiple coordination sites in a preorganised fashion. For instance, a number of examples have been reported on 1,3,5-2,4,6-functionalized benzene scaffoldings with 1,3,5-positions directed to one face of the ring leading to trifurcate anion receptors containing three arms with coordinating groups in a cooperative preorganization.[9]

From a different field, in the last years there has been an increasing interest in the blending of supramolecular concepts with porous inorganic solids in order to obtain hybrid organic-inorganic materials. These hybrid materials showed enhanced patterns of selectivity and new functional chemical properties. Recent examples in this area indicated that the combination of supramolecular models related with recognition/sensing procedures and nanoscopic supports can result to new perspectives of applicability of hetero-supramolecular concepts in siganlling protocols.[10] This does not refer to the simple anchoring of chemosensors to a solid support but to the search of new functional outcomes where the solid scaffolding itself would play a significant role in the recognition/sensing paradigm. This would lead to smart sensory materials where the information about the sensing outcome is somewhat

encoded in the functionalised solid via combination of a suitable binding sites, additional interactions provided by the solid support and a chromo-fluorogenic event.[11] What makes this approach especially attractive is the coming out of new molecular-solid synergic effects that are hardly achievable in molecular-based systems or in nanoscopic solids individually. In this context nice examples have been reported based on the use of nanoparticles[12] and mesoporous solids.[13]

The distinctive characteristics of functionalized mesoporous silica supports such as high homogeneous porosity, inertness, thermal stability, the presence of tunable pore sizes with a diameter of ca. 2-10 nm and the possibility of easily functionalize the external (or internal) surface, make of these solids ideal scaffoldings for hosting functional guest molecules.[14] However, although mesoporous solids have received much attention in certain fields such as adsorption,[15] optical and electronic applications,[16] delivery systems,[17] catalysis,[18] etc, they still have scarcely been used for supramolecular recognition or sensing protocols. Yet the combination of chemical binding centers with selected physical properties of mesoporous solids (especially bio-inspired properties such as the control of the hydrophobic properties near the recognition centre) is an appealing mode for modulating selectivity. Related with the later, it has been reported that the anchoring of suitable binding sites in the surface of certain mesoporous scaffoldings could lead to the formation of nanometer-sized binding pockets that can mimic the behaviour of certain complex biological superstructures.[19, 11a]

As a part of our interest in the development of chemosensors based on the use of solid scaffoldings,[20] we have recently prepared sensing protocols using displacement assays in mesoporous solids containing binding pockets (*vide infra*). In this additional work we were interested

in demonstrate that very simple mesoporous solids containing different binding pockets can be used to discriminate closely related organic anions. With this aim, suitable mesoporous materials of the MCM41-type have been functionalized with anion binding groups in one or two steps. The functionalized solids, further loaded with a certain dye, have been tested as potential colorimetric sensing systems for anions via displacement assays in pure water.

Results and discussion.

Preparation of functionalised mesoporous material containing functional binding pockets. For the preparation of solids for the chromo-fluorogenic recognition of anions we have followed a protocol relying on the use of nanoscopic hybrid "binding pockets" as mimicking systems of active-site cavities in biological systems. Moreover, interesting examples dealing with the functionalization of nanoscopic pockets on solid supports with suitable dyes have been reported for the development of colorimetric probes in water. In fact, there are an increasing number of recent examples dealing with the design of functionalised hybrid mesoporous silicas containing chromogenic or fluorogenic probes for the detection of metal ions. In most cases, the solid supports are MCM-41, MCM-48, SBA-15 or silica nanotube matrices in which certain selective probes are covalently anchored to the pore walls. Following this approach, chemosensors for the signaling of Hg^{2+}, [21, 22, 23] Cu^{2+}, [24, 25, 26] Fe^{3+}, [27] and Zn^{2+} [28] have been described. Optical pH sensors using mesoporous structures have also been reported.[29] In recent examples, and in order to develop simple synthetic procedures that avoid the covalent anchoring of the probe, Matsunaga and El-Safty have prepared a family of optical sensory materials for the detection of certain metal

ions in which the probes are electrostatically attached to the pore walls.[30-34]

However, despite these interesting examples for target metal cation sensing, the number of functionalised mesoporous supports for the design of chromo-fluorogenic probes for anions is very scarce.[35] Additionally, the approach followed in these examples for cation detection is based on the classical "binding site - signaling subunit" protocol. In contrast we have made use here of the so-called displacement paradigm. This is shown in Scheme 1. The signaling protocol involves several steps; (i) first the pores are functionalised with adequate binding sites, (ii) in a second step the pores are loaded with a dye that coordinates to these anchored sites and (iii) finally the presence of a target anion in the solution, that forms a stronger complex with the binding groups, induced the displacement of the dye and its diffusion into the bulk solution. This diffusion of the dye into the solution enables the colorimetric detection of the anionic guest. As in other displacement assays[36] a selective response is expected to be reached by the adequate choice of binding sites and dye.

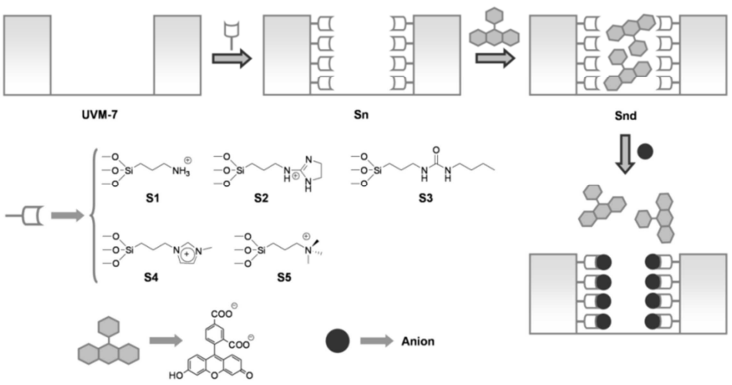

Scheme 1.- Protocol for anion signaling in water using mesoporous MCM-41-like solids containing nanoscopic binding pockets and suitable dyes.

Inspired by this concept shown in Scheme 1, the solid "host" UVM-7 was selected. This is a mesoporous MCM41-type material that is characterized by the presence of conglomerates of nanometric particles resulting in a bimodal pore system.[37] In a first step the UVM-7 mesoporous material was synthesized using the so-called "atrane route", based on the use of complexes that include triethanolamine($TEAH_3$)-related ligands (i.e. in general "atranes" and silatranes for the silicon containing complexes) as hydrolytic inorganic precursors and surfactants as porogen species. In a second step the template-free UVM-7 support was reacted with 3-aminopropyltrietoxysilane (**1**) to yield solid **S1** (see Scheme 2). From **S1**, the derivative **S2** was obtained by reaction with 2-methylthio-2-imidazoline hydroiodide (**2**) in refluxing methanol. **S3**, was synthesised by reaction of **S1** with butyl isocyanate (**3**) in THF in presence of triethylamine. Additionally, solid **S4** and **S5** were prepared by reaction of the starting mesoporous UVM-7 scaffolding with *N*-methyl-*N´*-propyltrimethoxysilyl imidazolium chloride (**4**) and with 3-(trimethoxysilyl)propyl-*N,N,N*-trimethylammonium chloride (**5**), respectively. In all cases the solids were filtered off after the reaction and meticulously washed with different solvents and dried.

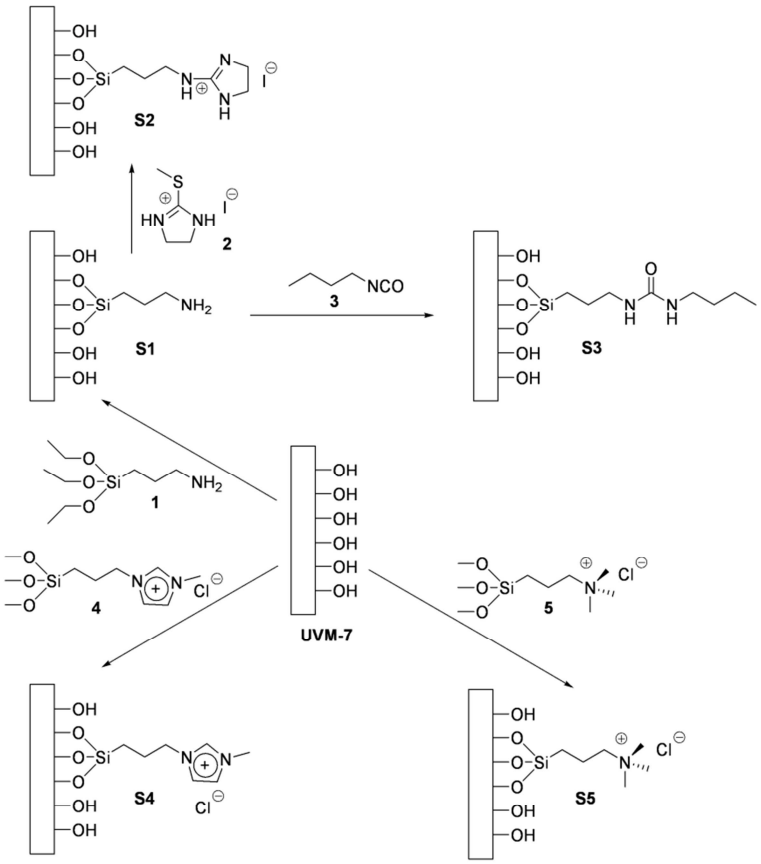

Scheme 2.- Synthetic route for the preparation of solids **S1**, **S2**, **S3**, **S4** and **S5**.

This synthetic procedure results in final solids able to give interactions with anions via electrostatic attractive forces (**S1**, **S2**, **S4**, **S5**) and hydrogen bonding interactions (**S1**, **S2**, **S3**, **S4**). In a second step, the final sensor supports were prepared by loading the pores with 5-carboxyfluorescein by reaction at room temperature in water at pH 7.5 for 24 hours to yield solids **S1d, S2d**, **S3d**, **S4d** and **S5d** that were isolated by filtration and washed until no release of the dye to the naked eye was observed.

Characterization of solids.

The prepared solids **S1**-**S5** and **S1d** - **S5d** were characterised using standard procedures. The powder X-ray pattern of the as-synthesized UVM-7 solid shows four low-angle reflections typical of a hexagonal array that can be indexed as (100), (110), (200), and (210) Bragg peaks with an a_0 cell parameter of 43.3 Å (d_{100} spacing of 37.6 Å). The X-ray pattern of the calcined UVM-7 solid shows a certain displacement of the (100) peak due to condensation of the silanol groups resulting in an approximate cell contraction of 5.7 Å. The X-ray diffraction patterns of the hybrid materials **S1**-**S5** are characterised by the presence of an intense peak at ca. 2θ = 2º (100 reflexion) typical of a surfactant-assisted mesoporous material, indicating that the different synthetic steps for their preparation from UVM-7 did not induce any significant effect on the mesoporous structure of the silica matrix. In fact, the X-ray powder pattern of UVM-7 and **S1**-**S5** solids are similar, whereas the low-angle (100) reflexion decreases in intensity for the corresponding dye-loaded solids **S1d** - **S5d** most likely due to a decrease in contrast as consequence of the pore filling with the organic dye. As a representative example the Figure 1 shows the X-ray diffraction patterns of the calcined UVM-7, **S5** and **S5d** solids.

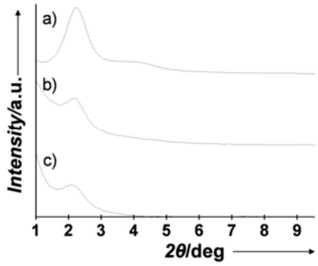

Figure 1.- X-ray diffraction patterns of the solids a) calcined UVM-7, b) **S5** and c) **S5d**

TEM images of all the studied solids show, additionally to the characteristic frindges of the mesoporous channels, the bimodal pore array typical of the UVM-7-like solids. Hence, this technique also indicate that the functionalization and further loading with the dye do not change the mesoporous structure of the starting scaffolding. Figure 2 shows a representative TEM image of the functionalized solids (solid **S4d**).

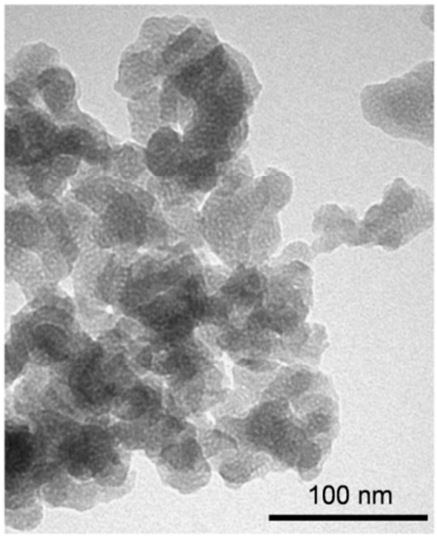

Figure 2.- TEM image of solid **S4d** showing the nanometric particle size.

The solids have also been studied via N_2 adsorption-desorption isotherms. The N_2 adsorption-desorption isotherm of UVM-7 calcined show two steps. The first, at $0.2 < P/P_0 < 0.6$ is originated from the capillary condensation of N_2 into the mesopores. There is no hysteresis loop in this interval and the pore distribution is very narrow suggesting the presence of uniform cylindrical mesopores. For this step a pore diameter of 2.97 nm and a pore volume of 0.98 $cm^3\ g^{-1}$ were calculated. The application of the BET model resulted in a value for the total specific

surface of 1075 $m^2 g^{-1}$. The second step, at higher relative pressures, is related with the filling of textural inter-particle pores typical of the UVM-7 scaffolding. In this case, the curves show hysteresis and a broader pore distribution. A volume of 1.42 $cm^3 g^{-1}$ and an average diameter of 66.5 nm for the textural pore were determined. For **S1**-**S5** materials typical pore diameters in the range 2.4-2.0 nm and pore volumes of 0.72-0.24 $cm^3 g^{-1}$ were calculated from N_2 adsorption-desorption isotherms. For these solids also volumes and diameters in the range of 0.68-0.56 $cm^3 g^{-1}$ and 41.1-33.0 nm for the textural pores were determined. When comparing these data with the non-functionalised solid UVM-7 it is evident that the higher degree of functionalization in **S1-S5** results in a reduction of both mesoporous and textural pores, which evidences the presence of the active sites in the inner surface of the solid. Additionally, the preparation of solids **S1d**-**S5d** by filling the pores of solids **S1**-**S5** with carboxyfluorescein resulted in curves that show a considerable reduction of the total specific surface to ca. 200-300 $m^2 g^{-1}$ as consequence of the inclusion of the dyes into the pores.

As a representative example, the ^{29}Si MAS NMR spectrum of functionalised solid **S1d** was also studied. It displays the presence of two groups of signals that correspond to T-silicon (-61 and -53 ppm) and Q-silicon (-105, -97 and -87 ppm) centres, indicative of the condensation of the aminosilane derivative with the silanol groups on the silica surface during the preparation of **S1**. Spectrum deconvolution gave an approximate relation between Q and T centres of 3:1 in good accordance with chemical analysis data.

The thermal analysis of the **S1-S5** and **S1d-S5d** solids showed three well defined steps; (i) a first weight loss between 25 and 150 ºC related with the elimination of solvent molecules, (ii) a second step, between 150

and 800 ºC due to the combustion of the organic groups (the binding groups and the corresponding dye) and (iii) a final weight loss in the ca. 800-1000 ºC range attributed to the condensation of the silanol groups.

The degree of functionalisation and dye loading of **S1-S5** and **S1d-S5d** solids was assessed by thermogravimetric studies and elemental analysis. From the elemental contents (C, H, N), the amount of groups contained in the materials were calculated in millimole per gram of SiO_2 (mmol g^{-1} SiO_2) using equation 1:

$$\alpha_A = \frac{\Delta W_i\% \times 1000}{\Delta W_{SiO_2}\% \times nM_i} \quad [\text{mmol g}^{-1}\ \text{SiO}_2] \qquad (1)$$

where $\Delta W_i\%$ (i = N, C) are the weight percentages of carbon or nitrogen, M_i is the corresponding atomic weight and n is the number of corresponding atoms in one molecule. $\Delta W_{SiO_2}\%$ is the inorganic SiO_2 content in weight percentage. These experiments show that the amount of organics content increases from the starting UVM-7 material to **S1-S5** due to the anchoring of organic groups and to **S1d-S5d** as consequence of the dye loading. For instance typical binding site contents in solids **S1-S5** range from 1.5 to 2 mmol groups per gram of SiO_2, whereas the dye loading obtained for the corresponding **S1d-S5d** materials range from 0.75 to 1.13 mmol of the fluorescein derivative per gram of SiO_2 (see Table 1).

	Binding site *mmol g^{-1}(α_A)*	*Binding sites* *groups nm^{-2} (β_A)*		*Dye* *mmol g^{-1}*
S1	1.9	1.1	**S1d**	1.13
S2	1.5	0.8	**S2d**	0.75
S3	1.9	1.1	**S3d**	0.75
S4	1.9	1.0	**S4d**	0.86
S5	2.0	1.1	**S5d**	1.05

Table 1. Binding sites and dye moles per SiO_2 gram and estimated inter-binding sites distances for the prepared materials.

Taking into account the contents of the binding sites and the value of the specific surface of the UVM-7 support, the average coverage (β_A in groups per nm^2) of the surface of the different solids by binding groups could be estimated by equation (2)

$$\beta_A = \alpha_A \times 10^{-3} \times S^{-1} \times 10^{-18} \times N_A = \alpha_A \times S^{-1} \times 602.3 \qquad (2)$$

where α_A is the binding groups content (mmol g^{-1} SiO_2), S the specific surface (m^2 g^{-1}) of the non-functionalized UVM-7 support and N_A Avogadro's number (see Table 1). From equation 2 a surface coverage ranging from 0.84 to 1.1 binding groups per nm^2 was calculated.

Displacement assays.

Inspired by the binding pocket concept shown above the "hosts" mesoporous solids **S1d-S5d** containing nanoscale binding cavities and loaded with a suitable dye were tested as signaling reporters. When we

designed the different binding pockets it was in our aim to demonstrate that the nature of the coordinating sites anchored on the inner surface of the mesopores could somehow control the response observed in the presence of the different anionic guests. Therefore, the prepared solids contained different kind of binding sites all of them suitable for anion coordination but still showing differential properties. Also, the anchoring of binding groups on the internal surface of the MCM-41-based solids would additionally result in an improvement of their coordination ability, due to cooperative effects that arises from the high density of coordinating subunits, which would enhance the electrostatic and hydrogen bonding interactions with anionic species into the binding pockets. This enhanced coordination ability of functionalised surfaces with binding groups has been widely reported on a variety of surfaces.[38] Anion coordination on the anchored binding groups on the nanoscopic binding pockets is expected to result in the displacement of the dye and have a significant role in the efficiency of the molecular recognition protocol.

Hybrid solid **S1** contains amino groups in its cavities. Additionally, the experiments were carried out in water at pH 7.5 and therefore it is expected that a number of amino moieties on **S1** will be partially protonated. Polyamines have been extensively explored as binding groups for the design of synthetic receptors able to give interactions with a large variety of inorganic, organic and biologically important anionic guests.[39] At acidic and neutral pH, amine-containing receptors are polycations (polyammonium receptors) and coordinate anionic guests through a combination of hydrogen bonding and Coulombic attractive forces. **S2** contain guanidinium groups on the pores of the inorganic mesoporous support. Guanidines have a very high protonation constant (pK_a > 13) and therefore at neutral pH the stable species are

the corresponding guanidinium groups. Guanidinium salts have been reported to be a very suitable anion coordination sites particularly through electrostatic interactions and via the formation of zwitterionic hydrogen bonds $H\text{-}N^{+\cdots}X^{-}$.[40] Whereas **S1** and **S2** use both hydrogen bonding and electrostatic attractive forces, **S3** is only able to display hydrogen bonding interactions through the use of urea binding groups. Urea moieties have also been used widely as anion binding sistems. It is known that urea groups can act as double hydrogen bond donors to give bidentate interaction with carboxylates.[41] These complexes have been reported to show appreciable stability even in polar solvents. Additionally, solids **S4** and **S5** contain imidazolium[42] and quaternary ammonium salts[43] as binding sites. Both of them have also been widely reported as suitable coordination sites for anions. Whereas ammonium salts can only display electrostatic interactions with anions, imidazolium has also been reported to interact with anions through $(C\text{-}H)^{+\cdots}X^{-}$ ionic hydrogen bonds.

The sensing ability towards certain anions (vide infra) of those solid receptors was studied in pure water. In a typical experiment the corresponding solid (30 mg) was suspended in water at pH 7.5 (HEPES 0.01 mol dm^{-3}) in the presence of a certain anion (C_{anion} = 6.66 x 10^{-4} mol dm^{-3}). After 10 minutes the mixture was filtered and the absorbance of the carboxyfluorescein visible band at 490 nm measured. In this study a number of carboxylate anions were selected; namely acetate, citrate, lactate, succinate, oxalate, tartrate, malate, mandelate and glutamate. As we will detail below the results can be rationalised bearing in mind that the final outcome is related with the nature of the binding sites. Also, in order to understand the observed behaviour it has to be taken into account that, from the pK_a values of the different anions, at pH 7.5 citrate is a trianion, succinate, oxalate, tartrate and malate are

dianions, whereas acetate, lactate, mandelate and glutamate are monoanions.[44] The colorimetric response solids **S1d**-**S5d** in the presence of those anionic species is shown in Figure 3.

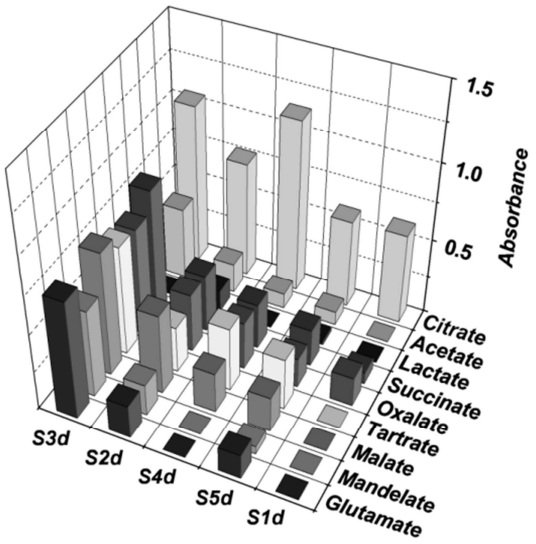

Figure 3.- Colorimetric response of solids **S1d**, **S2d, S3d**, **S4d**, and **S5d** in the presence of the single carboxylates acetate, citrate, lactate, succinate, oxalate, tartrate, malate, mandelate and glutamate in pure water at pH 7.5 (HEPES 0.01 mol dm^{-3}), C_{anion} = 6.66 x 10^{-4} mol dm^{-3}.

Additionally, it has to be taken into account that, as in other displacement assays, by an adequate choice of the binding sites and the dye it is possible to reach a selective response. This is possible if the stability constant between the binding pockets and the dye (K_{dye}) is lower than that with the target anion (K_{target}) but larger than the one with interfering anions ($K_{interferences}$); that is $K_{target} > K_{dye} > K_{interferences}$.

Solids **S4d** and **S5d** display a very similar behaviour; the displacement of the dye from the pore voids follows the order citrate > succinate ~

oxalate ~ tartrate ~ malate > acetate ~ lactate ~ mandelate ~ glutamate. This order is in agreement with the nature of the binding sites that can only display electrostatic interactions. Thus, a larger displacement of the dye from the pore voids is observed for the trianion citrate, whereas the dianions succinate, oxalate, tartrate and malate displace the dye in a lesser extent. The monoanions acetate, lactate, mandelate and glutamate are practically unable to induce displacement reactions of the also monoanionic dye carboxyfluorescein. Compared with this behaviour a very different displacement scheme is found for solid **S3d** that contain urea groups. As stated above, these are neutral receptor groups that can only display hydrogen bonding interaction. The figure shows that a number of carboxylates are able to displace the dye from the pores. Thus suspensions of **S3d** containing the anions succinate, oxalate, tartrate, malate, mandelate and glutamate show a similar optical response. This response is independent of the charge of the carboxylates. Additionally citrate shows a slightly larger ability to displace the dye from the pores of the inorganic support suggesting a better suitable fit of the anions within the cylindrical pores of the inorganic support. The anions acetate and lactate display a very poor response suggesting that the extraction from the water phase to the inner pores in the mesoporous material is not very effective for both anions.

The guanidinium-functionalised solid **S2d** display a behaviour that appears to be a mixture of both, electrostatic and hydrogen bonding interactions; the delivery is larger for trianions and dianions suggesting electrostatic forces, but at the same time monoanions such as mandelate, glutamate and acetate are also able to induce some displacement of the dye suggesting some hydrogen bonding interactions. The most remarkable behaviour is that found for solid **S1d**

that displays a citrate selective response indicating that the binding pockets in **S1d** are capable to bind this anion via favourable coordination preferentially over the dye ($K_{citrate} > K_{dye}$) but at the same time the interaction of the coordinating pocket with the dye is stronger than with the remaining carboxylates ($K_{dye} > K_{interferences}$).

Finally we were also interested in study the behaviour of these solids in the presence of other anions different to carboxylates. At this respect, except some anions such as phosphate that display sensing features with certain solids,[36b] the presence of typical inorganic anions (i.e. chloride, nitrate, sulphate,) and cations (i.e. sodium, potassium, calcium), in water resulted in a negligible or very poor displacement of the 5-carboxyfluorescein dye from the **S1d**-**S5d** solids. In these preliminary studies it was also found that the interaction of the solids with larger anions such as ATP, ADP and GMP resulted in a partial displacement of the dye. Therefore, in order to compare the behaviour of the prepared solids in the presence of other anions with the sensing abilities found for carboxylayes, further displacement assays were carried out in the presence of ATP, ADP and GMP in this case using the solids **S5d** (electrostatic interactions), **S3d** (hydrogen bonding interactions) and **S1d** (both electrostatic and hydrogen bonding interactions). The experimental procedure was similar to that followed above using the corresponding solid (30 mg) in water at pH 7.5 (HEPES 0.01 mol dm^{-3}). The coordination of the nanoscopic binding pockets with ATP, ADM and GMP was evaluated through the monitoring of the visible band centred at 490 nm that appeared when the dye was release to the solution. The results are found in Figure 4 that also show for comparative purposes the response of solids **S1d**, **S3d** and **S5d** to citrate (vide ante). From reported pK_a values,[45] it can be calculated that at pH 7.5, ATP exist in its tetraanionic form (ATP^{4-}), while ADP is a trianion

(ADP^{3-}) and GMP is a dianion (GMP^{2-}). As can be observed, solid **S5d** displays a colorimetric response that follows the order ATP > citrate ~ ADP > GMP that is in agreement with the existence of electrostatic interactions between the anions and the binding pockets functionalised with the quaternary ammonium derivatives. For solid **S1d** the response is ATP > ADP > GMP ~ citrate, also suggesting as main force the electrostatic interactions between the binding pockets (protonated amines) and the anions. Additionally the larger displacement observed for the nucleotides when compared with citrate also suggests that these anions form stronger complexes with the pocket most likely due to favourable hydrogen bonding interactions with the amino groups. In contrast with this behaviour solid **S3d** shows a displacement of the dye that follow the order citrate > ATP = ADP = GMP clearly pointing out that the main force are in this case the hydrogen bonding interactions, via the formation of stronger complexes with the carboxylates of the citrate anion that results in an enhanced signaling of citrate vs. ATP, ADP or GMP.

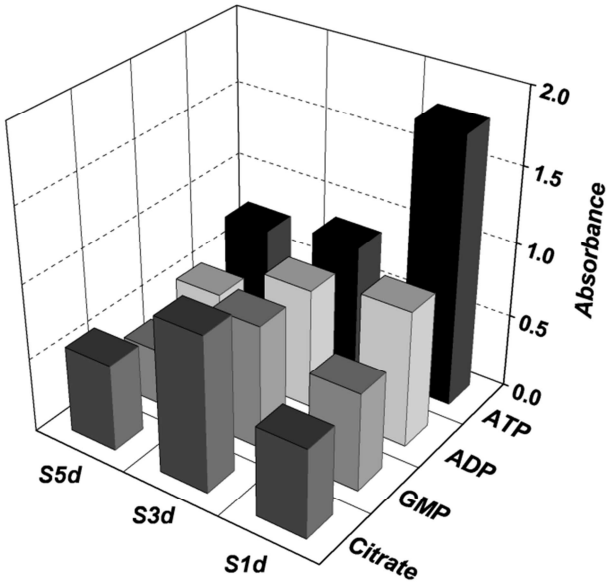

Figure 4.- Colorimetric response of solids **S1d**, **S3d**, and **S5d** in the presence of single citrate, ATP, ADP and GMP in pure water at pH 7.5 (HEPES 0.01 mol dm^{-3}), C_{anion} = 6.66 x 10^{-4} mol dm^{-3}.

In summary, the UV/vis studies carried out with **S1d**-**S5d** showed that the response to a family of carboxylates and nucleotides such as ATP, ADP and GMP can be modulated by the different binding moieties anchored into the inner pores of the inorganic mesoporous supports. In fact, the actual response to a certain anion depends on the characteristics of the binding pockets and the specific interaction of the anion with the binding groups in the mesopores that finally results in the displacement of the indicator. The response of a certain solid towards a certain anion therefore depends on the intrinsic chemical nature of the binding site, the charge of the anion, its size, the possibility of establish multiple hydrogen bonding contacts, etc. These subtle differences are reflected in the specific final response of each solid towards the anion

family studied. In fact this differential behaviour suggests that the response of solids **S1d** to **S5d** could be combined to form differential signaling ensembles for pattern recognition of anions. This implies to study the response of the **S1d**-**S5d** solids as a whole in an attempt to find selectivity fingerprints. This can be observed when the matrix of data is analysed by algorithms such as principal component analysis (PCA).[46] The PCA score plot of the results for solids **S1d**-**S5d** in the presence of carboxylates detailed above and the nucleotides ATP, ADP and AMP are shown in Figure 5 for three different trials. Recognition patterns can be identified clearly for most of the anions studied but especially for citrate and and the nucleotides. One more careful look to the PCA plot suggests that there is some correlation between the position in the axis PC1 and the charge of the anions. Thus, the cluster of ATP and citrate locate in the zone of more negative values of the first component PC1, whereas dianions (oxalate, tartrate, succinate and malate) are at middle values of PC1 and monoanins (lactate, acetate, mandelate and glutamate) are located at positive values of PC1. PC1 explain ca. 84 % of variance of data, therefore suggesting that, when considering all the receptors, the main driving force in the differentiation of the anions are the electrostatic interactions with the binding pockets. Additionally, and interestingly, different values in PC2 results in discrimination between different anions containing the same charge, finally allowing to obtain remarkable recognition patterns. Load plots (not shown) indicate that the response of solids **S2d**, **S4d** and **S5d** is quite similar, whereas **S1d**, and especially **S3d**, display a more differential behaviour. This last observation is in agreement with the results observed in Figure 3.

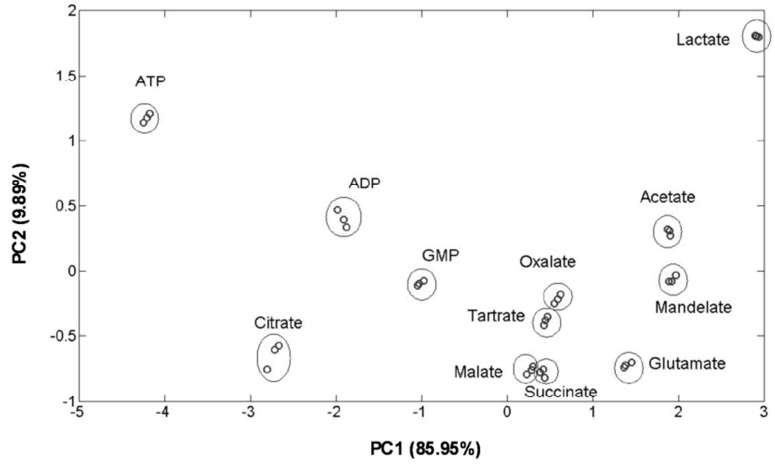

Figure 5.- Principal component analysis (PCA) score plot for the anions acetate, citrate, lactate, succinate, oxalate, tartrate, malate, mandelate, glutamate, ATP, ADP and GMP using the **S1d**-**S5d** chemosensing ensembles. Data shown from three different trials. PC axes are calculated to lie along lines of diminishing levels of variance in the data set.

Conclusions

In summary, we have shown that functionalised mesoporous solids can act as binding pockets in anion recognition processes. As a particular application we have developed solids for displacement colorimetric assays in water containing amines, guanidinium cations, ureas, imidazolium and quaternary ammonium salts as binding sites and 5-carboxyfluorescein as signaling reporter. The response of these solids in displacement assays has been studied in the presence of a family of carboxylates and also in the presence of ATP, ADP and GMP. In fact, the response toward a certain anion depends on the characteristics of the binding pockets and the specific interaction of the anion with the binding groups in the mesopores that finally results in the displacement of the indicator. A remarkable selective response for **S1d** and citrate has been

observed in pure water. The studies also indicate that the response to a certain guest in water can be tailor-made by designing binding pockets containing different simple binding sites. For instance a very different response was observed for the solid containing ureas (hydrogen bonding interaction) versus charged receptors (electrostatic interactions). It is also noteworthy that the systems tested are very simple and that to achieve similar differential colorimetric response in water for these anions would have required a tremendous synthetic effort in order to obtain receptors containing multiple coordination sites. Moreover, the non-covalent anchoring of binding sites and indicator groups allows to test with a minimum effort a large number of combinations in order to obtain tuned sensing systems. Additionally, these sensing ensembles work in pure water. We believe these findings can open new perspectives in the use of solids as hosts in conceptually new solid state–supramolecular chemistry ideas. Particularly, the possibility of using a large number of mesoporous materials functionalised with different binding sites makes the approach suitable for the design of new chromo/fluorogenic probes for target guests.

Experimental section

Reagents.

The products tetraethylorthosilicate (TEOS), *n*-cetyltrimethylammonium bromide (CTAB), sodium hydroxide (NaOH), triethanolamine ($TEAH_3$), 5-carboxyfluorescein, 3-aminopropyltriethoxysilane (**1**), 2-methylthio-2-imidazoline hydroiodide (**2**), butylisocyanate (**3**), 3-(trimethoxysilyl)propyl-*N,N,N*-trimethylammonium chloride (**5**), *N*-methylimidazol, 3-cloropropyltrimethoxysilane and all the anions used in this manuscript were provided by Aldrich and used as received. The

synthesis of *N*-methyl-*N´*-propyltrimethoxysilyl imidazolium chloride (**4**) has been previously described.[47]

Synthesis of the mesoporous UVM-7 support (MCM41-type material).
The synthesis strategy we have used to prepare UVM-7 silicas and hybrid related organosilicas is an application of the so-called "atrane route", a simple preparative technique based on the use of complexes that include triethanolamine($TEAH_3$)-related ligands (i.e. in general "atranes" and silatranes for the silicon containing complexes) as hydrolytic inorganic precursors and surfactants as porogen species. Then, the molar ratio of the reagents in the mother liquor was fixed to 7 $TEAH_3$:2 TEOS:0.52 CTAB:180 H_2O for the synthesis of **UVM-7**. TEOS and $TEAH_3$ mixture was heated to 120 ºC until no elimination of ethanol was observed. Then, the mixture was cooled to 90 ºC and the CTAB was added gradually in small portions and afterwards the water. The mixture was aged at room temperature for 24h. The resulting powder was collected by filtration, washed with water and ethanol and air-dried. The surfactant was removed by calcination at 550 ^{o}C for 5 hours.

Synthesis of the amine derivative S1*.*
The calcinated material (UVM-7) was first activated in a ethanol/HCl 1M solution. Template-free **UVM-7** activated material (3g) was suspended in anhydrous toluene (300 mL) and heated at 110 ºC in a Dean-Stark in order to remove the adsorbed water by azeotropic distillation under inert atmosphere (Ar atmosphere). Then a large excess of 3-(aminopropyl)triethoxysilane (**1**, 10.5 ml, 44.7 mmol) was added to the suspension at room temperature and stirred at reflux for 16 hours at 100 ºC. The final solid (**S1**) was filtered off, exhaustively washed with toluene and acetone and dried at 60 ºC for at least 12 hours.

Synthesis of the guanidine derivative S2*.*

Solid **S2** was obtained by reaction of **S1** with a large excess of 2-methylthio-2-imidazoline hydroiodide (**2**, 7 mmols per gram of **S1**) in refluxing methanol for 16h. The solid was filtered off, exhaustively washed with methanol and acetone and dried.

Synthesis of the urea derivative S3*.*

Solid **S3** was obtained by reaction of **S1** with an excess of butyl isocyanate (**3**, 5 mmols per gram of **S1**) in THF in presence of triethylamine. The solid was filtered off, washed with acetone and dried.

Synthesis of the imidazolium derivative S4.

Solid **S4** was obtained by reaction of UVM-7 with an excess of *N*-methyl-*N´*-propyltrimethoxysilyl imidazolium chloride (**4**) as follows. UVM-7 activated material (1g) was suspended in anhydrous acetonitrile (100 mL) and heated at 110 ºC in a Dean-Stark in order to remove the adsorbed water by azeotropic distillation under inert atmosphere (Ar atmosphere). Then *N*-methyl-*N´*-propyltrimethoxysilyl imidazolium chloride (**4**, 0.9 g, 3.3 mmol) dissolved in anhydrous acetonitrile was added to the suspension at room temperature and heated at 80 ºC in reflux system during 16h. The final solid **S4** was filtered off, washed with acetonitrile and acetone and dried.

Synthesis of the quaternary ammonium derivative S5*.*

Solid **S5** was obtained by reaction of UVM-7 with an excess of 3-(trimethoxysilyl)propyl-*N,N,N*-trimethylammonium chloride (**5**) as follows. UVM-7 activated material (1g) was suspended in anhydrous acetonitrile (100 mL) and heated at 110 ºC in a Dean-Stark in order to remove the adsorbed water by azeotropic distillation under inert atmosphere (Ar atmosphere). Then 3-(trimethoxysilyl)propyl-*N,N,N*-

trimethylammonium chloride (**5**, 1.2 g, 3.3 mmol) was added to the suspension at room temperature and heated at 80 ºC in reflux system during 16h. The final solid **S5** was filtered off, washed with acetonitrile and acetone and dried.

Synthesis of the dye-containing solids S1d, S2d, S3d, S4d and S5d.
The corresponding functionalised solids **S1**-**S5** (0.5 g) were suspended in water at pH 7.5 (50 mL) and 5-carboxyfluorescein (0.2 g) was added at room temperature. The mixture was stirred for 24 hours to yield the corresponding solids **S1d**, **S2d, S3d, S4d** and **S5d** that were isolated by filtration and exhaustively washed with water until no release of the dye was observed.

General Techniques and apparatus.
XRD, TG analysis, elemental analysis, TEM microscopy, N_2 adsorption-desorption, UV-visible spectrophotometer techniques were employed to characterize the materials. X-ray measurements were performed on a Bruker AXS D8 Advance diffractometer using Cu Kα radiation. Thermo-gravimetric analysis were carried out on a TGA/SDTA 851e Mettler Toledo balance, using an oxidant atmosphere (Air, 80 mL/min) with a heating program consisting on a heating ramp of 10 °C per minute from 393 K to 1273 K and an isothermal heating step at this temperature during 30 minutes. N_2 adsorption-desorption isotherms were recorded on a Micromeritics ASAP2010 automated sorption analyser. The samples were degassed at 120ºC in vacuum overnight. The specific surfaces areas were calculated from the adsorption data in the low pressures range using the BET model. Pore sized was determined following the BJH method. UV-visible spectroscopy was carried out with a Lambda 35 UV/Vis Spectrometer Perkin Elmer Instruments.

References.

[1] (a) F. P. Schmidtchen, M. Berger, *Chem. Rev.* **1997**, *97*, 1609-1646; (b) B. Dietrich, *Pure Appl. Chem.* **1993**, *65*, 1457-1464; (c) J. L. Atwood, K. T. Holman, J. W. Steed, *Chem. Commun.* **1996**, 1401-1407; (d) A. Ikeda, S. Shinkai, *Chem. Rev.* **1997**, *97*, 1713-1734; (e) P. A. Gale, *Acc. Chem. Res.* **2006**, *39*, 465-475; (f) V. McKee, J. Nelson, R. M. Town, *Chem. Soc. Rev.* **2003**, *32*, 309-325.

[2] (a) R. Martinez-Máñez, F. Sancenón, *Chem. Rev*. **2003**, *103*, 4419-4476; (b) C. Suksai, T. Tuntulani, *Top. Curr. Chem*. **2005**, *255*, 163-198; (c) R. Martínez-Máñez, F. Sancenón, *Coord. Chem. Rev*. **2006**, *250*, 3081-3093.

[3] (a) R. Martínez-Máñez, F. Sancenón, *J. Fluoresc*. **2005**, *15*, 267-285; (b) P.D. Beer, P. A. Gale, *Angew. Chem. Int. Ed*. **2001**, *20*, 487-516; *Angew. Chem.* **2001**, *113*, 502-532; (c) D. Parker, *Coord. Chem. Rev*. **2000**, *205*, 109-130; (d) L. Fabbrizzi, M. Licchelli, G. Rabaioli, A. Taglietti *Coord. Chem. Rev*. **2000**, *205*, 85-108.

[4] (a) H. Plenio, C. Aberle, Y. Al Shihadeh, J. M. Lloris, R. Martínez-Máñez, T. Pardo, J. Soto, *Chem. Eur. J*. **2001**, *7*, 2848-2861; (b) P. D. Beer, J. Cadman, J. M. Lloris, R. Martínez-Máñez, J. Soto, T. Pardo, M. D. Marcos, *J. Chem. Soc., Dalton Trans*. **2000**, 1805-1812; (c) J. M. Lloris, R. Martínez-Máñez, T. Pardo, J. Soto, M. E. Padilla-Tosta, *Chem. Commun*. **1998**, 837-838; (d) F. Sancenón, A. Benito, F. J. Hernández, J. M. Lloris, R. Martínez-Máñez, T. Pardo, J. Soto, *Eur. J. Inorg. Chem*. **2002**, 866-875; (e) P. D. Beer, S. R. Bayly, *Top. Curr. Chem*. **2005**, *255*, 125-162.

[5] (a) B. Valeur, I. Leray, *Coord. Chem. Rev.* **2000**, *205*, 3-40; (b) L. Fabbrizzi, A. Poggi, *Chem. Soc. Rev.* **1995**, 197-202; (c) K. Rurack, *Spectrochim. Acta A* **2001**, *57*, 2161-2195; (d) J. F. Callan, A. P. de Silva, D. C. Magri, *Tetrahedron* **2005**, *61*, 8551-8588.

[6] (a) P. de Silva, H.Q.N. Gunaratne, T. Gunnlaugsson, A:J:M: Huxley, C.P. McCoy, J.T. Rademacher, T.E. Rice, *Chem. Rev*. **1997**, *97*, 1515-1566; (b) S. L. Wiskur, H. Aït-Haddou, E. V. Anslyn, J. J. Lavigne, Acc. *Chem. Res.* **2001**, *34*, 963-972.

[7] (a) G.J. Mohr, *Chem. Eur. J*. **2004**, *10*, 1082-1090; (b) G.J. Mohr, *Sens. Actuators B* **2005**, *107*, 2-13; (c) G.J. Mohr, *Anal. Bional. Chem*. **2006**, *386*,

1201-1214; (d) T. D. James, S. Shinkai, *Top. Curr. Chem.* **2002**, *218*, 159-200; (e) S. Royo, R. Martínez-Máñez, F. Sancenón, A. M: Costero, M. Parra, S. Gil, *Chem. Commun.* **2007**, 4839-4847.

[8] S. L. Wiskur, H. Aït-Haddou, J. J. Lavigne, E. V. Anslyn, *Acc. Chem. Res*. **2001**, *34*, 963-972.

[9] (a) A. Metzger, E.V. Anslyn, *Angew. Chem. Int. Ed.* **1998**, *37*, 649-652; *Angew. Chem.* **1998**, *110*, 682-684; (b) S.L. Wiskur, E.V. Anslyn, *J. Am. Chem. Soc.* **2001**, *123*, 10109-10110; (c) H. Aït-Haddou, S.L. Wiskur, V.M. Lynch, E.V. Anslyn, *J. Am. Chem. Soc.* **2001**, *123*, 11296-11297.

[10] A.B. Descalzo, R. Martínez-Máñez, F. Sancenón, K. Hoffmann, K. Rurack, *Angew. Chem. Int. Ed*. **2006**, *45*, 5924-5948; *Angew. Chem.* **2006**, *118*, 6068-6093.

[11] (a) M. Comes, M. D. Marcos, R. Martínez-Máñez, F. Sancenón, J. Soto, L. A. Villaescusa, P. Amorós, D. Beltrán, *Adv. Mater*. **2004**, *16*, 1783-1786; (b) S. Basurto, T. Torroba, M. Comes, R. Martínez-Máñez, F. Sancenón, L. A. Villaescusa, P. Amorós, *Org. Lett*. **2005**, *7*, 5469-5472.

[12] (a) E. Katz, I. Willner, *Angew. Chem. Int. Ed*. **2004**, 43, 6042-6108; *Angew. Chem.* **2004**, *116*, 6166-6235; (b) U. Dreschsler, B. Erdogan, V. M. Rotello, *Chem. Eur. J*. **2004**, *10*, 5570-5579.

[13] (a) S. Huh, J. W. Wiench, J.–C. Yoo, M. Pruski, V. S.–Y. Lin, *Chem. Mater*. **2003**, *15*, 4247-4256; (b) V. S.–Y. Lin, C.–Y. Lai, J. Huang, S.–A. Song, S. Xu, *J. Am. Chem. Soc*. **2001**, *123*, 11510-11511.

[14] C.T. Kresge, M.E. Leonowicz, W.J. Roth, J.C. Vartuli, J.S. Beck, *Nature* **1992**, *359*, 710-712.

[15] See for instance: (a) X. Feng, G.E. Fryxell, L.Q. Wang, A.Y. Kim, J. Liu, K.M. Kemner, *Science* **1997**, *276*, 923-926; (b) L. Liu, X. Feng, G.E. Fryxell, L.Q. Wang, A.Y. Kim, M. Gong, *Adv. Mater*. **1998**, *10*, 161-165; (c) G. Rodríguez-López, M.D: Marcos, R. Martínez-Máñez, F. Sancenón, J. Soto, L.A. Villaescusa, D. Beltrán, P. Amorós, *Chem. Commun*. **2004**, 2198-2199; (d) J.V. Ros-Lis, R. Casasús, M. Comes, C. Coll, M.D: Marcos, R. Martínez-Máñez, F. Sancenón, J. Soto, P. Amorós, J. El Haskouri, N. Garró, K Rurack., *Chem. Eur. J*. **2008**, *14*, 8267-8278; (e) S.J. Lee, D.R. Bae, W.S. Has, S.S. Lee, J.H. Jung, *Eur. J. Inorg. Chem*. **2008**, 1559-1564.

[16] See for instance: (a) N.R.B. Coleman, M.A. Morris, T.R. Spalding, J.D. Holmes, *J. Am. Chem. Soc*. **2001**, *123*, 187-188; (b) H. Yang, Q. Shi, B. Tian, Q. Lu, F. Gao, S. Xie, J. Fan, C. Yu, B. Tu, D. Zhao, *J. Am. Chem. Soc*. **2003**, *125*, 4724-4725; (c) T. Abe, Y. Tachibana, T. Uematsu, M. Iwamoto, *J. Chem. Soc. Chem. Commun*. **1995**, *16*, 1617-1618; (d) Y. Han, J.M. Kim, G.D. Stucky, *Chem. Mater*. **2000**, *12*, 2068-2069; (e) B.J. Scott, G. Wirnsberger, G.D. Stucky, *Chem. Mater*. **2001**, *13*, 3140-3150.

[17] See for instance: (a) N.W. Clifford, K.S. Iyer, C.L. Raston*, J. Mater. Chem*. **2008**, *18*, 162-165; (b) Q. Ji, M. Miyahara, J.P. Hill, S. Acharya, Z. Vinu, S.B. Yoon, J.-S. Yu, K. Sakamoto, K. Ariga, *J. Am. Chem. Soc*. **2008**, *130*, 2376-2377; (c) R. Casasús, E. Climent, M.D. Marcos, R. Martínez-Máñez, F. Sancenón, J. Soto, P. Amorós, J. Cano, E. Ruiz, *J. Am. Chem. Soc*. **2008**, *130*, 1903-1917; (d) A. Bernardos, E. Aznar, C. Coll, R. Martínez-Máñez, J.M. Barat, M.D. Marcos, F. Sancenón, A. Benito, J. Soto, *J. Control. Release* **2008**, *131*, 181-189; (e) C. Park, K. Oh, S.C. Lee, C. Kim, *Angew. Chem. Int. Ed*. **2007**, *46*, 1455-1457; *Angew. Chem.* **2007**, *119*, 1477-1479; (f) B.G. Trewyn, I.I. Slowing, S. Giri, H.T. Chen, V.S.Y. Lin, *Acc. Chem. Res*. **2007**, *40*, 846-853; (g) M. Vallet-Regí, F. Balas, D. Arcos, *Angew. Chem. Int. Ed*. **2007**, *46*, 7548-7558; *Angew. Chem.* **2007**, *119*, 7692-7703; (h) R. Hernandez, H.-R. Tseng, J.W. Wong, J.F. Stoddart, J.I. Zink, *J. Am. Chem. Soc*. **2004**, *126*, 3370-3371; (i) N.K. Mal, M. Fujiwara, Y. Tanaka, *Nature* **2003**, *421*, 350-353.

[18] See for instance: (a) A. Stein, B.J. Melde, R.C. Schroden, *Adv. Mater*. **2000**, *12*, 1403-1419; (b) J.Y. Ying, C.P. Mehnert, M.S. Wong, *Angew. Chem. Int. Ed*. **1999**, *38*, 56-77; *Angew. Chem.* **1999**, *111*, 58-82; (c) I.K. Mbaraka, K.J. McGuire, B.H. Shanks, *Ind. Eng. Chem. Res*. **2006**, *45*, 3022-3028; (d) D.S. Shephard, T. Maschmeyer, B.F.G. Johnson, J.M. Thomas, G. Sankar, D. Ozkaya, W. Zhou, R. D. Oldroyd, R.G. Bell, *Angew. Chem. Int. Ed*. **1997**, *36*, 2242-2245; *Angew. Chem.* **1997**, *109*, 2337-2341.

[19] A.B. Descalzo, K. Rurack, H. Weisshoff, R. Martínez-Máñez, M.D. Marcos, P. Amorós, K. Hoffmann, J. Soto, *J. Am. Chem. Soc*. **2005**, *127*, 184-200.

[20] (a) M. Comes, M.D: Marcos, R. Martínez-Máñez, F. Sancenón, L.A: Villaescusa, A. Graefe, G.J. Mohr, *J. Mater. Chem*. **2008**, *18*, 5815-5823; (b) E. Climent, P. Calero, M.D: Marcos, R. Martínez-Máñez, F. Sancenón, J. Soto,

Chem. Eur. J. **2009**, *15*, 1816-1820; (c) E. Climent R. Casasús, M.D. Marcos, R. Martínez-Máñez, F. Sancenón, J. Soto, *Chem. Commun*. **2008**, 6531-6533; (d) P. Calero, E. Aznar, J.M. Lloris, M.D. Marcos, R. Martínez-Máñez, J.V. Ros-Lis, J. Soto, F. Sancenón, *Chem. Commun*. **2008**, 1668-1670; (e) A.B. Descalzo, M.D. Marcos, C. Monte, R. Martínez-Máñez, K. Rurack, *J. Mater. Chem*. **2007**, *17*, 4716-4723; (f) C. Coll, R. Martínez-Máñez, M.D. Marcos, F. Sancenón, J. Soto, *Angew. Chem. Int. Ed*. **2007**, *46*, 1675-1678; *Angew. Chem.* **2007**, *119*, 1705-1708; (g) R. Casasús, E. Aznar, M.D. Marcos, R. Martínez-Máñez, F. Sancenón, J. Soto, P. Amorós, *Angew. Chem. Int. Ed*. **2006**, *45*, 6661-6664; *Angew. Chem.* **2006**, *118*, 6813-6816; (h) M. Comes, M.D. Marcos, R. Martínez-Máñez, .C. Millán, J.V. Ros-Lis, F. Sancenón, J. Soto, L.A. Villaescusa, *Chem. Eur.J*. **2006**, *12*, 2162-2170; (i) J.V. Ros-Lis, M.D. Marcos, R. Martínez-Máñez, K. Rurack, J. Soto, *Angew. Chem. Int. Ed*. **2005**, *44*, 4405-4407; *Angew. Chem.* **2005**, *117*, 4479-4482.

[21] M. H. Lee, S. J. Lee, J. H. Jung, H. Lim, J.S. Kim, *Tetrahedron* **2007**, *63*, 12087-12092.

[22] R. Métivier, I. Leray, B. Lebeau, B. Valeur, *J. Mater. Chem*. **2005**, *15*, 2965-2973.

[23] S. J. Lee, J.-E. Lee, J. Seo, I. Y. Jeong, S. S. Lee, J. H. Jung, *Adv. Funct. Mater*. **2007**, *17*, 3441-3446.

[24] L. Gao, J. Q. Wang, L. Huang, X. X. Fan, J. H. Zhu, Y. Wang, Z. G. Zou, *Inorg. Chem*. **2007**, *46*, 10287-10293.

[25] H. Zhang, P. Zhang, K. Ye, Y. Sun, S. Jiang, Y. Wang, W. Pang, *J. Lumin*. **2006**, *117*, 68-74.

[26] L.-L. Li, H. Sun, C.-J. Fang, J. Xu, J.-Y. Jin, C.-H. Yan, *J. Mater. Chem*. **2007**, *17*, 4492-4498.

[27] J.-Q. Wang, L. Huang, M. Xue, Y. Wang, L. Gao, J. H. Zhu, Z. Zou, *J. Phys. Chem. C* **2008**, *112*, 5014-5022.

[28] L. Gao, Y. Wang, J. Wang, L. Huang, L. Shi, X. Fan, Z. Zou, T. Yu, M. Zhu, Z. Li, *Inorg. Chem*. **2006**, *45*, 6844-6850.

[29] G. Wirnsberger, B. J. Scott, G. D. Stucky, *Chem. Commun*. **2001**, 119-120.

[30] T. Balaji, M. Sasidharan, H. Matsunaga, *Anal. Bioanal. Chem*. **2006**, 384, 488–494.

[31] T. Balaji, S. A. El-Safty, H. Matsunaga, T. Hanaoka, F. Mizukami, *Angew. Chem. Int. Ed*. **2006**, *45*, 7202–7208; *Angew. Chem.* **2006**, *118*, 7360-7366.

[32] S. A. El-Safty, A. A. Ismail, H. Matsunaga, F. Mizukami, *Chem. Eur. J*. **2007**, *13*, 9245–9255.

[33] S. A. El-Safty, D. Prabhakaran, A. A. Ismail, H. Matsunaga, F. Mizukami, *Adv. Funct. Mater*. **2007**, *17*, 3731-3745.

[34] S. A. El-Safty, A. A. Ismail, H. Matsunaga, H. Nanjo, F. Mizukami, *J. Phys. Chem*. **2008**, *112*, 4825-4835.

[35] (a) M. Comes, G. Rodríguez-López, M.D. Marcos, R. Martínez-Máñez, F. Sancenón, J. Soto, L.A. Villaescusa, P. Amorós, D. Beltrán, *Angew. Chem. Int. Ed*. **2005**, *44*, 2918-2922; *Angew. Chem.* **2005**, *117*, 2978-2982; (b) M. Comes, M.D. Marcos, R. Martínez-Máñez, . Sancenón, J. Soto, L.A. Villaescusa, P. Amorós, *Chem. Commun*. **2008**, 3639-3641.

[36] (a) B. T. Nguyen, E. V. Anslyn, *Coord. Chem. Rev*. **2006**, *250*, 3118-3127; (b) L. Fabbrizzi, N. Marcotte, F. Stomeo, A. Taglietti, *Angew. Chem. Int. Ed*. **2002**, *41*, 3811-3814; *Angew. Chem.* **2002**, *114*, 3965-3968.

[37] (a) J. El Haskouri, D. Ortiz, C. Guillem, J. Latorre, M. Caldés, A. Beltrán, D. Beltrán, A.B. Descalzo, G. Rodríguez-López, R. Martínez-Máñez, M.D. Marcos, P. Amorós, *Chem. Commun*. **2002**, 330-331; (b) L. Huerta, C. Guillem, J. Latorre, A. Beltrán, R. Martínez-Máñez, M.D. Marcos, D. Beltrán, P. Amorós, *Solid. State. Sciences* **2006**, *8*, 940-951.

[38] (a) A. B. Descalzo, D. Jiménez, M. D. Marcos, R. Martínez-Máñez, J. Soto, J. El Haskouri, C. Guillém, D. Beltrán, P. Amorós, P. *Adv. Mater.* **2002**, *14*, 966-969; (b) A. B. Descalzo, M. D. Marcos, R. Martínez-Máñez, J. Soto, D. Beltrán, P. Amorós, *J. Mater. Chem.* **2005**, *15*, 2721-2731; (c) A. K. Boal, V. M. Rotello, *J. Am. Chem. Soc.* **1999**, *121*, 4914-4915; (d) A. K. Boal, V. M. Rotello, *J. Am. Chem. Soc.* **2000**, *122*, 734-735; (e) A. K. Boal, V. M. Rotello, *J. Am. Chem. Soc.* **2002**, *124*, 5019-5024; (f) A. Callegari, M. Marcaccio, D. Paolucci, F. Paolucci, N. Tagmatarchis, D. Tasis, E. Vazquez, M. Prato, *Chem. Commun.* **2003**, 2576-2577.

[39] (a) A. Bianchi, M. Micheloni, P. Paoletti, *Inorg. Chim. Acta* **1988**, *151*, 269-272; (b) V. Král, A. Andrievsky, J.L. Sessler, *J. Chem. Soc., Chem. Commun.* **1995**, 2349-2350; (c) C. De Stefano, C. Foti, A. Gianguzza, O. Giuffrè, S. Sammartano, *J. Chem. Soc., Faraday Trans.* **1996**, *92*, 1511-1518; (d) M.T.

Albelda, M.A. Bernardo, E. García-España, M.L. Godino-Salido, S.V. Luis, M.J. Melo, F. Pina, C. Soriano, *J. Chem. Soc., Perkin Trans. 2* **1999**, 2545-2549; (e) F. Sancenón, A. Benito, J.M. Lloris, R. Martínez-Máñez, T. Pardo, J. Soto, *Helv. Chim. Acta* **2002**, *85*, 1505-1516; (f) M.T. Albelda, J. Aguilar, S. Alves, R. Aucejo, P. Diaz, C. Lodeiro, J.C. Lima, E. García-España, F. Pina, C. Soriano, *Helv. Chim. Acta* **2003**, *86*, 3118-3135; (g) J.M. Lloris, R. Martínez-Máñez, M. Padilla-Tosta, T. Pardo, J. Soto, M.J.L. Tendero, *J. Chem. Soc., Dalton Trans.* **1998**, 3657-3662; (h) J.M. Lloris, R. Martínez-Máñez, T. Pardo, J. Soto, M.E. Padilla-Tosta, *J. Chem. Soc. Dalton Trans* **1998**, 2635-2641.

[40] (a) P. Blondeau, M. Segura, R. Pérez-Fernández, J. de Mendoza, *Chem. Soc. Rev.* **2007**, *36*, 198-210; (b) M. D. Best, S. L. Tobey, E. V. Anslyn, *Coord. Chem. Rev.* **2003**, *240*, 3-15; (c) S. L. Wiskur, J. J. Lavigne, A, Metzger, S. L. Tobey, V. Lynch, E. V. Anslyn, *Chem. Eur. J.* **2004**, *10*, 3792-3804; (d) S. L. Tobey, E. V. Anslyn, *J. Am. Chem. Soc.* **2003**, *125*, 14807-14815.

[41] See for example: (a) V. Amendola, D. Estebán-Gómez, L. Fabbrizzi, M. Licchelli, *Acc. Chem. Res.* **2006**, *39*, 343-353; (b) M. Boiocchi, L. Del Boca, D. Estebán-Gómez, L. Fabbrizzi, M. Licchelli, E. Monzani, *Chem. Eur. J.* **2005**, *11*, 3097-3104; (c) J. Y. Kwon, Y. J. Jang, S. K. Kim, K. –H. Lee, J. S. Kim, J. Yoon, *J. Org. Chem.* **2004**, *69*, 5155-5157; (d) E. Quinlan, S. E. Matthews, T. Gunnlaugsson, *J. Org. Chem.* **2007**, *72*, 7497-7503; (e) C. M. G. dos Santos, T. McCabe, G. W. Watson, P. E. Kruger, T. Gunnlaugsson, *J. Org. Chem.* **2008**, *73*, 9235-9244; (f) D. A. Jose, D. K. Kumar, B. Ganguly, A. Das, *Org. Lett.* **2004**, *6*, 3445-3448.

[42] See for instance: (a) J. Y. Kwon, N. J. Singh, H. Kim, S. K. Kim, K. S. Kim, J. Yoon, *J. Am. Chem. Soc.* **2004**, *126*, 8892-8893; (b) S. K. Kim, B.-G. Kang, H. S. Koh, Y. J. Yoon, S. J. Jung, B. Jeong, K.-D. Lee, J. Yoon, *Org. Lett.* **2004**, *6,* 4655-4658; (c) J. Yoon, S. K. Kim, N. J. Singh, J. W. Lee, Y. J. Yang, K. Chellappan, K. S. Kim, *J. Org. Chem.* **2004**, *69*, 581-583; (d) C. E. Willans, K. M. Anderson, P. C. Junk, L. J. Barbour, J. W. Steed, *Chem. Commun.* **2007**, 3634-3636; (e) C. Coll, R. Casasús, E. Aznar, MD. Marcos, R. Martínez-Máñez, F. Sancenón, J. Soto, P. Amorós, *Chem. Commun*. **2007**, 1957-1959; (f) J. Yoon, S. K. Kim, N. J. Singh, K. S. Kim, *Chem. Soc. Rev.* **2006**, *35*, 355-360.

[43] (a) J. M. Llinares, D. Powell, K. Bowman-James, *Coord. Chem. Rev.* **2003**, *240*, 57-75; (b) C. A. Ilioudis, J. W. Steed, *J. Supramol. Chem.* **2001**, *1*, 165-187.

[44] pK_a values for these acids are: citrate (3.15, 4.77, 6.40), acetate (4.76), lactate (3.87), succinate (4.19, 5.64), oxalate (1.27, 4.28), tartrate (2.98, 4.34), malate (3.14, 5.13), Mandelate (3.37), glutamate (2.2, 4.5, 9.7).

[45] Log protonation constants for ATP, ADP and GMP are; ATP: 6.75, 4.09; ADP: 6.54, 3.86 and GMP: 6.1, 2.4 in water. See for instance: Q. Lu, A.E. Martell, R.J. Motekaitis, *Inorg. Chim. Acta* **1996**, *251*, 365-370.

[46] I.T. Jolliffe, Principal Component Analysis; Springer; New York, **2002**.

[47] M. H. Valkenberg, C. de Castro, W. F. Hölderich, *Top. Catal.* **2001**, *14*, 139-144.

Chapter 6

Conclusions

Design of hybrid organic-inorganic materials has attracted significant attention especially in the area of molecular recognition. This thesis work has attempted to contribute to this field.

A general introduction showing the principles, perspectives and recent developments in the field of supramolecular chemistry has been incorporated. The effects induced by the integration of organic functionalizations on solid supports have been explained in order to understand the interactions involved in the design of sensing systems.

At the end of the introduction a brief description of some significant hybrid materials for these aplications have been included.

Following the plan described in the chapter 2, the work carried out in the thesis has been divided in two chapters with the aim of descriving the results obtained when using different hybrid organic-inorganic materials implied in a chemodosimeter process or in a displacement assay.

Chapter 4 was focused on the design and synthesis of new hybrids materials for chromogenic sensing using a chemodosimeter approach. From this chapter it can be concluded that:

- It has been synthesized a trimethoxysilyl aniline derivative as an organic precursor for the preparation of different dyes and it has been incorporated into the inorganic mesoporous and microporous silica materials by co-condensation method.
- The sensing ability of the 4-(4-amino-phenyl)-2,6-diphenylpyrylium chromogenic derivative in the mesoporous solid has been studied in water obtaining a discrimination of closely related aliphatic amines when the inorganic matrix has been hydrophobated with hexamethyldisilazane. In particular, using this solid, n-heptylamine, n-octylamine and n-nonylamine gave a colour change whereas no significant colour change was observed for amines with shorter and longer aliphatic chains.
- The sensing ability of the 4-(4-amino-phenyl)-2,6-diphenylpyrylium chromogenic derivative was also tested when it was inside a microporous matrix such as zeolite beta. The response of this dye-containing solid to a number of amines demonstrated that microporous materials can act as suitable

selective hetero-supramolecular host in selective optical sensing protocols.

- It has been demonstrated that the trimethoxysilyl aniline covalently incorporated into the microporous or mesoporous structures is a suitable precursor for the preparation of other materials containing dyes such as tricyanovinylbenzene, triphenylpyrylium, azoic and squarine derivatives.
- Some of those materials have been included into a polymeric matrix and it has been demonstrated that this presents some advantatges as an enhancement of the selective response and a large resistance to leaching. This study demonstrates that the combination of mesoporous supports with polymeric matrices can be a suitable method for the fabrication of optical materials.

Chapter 5 was focused on the design of functionalized binding pockets as a procedure to prepare new sensing materials using a displacement approach. From this chapter it can be concluded that:

- It has been prepared a mesoporous solid functionalized with 3-aminopropyltrietoxysilane and loaded with three different dyes (Methyl Red, 5-Carboxyfluorescein and Methylthymol Blue). This material has been used as a sensory material for the chromo-fluorogenic detection of different anions (NO_3^-, PO_4^{3-}, SO_4^{2-},CH_3COO^-, I^-, Br^- and F^-) and it has been found a phosphate-selective response.
- Moreover from the solid functionalized with 3-amino-propyltriethoxysilane other materials functionalized with guanidinium groups (by reaction with 2-methylthio-2-imidazoline hydroiodide) and another with urea groups (by reaction with butyl isocyanate) were prepared. Two more

solids were obtained by reaction with N-methyk-N''-propyltrimethoxysilyl imidazolium chloride, given a imidazolium-functionalized solid, and with 3-(trimethoxysilyl)propyl-N,N,N-trimethylammonium, resulting in a quaternary ammonium functionalized material. These solids have been loaded with 5-Carboxyfluorescein and were tested in displacement assays in the presence of a family of carboxylates and ATP, ADP and GMP.